

This item was submitted to [Loughborough's Research Repository](#) by the author.
Items in Figshare are protected by copyright, with all rights reserved, unless otherwise indicated.

Suspension polymerisation of methyl methacrylate: the use of polyelectrolyte stabilisers

PLEASE CITE THE PUBLISHED VERSION

PUBLISHER

© Styliani Georgiadou

PUBLISHER STATEMENT

This work is made available according to the conditions of the Creative Commons Attribution-NonCommercial-NoDerivatives 4.0 International (CC BY-NC-ND 4.0) licence. Full details of this licence are available at: <https://creativecommons.org/licenses/by-nc-nd/4.0/>

LICENCE

CC BY-NC-ND 4.0

REPOSITORY RECORD

Georgiadou, Stella. 2018. "Suspension Polymerisation of Methyl Methacrylate: The Use of Polyelectrolyte Stabilisers". figshare. <https://hdl.handle.net/2134/34983>.



University Library

Author/Filing Title GEORGIADOU, S

Class Mark T

Please note that fines are charged on ALL
overdue items.

FOR REFERENCE ONLY

0403176972



**SUSPENSION POLYMERISATION OF METHYL
METHACRYLATE.
THE USE OF POLYELECTROLYTE STABILISERS.**

by


Styliani Georgiadou

Dipl.-Eng. MSc.

A thesis submitted in partial fulfilment of the requirements for the award of the
Degree of Doctor of Philosophy

**Chemical Engineering Department
Loughborough University**

April 2005

	Loughborough University Pilkington Library
Date	JAN 2006
Class	T
Acc No	0403176972

*To my beloved parents
Spyros and Kaiti*



Abstract

The suspension polymerisation of Methyl Methacrylate (MMA), using polyelectrolyte solutions, Sodium polymethacrylate (PMA-Na) and Ammonium polymethacrylate (APMA), as suspending agents (stabilisers) was experimentally investigated in this project. The topics examined were, the rheological behaviour of the aqueous polyelectrolyte solutions, the factors that affect drop and particle sizes, dispersion and stabilisation mechanism and the factors that affect the critical conversion where the onset of the gel effect occurs. The main advantage of using PMA-Na and APMA as stabilisers for the suspension polymerisation is that these stabilisers are not grafted on to the polymer beads' surface, and they are easily washed off and removed after the polymerisation.

Rheological behavior of PMA-Na and APMA: Aqueous solutions of PMA-Na and APMA are characterised by high viscosity. They exhibit a non-Newtonian shear thinning behaviour, in contrast to the polymethacrylic acid (PMA), from which they are derived, and which shows a shear thickening behaviour. The viscosity of PMA-Na aqueous solutions depends on shear rate, but it is independent of pH and shear history. The viscosity of APMA solutions depends on, both, pH and shear history. Below, a certain pH value, the behaviour of the PMA-Na and APMA aqueous solutions, resembles the behaviour of the acid (PMA), showing a shear thickening behaviour. Hence, despite the advantage of using PMA-Na and APMA as stabilisers, their use induces various complexities in the flow in the reactor, because of their rheological behaviour.

Factors that affect the drop and particle sizes: The factors that were found to influence the drop and particle sizes were, the stabiliser concentration, the continuous phase viscosity, the stirring speed, the monomer hold-up fraction, the dispersed phase viscosity, the initial pH of the continuous phase, and the reaction temperature. The formation of fine particles, with diameters smaller than 10 μ m, was observed, for certain conditions.

Dispersion mechanism. The dispersion mechanism of the drops when APMA and PMA-Na are used as stabilisers was investigated. Experimental data of the maximum

drop size, d_{\max} , were compared with predictions of d_{\max} , from the Kolmogoroff theory of inertia break-up and from Taylor's theory of viscous shear break-up. Taylor's theory of viscous shear break-up seems to describe satisfactorily the experimental data and, therefore, the viscous shear break-up mechanism is considered to be the prevailing dispersion mechanism. The low Reynolds and Taylor numbers were consistent with this conclusion.

Stabilisation mechanism. The initial pH of the continuous phase plays a very important role for the MMA dispersion stability. The increase of the pH enhances the stability of the system, causing the drop sizes to decrease. Also, the required concentration of suspending agent, to stabilise the MMA dispersion, decreases as the pH increases. 'Electrosteric stabilisation' accounts for this behaviour. The polyelectrolyte solutions can promote the stability of the drops by functioning in a dual way, by steric stabilisation, and by electrostatic stabilisation. The adsorption of the polymer chain of the stabiliser on the monomer drops' surface, provides steric stabilisation, whereas, the ionisation of the electrolyte species and the charge of the polymer chain induces electrostatic repulsion, providing electrostatic stabilisation. The combination of the two is called electrosteric stabilisation.

Factors that affect the critical conversion (x_{crit}). The effect of temperature and of the molecular weight of the polymer produced in the polymerisation, on x_{crit} were examined by using a statistical approach. This approach eliminates the experimental error in the estimation of x_{crit} , which is induced by the difficulty in achieving completely isothermal conditions. The results that derive from the statistical analysis are compared with predictions from the free volume theory, which is the prevailing theory used to explain the gel effect. Analysis of variance and K-means cluster analysis were used to analyse a large number of experimental results. The results showed that x_{crit} depends on temperature, and on the molecular weight of the polymer produced in the polymerisation. The temperature dependence is consistent with the free volume theory, whereas, the molecular weight dependence is not taken into account by the free volume theory. Another very significant factor that was found to affect the kinetics of the polymerisation, was the type of stabiliser used. APMA and benzoyl peroxide (BPO), which was used as initiator, were found to interact. This interaction was manifested by a phenomenal decrease of the x_{crit} . This effect was

attributed to an acceleration of the polymerisation reaction rate, caused by APMA, which acts as a catalyst for the decomposition of BPO. APMA accelerates the decomposition of BPO, and this effect was found to depend on the concentration of stabiliser. The magnitude of the interfacial area, between the continuous and monomer phases, also influences the decomposition of BPO, and hence the polymerisation rate, suggesting that the interaction between the two variables, is related to the interfacial area between the two phases.

Keywords: Suspension polymerisation, polyelectrolyte solutions, suspending agents, non-Newtonian fluids, sodium polymethacrylate, ammonium polymethacrylate, gel effect

Acknowledgements

I would like to express my gratitude to my supervisor, Professor Brian W. Brooks, for his guidance, his valuable scientific advice, his support and help, and for his immediate response to my every query and request, throughout this project. I would also like to express my thanks to my second supervisor, Professor Chris Rielly, for his support.

I would like to thank Lucite International for the financial support of this project, the provisions of materials, and the analysis of samples carried out at Lucite premises.

I would like to express special thanks to Dr Michael Chisholm, Resins Business Research Associate (Lucite International), for his valuable contribution, his scientific advice, his support and help, during this project. I would also like to express special thanks to Dr Sera Abed-Ali, R&D Manager (Lucite International), for his scientific advice and help, and the for the enlightening discussions that we had. I would also like to thank Mrs Helen Harte, Research Scientist (Lucite International), for carrying out the analysis of polymer samples with Gel Permeation Chromatography, for this project.

I would like to thank Mr Andy Milne, Laboratory Technician in Loughborough University, for his valuable help in the laboratories. I would also like to thank Mr Dave Smith, Laboratory Technician for his help.

CONTENTS

Abstract	I
Acknowledgements	IV
Contents	V
List of figures	X
List of Tables	V
Nomenclature	XIII
SECTION 1- INTRODUCTION AND LITERATURE REVIEW	1
CHAPTER 1. INTRODUCTION	1
CHAPTER 2. LITERATURE REVIEW	2
2.1. Liquid-liquid dispersions	2
2.1.1. Breakage and coalescence of drops	3
2.1.2. Effect of hold-up fraction	4
2.1.3. Effect of the dispersed phase viscosity	5
2.1.4. Effect of the continuous phase viscosity	6
2.1.5. Effect of the non-Newtonian flow behavior	7
2.1.6. Dispersion mechanisms	7
2.1.6.1. Inertial breakup theory	8
2.1.6.2. Viscous shear breakup theory	11
2.2. Suspending agents and effects on particle size and morphology	14
2.2.1. Ammonium and Sodium salts of Polymethacrylic acid	18
2.3. Production of fine particles	21
2.4. pH	21
2.5. Kinetics	24

2.5.1. Trommsdorff effect (gel effect)	24
2.6. Effect of molecular weight (M_w)	28
2.7. Benzoyl peroxide – amine interactions	31

SECTION 2 – EXPERIMENTAL AND STATISTICAL PART

CHAPTER 3. EXPERIMENTAL PART	36
-------------------------------------	-----------

3.1. Materials	36
3.2. Polymerisation reactor	36
3.3. Analytical procedures	37
3.3.1. Determination of conversion	38
3.3.2. Determination of viscosity	38
3.3.3. Drop size distributions	40
3.3.4. Calculation of interfacial area	42
3.3.5. Calculation of the critical conversion (x_{crit})	43
3.3.6. Molecular weight averages and distributions	45

CHAPTER 4. STATISTICAL METHODS AND TESTS	46
---	-----------

4.1. Basic statistical concepts	46
4.2. Probability-Probability plots	47
4.3. Pearson's correlation	48
4.4. Levene's test of homogeneity of variance	49
4.5. One-Way Analysis of Variance (ANOVA)	50
4.6. Post Hoc tests	52
4.7. T-test	52
4.8. K-means clustering	53

SECTION 3 – RESULTS AND DISCUSION

CHAPTER 5. BEHAVIOUR OF PMA-Na AND APMA AS SUSPENDING AGENTS	54
5.1. Rheology	54
5.1.1. Polymethacrylic acid	54
5.1.2. Ammonium polymethacrylate (APMA)	58
5.1.3. Sodium polymethacrylate (PMA-Na)	61
5.1.4. Conclusions	64
5.2. Interfacial tension	66
5.2.1. APMA	66
5.2.2. PMA-Na	67
5.2.3. Conclusions	67
5.3. Factors that affect the drop and particle sizes and their distributions	68
5.3.1. Effect of the stabiliser concentration - continuous phase viscosity	68
5.3.2. Effect of the stirring speed	74
5.3.3. Effect of the monomer hold-up	77
5.3.4. Effect of the dispersed phase viscosity	80
5.3.5. Effect of pH	82
5.3.6. Effect of temperature	88
5.3.7. Effect of the chain transfer agent	94
5.3.8. Evolution of the particle size distribution during suspension polymerisation	98
5.3.9. Conclusions	102
5.4. Factors required for the investigation of the dispersion mechanism	104
5.4.1. Required stabiliser concentration	105
5.4.2. Apparent viscosity of the non-Newtonian continuous phase.	109

5.4.3. Density and interfacial tension	113
5.4.4. Dissipated power	114
5.4.5. Kolmogoroff turbulence macroscale	115
5.4.6. Conclusions	117
5.5. Determination of the dispersion mechanism	118
5.5.1. Experimental results and inertial breakup mechanism	119
5.5.2. Experimental results and viscous shear break up mechanism	120
5.5.3. Effect of the dispersed phase viscosity	125
5.5.4. Conclusions	127
5.6. Stabilisation mechanism	129
5.6.1. pH	129
5.6.2. Viscosity decrease (APMA)	132
5.6.3. Ionization / Dissociation degree.	132
5.6.4. Conclusions	133
CHAPTER 6. FACTORS THAT AFFECT THE ONSET OF THE GEL EFFECT	134
6.1. Experiments	135
6.2. Preliminary tests of the variables	139
6.2.1. Conclusions	140
6.3. Effect of temperature on x_{crit}	141
6.3.1. Conclusions	143
6.4. Effect of the initiator concentration on x_{crit}	144
6.4.1. One way Analysis of Variance (A-NOVA)	145
6.4.2. K-means cluster analysis	149
6.4.3. Effect of predissolved polymer on x_{crit}	153

6.4.4. Conclusions	155
6.5. Effect of the type of stabiliser on x_{crit}	156
6.5.1. T-test	157
6.5.2. Combined effect of increasing BPO and APMA concentrations	158
6.5.3. Effect of APMA concentration on x_{crit}	161
6.5.4. Effect of interfacial area	162
6.5.5. Conclusions	166
6.6. Effect of AMPA on M_w	167
6.6.1. Effect of APMA concentration on MWD	167
6.6.2. Effect of interfacial area on MWD	169
6.6.3. Conclusions	170
 SECTION 4- CONCLUSIONS and FUTURE WORK	 172
CHAPTER 7. GENERAL CONCLUSION	172
7.1. Rheological behaviour and interfacial properties	172
7.2. Behavior of PMA-Na and APMA as suspending agents	173
7.2.1 Factors that affect the drop / particle sizes	173
7.2.2. Dispersion mechanism	175
7.2.3. Stabilisation mechanism	175
7.3. Factors that affect the onset of the gel effect	176
 CHAPTER 8. FUTURE WORK	 178
 REFERENCES	 179

List of figures

Chapter 2

Figure 2.7.1. Possible mechanism for the interaction between amines and benzoyl peroxide	34
--	----

Chapter 3

Figure 3.2.1. Experimental set up	37
Figure 3.3.1. Typical example of viscosity and shear stress data obtained by using the Haake rheometer, and the fit to the power law model (solid line).	40
Figure 3.3.2. Typical particle size distribution	42
Figure 3.3.3. Experimental conversion data in comparison with theoretically predicted conversion values versus time	44

Chapter 4

Figure 4.2.1. Typical P-P plot	48
--------------------------------	----

Chapter 5

Figure 5.1.1. Effect of shearing time on a 3% aqueous PMA solution	55
Figure 5.1.2. Viscosity for increasing shear rate, for 3% PMA at 70°C	57
Figure 5.1.3. Viscosity under constant shear 108s^{-1} , for a 0.78% APMA solution, at 70°C, versus time.	58
Figure 5.1.4. The effect of pH and shear rate on the viscosity of a 0.93% APMA solution at 70°C	60
Figure 5.1.5.a) Effect of subsequent runs of shear on the viscosity of 0.93% APMA solution, at pH 8 and 70°C	60
Figure 5.1.5.b) Effect of subsequent runs of shear on the viscosity of 0.93% APMA solution, at pH 9 and 70°C	61

Figure 5.1.6. Effect of shearing time on viscosity	62
Figure 5.1.7. Effect of the pH on the viscosity of 0.6% PMA-Na aqueous solution	62
Figure 5.1.8. Viscosity dependence on shear rate and history for various pH values: a)pH 7, b)pH=8, c)pH=12	63
Figure 5.2.1. Interfacial tension between the monomer and the APMA continuous phase versus pH at 70°C	66
Figure 5.2.2. Interfacial tension between the monomer and the PMA-Na continuous phase versus pH at 70°C	67
Figure 5.3.1. Particle size distributions for increasing PMA-Na concentration in the continuous phase, at 70°C, 12.5s ⁻¹ , and initial pH=10	69
Figure 5.3.2. Effect of increasing APMA concentration in the continuous phase, at 70°C, 12.5s ⁻¹ , and initial pH=10	69
Figure 5.3.3. Effect of the continuous phase viscosity on the Sauter mean diameter, at 70°C, 12.5s ⁻¹ , and initial pH =10 for a)PMA-Na and initial pH =9 for b)APMA	71
Figure 5.3.4. d ₃₂ for PMA-Na and APMA, at 70°C, 12.5s ⁻¹ , for increasing continuous phase viscosity	72
Figure 5.3.5. Interfacial tension between monomer and the continuous phase for increasing stabiliser concentration, at 70°C	73
Figure 5.3.6. PSDs for 0.6% PMA-Na and increasing stirring speed at 70°C, and initial pH=10	75
Figure 5.3.7. PSDs for 1.2% PMA-Na and increasing stirring speed at 70°C, and initial pH=10	75
Figure 5.3.8. PSDs for various PMA-Na concentrations at 850 rpm, at 70°C, and initial pH=10	76
Figure 5.3.9. PSDs for various PMA-Na concentrations at 950 rpm, at 70°C, and initial pH=10	76

Figure 5.3.10. d_{32} for increasing stabiliser concentration at different stirring speeds	77
Figure 5.3.11. PSDs for increasing holdup and 0.6% PMA-Na, at pH 10 and 750rpm	79
Figure 5.3.12. d_{32} for increasing hold-up and various PMA-Na concentrations, at pH 10	80
Figure 5.3.13. PSD for increasing dispersed phase viscosity, for PMA-Na, at 70°C and 12s ⁻¹	81
Figure 5.3.14: The effect of the dispersed phase viscosity on d_{max} for PMA-Na, at 70°C and 12s ⁻¹	81
Figure 5.3.15. pH decrease during the course of polymerisation, at 70°C	82
Figure 5.3.16. Effect of increasing initial pH on the PSD, for 0.45% PMA-Na	83
Figure 5.3.17.a. Effect of increasing pH on peak 1	84
Figure 5.3.17.b. Effect of increasing pH on peak 2.	85
Figure 5.3.17.c.Effect of increasing pH on the main peak.	85
Figure 5.3.18.a. Effect of pH on peaks 1 and 2	87
Figure 5.3.18.b. Effect of pH on the main peak (peak 3)	87
Figure 5.3.18.c. d_{32} for total distribution and increasing pH	87
Figure 5.3.19. Volume % of each peak for increasing pH	88
Figure 5.3.20. Continuous phase viscosity (PMA-Na) for various temperatures, for series A and B	89
Figure 5.3.21. pH decrease with time for various temperatures	90
Figure 5.3.22. Conversion-time for various temperatures, and BPO 0.06mole/l	91
Figure 5.3.23. PSDs for various temperatures and 0.6% PMA-Na	91
Figure 5.3.24. d_{32} series A and for PMA-Na concentrations 0.6, 0.9 and 1.2%	92
Figure 5.3.25. Conversion-time for various T, and BPO concentration adjusted	92

to achieve the same reaction rate

Figure 5.3.26. d_{32} of the final particles for series B and for PMA-Na concentrations: 0.6, 0.9 and 1.2%	93
Figure 5.3.27. d_{32} for series A and B and for PMA-Na concentrations 0.6, 0.9 and 1.2%	93
Figure 5.3.28. Conversion-time data for polymerisation with and without DMA	95
Figure 5.3.29. PSDs for runs with DMA and pure monomer, for 0.6% PMA-Na	96
Figure 5.3.30. PSDs of fine particles, for runs with DMA and pure monomer, and for 0.6% PMA-Na	96
Figure 5.3.31. Evolution of the PSD, with DMA, and for 0.4% PMA-Na	97
Figure 5.3.32. Evolution of the PSD for the fine particles, with DMA, and for 0.4% PMA-Na	97
Figures 5.3.33. Conversion time data for 0.04mole/l BPO, at 70°C	98
Figure 5.3.34. Evolution of the PSD for particles with diameter larger than 10 μ m, and 0.2% PMA-Na	99
Figure 5.3.35. Evolution of the PSD for particles with diameter smaller than 10 μ m, and 0.2% PMA-Na	100
Figure 5.3.36. Evolution of the PSD for particles with diameter larger than 10 μ m, and 0.4% PMA-Na	101
Figure 5.3.37. Evolution of the PSD for particles with diameter smaller than 10 μ m, and 0.4% PMA-Na	101
Figure 5.4.1: Evolution of d_{32} with conversion for various stabiliser concentrations at 70°C, (a) PMA-Na (b) APMA	107
Figure 5.4.2: Sauter mean diameter with the conversion for various concentrations of predissolved PMMA, for 0.6% PMA-Na	108
Figure 5.4.3. PSD for increasing conversion for 0.6% PMA-Na	108

Figure 5.4.4: Viscosity and shear stress versus shear rate for various PMA-Na concentrations at the reaction temperature (70°C)	111
Figure 5.4.5: Viscosity and shear stress versus shear rate for series B ₁ , for various	112
Figure 5.5.1. Ind_{max} versus $\ln(\sigma v_c / \epsilon \rho_c)$ for PMA-Na (series A ₁)	119
Figure 5.5.2. Ind_{max} versus $\ln(\sigma v_c / \epsilon \rho_c)$ for APMA (series B)	120
Figure 5.5.3. d_{max} versus $\sigma / \mu_c f(p)$ for PMA-Na and various stirring speeds	122
Figure 5.5.4. d_{max} versus $\sigma / \mu_c f(p)$ for APMA	123
Figure 5.5.5. d_{max} versus $\sigma / \mu_c f(p)$ for PMA-Na. Comparison of the stirring speeds.	123
Figure 5.5.6. d_{max} versus Taylor number for various stirring speeds	124
Figure 5.5.7 (a). d_{max} versus Taylor number for all stirring speeds (series A)	125
Figure 5.5.7 (b). d_{max} versus Taylor number for APMA (series B)	125
Figure 5.5.8. d_{max} versus $\sigma / \mu_c f(p)$ for increased dispersed phase viscosity	126
Figure 5.5.9. d_{max} versus $\frac{\sigma}{\mu_c f(p)}$ at 750rpm. Comparison for simple runs (MMA only) and runs with predissolved PMMA	127
Figure 5.6.1. d_{32} for various PMA-Na concentration at various pH values	130
Figure 5.6.2. d_{32} for various APMA concentration at various pH values	131
Figure 5.6.3. Required amount of stabiliser to prevent coalescence for increasing pH	131
Figure 5.6.4. Required stabiliser concentration to stabilise a dispersion for increasing pH	131
Chapter 6	
Figure 6.2.1. P-P plots for x_{crit} and Mv	140
Figure 6.3.1. x_{crit} for various temperatures	141

Figure 6.4.1. Effect of initiator concentration on monomer conversion, for PMA-Na and pH 10	144
Figure 6.4.2. x_{crit} for various BPO concentrations	146
Figure 6.4.3. Mean values of x_{crit} for increasing BPO concentration	148
Figure 6.4.4. Samples (labelled with BPO concentration) comprising the clusters	150
Figure 6.4.5. Percentage of samples type in each cluster	151
Figure 6.4.6. M_v and x_{crit} for each cluster	153
Figure 6.4.7. MWD of PMMA at 0.336 conversion	154
Figure 6.4.8. M_v of predissolved PMMA and corresponding x_{crit}	155
Figure 6.5.1. The effect of the type of stabiliser on conversion	156
Figure 6.5.2. Conversion for increasing BPO concentration, with APMA at 70°C	158
Figure 6.5.3 x_{crit} for increasing BPO concentration, for APMA	159
Figure 6.5.4 Comparison between PMA-Na and APMA for increasing BPO concentration	160
Figure 6.5.5. Conversion for increasing APMA concentration in the continuous phase	161
Figure 6.5.6. Particle size distributions for APMA and increasing stirring speed	162
Figure 6.5.7. Interfacial area for increasing APMA concentration	163
Figure 6.5.8. Conversion for 0.78% APMA and increasing stirring speed and BPO 0.06mole/l.	164
Figure 6.5.9. x_{crit} for APMA and increasing stirring speed	164
Figure 6.5.10. x_{crit} for increasing interfacial area	165
Figure 6.6.1. MWDs for PMA-Na and APMA, produced under similar conditions	168

Figure 6.6.2. MWDs for increasing stirring speed, produced with 0.93% APMA, at initial pH 9	170
---	-----

List of tables

Chapter 3

Table 3.3.1. Typical output of the laser particle sizer and the calculated %volume	41
Table 3.3.2. Interfacial area for each size fraction	43

Chapter 4

Table 4.4.1. Example of Levene's test	49
Table 4.5.1. A typical example of an output for ANOVA	51

Chapter 5

Table 5.4.1. Experimental conditions	105
Table 5.4.2: Values of K, viscosity index n, and k_s , for series A	113
Table 5.4.3: Density and interfacial tension for various PMA-Na and APMA concentrations.	114
Table 5.4.4. Results for PMA-Na (series A): Viscosity, Re, N_p , power, dissipated power, Kolmogoroff scale, viscosity ratio, maximum diameter, and Taylor number	116
Table 5.4.5. Results for APMA (series B): Viscosity, Re, N_p , power, dissipated power, Kolmogoroff scale, viscosity ratio, maximum diameter, and Ta	117
Table 5.4.6. Results from series C: % concentration of PMMA predissolved in MMA, maximum diameter, Kolmogoroff length, interfacial tension, viscosity, viscosity ratio, power number, power and dissipated power	117

Chapter 6

Table 6.1.1. Results for series A	136
Table 6.1.2. Results for series B ₁	136
Table 6.1.3. Results for series B ₂	137
Table 6.1.4. Results for series C	138

Table 6.3.1. Descriptive statistics for x_{crit} and various temperatures (series A)	141
Table 6.3.2. Test of Homogeneity of Variances	142
Table 6.3.3. ANOVA	142
Table 6.3.4. Tukey test	143
Table 6.4.1. Descriptive statistics for x_{crit}	145
Table 6.4.2. Test of Homogeneity of Variances for x_{crit}	147
Table 6.4.3. ANOVA for the mean values of x_{crit} for various BPO concentrations	147
Table 6.4.4. Pearson correlation	148
Table 6.4.5. Initial Cluster Centres	149
Table 6.4.6. Final Cluster Centres	149
Table 6.4.7. Distances between Final Cluster Centres	149
Table 6.4.8 Number of Cases in each Cluster	150
Table 6.4.9. Descriptive statistics for the clusters	151
Table 6.4.10. Test of Homogeneity of Variances for x_{crit} in the clusters	152
Table 6.4.11. ANOVA for x_{crit} in the clusters	152
Table 6.4.12. Pearson Correlations	152
Table 6.4.13. Viscosity average molecular weight M_v , concentration of predissolved PMMA, x_{crit} and BPO concentration	154
Table 6.5.1. Descriptives	156
Table 6.5.2. Independent Samples T-test	157

Nomenclature

a = constant

a_2 = constant

A = (1) sample in chapter 4, (2) constant for the empirical equations in chapter 5

B = (1) sample in chapter 4, (2) constant for the empirical equations in chapter 5

b = impeller blade width (m)

B_k = constant

C = concentration of suspending agent (kg m^{-3})

D = impeller blade diameter (m)

d = drop diameter (m)

d_{32} = Sauter mean diameter (m)

df = degrees of freedom

d_{max} = maximum stable droplet diameter (m)

$(du/dr)_A$ = average shear rate (s^{-1})

e = distance between impeller blade and wall of reactor (m)

f = initiator efficiency

F = F statistic (F distribution)

f_i = frequency of drops with diameters within the range $(d_i + d_{i+1})/2$

$f(p)$ = function of p , $f(p) = \frac{19p+16}{16p+16}$

f_v = volume frequency distribution

G = velocity gradient (s^{-1})

G_{max} = velocity gradient at breakup of droplet (s^{-1})

H_0 = null hypothesis

I_0 = initial initiator concentration (mole/l)

I = initiator concentration (mole/l)

k = constant

k_1 = constant

k_2 = constant

K = constant from the power law model (Pas^n)

k_d = initiator decomposition rate coefficient (s^{-1})

k_p = propagation rate coefficient ($\text{l mol}^{-1} \text{s}^{-1}$)

k_s = constant

k_t = termination rate coefficient ($\text{l mol}^{-1} \text{s}^{-1}$)

k_{to} = termination rate coefficient at low conversion ($\text{l mol}^{-1} \text{s}^{-1}$)

L = Levene's statistic

m_i = level mean

N = stirring speed (rpm)

n = viscosity index

n_T = total number of data points

N_P = power number

N_i = number of drops

P = power consumption (W)

p = viscosity ratio = μ_d / μ_{appc}

r = Pearson's correlation

R = universal gas constant

$$R^2 = \frac{SSR}{SST} = \frac{\sum_{i=1}^{n_T} (\hat{y}_i - \bar{y})^2}{\sum_{i=1}^{n_T} (y_i - \bar{y})^2}$$

Re = Reynolds number

R_p = Propagation rate (s^{-1})

s = sample standard deviation

s^2 = sample variance

S_c = critical surface coverage ($\text{m}^2 \text{ kg}^{-1}$, or $\text{cm}^2 \text{ g}^{-1}$)

S_{di} = surface area of a single drop with diameter d_i (m^2)

S_i = interfacial area of fraction of drops with diameter d_i (m^2)

T = tank diameter (m)

t = time (s)

$$Ta = \text{Taylor number, } Ta = (ND\pi e / \nu_c) \sqrt{\frac{2e}{D}}$$

\bar{u}^2 = mean square turbulent velocity for the droplet ($\text{m}^2 \text{s}^{-2}$)

V = volume of the reaction mixture (m^3)

V_{di} = volume of a single drop with diameter d_i (m^3)

V_i = volume of fraction of drops with diameter d_i

Vi, λ = viscosity number of Ohnesorge number = $\mu_d / (\rho_d \sigma d)^{0.5}$

$V_{i,T}$ = tank viscosity group of the discontinuous phase = $(\rho_d / \rho_d)^{0.5} (\mu_d ND / \sigma)$

We = Weber number

$(We)_{crit}$ = critical Weber number

$(We)_T$ = Weber number of tank = $(\rho_c N^2 D^3)/\sigma$

$(We)_\lambda$ = Weber number for droplet = $(\rho u^{-2} d)/\sigma$

$(We)_o$ = Weber number when $Vi \cong 0$

x = (1) fractional conversion of monomer (2) a variable in chapter 4

x_{crit} = critical conversion

x_i = experimental value for variable x

\bar{x} = mean value of variable x

y = constant for the empirical equations in chapter 5

y = a variable in chapters 3 and 4

\bar{y} = the average of the y_i data points, or sample mean

y_i = data point, experimental value of variable y

\hat{y}_i = the predicted value for y_i

\bar{y}_i = the mean of the i_{th} subgroup

\bar{z}_i = the group means of the z_{ij}

\bar{z} = the overall mean of the z_{ij}

Greek letters

γ = shear rate (s^{-1})

γ_e = effective rate of deformation (s^{-1})

Δ = pressure difference across droplet – fluid interface (Pa)

\mathcal{E} = dissipated power per unit mass of the fluid ($W\ kg^{-1}$)

η = Kolmogoroff scale (m)

η_e = effective viscosity (Pa s)

θ = dimensionless time

λ = number of experiments

μ = dynamic viscosity (Pa s)

μ_{app} = apparent viscosity (Pa s)

ν = kinematic viscosity ($m^2\ s^{-1}$)

Π = disruptive pressure difference across droplet-fluid interface (Pa)

ρ = density (kg m^{-3})

σ = interfacial tension (kg s^{-2})

τ = shear stress (Pa)

ϕ = monomer volume fraction

Subscripts

c = continuous phase

d = dispersed phase

m = reaction mixture

Abbreviations

APMA = ammonium polymethacrylate

BPO = benzoyl peroxide

CTA = chain transfer agent

HQ = hydroquinone

M = molecular weight

MAA = methacrylic acid

MMA = methyl methacrylate

M_v = viscosity average molecular weight

M_w = weight average molecular weight

n-DDM = n-dodecyl mercaptan

PD = polydispersity index

PMA = poly methacrylic acid

PMA-Na = sodium polymethacrylate

PMMA = poly methyl methacrylate

PVA = poly vinyl alcohol

PVC = poly vinyl chloride

SSR = regression sum of squares

SST = total sum of squares

VCM = vinyl chloride monomer

SECTION 1. INTRODUCTION AND LITERATURE REVIEW

CHAPTER 1. INTRODUCTION

Suspension polymerisation is a process in which a monomer is dispersed in an aqueous medium by the combined action of agitation and of a suspending agent (stabiliser). The solubilities of the dispersed phase and of the produced polymer in the aqueous phase are usually low. Polymerisation occurs in the drops, and in most cases, by a free-radical mechanism. The size distribution of both the initial drops and the final particles depends upon the balance between breakup and coalescence mechanisms. This in turn depends upon the agitation intensity and the type and concentration of the suspending agent used (for given reactor and agitator geometry).

Free radicals are (usually) formed by thermal decomposition of the initiator. Once formed, these radicals propagate by reacting with monomers to form long macro-radical chains. The growing chain terminates when two radicals react.

The polymerisation reaction takes place in the following main steps: initiation, propagation, chain transfer and termination. During the course of polymerisation the physical properties of the reacting medium are subjected to significant changes. As a consequence, the kinetic parameters exhibit aberrations from “classical” kinetics, and in particular the termination rate becomes diffusion controlled, resulting in a great increase in the polymerisation rate, known as the auto-acceleration or ‘gel effect’. These events influence both the molecular weight and molecular weight distribution (MWD) of the polymer products which under the influence of these phenomena becomes broader and some times bimodal.

Suspension polymerisation is a widely used process, by which, polymer is produced in the form of particles or beads. The most important factors that determine the attributes of the final product are the particle size distribution and the molecular weight distribution of the polymer.

SECTION 1. INTRODUCTION AND LITERATURE REVIEW

CHAPTER 1. INTRODUCTION

Suspension polymerisation is a process in which a monomer is dispersed in an aqueous medium by the combined action of agitation and of a suspending agent (stabiliser). The solubilities of the dispersed phase and of the produced polymer in the aqueous phase are usually low. Polymerisation occurs in the drops, and in most cases, by a free-radical mechanism. The size distribution of both the initial drops and the final particles depends upon the balance between breakup and coalescence mechanisms. This in turn depends upon the agitation intensity and the type and concentration of the suspending agent used (for given reactor and agitator geometry).

Free radicals are (usually) formed by thermal decomposition of the initiator. Once formed, these radicals propagate by reacting with monomers to form long macro-radical chains. The growing chain terminates when two radicals react.

The polymerisation reaction takes place in the following main steps: initiation, propagation, chain transfer and termination. During the course of polymerisation the physical properties of the reacting medium are subjected to significant changes. As a consequence, the kinetic parameters exhibit aberrations from “classical” kinetics, and in particular the termination rate becomes diffusion controlled, resulting in a great increase in the polymerisation rate, known as the auto-acceleration or ‘gel effect’. These events influence both the molecular weight and molecular weight distribution (MWD) of the polymer products which under the influence of these phenomena becomes broader and some times bimodal.

Suspension polymerisation is a widely used process, by which, polymer is produced in the form of particles or beads. The most important factors that determine the attributes of the final product are the particle size distribution and the molecular weight distribution of the polymer.

CHAPTER 2. LITERATURE REVIEW

The drop and particle size distribution of polymethyl methacrylate (PMMA) and the molecular weight distribution have been the subject of excessive study. In order to control the particle sizes various suspending agents have been used and their behaviour has been investigated for suspension polymerisation. Nevertheless, the use of polyelectrolyte solutions, which are widely used as means to stabilise dispersions or suspensions in other industrial fields such as the ceramics industry, has not been investigated. The literature review covers the topics that are discussed in this study, which include the main topics of investigation for the suspension polymerisation processes, and additionally some topics that are not commonly encountered in suspension polymerisation studies. The main topics of investigation for suspension polymerisation processes are, liquid-liquid dispersions, suspending agents, dispersion mechanisms and polymerisation kinetics. Other topics also reviewed here are, the use polyelectrolyte stabilisers for dispersions, the effect of the pH on the formation of drops/ particles, and compounds that act as accelerators for radical polymerisations.

2.1. Liquid-liquid dispersions

When two immiscible liquids are brought into contact in an agitated vessel a dispersion is formed by the combined action of agitation and surface energy. In suspension polymerisation a monomer phase is dispersed in a continuous aqueous medium. In the first stages of suspension polymerisation, it is crucial that a uniform liquid – liquid dispersion is formed, since this dispersion determines the attributes of the final particles. The dispersion is maintained by agitation and the use of suspending agents. Consequently, it is controlled by the agitation intensity, the monomer volume fraction and the type and concentration of the suspending agent used (Dowding and Vincent, 2000). It was also observed that an increase in the viscosity of the suspending medium influences drop size and has different effect on drops of different sizes (Wang and Calabrese, 1986). The final drop size is determined by a balance between break up and coalescence.

2.1.1. Breakage and coalescence of drops

For a breakage to occur, it is necessary that enough energy be supplied to the drop to overcome the force that holds it together as a function of surface tension. The energy for the breakage is provided from the field outside the drop either as kinetic energy in the turbulent eddies, shear energy or as a combination of both. For isotropic turbulence, when the diameter of the drops is less than the Kolmogorov length η , drop breakage results from viscous shear; if the drop diameter exceeds η , drop breakage is caused by turbulent pressure fluctuations (Borwankar et al., 1986; Brooks, 1990). As the viscosity of the continuous phase increases or the rotational speed of the agitator decreases, the turbulent eddies diminish and the shear forces exerted on the drops from the flow field become more important. Thus, the drop breakage rate depends on the surface tension and on the hydrodynamic field outside the drops. The drop coalescence rate is also influenced by several factors, such as the collision rate between the drops and the coalescence efficiency between colliding drops. The latter is a function of the time that two colliding drops remain in contact and the time required for the intervening liquid film to drain out to achieve film rupture and thus coalescence. For systems of higher continuous phase viscosities, a lower film drainage rate would be expected and thus lower coalescence rate. The collision frequency increases with increasing stirring speed causing the coalescence frequency to increase, as well. (Howarth, 1963; Coulaloglou and Tavlarides, 1976).

Breakage and coalescence frequencies are not uniform throughout the volume of the reactor. Drop breakup occurs near the impeller and droplet coalescence predominates at other locations to a great extent. Beyond distances from the impeller region of the order of only 1/6 of the impeller diameter, breakup has been found to be virtually non-existent (Park and Blair, 1975). Experimental work by Park and Blair (1975) also showed that only binary coalescence occurs even at the highest dispersed phase concentration investigated, although the collision frequency, and consequently the coalescence rate, increases with the increase of dispersed phase concentration. Sprow (1967) studied the effect of coalescence on the drop size distribution in turbulent liquid-liquid dispersions, and he found that the maximum drop diameter, d_{\max} , increased for increasing stirring speed and increasing volume fraction. Zerfa and Brooks (1996(a)) also studied drop coalescence in suspension polymerisation and

showed that the extent of coalescence rises but only slowly with mixing time is roughly proportional to the agitation speed and decreases sharply when the concentration of the stabiliser increases.

The size dependence on drop coalescence frequency was investigated by Tobin et al. (1990) by measurement of transient drop size distributions in coalescing systems. The results indicated that the coalescence frequency of small drops (10-50 μ m in diameter) is lower than that predicted from a constant coalescence efficiency model, and the coalescence frequency is an increasing function of the drop pair sizes.

Various models describing the breakage and coalescence of drops in turbulent flows have been developed, either based on the mechanism of coalescence of drops by film drainage (Valentas et al., 1966; Coulaloglou and Tavlarides, 1977; Narsimhan et al. 1979; Sovova H., 1981, Kumar et al., 1991; Kumar et al., 1998) or on a population balance model (Alvarez et al., 1994; Maggioris et al., 1998; Ni et al., 2001; Jahanzad et al., 2005). More recently, the models established take into consideration the non-homogeneity of turbulence (Maggioris et al., 2000)

2.1.2. Effect of hold-up fraction (ϕ)

Zerfa and Brooks (1996 (b)) have established a relationship between drop size, volume fraction and Weber number in a turbulent dispersion. Increases in volume fraction of the dispersed phase led to widening of the drop size distribution. The effect of the dispersed phase concentration, ϕ , was also investigated by Kumar et al. (1991) who found that for low ϕ , the largest stable diameter increases with increasing ϕ , but decreases with increasing ϕ at high ϕ . They identified shear and accelerating flows prevailing in stirred vessels as alternative sources of drop breakup, and concluded that the observed d_{\max} at high ϕ could be explained by drop breakage in shear flows.

Similar observations were made by Boye et al. (1996) who studied the effect of the dispersed phase concentration on the Sauter mean diameter, as well as the effect of increase in the apparent viscosity of the dispersion due to the increase of the dispersed phase concentration on drop breakup, for xylene in water dispersions. They found that the viscosity of the dispersion exhibited strong non-Newtonian characteristics for

dispersed phase concentrations greater than approximately 50% by volume. The development of non-Newtonian flow properties and the increase in the apparent viscosity of the dispersion with increasing dispersed phase concentration changed the flow conditions in the tank from a turbulent regime to transitional and laminar flow regime. The sauter mean drop diameter measured as a function of the dispersed phase volume fraction (ϕ) was successfully interpreted in terms of inertial breakage mechanism for $\phi < 50\%$, and by a boundary layer drop breakage model for $\phi > 50\%$ by volume. For $\phi < 50\%$ the turbulence prevailed in the reactor, whereas for $\phi > 50\%$ the flow was not turbulent because of the high monomer hold-up which leads to high viscosity. In the turbulent flow regime, d_{32} increased with increasing ϕ , while in the non-turbulent regime the opposite effect was observed.

Desnoyer et al. (2003) carried out an experimental investigation in order to analyse the drop size distributions of a liquid-liquid dispersion in a stirred vessel at high phase ratio (ϕ) up to $\phi=0.6$. Two liquid- liquid systems have been investigated, one at low and one at high coalescence rate. They concluded that for a given impeller speed the mean diameter increased as ϕ increased, for both coalescing and non-coalescing systems. The linear relationship between the logarithm of d_{32} and the logarithm of the stirring speed predicted by Kolmogorov – Hinze theory was well verified with both systems suggesting that the correlation between the turbulent energy spectrum and the maximum stable diameter is still valid at high phase fraction. The formation of a secondary distribution was reported.

2.1.3. Effect of the dispersed phase viscosity

The effect of the dispersed phase viscosity on the maximum stable drop size in a turbulent flow was studied by Arai et al. (1977) who showed that the maximum stable drop size is controlled by two dimensionless groups, the Weber number,

$$We = \frac{\rho \bar{u}^2 d}{\sigma}, \text{ and the Viscosity number, } V_{i,\lambda} = \frac{\mu_d}{\sqrt{\rho_d \sigma d}}.$$

Calabrese et al. (1986) and, Wang and Calabrese (1986) investigated the effect of the dispersed phase viscosity alone and in relation to the interfacial tension on the drop breakup. They found that the drop size distribution broadens considerably as the

dispersed phase viscosity increases. The Sauter mean diameter was well correlated for various dispersed phase viscosities with either the Reynolds number or the impeller tip speed. They also showed that the relative influence of interfacial tension decreases as the viscosity increases.

2.1.4. Effect of the continuous phase viscosity

Little work has been done on the effect of the continuous phase viscosity on bead diameter. Stamatoudis and Tavlarides (1985) worked with continuous phase viscosities ranging from 3.6 cP to 223.1 cP and found that the effect of continuous phase viscosity on the drop size distribution is most pronounced for systems of high dispersed viscosities. A logarithmic plot of the Sauter mean diameter as a function of the impeller speed is a straight line, the slope of which varies with the continuous phase viscosity. The slope increases, reaches a maximum and then decreases with increasing continuous phase viscosity. This is attributed to an initial decrease of the breakage rate with the increasing viscosity of the continuous phase which results in an increase of the Sauter mean diameter. A still further increase of μ_c causes the coalescence rate to decrease, resulting in a decrease of d_{32} after reaching a maximum. To increase μ_c still further results in a region where d_{32} remains almost constant. This occurs because the decrease in the breakage rate is counterbalanced by the decrease in the coalescence rate. For higher impeller speeds the Sauter mean diameter changes little with increasing viscosity.

Jegat et al., (1998) used sucrose and acacia gum solutions as the continuous phase for suspension polymerisation experiments, in order to study the effect of the increasing continuous phase viscosity on the bead diameter. It was concluded that the viscous shear break up theory was valid for the prediction of the beads maximum diameter.

The effect of the continuous phase viscosity on the bead diameter has also been studied by Gaillard et al. (2000) who used solutions of acacia gum that displayed Newtonian behaviour, in order to increase the viscosity of the continuous phase. But the effect of a non-Newtonian highly viscous continuous phase on the bead diameter during suspension polymerisation has not yet been investigated.

2.1.5. Effect of non-Newtonian flow behaviour

Lagisetty et al. (1986) and Koshy et al. (1988) investigated the effect of non-Newtonian flow behaviour of the dispersed phase on drop breakage. Shimizu et al. (1999) investigated the effect of the non-Newtonian flow behaviour on the drop breakage in liquid-liquid dispersions by using palm oil as the dispersed phase and aqueous solutions of carboxymethyl cellulose and xanthan gum as the continuous phase. They found that the non-Newtonian characteristics of the continuous phase caused an increase in the maximum drop size particularly at low impeller speeds and wide drop size distributions. The Sauter mean diameter was proportional to the maximum drop diameter in non-Newtonian and Newtonian systems.

2.1.6. Dispersion mechanisms

Breakage is the result of viscous shear forces and turbulent pressure fluctuations in the vicinity of a droplet (Walstra, 1993). There are two main theories to account for the d_{\max} of stable droplets in stirred liquid-liquid dispersions: the inertial breakup theory established by Hinze (1955) from the homogeneous isotropic turbulence of Kolmogorov and the shear viscous breakup theory established by Taylor (1932, 1934).

Leng and Quaderer (1982) proposed 4 models, two based on laminar shear and two based on turbulent flow, to describe drop dispersion in non coalescing systems. The models predict the largest surviving drop size d_{\max} as a function of geometry, speed and physical property variables. Experimental evidence supports the boundary layer laminar shear model for drops larger than approximately 200 microns, while the presence of smaller drops supports a turbulence model. Both shear and turbulent mechanisms can produce stable dispersions (dispersions formed for non – coalescing conditions). The transition occurred at a Re of about 1000.

Jegat et al., (2001) found that when the viscosity of the continuous phase μ_c increases, the ratio $\sigma / [\mu_c f(p)]$, where p is the ratio of the viscosities of the two phases,

σ is the interfacial tension, and μ_c is the continuous phase viscosity (see equation 2.1.6.22), as well as the maximum drop diameter d_{\max} decreases. A linear relation of the maximum diameter d_{\max} to the ratio $\sigma/[\mu_c f(p)]$ was found in two peculiar regions separated by a break point. These workers attributed this breakpoint to changes in the nature of flow as a function of the Taylor number, which is given by the equation

$$Ta = (ND\pi e / \nu_c) \sqrt{\frac{2e}{D}}, \text{ where } N = \text{stirring speed (rps)} \quad D = \text{impeller blade diameter (m)}$$

e = distance between radius of small and big coaxial cylinders or between the impeller blade and the wall of reactor (without baffles) ν_c = kinematic viscosity of continuous phase ($\text{m}^2 \text{ s}^{-1}$). On one side of the breakpoint and for lower continuous phase viscosity, the Taylor number is $Ta > 400$ and the flow is turbulent. On the other side of the breakpoint and for higher continuous phase viscosity, the Taylor number is $Ta \leq 400$ and the flow is laminar with Taylor vortices. Therefore, the breakpoint corresponds to changes in the nature of the flow.

2.1.6.1. Inertial breakup theory

In a turbulent dispersion, three different forces act on an isolated droplet: a dynamic pressure due to the surrounding liquid (τ) a viscous shear of the droplet related to the

viscosity of the droplet, $\frac{\mu_d}{d} \sqrt{\frac{\tau}{\rho_d}}$, and the pressure difference whose order of

magnitude is σ/d . The dynamic pressure and the pressure difference always act on the droplet, while the viscous shear is only taken into account for high droplet viscosity.

When the viscous shear is negligible, the ratio of the dynamic pressure to the pressure difference reduces to a function of σ : $\frac{\tau/d}{\sigma} = (We)_\lambda$.

The We for the droplet $(We)_\lambda$ can be expressed as

$$(We)_\lambda = \frac{\rho_c \bar{u}^2 d}{\sigma} \quad (2.1.6.1)$$

where \bar{u}^2 is the mean square turbulent velocity for a droplet of dimension d .

$$(We)_{crit} = \frac{\rho_c \bar{u}^2 d_{\max}}{\sigma} \quad (2.1.6.2)$$

where $(We)_{crit}$ is the critical We, which is the value of $(We)_\lambda$ corresponding to the breakup of the droplet.

When the viscosity of the droplet liquid increases, the ratio of the external forces to the internal forces cannot simply be expressed in term of $(We)_\lambda$. The viscous shear is no longer negligible. Therefore, $(We)_{crit}$ must be expressed as a function ϕ of μ_d and σ by using the viscous (Ohnesorge) number $V_{i,\lambda}$:

$$V_{i,\lambda} = \frac{\mu_d}{\sqrt{\rho_d \sigma d}} \quad (2.1.6.3).$$

Hinze (1955) proposed the following relation for $(We)_{crit}$, taking into account $V_{i,\lambda}$:

$$(We)_{crit} = (We)_0 (1 + \phi(V_{i,\lambda})) \quad (2.1.6.4)$$

where $(We)_0$ is constant. The function $\phi(V_{i,\lambda})$ decreases to zero when $(V_{i,\lambda})$ tends to zero.

It is known that $(We)_{crit}$ is nearly constant when the viscosity number is smaller than 0.1 (Tarnogrodzki, 1993). In this case, the dynamic pressure induced by the turbulent flow is the determining factor for the greatest droplet diameters. Unfortunately, the We for a droplet cannot be determined. To avoid this difficulty, the Weber number of the chemical reactor $(We)_T$ is generally used (for stirred tank reactors), because it is proportional to the We of the droplet $(We)_0$.

$$(We)_T \propto (We)_0, \text{ and } (We)_T = \frac{\rho_c N^2 D^3}{\sigma} \quad (2.1.6.5)$$

When the stirring speed is constant in a given reactor the $(We)_T$ becomes

$$(We)_T \propto \frac{\rho_c}{\sigma} \quad (2.1.6.6)$$

According to Kolmogorov's theory of isotropic homogeneous turbulence, the \bar{u}^{-2} is independent of the of the macroscopic parameters of the flow. When the d of small eddies (i.e. the size of droplets) is much smaller than the D of the largest eddies (i.e. the impeller diameter) Kolmogorov defined the scale η as $\eta = \varepsilon^{-1/4} \nu_c^{3/4}$ where ε is the dissipated mechanical power per unit mass of the stirred suspension and ν_c is the kinematic viscosity of the continuous phase.

$$\text{When } D \gg d \gg \eta, \quad \bar{u}^{-2} \propto \varepsilon^{2/3} d^{2/3} \quad (2.1.6.7)$$

$$\text{When } D \gg \eta \gg d, \bar{u}^2 \propto \frac{\varepsilon}{\nu_c} d^2 \quad (2.1.6.8)$$

By replacing these two relationships for \bar{u}^2 to $(We)_{crit} = \frac{\rho_c \bar{u}^2 d_{max}}{\sigma}$, Shinnar and Church (1960) obtained the following relations:

$$\text{When } D \gg d \gg \eta, d_{max} \propto \varepsilon^{-6/15} \left(\frac{\sigma}{\rho_c} \right)^{3/5} \quad (2.1.6.9)$$

$$\text{When } D \gg \eta \gg d, d_{max} \propto \left(\frac{\sigma \nu_c}{\varepsilon \rho_c} \right)^{1/3} \quad (2.1.6.10)$$

Replacing (σ/ρ_c) by $(We)_T$ leads to

$$d_{max} \propto \varepsilon^{-6/15} (We)_T^{3/5} \quad (2.1.6.11)$$

When $(We)_{crit}$ differs from $(We)_0$ for highly viscous drops, then

$$(We)_{crit} = (We)_T (1 + \phi(V_{i,\lambda})) \quad (2.1.6.12)$$

$$\text{and } d_{max} \propto \varepsilon^{-6/15} [(We)_T (1 + \phi(V_{i,\lambda}))]^{3/5} \quad (2.1.6.13)$$

Experimental relationships based on inertial break up theory

Equation 2.1.6.11 validates the experimental relationships, established by several authors (Shinnar and Church, 1960; Coulaloglou and Tavlarides, 1976) for the mean diameter of a drop, when the viscosities μ_d and μ_c are close to each other and to the viscosity of water at the reaction temperature :

$$d_{32} = k_1 (1 + \alpha\phi) (We)_T^{-3/5} \quad (2.1.6.14)$$

It is generally accepted that $\varepsilon^{-2/5}$ from eq. 2.6.1.11 is proportional to $k_1 (1 + \alpha\phi)$ from eq. 2.1.6.14.

Equation 2.1.6.13 is analogous to the following experimental relation established by Calabrese and co-workers. (Calabrese et al., 1986a; 1986b)

$$\frac{d_{32}}{D} = k_2 [(We)_T^{-3/5} (1 + \alpha_2 V_{i,T})^{1/3}]^{3/5} \quad (2.1.6.15)$$

where $k_2 \sim 0.05$ and $\alpha_2 \sim 4.5$, and

$$V_{i,T} = \sqrt{\frac{\rho_c}{\rho_d}} \frac{\mu_d ND}{\sigma} \quad (2.1.6.16)$$

A simpler relationship was proposed by Das (1996)

$$d_{32} \propto [[(We)_T] - V_{i,T}]^{3/4} \quad (2.1.6.17)$$

2.1.6.2. Viscous shear breakup theory

The first work of significance which considered the distortion of a droplet caused by the viscous stresses exerted by the surrounding continuous phase was the work of G.I. Taylor in 1934 (Taylor, 1934). His work provided a theoretical and practical analysis of the drop break-up process as a result of the local shear field experienced by a drop. In effect, the first stage in understanding the action of emulsification was to consider the break-up of drops in homogeneous fields. The theoretical analysis was supported by experimental results. Taylor's paper provided the first photographic record of the break-up process for a variety of conditions.

According to Taylor's theory, a drop will continue to survive as long as its surface energy exceeds the local fluid energy. Drop breakage occurs when fluid stresses exceed surface resistance. This leads to the statement of conditions for the survival of a drop of a given diameter d . The pressure difference at the droplet-liquid interface

$$(\Delta) \text{ is } \Delta = \frac{4\sigma}{d} \quad (2.1.6.20)$$

Taylor (1934) showed that the disruptive pressure difference across the interface (Π) is

$$\Pi = 4G\mu_c f(p) \quad (2.1.6.21)$$

$$\text{where } f(p) = \left(\frac{19p+16}{16p+16} \right) \text{ with } p = \left(\frac{\mu_d}{\mu_c} \right) \quad (2.1.6.22)$$

where $f(p)$ is the function f of the viscosity ratio p and G is the velocity gradient of shear rate.

Taylor assumed that in a laminar or semi laminar flow a droplet breaks up when the disruptive pressure is greater than the pressure difference: $\Pi \geq \Delta$

The equality is the limiting value that corresponds to the largest stable droplet diameter. So, d_{\max} can be obtained from the relationships

$$\frac{4\sigma}{d_{\max}} \approx 4G_{\max}\mu_c f(p) \quad (2.1.6.23)$$

$$\text{and} \quad d_{\max} \approx \frac{\sigma}{G_{\max}\mu_c f(p)} \quad (2.1.6.24)$$

where G_{\max} is the velocity gradient at the breakup of the droplet. It is difficult to express G_{\max} as a function of μ_c . The Blasius solution for a boundary layer flow perpendicular to the cylinder axis is

$$G_{\max} = \frac{2.25\sqrt{\rho_c}V^{3/2}}{\sqrt{R\mu_c}} \quad (2.1.6.25)$$

where R is the radius of the cylinder and V is the relative velocity between the fluid and impeller. In this case d_{\max} should be a function of $\mu_c^{-1/2}$

Taylor's theory assumes that the breakup process is due to a viscous shear. The viscosities of the two phases do not play the same role: μ_c is a determining factor, while μ_d appears in function $f(p)$ as $p = \mu_d / \mu_c$. The influence of the μ_c has received relatively little attention, and there are not many experimental relationships that describe the effect of the continuous phase viscosity on the drop or particle sizes.

Experimental relationships based on viscous shear breakup theory

Experimental relationships that relate a mean diameter \bar{d} with the continuous phase viscosity μ_c are the following:

$$\frac{d_{50}}{D} = \sqrt{\text{Re}}((We)_T)^{-1} \left(\frac{\mu_d}{\mu_c} \right)^{0.1} \quad (2.1.6.26)$$

established by von Hopff, (1964) and

$$d_{10} \propto \mu_c^{-0.5} \quad (2.1.6.27)$$

$$\text{where } d_{pq} = \frac{\sum x_i d_i^p}{\sum x_i d_i^q}$$

established by Leng and Quarderer (1982). These relationships, though, have not been confirmed by other authors.

2.2. Suspending agents and their effects on particle size and morphology

Aqueous suspensions can be stabilised by a combination of agitation and the use of water soluble stabilisers. These may include electrolytes to increase the interfacial tension between the phases, and water soluble polymers which are absorbed on the monomer water interface providing stabilization of the suspension by a steric mechanism. Stabilisers may also include finely divided insoluble organic or inorganic materials which interfere with agglomeration mechanically.

As the polymeric stabiliser dissolves in the aqueous phase it acts in two ways: First it decreases the interfacial tension between the monomer droplet and water to promote the dispersion of droplets. Second, the stabiliser molecules are adsorbed on the monomer / water interface and prevent other drops from approaching because of steric repulsion forces. This causes reduction of immediate coalescence due to the increasing strength of the liquid film entrapped between two colliding drops. The presence of a protective film prolongs the contact time for drop coalescence, thus increasing the probability of drop separation by agitation. However, some collisions do result in adhesion of the colliding drops. In this case the thickness of the intervening film tends to decrease with time and finally collapses, permitting thus the coalescence of droplets (Chatzi et al., 1991; Yan et al., 1991; Vivaldo-Lima et al., 1997)

One of the most important issues in the practical operation of suspension polymerisation is the control of the final particle size distribution. The main factors that determine the particle size and the particle size distribution of the polymer are the type, attributes and concentration of the stabiliser. The presence of suspending agents hinders the coalescence of monomer droplets and the adhesion of partially polymerized particles during the course of polymerisation. Much research has been carried out in order to determine the effects of the suspending agents on the final particles under various operating conditions.

Zerfa and Brooks (1997) demonstrated that the type of stabiliser can affect the poly-vinyl chloride (PVC) particle's shape, size distribution and porosity. The effects of the suspending agent on the morphology of the resulting particles was examined by Lerner and Nemet (1999) and more specifically the effects of poly-vinyl alcohol

(PVA) which is one of the more extensively used stabilisers, on the suspension polymerisation of vinyl chloride. At the initial steps of polymerisation PVC molecules are grafted onto the molecules of the suspending agent forming a PVC-PVA membrane. The properties of this membrane depend on the type of suspending agent, the polymerisation temperature, the mixing efficiency and other factors. The morphology of the growing PVC particles and the properties of the PVC resin depend in turn on the characteristics of the suspending agent. Growing PVC particles are covered by a PVA-PVC membrane, which regulates the degree of particle contraction. If the degree of PVC grafting on the suspending agent is sufficiently high, the membrane toughness will also be higher resulting in a lower degree of particle shrinking and therefore higher PVC porosity. Porosity is also related to the surface tension of the suspending medium. A combination of low surface tension PVA and intense agitation results in high porosity particles of PVC, while a combination of medium surface tension PVA solution and low agitation results in low porosity dense particles (Ormondroyd, 1988). The importance of grafting of PVA on MMA during emulsion polymerisation was shown by the experimental work performed by Ohoya and co-workers (1999). Kiparissides et al. (1993) investigated quantitatively the electrostatic and steric stabilisation of primary PVC particles. Electrostatic stabilisation takes place as electrolytically active species (i.e. HCl) formed during the polymerisation are initially concentrated on the surface of the primary particles, thus providing the necessary negative electrostatic stabilizing forces. However, as the size of the primary particles increases, the contribution of the electrolytically active species decreases, resulting in a corresponding decrease of the particles' electrostatic stability. Steric stabilisation is achieved by the adsorption of PVA polymer chains on the drop surface.

The effect of continuous phase viscosity on the drop size of liquid-liquid dispersions in agitated vessels was examined experimentally by Stamatoudis and Tavlarides, (1985). Their experimental results indicate a decrease in Sauter mean diameter with increasing viscosity. The effect of continuous phase viscosity, though, is more pronounced for systems of high dispersed-phase viscosities and therefore for this system the drop size distribution becomes narrower and is shifted towards smaller drop sizes. The influence of the viscosity of the suspension medium in relation to molecular weight distribution and particle morphology was examined by Cebollada et

al., (1989) and the experimental results demonstrate that there is no appreciable influence of the characteristics of the suspension medium on the molecular weight distribution. In the case of particle size, high viscosity media produce larger size, unicellular spherical particles retaining their identity as individual droplets. Conversely, low viscosity media favour the formation of smaller particles. At lower viscosities, however, coalescence mechanisms become active simultaneously, resulting in multicellular structures. As a consequence, particle size will exhibit a minimum at a critical value of viscosity when all other parameters are kept constant.

Viscosity is predicted to have no effect when turbulence governs dispersion. When shear controls breakage, drop sizes should respond to $\mu_c^{-0.5}$. Increasing viscosity leads to a decrease in the drop size. Changes in viscosity were accomplished by increasing the PVA concentration. These changes in PVA concentration did not affect σ at the high concentration used (Leng and Quadrerer, 1982). The concentration of suspending agent which just prevented coalescence was noted. It was found that there was a critical surface coverage, S_c , for each suspending agent, such that if the ratio of the interfacial area of the dispersion over the weight of the suspending agent in the dispersion was higher than S_c ,
$$\frac{\text{interfacial_area}}{\text{weight_of_suspending_agent}} \geq S_c$$
, coalescence occurred. If the ratio was smaller than S_c ,
$$\frac{\text{interfacial_area}}{\text{weight_of_suspending_agent}} \leq S_c$$
, the system was stable.

The concentration of suspending agent necessary to stabilize a liquid dispersion is

$$C = 6\phi S_c / ((1-\phi)d_{32}) \text{ (Leng and Quadrerer, 1982)}$$

And the critical surface coverage may be calculated from the expression,

$$S_c = \frac{(1-\phi)d_{32}C}{\phi} \text{ (Borwankar et al., 1986). The Sauter mean diameter } d_{32} \text{ is defined}$$

as $d_{32} = \sum f_i \bar{d}_i^3 / \sum f_i \bar{d}_i^2$ and $\bar{d}_i = (d_i + d_{i+1})/2$, where f_i is the frequency of drops in the size range d_i and d_{i+1} . The frequency of the drops f_i is calculated from the drop size distribution

Zerfa and Brooks (1998) studied the kinetic mechanism of PVA adsorption at the vinyl chloride/water interface in monomer suspensions for different experimental

conditions. The surface coverage was found to be independent of both the turbulence intensity and the vinyl chloride drop size. The quantity of PVA adsorbed was found to be proportional to the volume fraction of the monomer and a multilayer is formed when high concentrations of PVA are used. The results lead to the conclusion that although saturation of vinyl chloride/water interface with PVA was reached relatively quickly (in less than 5 min) due to the fact that PVA molecules diffuse relatively quickly to the interface, the stability of VCM droplets was not reached before 30 min. This delay was attributed to the rearrangement and spreading of the PVA molecules on the interface until they reach a favourable conformation. For another monomer, MMA, and in the case of PVA adsorption on the interface of MMA/water system, the concentration of PVA adsorbed was found to vary with increasing impeller speed. It was observed that in the absence of polymerisation reaction, the concentration of PVA adsorbed increases with impeller speed, reaching a maximum at 400 rpm and then decreases with increasing impeller speed (at high speeds) (Lazrak et al., 1998).

PVA adsorption on the monomer (styrene)/ water interface has also been studied by means of interfacial tension variations with time and PVA concentration at different temperatures (Chatzi et al., 1991). It was demonstrated that both the time required to reach equilibrium and the interfacial tension decrease with increasing PVA concentration. Initially, it appears that surface tension is relatively independent of concentration up to about 0.01 g/L. For PVA concentrations higher than 0.01 g/L there is a break point and the surface tension decreases almost linearly on a semilog scale. A possible explanation for the observed variations of interfacial tension with respect to PVA concentration may be a complete and rapid unfolding of the very flexible PVA molecules for low PVA concentrations, resulting in an extended conformation of PVA with a large number of segments per molecule in the interfacial region. The break point marks the onset of almost complete coverage of the interface and its saturation with molecules having an extended conformation. The rather steep decrease of interfacial tension at higher concentrations is probably due to increased adsorption of molecules and the appearance of strong repulsive forces. The conformation of adsorbed molecules will be random initially. However, as the number of adsorbed segments increases, the packing of the molecules in the surface layer increases up to the formation of a monolayer. Above this concentration no significant changes of the drop size distribution are expected.

The experimental investigation of the effect of PVA on styrene, conducted by Yang et al., (2000) demonstrated that an increase in PVA concentration decreases the mean drop size and narrows the drop size distribution. There is a critical concentration of PVA that depends on the monomer volume fraction, above which, further increases in PVA concentration do not have a great effect on the drop size and volume distribution.

Although, most of experimental work reported on suspending agents, refers to the use of PVA, (Konno et al., 1982; Chatzi et al., 1991; Lazrak et al., 1998; Yang, 2000, He et al., 2002), the stabilising effects of some polyelectrolytes such as polymethacrylic acid and copolymers of methacrylic acid with methyl methacrylate were also investigated (Ryabov and Panova, 1972). It was concluded that the stabilising effect of the PMMA and of the MAA+MMA copolymer becomes evident at pH values 5-7, while it decreases at pH below 4. The stabilising effect is improved at pH values above 7, when the carboxyl groups are ionised.

The effect of the type of stabiliser on particle size, porosity and morphology was also investigated experimentally (Konno et al., 1982) and in particular the effect of PVA on the suspension polymerisation of styrene. It was demonstrated that the dispersed drop size does not depend upon stabiliser concentration at the early stage of the reaction, but is influenced by it after the middle stage of the reaction. A bimodal drop size distribution appears during the reaction and the lower drop size mode in the distribution maintains a constant diameter, while the second drop size mode is shifted to larger sizes. The experimental results show that the stabiliser does not effectively prevent the coalescence of dispersed drops of a size larger than d_{\max} , owing to the considerable deformation of the dispersed drops.

2.2.1. Ammonium and Sodium salts of Polymethacrylic acid

Polyelectrolyte solutions are widely used to stabilise large colloidal particles and have found applications in many industrial fields such as the cosmetics industry, the adhesives industry and the paper industry. Sodium polymethacrylate (PMA-Na) is also used in the ceramic industry as a suspending agent to stabilise alumina suspensions (Cesarano et al., 1988; Sundlof and Carty, 2000). Although, it has not

been reported previously (to our knowledge) PMA-Na may also be used in the polymer industry as a suspending agent for suspension polymerisation reactions. The fact that it is listed within the non-hazardous chemicals list (environmental friendly) is one of the benefits of using this polyelectrolyte salt. The most significant advantages, though, of using PMA-Na as suspending agent for suspension polymerisation reactions are that PMA-Na is easily removed with water and washed off from the final polymer product at the end of the reaction, and secondly it is not grafted on the particle surface like other common stabilisers are, e.g. polyvinyl alcohol (Lerner and Nemet, 1999).

The latter is a very important advantage, especially when a high purity polymer is required. Despite the obvious advantages, the use of PMA-Na induces various complexities, because of the high viscosity and the non-Newtonian behavior that characterises the aqueous solutions of PMA-Na.

The Ammonium Salt of Polymethacrylic acid (APMA), known as 'Darvan C', has been widely used in the ceramic industry as a suspending agent in order to stabilise ceramic powders in aqueous suspensions (Cesarano et al., 1988; Kelso and Ferrazzoli, 1989; Beattie and Djerdjev, 2000; Sundolf and Carty, 2000; Cho and Dogan, 2001). In general, suspensions can be stabilised by electrostatic, steric or electrosteric mechanisms. Electrostatic stabilisation is accomplished by generating a common surface charge on the particles. Steric stabilisation is achieved by adsorption of polymeric additives which serve to form protective colloids. Electrosteric stabilisation, is a combination of the two aforementioned, and requires the presence of adsorbed polymer or polyelectrolyte and significant electrical layer repulsion. The use of polyelectrolyte species promotes the stability of the suspension through an electrosteric mechanism.

The critical factors that determine the stability of a suspension in the case of aqueous ceramic suspension are apart from the surface chemistry of the powders, the pH, the degree of polyelectrolyte dissociation, the molecular weight of the polyelectrolyte and the quantity of polyelectrolyte.

The dissociation of APMA and PMA-Na is strongly affected by the pH of the solvent. The fraction of dissociation of APMA at different pH values increases from 0 at pH=2

to 1.0 at pH=11-12. Therefore, APMA changes from a relatively neutral polymer at pH=2 to a fully negatively charged polymer at pH=11-12. Ionised APMA is expected to have a more stretched conformation with increasing pH because of the electrostatic repulsive force between negatively charged side groups (Jean and Wang, 1998). More specifically, the degree of APMA dissociation was studied by Cho and Dogan, (2001) who conducted ESA (Electrokinetic Sonic Amplitude) measurements. According to these measurements, below pH =8 dissociation of APMA molecules decreases approaching 0, while above pH=8 the ESA values remain constant, indicating that APMA molecules are fully dissociated.

The stability of aqueous Barium Titanate suspensions as a function of pH was investigated experimentally and the adsorption of APMA was found to decrease as pH increases and the amount of APMA required to stabilise a suspension decreases as pH increases. A combination of electrostatic and steric stabilization, electrosteric stabilization is believed to be operative at pH =7-12 with the various concentrations of APMA investigated (Jean and Wang, 1998).

The investigation of alkaline earth titanates' suspensions shows that the suspension is stable at a critical addition of APMA. With further addition of the polyelectrolyte a transition from stabilization to flocculation occurs. It was also concluded that at acidic pH range the steric repulsion of APMA has a positive contribution on the dispersion (Shih and Hon, 1999).

The experimental investigation of alumina suspension with APMA showed that the adsorption density of APMA continuously decreases with increasing pH up to about pH =9 and thereafter becomes insignificant due to electrostatic repulsion. Desorption studies also indicate that cumulative percentage desorption of APMA from the alumina surface increases with increasing pH. Hydrogen bonding, electrostatic and chemical interactive forces are postulated to govern the adsorption process. Conformational changes also take place as a function of pH. At alkaline pH values, the polymer is fully ionized and the negatively charged sites on the polymer chains tend to repel each other and this leads to a stretched conformation, with the polymeric chains dangling into the solution phase. Such a stretched configuration of the polymer should favour hydrogen bonding. However, at acidic pH values, namely at pH 3, the polymer chains have a coiled conformation due to the absence of intrapolymer-chain

electrostatic repulsion. Consequently, each polymeric chain covers a relatively large surface area and enhanced adsorption is observed. Thus both electrostatic and conformational factors govern polymer adsorption as a function of pH, while FTIR analyses demonstrated the existence of hydrogen bonding (Santhiya et al., 2000).

2.3. Production of fine particles

The existence of one or more secondary distributions of fine or emulsion particles is of major importance in many industrial processes (solvent losses or pollution). It is well known that the breakage of a single drop in two equivalent daughter drops may be accompanied by the formation of smaller drops or 'satellite' drops (Karam and Bellinger, 1968). These drops may result from the stretching of the liquid filament that develops just before the daughter drops' separation (Stone 1994). Shreekumar et al. (1996) found that, at least during breakage of a drop of diameter greater than d_{\max} by interaction with a fluctuation of equal length scale, a satellite drop is always formed between two larger drops. When very large drops are broken by smaller-length-scale fluctuations, highly deformed shapes are produced suggesting the possibility of further fragmentation due to instabilities. The emulsion particles may also result from molecular diffusion causing partial dissolution of the monomer/polymer droplets (Azad and Fitch., 1978). This occurs faster for smaller drops because of their higher surface energy. The addition of inhibitor has been found to suppress the formation of the emulsion particles by consuming the initiator particles formed in the aqueous phase (Jahanzad et al., 2004)

2.4. Effects of pH

In agitated liquid-liquid dispersions, four primary factors are known to affect the coalescence process. These factors are

1. energy dissipation rate, which governs the energies of the drop collision process and to some extent the frequency of coalescence

2. the dispersed phase concentration which directly determines the collision frequency
3. the viscosities of the continuous and dispersed phases, all of which affect the rate of film drainage between two colliding drops
4. the interfacial tension of the system, which bears on the deformability of the drops

In addition to the above factors, there is evidence that drop surface charge can also be important for determining coalescence rates in agitated dispersions. Experimental work performed by Howarth (1967) showed that in the case of an organic substance in water dispersion (5% benzene/ CCl_4 in water) where the surface was charged by the addition of an electrolyte, the electrolyte type and concentration plays a definite role in determining the coalescence rate of the organic droplets. Reddy and Fogler (1980) showed that emulsion droplets can be substantially stabilised against coalescence merely by increasing the pH of the system. They investigated possible alternative explanations but were eventually led to the conclusion that the drop surface charges were due to preferential adsorption of hydroxide ions.

Doxastakis and Sherman (1984) studied the rate of drop coalescence in concentrated corn oil-in-water emulsions stabilized with sodium caseinate, glyceryl monostearate and glyceryl distearate. Both pH and the monoglyceride/diglyceride ratio influence coalescence. At any pH, minimum coalescence was observed at a 5/2 monoglyceride/diglyceride ratio. This was attributed to association of caseinate with a previously formed 'complex' of monoglyceride and diglyceride, so supporting an interpretation previously proposed on the basis of rheological data for the emulsions and for films of caseinate-glycerides at the oil-water interface.

Ggillc et al. (1986) examined the separation of fine dispersions of organic solvents in water by passage through glass fiber beds. Dispersions were generated in a stirred tank and the Sauter mean diameter of organic droplets was between 10 and 30 μm for a wide range of Interfacial tensions as well as viscosities of organic solvents. They showed that the pH of the aqueous phase affects the coalescence rate considerably.

Tobin et al. (1991) studied the effect of the drop charge as a function of pH, on coalescence in agitated liquid-liquid dispersions and demonstrated that drop charges

can substantially alter the coalescence rate of droplets in an agitated dispersion. Elevation of the pH causes the drop size distributions to narrow and shift towards smaller sizes. In addition, the presence of a drop charge in such dispersions appeared to be latent, and was attributed to the preferential adsorption of hydroxide ions onto the organic-water interface. The effect of drop charge on coalescence was strongly size-dependent, and reduction of the electrostatic repulsion promoted coalescence of the largest drops primarily. Tobin and Ramkrishna (1992) studied the effect of the pH of the aqueous phase on the coalescence rate of drops of benzene and carbon tetrachloride dispersed in water. They found that an increase in pH inhibited substantially the coalescence of drops, an effect that was attributed to the preferential adsorption of hydroxide ions onto the water organic interface

Kawashima et al. (1993) controlled the size of ibuprofen microspheres fabricated by the o/w emulsion solvent diffusion method by adjusting the pH in an aqueous dispersion phase.

Velev et al. (1994) performed experimental research into model oil-in-water emulsion systems stabilized with non-ionic surfactant blends: thin aqueous films between oil phases and oil drops coalescing against their homophase. Xylene was chosen as the oil phase and Tween 20 and Span 20, alone or in mixtures at different molar ratios, were used as stabilisers. The roles of the electrolyte concentration and pH were studied. It was shown that there is considerable electrostatic repulsion within the aqueous films, and that the pH affects significantly the coalescence rate.

Deshiikan and Papadopoulos (1995) studied the coalescence of n-hexadecane oil drops with diameters within the range 70-100 μm , suspended in an aqueous medium of varying pH and ionic strength. They found that pH is more important than ionic strength in controlling the coalescence of charged oil drops. They also observed that the coalescence times indicated faster coalescence at acidic pH than at alkaline pH.

Ruiz et al. (2002) studied the effect of pH changes on the breakage rate of organic drops. The organic phase they used was a 1:1 mixture of a salicylaldoxime and a ketoxime in an aliphatic diluent. They found that changes in the surface charge of the organic drops in liquid-liquid dispersions, would produce variations in the resistance to deformation (stiffness) of the drop surface, which in turn will change the tendency

of the drops to undergo breakage. A decrease of the pH increased progressively the tendency of the organic drops to undergo breakage, giving finer drops, due to changes in the surface charge of the drops produced by the pH change.

Kraume et al. (2004) carried out an experimental investigation to analyse the influence of coalescence behaviour on drop size distributions in stirred liquid-liquid dispersions. They studied the influence of pH and addition of ions and found that the pH exerts a significant influence on the coalescence rate.

2.5. Kinetics

Free radical polymerisation of MMA, as with many other monomers, exhibits an autoacceleration of the polymerisation rate known as Trommsdorff or 'gel effect' which leads to an increase of the molecular weight of the polymer, accompanied by a sudden temperature rise. Consequently "classical" kinetics do not apply during autoacceleration regime and the modeling of polymerisation all over the conversion range has not yet been achieved due to a incomplete understanding of the origin of the phenomenon.

2.5.1. Trommsdorff effect (gel effect)

Many theories have been proposed trying to interpret the autoacceleration phenomenon or gel effect. Experimental tests, though, to discern among these theories have been lacking. The most widely accepted interpretation of the phenomenon is based upon the changes in apparent kinetic parameters of the elementary reactions which occur during the course of the polymerisation.

The kinetic expression describing free radical polymerisation at low conversions is

$$R_p = k_p [M] (fk_d[I]/k_t)^{1/2}$$

where R_p is the propagation rate, k_p is the propagation rate constant, M is the concentration of monomer, f is the initiator efficiency, I is the initiator concentration and k_t is the termination rate constant. This expression does not apply, though, to

higher conversions, where R_p undergoes a sharp increase with an accompanying rise in system temperature and degree of polymerisation. The phenomenon was associated with a decreased termination rate constant.

During the autoacceleration regime dramatic changes in the solution properties take place. Various approaches have sought the onset of autoacceleration to a 'critical' polymer concentration and a 'critical' molecular weight (Dvornic and Jacovic, 1981). Abuin et al. (1977) suggested that both the conversion at which the gel effect appears and the value of k_t at a given conversion depend on the molecular weight of the 'dead polymer'. The mean size of the growing radicals is also found to influence k_t .

The onset of the autoacceleration of the propagation rate was attributed to the increasing bulk viscosity, which severely impeded the diffusion of the propagating chains causing a restriction or decrease of the termination reaction which in turn leads to a higher radical population and consequently an increase of R_p . In other words, with increasing monomer conversion the viscosity of the reaction mixture increases by many orders of magnitude until it becomes high enough to induce diffusion control over the termination steps of the polymerisation reaction, resulting in a significant decrease in the apparent rate constant of the termination reaction k_t . As a consequence, a large autoacceleration in the rate of polymerisation occurs which is associated with a simultaneous increase in the molecular weight of the polymer produced.

Brooks (1977) investigated the kinetics of free-radical polymerisation at high viscosities, the relationship between radical mobility and viscosity and polymer volume fraction, and related the chain termination rate coefficient with the viscosity. Bogunjoko and Brooks (1983 (a)) investigated the influence of increasing solution viscosity on the molecular weight distribution suggesting that the mobilities of the growing radicals are not equally influenced by the solution viscosity (Bogunjoko and Brooks, 1983 (b)).

Dvornic and Jacovic (1981) investigated the kinetics of the suspension polymerisation of methyl methacrylate initiated by benzoyl peroxide and the effect of the concentration of the molecular weight regulator (dodecyl mercaptan) at the onset of the gel effect. They drew the conclusion that there exists a critical viscosity of the

polymerisation mixture at which the termination reaction becomes diffusion controlled and that autoacceleration begins when the critical viscosity is reached.

Cioffi et al. (2001) carried out rheokinetic studies of free radical polymerisation (in bulk) of styrene and n-butylmethacrylate at high degrees of conversion and they showed that the viscosity of the reacting mixture initially increases and then after reaching a certain value decreases suddenly exhibiting a highly irregular trend with time. This phenomenon was attributed to phase separation which occurred when the polymer concentration increased and therefore it was no longer soluble to the residual monomer.

In the last decades, three approaches have been presented that could potentially explain this phenomenon. The first is that the formation of chain entanglements plays a pivotal role in restricted chain mobility, leading to the decrease in k_t . Tulig and Tirrell (1981) developed an entanglement based model, which related k_t to the diffusion coefficient of the propagating chains and included molecular weight and concentration scaling for the diffusion constant. There also exist experimental data (Abuin and Lisi, 1977; Abuin et al., 1977) that link entanglements to the gel effect. It was observed that there appears to be a higher gel effect onset concentration when lower molecular weight polymer is formed. This observation was qualitatively consistent with the entanglement theory, as entanglements should form at higher conversions for lower molecular weight. O'Shaughnessy and Yu (1994) also attributes the onset of gel effect to entanglement - dominated kinetics (k_t is controlled by polymer self diffusion which in turn exhibit entangled polymer dynamics) and suggests that the long chain mobility is reduced by entanglements to such an extent that short mobile chains provide a faster termination mechanism despite their small numbers. Abuin and Lissi, (1977) and Lachinov et al., (1979) had already related the free volume on the onset of gel effect with the chain length and the conversion at which the gel effect appeared to a critical entanglement. Recent experimental work, though, indicates that the gel effect occurs in the absence of entanglements, and eliminating the formation of chain entanglements does not result in a corresponding elimination or delay of the gel effect onset (Neil et al., 1996). Moreover, the onset of gel effect does not correlate with molecular weight quantitatively in a way that would be consistent with the entanglement theory.

A second approach is that termination at intermediate conversions is dominated by short active chains (unentangled) reacting with long active chains (entangled) a process governed by the diffusion of the shorter, more mobile chains. This different approach to describe termination kinetics on the basis of "short-long" termination has emerged recently. O'Shaughnessy and Yu, (1994) have advanced a theory to explain the kinetics during the gel effect on the basis of short-long termination. This picture postulates that during the gel effect the termination of a long chain becomes so hindered due to diffusional limitation that it can only terminate when a short chain diffuses to its vicinity. The gel effect is then related to a depletion of short chains in the system. But this theory as well has not been tested experimentally, and besides, it does not explain the presence of the gel effect in the absence of entanglements.

Zhu and Hamielec (1989) and Zhu et al. (1990) investigated the bulk free radical polymerisation of MMA and found that a fraction of the radical population is trapped during the course of polymerisation and therefore there exist two radical populations in the reacting mass - free radicals in the liquid state and trapped radicals in the solid state. Consequently the reacting mass is heterogeneous and the probability of a radical center becoming trapped is a strong function of its chain length.

A third theory is related to free volume of the monomer as it is converted into polymer. The free volume of the monomer is higher than the free volume of the polymer. As monomer is converted to polymer the free volume is decreasing, and the mobility of the free radicals is restricted. The essential idea is that the restricted mobility, associated with the decreasing free volume as monomer is converted to polymer, is adequate to account for the observed decrease in k_t . In other words, when a critical value of conversion is reached, the termination rate k_t decreases rapidly and its decrease can be described as a function of the free volume of the system. Experimental investigation of this approach shows that the dependence of the conversion at which the gel effect begins on temperature is consistent with that predicted by the free volume theory. The last approach prevails among the various theories reported (Arai and Saito, 1976; Neil et al., 1998).

Most attempts to explain the gel effect have fallen into one of two categories: entanglement theories and free volume theories. However, neither is adequate to describe the gel effect completely. The theory that the onset of gel effect is caused by

the onset of entanglements, fails to predict trends concerning the effects of temperature, polymer concentration, and molecular weight on the gel effect onset conversion (Neil and Torkelson, 1999). The free volume theory is consistent with experimental results when critically tested (Neil et al., 1998) it cannot be used though by itself to predict accurately conversion – time results for a broad range of conditions and is not a molecular – level theory as it does not account for radical chain length effects on the rate of termination.

The gel effect has been associated with a number of physical parameters that were related to the changes observed during the course of the event. Enormous effort has been put into the interpretation of the phenomenon and the determination of the factors that cause this autoacceleration of the reaction rate. It is well understood that the characteristic autoacceleration in polymerisation rate associated with the gel effect is due to a decrease in the termination rate parameter k_t . This decrease of k_t , in turn, is related to a restriction of chain mobility as monomer is converted to polymer, while for high mass fraction of polymer k_p also decreases. Nevertheless, a quantitative understanding of autoacceleration has not been yet achieved.

2.6. Effect of molecular weight (Mw)

In suspension polymerisation of MMA the concentrations, physical properties and kinetic parameters change dramatically during the reaction and produce polymer chains of different lengths with consequent variations in the weight average molecular weight Mw and the molecular weight distribution (MWD). In particular, the increase in the polymer concentration during the reaction affects strongly the process dynamics: the resulting increase in the viscosity of the reacting system gives rise to a reduction in the mobility of the polymer chain; this may lead to a situation in which the termination and the propagation rates are controlled by diffusion, the gel and glass effects. In both cases (glass and gel effect) the consequence is a broadening of the MWD curves. In the polymerisation of MMA the influence of the gel effect on the Mw is very strong, so the instantaneous values of the average chain length increase rapidly during the process. As a consequence, under isothermal conditions, the MWD shows bimodality, as observed experimentally.

The main mechanical and thermal properties of the polymeric products are related with the value of the M_w and the MWD. In order to control the M_w of the polymers chain transfer agents are used. Chain transfer agents affect not only the M_w of the resulting polymer but also the magnitude and the onset of the gel effect. It has been pointed out that increasing the concentration of the chain transfer agent (CTA) delays the onset of the gel effect and reduces its magnitude. Moreover, the presence of CTAs in a system may modify the final conversion of the polymer produced (Abuin and Lissi, 1979; Madruga et al., 1990; Wang and Ruckenstein, 1993). Consequently, the MWD is shifted to a lower M_w (Madruga and San Roman, 1984).

An extensive review of previous work on batch polymerisation processes and strategies to narrow the MWD was carried out by Louie and Soong (1985 (a)). They distinguish between two categories of partial optimizations: minimizing the batch time which leaves the M_w uncontrolled, and narrowing the MWD which minimizes the polydispersity index, PD, but leaves the M_w and the batch time uncontrolled. Optimum strategies are then analyzed, by means of a mathematical model which accounts for gel and glass effects. Among them, reactor temperature, initiator, monomer and solvent addition and a combination of these are examined. Solvent addition is indicated as the most promising policy and is experimentally analyzed in a second paper (Louie and Soong, 1985 (b)) showing that sensible improvements can be achieved.

In some cases analysis of MWD showed that the MWD of the PMMA formed by the reaction is bimodal (Bogunjoko and Brooks, 1983 (a)) and is influenced by the presence of PMMA which is dissolved in the monomer prior to polymerisation. The predicted changes would occur in the MWD of the new polymer when the solution viscosity increased.

In batch isothermal runs the polydispersity (PD) increases with conversion and the final MWD becomes broad up to cases in which bimodality may be observed. Changing the operating temperature during the batch according to an operating temperature profile makes it possible to obtain a narrow unimodal MWD. Optimum temperature profiles have been extensively used to control the MWD and produce a polymer having the desired chain length and polydispersity so as to meet the product specifications while minimizing batch times (Driscoll and Ponnuswamy, 1990; Chang

and Lai, 1992; Crowley and Choi, 1997; Chang and Laio, 1999). Scali et al. (1995) presented a method to determine an optimal temperature profile which leads to products with controlled MWD (by maintaining the PD as close as possible to its minimum value and desired values of Mw. Based on a kinetic model, the optimal temperature profile is determined so as to maintain the value of the instantaneous chain length constant. The experimental results suggest that it is possible to decouple the problem: acting on the operating temperature to control the MWD, and acting on the initial temperature and initiator concentration to influence the Mw. According to the optimal temperature profile suggested, the required temperature is almost constant at the initial stage of the reaction. Then the temperature shows an increase with conversion that becomes larger when the conversion and consequently the viscosity increase owing to gel effect, which slows the termination rate compared with the propagation rate. In the final part of the reaction, owing to the diminution of initiator and monomer concentration, the polymerisation rate is strongly reduced and a decrease in temperature is required. The optimal profile requires a temperature increase before the onset of the gel effect in order to counteract the effect of the increase of viscosity, which leads to a broad MWD for the product. The positive effect of an increase of temperature, even if different from the optimal one, is confirmed by experimental results. Maschio and Scali (1992) and Maschio et al. (1994) investigated operation strategies for the control of the MWD of polymer products. In isothermal conditions, the onset of the gel effect causes a strong increase of the Mw and the polydispersity. Therefore, for the suspension polymerisation, they suggest a batch operation under isothermal followed by adiabatic conditions. This operation approaches the optimal temperature profile and makes it possible to eliminate bimodality in the molecular weight distribution. In the final part of the reaction also the propagation rate becomes very slow and a decrease in temperature is required.

Cunningham and Mahabadi (1996) proposed the deconvolution of the MWD and the use of the constituent distributions to analyze the MWD in free radical systems and to further investigate the nature of the gel effect. The deconvolution of the MWD for the polymerisation of MMA reveals the presence of three distinct instantaneous MWDs that are produced at different times during the polymerisation. A single distribution characterizes the low conversion zone, while two distributions are shown to exist or

are formed after the onset of the gel effect, the intermediate-conversion MWD and the high-conversion MWD. These observations are not consistent with the existence of one type of radical. It was also observed that all subsequent broad pseudoinstantaneous MWDs were a combination of the intermediate and high conversion instantaneous MWD.

Maschio et al. (1999) suggested the deconvolution technique to analyze the effect of diffusive phenomena on the MWD of the polymer and also to determine the influence of some kinetic parameters on the conversion and the molecular weight. It was observed that the cumulative MWD curve at low conversion, before the onset of the gel effect, can be described by a single distribution curve. At higher conversions, two distributions, centered at different peak values, must be used to describe the cumulative distribution. These can be considered indicative of the two extreme situations of chemical and diffusive control. When the value of the gel effect onset concentration is reached, the contribution of the first peak decreases with conversion, while at the same time the contribution of the second peak increases with conversion.

2.7. Benzoyl peroxide – amine interactions

Acrylic resins commonly used in dentistry are cured by a free-radical initiated polymerisation. The thermal decomposition of benzoyl peroxide (BPO) which is used as initiator or catalyst, yields these radicals for the heat cure of denture base materials. Amines are used as curing accelerators or promoters for the polymerisation of methyl methacrylate or styrene. Three basic promoter systems are generally used, metallic salt plus methyl- ethyl- ketone peroxide catalyst; amine promoter plus benzoyl peroxide catalyst; and double promoted system such as amine promoter and metallic salt plus methyl- ethyl- ketone peroxide (Werts, 1971). Berndtsson (1954) and Maltha (1956) found that tertiary amines also react with benzoyl peroxide to accelerate radical-initiated processes. Tertiary aromatic amines have been used for a number of years together with benzoyl peroxide (BPO) as an effective initiation system in the free-radical polymerisation of acrylic resins and especially of methyl methacrylate. (Moad and Solomon, 1995). The resultant polymers have been widely used as biomaterials in dentistry and in orthopedic surgery as bone cements. The role of the amine is to carry out the reaction in a short period of time at body temperature.

Amine accelerators facilitate the formation of radicals from benzoyl peroxide. The kinetics of the reaction of benzoyl peroxide with dimethylaniline, triethylamine, or aniline in solutions or emulsions of benzene were studied by Margaritova and Rusakona in 1969. The order of the reaction relative to each component was always 1; this was irrespective of whether it took place in solution or in an emulsion. The activation energies of these reactions were calculated, and the conditions were found not to affect them (in solution or emulsions). Ades and Fontanille (1978) studied the kinetics of the radical polymerisation of phenyl glyceric ether methacrylate, taken as model of the corresponding derivative of bisphenol A, initiated by the system benzoyl peroxide/dimethyl p-toluidine p-toluene sulfinic acid salt.

Brauer (1981) studied amino-containing redox systems which are very effective accelerators for composites, yielding restoratives with excellent mechanical properties and minimum discoloration. Other redox systems such as BP-sulfinic acids, peroxide-thiourea, hydro-peroxide-ascorbic acid or trialkylborane-oxygen also yield rapid polymerisation of acrylic resins.

Pittman and Jada (1982) investigated the effect of polymer-bound amines accelerators on the radical-initiated curing of unsaturated polyesters with styrene. They compared the polymer-bound tertiary amine accelerators to their freely added monomeric analogues as catalysts for the curing of poly(diethylene glycol maleate) prepolymers with styrene. Benzoyl peroxide was used as the initiator. The polymer-anchored accelerators gave shorter curing times and lower energies of initiation than their monomeric analogues. Each of the polymer-bound accelerators tested was found to be significantly more efficient than its free analogue. When the accelerators were attached to the polymer being cured, the curing rate increased. Polymer bound accelerators exerted a promoted effect. A probable mechanism sequence is shown in figure 2.7.1 (Pittman and Jada, 1982). An initial amine complex with benzoyl peroxide is formed with free amines. The polymer-anchored analogue of this complex is represented by 6 in figure 2.7.1. Higher electron density at nitrogen favours the formation of salt 6. The accelerating effect of amines on curing derives from the decomposition of 6 to 7 and 8. Both 7 and 8 may initiate styrene polymerisation, or form new radical sites along the prepolymer chain, either by addition to the double bonds remaining from maleic anhydride moieties or by hydrogen abstraction a to ether

oxygens. Also, radical cation 8 may directly initiate a polymerising styrene chain giving a quaternary ammonium salt site at the N. The fastest initiation was achieved by dimethylaniline.

Yefremova et al. (1985) studied the reactions of benzoyl and lauryl peroxides with various tertiary aromatic amines. The presence of 2 stages in the reaction of benzoyl peroxide with tetramethylphenylene diamine, differing in reaction rate, was demonstrated. It has been shown that the radical-initiated polymerisation of styrene is due both to decomposition of a primary peroxide-amine complex and to a further transformation of the decomposition products.

Vazquez et al., (1998) presented a review on the accelerating effect of tertiary aromatic amines used as activator in the benzoyl peroxide/amine system for the curing of acrylic resins. The kinetics, mechanism and activation energy of the reaction are considered, together with some toxicity, residuals and leaching data concerned with biomedical applications of this system, e.g. denture resins or acrylic bone cements. Furthermore, some results relating the effect of the temperature of the surroundings on the curing parameters of the cements prepared with three amines (N,N-dimethyl-4-toluidine, N,N-dimethylbenzyl alcohol and N,N-dimethylbenzyl methacrylate) are shown. The results indicate that the temperature has a significant effect on the curing parameters, and must be considered in the evaluation of new activators. The relevance of these results lies with the importance of thermal trauma generally associated with the implantation of acrylic bone cements.

Oldfield and Yasuda (1999) studied the polymerisation of MMA with a peroxide/amine system for bone cement formation. Methyl methacrylate was polymerized using a N,N-dimethyl-p-toluidine (TD)/benzoyl peroxide (BPO) redox system in the presence of polymethyl methacrylate (PMMA) powder. While the optimum free radical concentration was observed near the equimolar amine/BPO concentration, excess amine led to a change in the chemical structure of the trapped radical and inhibited the polymerisation process. At a high amine/BPO ratio a nitroxide-based radical appeared. The appearance of this nitroxide radical seems to depend on the amine/BPO molar ratio and on the presence of PMMA.

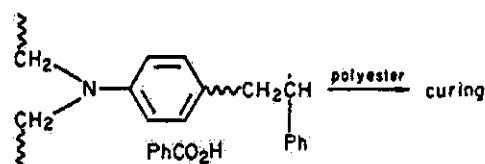
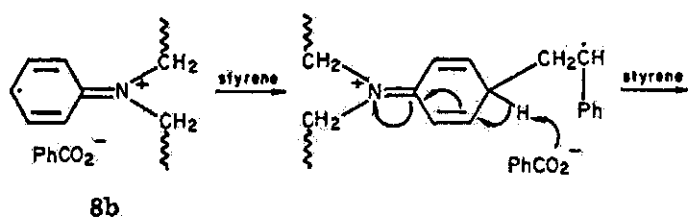
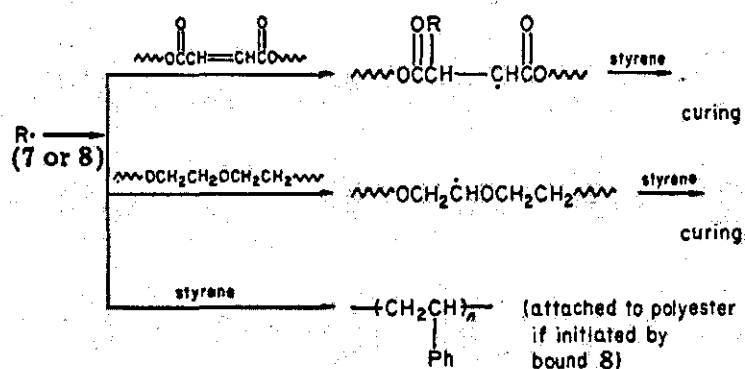
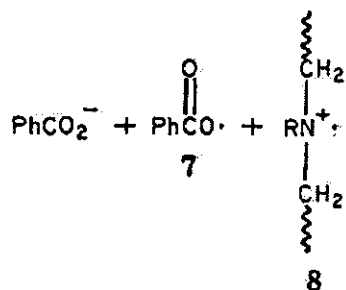
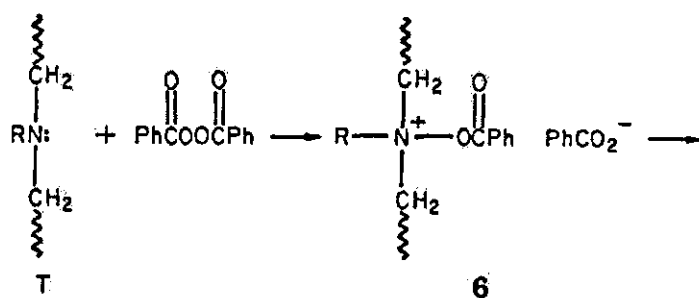


Figure 2.7.1. Possible mechanism for the reaction between amines and benzoyl peroxide (Pittman and Jada, 1982)

An excess amount of amine with respect to BPO was found to inhibit the polymerisation process. When BPO was removed, the system still polymerized but with a longer gelation time and a lower radical concentration. These results demonstrate that trapped free radicals in the bulk polymerisation of MMA convert to polymeric peroxides that act as initiators in bone cement. When the accelerator 4-dimethylamino phenethyl alcohol (TDOH) was used, a higher radical concentration was observed in the polymerizing system. TDOH shows potential for being a more effective accelerator than TD for bone cement curing.

Achilias and Sideridou (2002) studied the kinetics of the free radical bulk polymerisation of methyl methacrylate (MMA) using the benzoyl peroxide (BPO)/amine initiation system. N,N dimethyl-4-aminophenethyl alcohol (DMPOH) which is a newly synthesized amine used in the preparation of acrylic dental resins and bone cements was examined, and the results compared to the most commonly used amine in these applications, the N,N dimethyl-p-toluidine (DMT). For both amines, the effect of the molar ratio of BPO/amine and of the reaction temperature, on the polymerisation kinetics was investigated. The prepared polymers were characterized by determination of the average molecular weights and molecular weights using Gel Permeation Chromatography. DMPOH was found to lead in slightly higher polymerisation rates, lower gel times and lower average molecular weights than DMT. The values of these parameters for both amines were influenced by the molar ratio of BPO to amine, when the product of the concentrations of these was kept constant. The highest polymerisation rate occurred in the lowest gel time, resulting in polymers with the lowest molecular weight, and was observed when a molar ratio of about 1.5 BPO/amine was used. However, the final monomer conversion was found to be independent of the molar ratio and amine used. The overall activation energy of polymerisation was found to be 51.8 kJ/mol K for BPO/DMPOH and 47.1 kJ/mol K for BPO/DMT.

SECTION 2. EXPERIMENTAL AND STATISTICAL PROCEDURES

CHAPTER 3. EXPERIMENTAL PROCEDURES

3.1. Materials

Methyl Methacrylate (MMA) (analytical grade, Aldrich) was distilled at reduced pressure to remove the polymerisation inhibitor. Aqueous solutions of Sodium polymethacrylate (PMA-Na) or Ammonium polymethacrylate (APMA) in distilled water were used as the continuous phase. Sodium polymethacrylate was produced by neutralising the 3% Polymethacrylic acid (PMA) gel in water, which was provided by Lucite International, with NaOH (97+%, analytical grade, Aldrich). APMA was provided by Lucite International as an aqueous solution of 14% APMA in water, and was used as received. Benzoyl peroxide (BPO) (75%, Aldrich), hydroquinone (HQ) (99%, Aldrich) and n-dodecyl mercaptan (n-DDM) (98+%, Aldrich) were used as received, without any further purification.

Additional chemicals including NH_3 , acetone, and methanol were analytical grade purchased from Aldrich and were used as received.

3.2. Polymerisation Reactor

Set up: For the suspension polymerisation experiments a glass reactor with capacity 0.5-litre and 10 cm diameter was used, as shown in figure 3.2.1. The reactor had a flanged top and a dish base. A double flat 4-bladed impeller with diameter 4 cm was used in order to ensure the complete dispersion of the monomer in the highly viscous continuous phase. Four equidistant baffles were used of width 1 cm. The suspension polymerisation experiments were run with a nitrogen atmosphere in the reactor. The reactor vessel was placed in a water bath in order to control the temperature within $\pm 1^\circ\text{C}$ from the desired reaction temperature. The temperature of the reaction mixture was monitored using a thermocouple. An overhead reflux condenser was used and samples were drawn from the reactor at frequent time intervals by using a pipette. The

pH of the reaction mixture was also monitored by using a pH meter. The impeller speed was adjusted at the desired level at the start of each experiment.

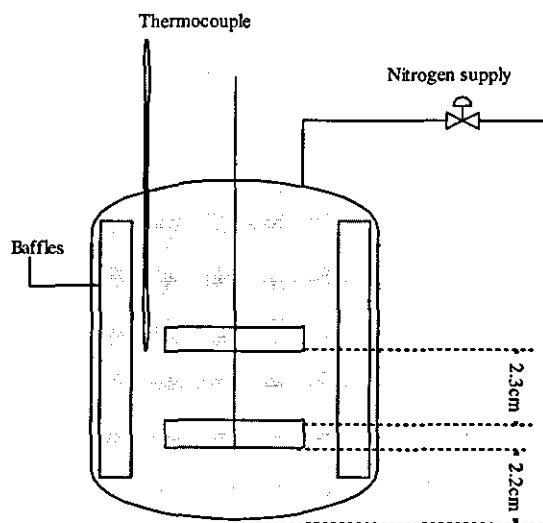


Figure 3.2.1. Experimental set up

Suspension polymerisation experiments: The required quantity of PMA-Na or APMA gel was dissolved in pre-weighed amount of deionised water. The aqueous phase (deionised water and stabiliser) was purged with nitrogen for 60 minutes before the addition of the organic phase (monomer and initiator). The continuous phase was heated and stirred and the pH was adjusted at the desired value, by the addition of NaOH for PMA-Na continuous phase or NH_3 for APMA continuous phase. The initiator and the dispersed phase were weighed. The initiator was dissolved in the dispersed phase just prior to the addition in the reaction vessel. The total volume of the reaction mixture was always kept constant at 500 cm^3 .

3.3. Analytical Procedures

The viscosity of the dispersed phase was measured by using a U-tube viscometer, which was calibrated with standard liquids such as olive oil and glycerol. The interfacial tension was measured with the Du Nouy ring technique, using a White surface tensionmeter manufactured by White Electrical Instruments Co. Ltd. (Malvern Link, Worcestershire, UK). The pH was measured by using a Mettler Toledo pH meter (Greifensee, Switzerland). The particle diameters after polymerisation were

measured by using a Leica optical microscope (Leica Microscope Systems, Nusloch, Germany). At the end of polymerisation, the beads were photographed by a JVC camera (Victor Co. Ltd., Japan) attached to the microscope. The diameters of 500 polymer beads were measured per run and the average diameter of the 5 biggest beads was considered to be the maximum diameter for each run. The molecular weight averages and distributions were measured by Gel Permeation Chromatography at Lucite premises.

3.3.1. Determination of conversion

The monomer conversion was measured gravimetrically. Small quantities of the reaction mixture were withdrawn from the reactor and transferred into small aluminium weigh 'boats' for weighing. Methanol containing inhibitor was added to quench the reaction and precipitate the polymer. The samples were kept in a vacuum oven at 60°C for more than 16 hours. Monomer, water and methanol evaporated in the vacuum oven. The samples were considered dry when their weight was constant and did not change with further heating in the vacuum oven. The solid residue left, was weighed again and the monomer conversion was calculated by the expression:

$$\text{conversion} = \frac{\frac{\text{weight.residue}}{\text{aliquot.weight}} - \text{solid.fraction}}{\text{monomer.fraction}}$$

The additives account for the initiator, the stabiliser, NaOH used to control the pH, the chain transfer agent and any other solid additive used. The monomer accounts for the quantity of monomer in the liquid sample, and was calculated as follows:
monomer = monomer fraction x liquid sample.

3.3.2. Determination of viscosity

The viscosity of the continuous phase was measured by using a Haake viscometer, manufactured by Thermo Haake (Karlsruhe, Germany). The continuous phase is non-Newtonian, and its viscosity is shear dependent and more specifically shear thinning. Therefore, viscosity depends on the stirring speed in the reactor, and it will change for

different stirring speeds. Hence, an appropriate method has to be used in order to relate the stirring speed in the reactor for the various experiments with the corresponding apparent viscosity of the continuous phase. Solutions of various stabiliser concentrations were prepared, and their viscosity and shear stress over a range of shear rates from 0 to 648 s⁻¹ was measured, at the reaction temperature. The series of data points obtained by these measurements were then fitted, to various models. The best fit was given by the power law model described by the expressions:

$$\tau = K\gamma^n \quad \text{or} \quad \mu = K\gamma^{n-1}$$

with the values of the correlation coefficient R^2 ranging from 0.960 to 0.999 for the various solutions. The correlation coefficient R^2 is computed as the ratio of the regression sum of squares (SSR) to the total sum of squares (SST), by the following expression

$$R^2 = \frac{SSR}{SST} = \frac{\sum_{i=1}^{n_T} (\hat{y}_i - \bar{y})^2}{\sum_{i=1}^{n_T} (y_i - \bar{y})^2}$$

where, \hat{y}_i is the predicted value for y_i , \bar{y} is the average of the y data points and n_T is the total number of data points. R^2 is a measurement of how well the experimental data points are described by the model. R^2 is a number between 0 and 1.

A typical example of the data obtained by these measurements and the fit to a power law model is shown in figure 3.3.1, where the solid line represents the power law model. The data points represent the viscosity and shear stress values for increasing stirrer speed and therefore for increasing shear rate.

The power law model provides values for the viscosity index n and for the constant K . Since, K and n are provided by the power law model, the apparent viscosity of the continuous phase for any impeller speed can be calculated by using the Metzner-Otto theory, as will be described in chapter 5.4.2

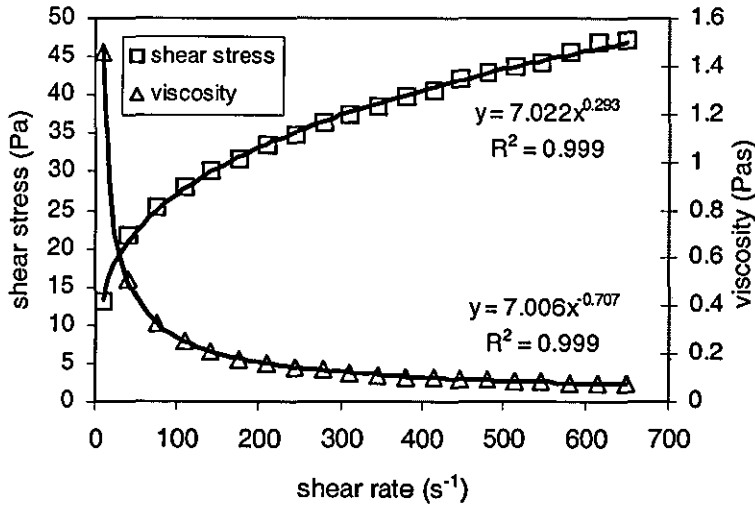


Figure 3.3.1. Typical example of viscosity and shear stress data obtained by using the Haake rheometer, and the fit to the power law model (solid line).

3.3.3. Drop size distributions

The drop and particle size distributions, before and during the polymerisation, were measured by using the laser diffraction technique, which is based on the measurement and interpretation of the angular distribution of light diffracted by the drops and uses the Fraunhofer theory. A laser particle sizer (Coulter LS130) with 85 channels, was used. These channels change logarithmically and cover the size range of 0.43-822 μm . An aqueous solution of the stabiliser was used in the sampling cell to prevent particles from coalescing.

The output of the particle sizer is given as volume of drops in each bin size. This can be transformed to a volume frequency distribution (f_v),

$$f_v(d_i) = \frac{V_i}{\sum V_i}$$

where V_i is the volume of drops with diameter between d_i and $d_i + \Delta \ln(d_i)$

and the % volume for each size range is given by $\% \text{volume} = 100 * V_i / \sum V_i$. The aim of this transformation is to normalise the data, on a logarithmic scale, so that data from different experimental runs can be plotted together and compared.

A typical output obtained from the laser diffraction particle sizer, as well as the %volume transformed data, are given in table 3.3.1.

Table 3.3.1. Typical output of the laser particle sizer and the calculated %volume

d_i (μm)	volume (μm^3)	% volume
0.4292	50.423	0.0578
0.4701	63.666	0.0730
0.5149	90.588	0.1038
0.564	118.27	0.1356
0.6178	144.39	0.1655
0.6766	169.81	0.1946
0.7411	193.05	0.2213
0.8118	214.55	0.2459
0.8892	232.46	0.2665
0.974	244.52	0.2803
1.066	247.93	0.2842
1.168	245.62	0.2815
1.279	239.14	0.2741
1.401	229.42	0.2630
1.535	216.76	0.2485
1.681	202.14	0.2317
1.842	186.41	0.2137
2.017	170.42	0.1953
....
48.85	1557	1.7847
53.5	2283.8	2.6178
58.6	3146.5	3.6067
64.19	4130.7	4.7348
70.31	5216.9	5.9799
77.01	6325.7	7.2509
84.36	7283.6	8.3489
92.4	7856.8	9.0059
101.2	7845.8	8.9933
110.8	7189.1	8.2405
121.4	6015.2	6.8950
133	4599.3	5.2720
145.6	3247	3.7219
159.5	2180.1	2.4990
174.7	1482.9	1.6998
191.4	916.3	1.0503
209.6	506.26	0.5803
229.6	221.18	0.2535
251.5	54.28	0.0622
275.5	14.76	0.0169
301.8	5.16	0.0059
330.5	1.23	0.0014

A typical drop size distribution obtained from the transformed data shown in the previous table article sizer is depicted in figure 3.3.2.

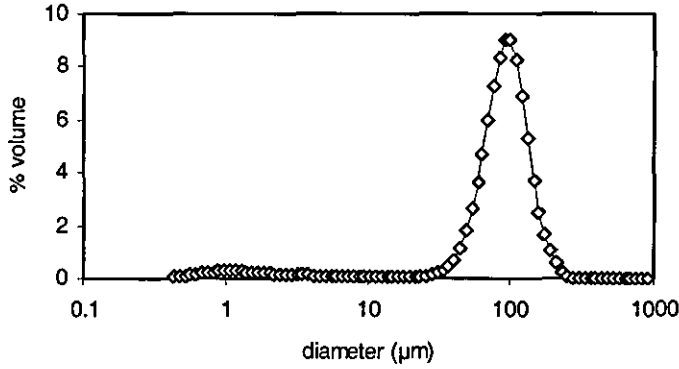


Figure 3.3.2. Typical particle size distribution

3.3.4. Calculation of interfacial area

The interfacial area between the continuous and dispersed phases was calculated from the drop size distribution. The number of the drops per size fraction and the interfacial area are calculated from the type of data shown in table 3.1, as follows:

- The volume, V_{di} , and the surface area, S_i , of one single drop corresponding to each size fraction, is calculated by using the drop diameter, d_i , as follows:

$$V_{di} = \frac{4}{3} \pi (d_i/2)^3$$

$$S_{di} = 4 \pi (d_i/2)^2$$

- The number of drops, N_i , having a certain diameter, d_i , is calculated by dividing the volume of the size fraction over the volume of a single drop $N_i = V_i/V_{di}$
- The interfacial area, S_i , of these size fractions of drops having a certain diameter d_i is then calculated by multiplying the surface area of a single drop times the number of drops $S_i = N_i S_{di}$

A typical example of these data is given in table 3.3.2.

Table 3.3.2. Interfacial area for each size fraction

d_i (μm)	V_{di} (μm^3)	S_{di} (μm^2)	V_i (μm^3)	N_i	S_i (μm^2)
...
1.066	0.6339	3.5682	247.93	391.092	1395.478
1.168	0.8339	4.2837	245.62	294.548	1261.747
1.279	1.0949	5.1365	239.14	218.405	1121.845
1.401	1.4391	6.1632	229.42	159.418	982.527
1.535	1.8928	7.3985	216.76	114.518	847.270
1.681	2.4859	8.8729	202.14	81.315	721.499
1.842	3.2707	10.6539	186.41	56.993	607.199
2.017	4.2943	12.7744	170.42	39.685	506.951
2.21	5.6488	15.3361	155.23	27.480	421.439
2.42	7.4169	18.3891	141.37	19.060	350.504
2.651	9.7501	22.0673	129.78	13.311	293.731
2.904	12.8165	26.4803	120.32	9.388	248.595
...

3.3.5. Calculation of the critical conversion (x_{crit})

In suspension polymerisation the monomer to polymer conversion was calculated from the well-known rate expression (Neil et al., 1996)

$$\left(\frac{dx}{dt}\right) = \left(\frac{2fk_d I}{k_t}\right)^{1/2} k_p (1-x) \quad (3.3.1)$$

At low monomer conversion, chain termination is unaffected by diffusion control and the value of the termination constant, k_t , is that expected in the absence of the gel effect (i.e. $k_t = k_{t0}$). Also, the half-life of benzoyl peroxide is more than 10 h at the reaction temperature. Therefore, at short times, the initiator concentration, I , remains at its initial value (I_0). Thus,

$$x = 1 - e^{-\theta} \quad (3.3.2)$$

$$\text{where } \theta = \left(\frac{2fk_d I_0}{k_{t0}}\right)^{1/2} k_p t, \text{ is dimensionless time}$$

Samples were drawn from the reactor and monomer conversion was measured gravimetrically, as described in section 3.3.1. Figure 3.3.3, shows that the

experimental conversion was identical to the predicted conversion at low times. As the conversion increases, and diffusion control causes the k_t to diminish, the experimental conversion-time data, start to deviate from the predicted ones by the expression 3.3.1. The critical conversion, that heralds the onset of the gel effect, is defined as the conversion at which the experimental data deviate 5% from the theoretically predicted (from equation 3.3.1) values of conversion.

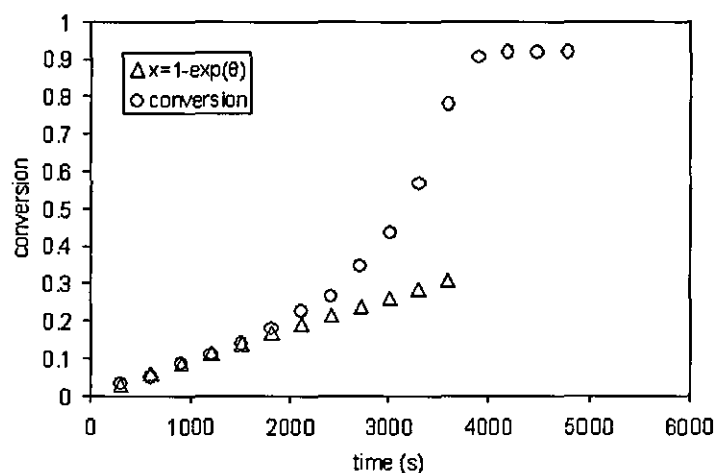


Figure 3.3.3. Experimental conversion data in comparison with theoretically predicted conversion values versus time

Therefore, all the values for the critical conversion in this work, were calculated as the 5% deviation from classical kinetics predictions.

The values of the reaction constants used for the x_{crit} calculations for the suspension polymerisation of MMA, are

- $k_d [s^{-1}] = 1.25 \times 10^{18} \exp(-35473/RT)$ (Ahn et al., 1996)
- $k_p [l \text{mol}^{-1} s^{-1}] = 2.94 \times 10^6 \exp(-5656/RT)$ (Ahn et al., 1996)
- $k_{to} [l \text{mol}^{-1} s^{-1}] = 5.20 \times 10^8 \exp(-1394/RT)$ (Ahn et al., 1996)
- $f = 0.7$ (Clarke-Pringle and MacGregor, 1998)

where R is the universal gas constant and T is the temperature.

3.3.6. Molecular weight averages and distributions

The molecular weight measurements were carried out at Lucite's premises, by using Gel Permeation Chromatography (GPC). The instrument had a refractive index detector and a 2xPLgel mix B, 10 micron, column. The conditions for running the GPC were, ambient temperature and 1ml/min flow. The solvent used was Tetra hydro furan (THF). Toluene was used as internal standard and PMMA was used for the calibration.

CHAPTER 4. STATISTICAL METHODS AND TESTS

One of the aims of this work is to investigate the factors that affect the onset of gel effect, which is described by the critical conversion, x_{crit} , in suspension polymerisation of MMA. A statistical assessment was used to estimate the effect of various factors on the critical conversion.

The difficulty in estimating the critical conversion, x_{crit} derives from the difficulty in achieving isothermal experiments. There is usually, at least a small fluctuation in temperature, at the onset and during the gel effect, which affects the x_{crit} . These temperature fluctuations introduce an error which may lead to a large variance of the values of x_{crit} for replicates of the same experiment. The narrow range of values within which x_{crit} varies, in combination with the difficulty in achieving completely isothermal experiments, has often led to an overestimation of x_{crit} . In order to eliminate the error introduced by these experimental uncertainties, a large number of suspension polymerisation experiments were run and a statistical approach was used (chapter 6), to clarify the underlying factors that affect the onset of the gel effect.

4.1. Basic statistical concepts

The objective of statistical inference is to draw conclusions about a population using a sample from that population. This sample consists of a number of observations or experiments. The probability structure of the variables that describe these observations or experiments is described by its probability distribution. A statistic of a variable is defined as any function of the observations in the sample that does not contain unknown parameters. The most commonly used statistics are, the mean, the variance, and the standard deviation of the probability distribution. The mean of a probability distribution is a measure of its central tendency or location. The variance is a measure of the spread or dispersion of the probability distribution. The standard deviation is the square root of the variance and is also used as a measure of dispersion of a variable (Montgomery, 1991).

If y_1, y_2, \dots, y_n represent a sample, these statistics are defined as follows:

- sample mean : $\bar{y} = \frac{\sum_{i=1}^n y_i}{n_T}$
- sample variance : $s^2 = \frac{\sum_{i=1}^n (y_i - \bar{y})^2}{n_T - 1}$, where the numerator is called the sum of squares, SS, and the denominator is called the number of degrees of freedom of the sum of squares
- sample standard deviation: $s = \sqrt{s^2}$

The sample mean \bar{y} , is a point estimator of the population mean m , and the sample variance is a point estimator of the population variance s^2 . A particular value of an estimator, computed from sample data, is called an estimate.

4.2. Probability-Probability plots

This test plots a variable's cumulative proportions against the cumulative proportions from any of a number of test distributions (beta, chi-square, exponential, gamma, half-normal, Laplace, Logistic, Lognormal, Normal, Pareto, Student's t, Weibull, and uniform). Probability plots are generally used to determine whether the distribution of a variable matches a given distribution. If the selected variable matches the test distribution, the experimental points cluster around a straight line. The more the experimental data deviate from the straight line the more, their distribution deviated from the test distribution (Montgomery, 1991). A typical example of a probability-probability plot (P-P plot) is shown in the figure 4.2.1.

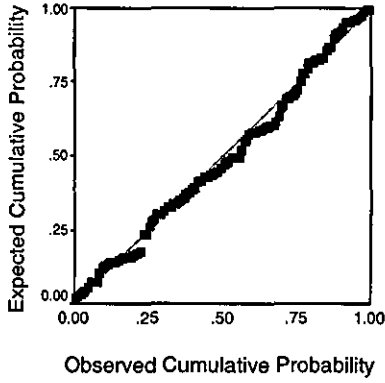


Figure 4.2.1. Typical P-P plot

4.3. Pearson's correlation

Pearson's correlation (r) reflects the degree of linear relationship between two variables. It ranges from +1 to -1. A correlation of +1 means that there is a perfect positive linear relationship between variables (Mason, 2003).

The formula for Pearson's correlation takes on many forms. A commonly used formula is shown below:

$$r = \frac{\sum_{i=1}^{\lambda} (X_i - \bar{X})(Y_i - \bar{Y})}{(\lambda - 1)S_x S_y} \quad (4.3.1)$$

where r = Pearson's correlation,

X_i and Y_i = the experimental values for x, y variables

\bar{X}, \bar{Y} = mean values of X, Y variables

S_x, S_y = standard deviations for x, y variables respectively

λ = the number of experiments

4.4. Levene's test of homogeneity of variance

Levene's test (Dean and Voss, 1999) is used to test if n samples have equal variances. Equal variances across samples is called homogeneity of variance. Some statistical tests, for example the analysis of variance, assume that variances are equal across groups or samples. The Levene test can be used to verify that assumption. A typical example of an output of Levene's test is described in table 4.4.1. The output includes the Levene's statistic, L , the degrees of freedom $df1$ and $df2$, defined in the table, and the p -value which reflects the significance level for the result given by L .

Table 4.4.1. Example of Levene's test

Levene statistic	df1	df2	Significance
L	$u-1$	$u(\lambda-1)$	p -value

Where

$$L = \frac{(\lambda - u) \sum_{i=1}^u \lambda_i (\bar{z}_i - \bar{z})^2}{(u-1) \sum_{i=1}^u \sum_{j=1}^{\lambda_i} (z_{ij} - \bar{z}_i)^2} \quad (4.4.1)$$

u = the number of treatments or levels or groups,

λ = the number of experiments or replicates per group

$$z_{ij} = |y_{ij} - \bar{y}_i|$$

\bar{z}_i = the group means of the z_{ij}

\bar{z} = the overall mean of the z_{ij}

\bar{y}_i = the mean of the i_{th} subgroup

When the p -value (sig) is higher than 0.05 then the sample variances are equal, homogeneity of variance can be considered. If the p -value is lower than 0.05 then the variances are not equal and the hypothesis of equality is rejected.

4.5. One-Way Analysis of Variance (ANOVA)

The one-way ANOVA is a method of analysis that requires multiple experiments. The one-way ANOVA provides a comparison of the means of a number of replications of experiments performed where a single input factor is varied at different settings or levels (Cobb, 1998). The object of this comparison is to determine the proportion of the variability of the data that is due to the different "treatment" levels or "factors" as opposed to variability due to random error. In other words, ANOVA is a useful tool which helps to identify sources of variability from one or more potential sources. By varying the factors in a predetermined pattern and analysing the output, one can use statistical techniques to make an accurate assessment as to the cause of variation in a process.

The model deals with specific treatment levels and is involved with testing the null hypothesis that the level means are equal,

$$H_0: m_1 = m_2 = \dots = m_i$$

where m_i represents the level mean.

Analysis of variance tests the null hypothesis that all the population means are equal, by comparing two estimates of variance (s^2 where s^2 is the variance within each of the "a" treatment populations), as shown in table 4.5.1. One estimate (called the Mean Square Error or "MSE" for short) is based on the variances within the samples. The MSE is an estimate of s^2 whether or not the null hypothesis is true. The second estimate (Mean Square Between or "MSB" for short) is based on the variance of the sample means. The MSB is only an estimate of s^2 if the null hypothesis is true. If the null hypothesis is false then MSB estimates something larger than s^2 . The logic by which analysis of variance tests the null hypothesis is as follows: If the null hypothesis is true, then MSE and MSB should be about the same since they are both estimates of the same quantity (s^2); however, if the null hypothesis is false then MSB can be expected to be larger than MSE since MSB is estimating a quantity larger than s^2 .

Table 4.5.1. A typical example of an output for ANOVA

Source of variance	Sum of squares (SS)	Degrees of freedom (df)	Mean square (= SS / df)	F	Sig.
Between treatments	SS_B	$u - 1$	$MSB = \frac{SS_B}{(u-1)}$	$\frac{MSB}{MSE} = \frac{SSB/(u-1)}{SSW/u(\lambda-1)}$	p-value
Within treatments (Residual)	SS_W	$u(\lambda - 1)$	$MSE = \frac{SS_W}{u(\lambda-1)}$		
Total	SS_T	$(u \lambda) - 1$			

Where

u = the number of treatments or levels or groups,

λ = the number of experiments or replicates,

SS =sum of squares

SS_B =sum of squares between treatments or groups

SS_W = sum of squares within treatments or groups

df =degrees of freedom

F = F statistic

The significance test involves the statistic F which is the ratio of MSB to MSE: $F = MSB/MSE$. If the null hypothesis is true, then the F ratio should be approximately one since MSB and MSE should be about the same. If the ratio is much larger than one, then it is likely that MSB is estimating a larger quantity than is MSE and that the null hypothesis is false. In order to conduct a significance test, it is necessary to know the sampling distribution of F given that the null hypothesis is true. From the sampling distribution, the probability of obtaining an F as large or larger than the one calculated from the data can be determined. This probability is the probability value. If it is lower than the significance level, then the null hypothesis can be rejected.

Basically, rejection of the null hypothesis indicates that variation in the output is due to variation between the treatment levels and not due to random error. If the null hypothesis is rejected, there is a difference in the output of the different levels at a significance 'a' and it remains to be determined between which treatment levels the actual differences lie.

In addition to determining that differences exist among the means, it may also be required to determine which means differ. There are two types of tests for comparing means: a priori contrasts and post hoc tests. Contrasts are tests set up before running the experiment, and post hoc tests are run after the experiment has been conducted.

4.6. Post Hoc tests

Once it has been determined that differences exist among the means with ANOVA, post hoc range tests and pairwise multiple comparisons can determine which means differ. The post hoc tests examine all possible combinations to identify significant differences among groups. Range tests identify homogeneous subsets of means that are not different from each other. Pairwise multiple comparisons test the difference between each pair of means, and yield a matrix where asterisks indicate significantly different group means at an alpha level of 0.05.

Tukey's significant difference test, Hochberg's GT2, Gabriel's test, and Scheffé's test are multiple comparison tests and range tests. The Scheffe' test is customarily used with unequal sample sizes, although it could be used with equal sample sizes.

4.7. T-test

A t-test is a statistical tool used to determine whether a significant difference exists between the means of two distributions or the mean of one distribution and a target value. The t test employs the statistic (t), with $n_T - 1$ degrees of freedom, (n_T =number of replications or experiments) to test a given statistical hypothesis about a population parameter (Dean and Voss, 1999). It is usually used with small sample sizes (<30). It is used when population standard deviation is unknown. It tests the null hypothesis that two sample means are equal. It involves the test statistic,

$$T = \frac{\bar{y}_A - \bar{y}_B}{\sqrt{s_A^2 / N_A + s_B^2 / N_B}}, \quad (4.7.1)$$

where

\bar{y} = mean

s^2 = variance

N = number of experiments per sample

A, B = samples A and B

If the p-value for the T-statistic is smaller than 0.05 then the null hypothesis that the group means are equal is rejected. If the p-value is higher than 0.05, then the null hypothesis is rejected, and the mean values are considered equal.

4.8. K-means clustering

K-means clustering can best be described as a partitioning method. That is, the function K-means partitions the observations in a set of data into k mutually exclusive clusters, and returns a vector of indices indicating to which of the k clusters it has assigned each observation. Unlike the hierarchical clustering methods used in linkage, k-means does not create a tree structure to describe the groupings in the data, but rather creates a single level of clusters. Another difference is that K-means clustering uses the actual observations of objects or individuals in the data, and not just their proximities. These differences often mean that K-means is more suitable for clustering large amounts of data.

K-means treats each observation in the data as an object having a location in space. It finds a partition in which objects within each cluster are as close to each other as possible, and as far from objects in other clusters as possible. Each cluster in the partition is defined by its member objects and by its centroid, or centre. The centroid for each cluster is the point to which the sum of distances from all objects in that cluster is minimized. K-means uses an iterative algorithm that minimizes the sum of distances from each object to its cluster centroid, over all clusters (Morgan et al. 2004). This algorithm moves objects between clusters until the sum cannot be decreased further. The result is a set of clusters that are as compact and well-separated as possible.

SECTION 3. RESULTS AND DISCUSSION

CHAPTER 5. BEHAVIOUR OF PMA-Na AND APMA AS SUSPENDING AGENTS

5.1. Rheology

Polymer solutions may often exhibit a rheological behaviour that is shear dependent, or time dependent. The shear dependent behaviour describes the variation of viscosity with shear rate. According to their shear dependent behaviour the polymer solutions can be classified as pseudoplastic or shear thinning and dilatant or shear thickening fluids. The first term is used, when the solution viscosity decreases with increasing shear rate, the latter term is used when the solution viscosity increases with increasing shear rate. The time dependent behaviour describes the variation of viscosity with time for a constant shear rate. It may be either thixotropic or rheopectic, which corresponds to a decrease or increase, of the solution viscosity with time, respectively.

This chapter refers to the rheological behaviour of polymethacrylic acid (PMA) and its salts, sodium polymethacrylate (PMA-Na) and ammonium polymethacrylate (APMA). The solutions are examined for time-dependent behaviour, shear dependent behaviour, and for any dependence on shearing history.

5.1.1. Polymethacrylic acid

Polymethacrylic acid (PMA) does not represent a typical polyelectrolyte due to the presence of the hydrophobic methyl side group. PMA solutions exhibit an anomalous rheological behaviour indicated by a time-dependent increase in viscosity at constant shear rate, and by a shear dependent viscosity increase or shear thickening behaviour (Ohoya et al., 2000; Katsumichi Ono and Kenkichi Murakami, 1977). The rheopectic behaviour (time – dependent viscosity increase) was reported for PMA solutions with molecular weight higher than 7×10^5 or higher, while for solutions with molecular weight 5.9×10^5 , no rheopectic behaviour was observed. The experimental work reported in the literature that investigates the shear induced viscosity increase of PMA refers to low shear rates and to angular velocities up to 200 rpm (Ohoya et al., 2000;

Katsumichi Ono and Kenkichi Murakami, 1977). Therefore, it is unknown whether the behaviour is similar for higher shear rates or if the possible explanations proposed for these conditions apply to higher shear rates.

Time dependent behaviour: Initially, the dependence of the PMA solutions on shearing time is examined for a 3% polymethacrylic acid (with molecular weight 5×10^5) aqueous solution, at 70°C . The viscosity of two samples of the same solution was measured every 2 min, for a period of 200 min, and for two different shear rates, 100 s^{-1} and 200 s^{-1} . The measurements were conducted using a HAAKE viscometer. The results are shown in figure 5.1.1. The viscosity of the solutions, for both shear rates, seem to be almost independent of the shearing time, and no rheopectic effects were observed. This is consistent with the data reported in the literature (Ohoya et al., 2000). The viscosity of the solution was higher at 200 s^{-1} , indicating a possible shear thickening behaviour.

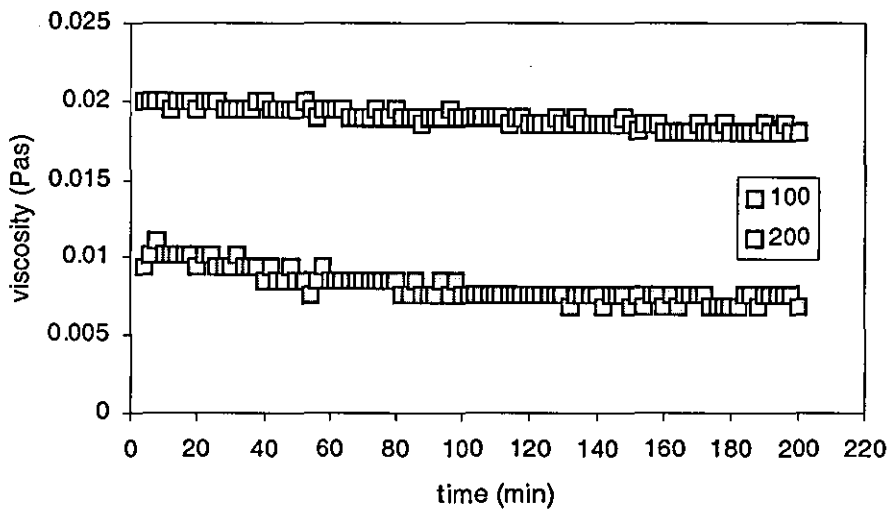


Figure 5.1.1. Effect of shearing time on a 3% aqueous PMA solution, at pH 3

Shear rate and shear history dependence: The 3% aqueous solution of PMA was then examined for shear rate dependence and dependence on the shearing history. In order to examine the solution dependence on the shear rate, the viscosity of the solution was measured for increasing shear rate, at 70°C . In order to examine the dependence on the shearing history, the solution was subjected to subsequent runs as shown in figure 5.1.2. If there is no dependence on the shearing history, the measurements for all the

subsequent runs should be identical, otherwise, the measurements for the subsequent runs will differ. The time lapse between the subsequent runs was 2 min. Since no time dependence of the viscosity was observed previously (figure 5.1.1), the time was not considered to have any effect on these measurements. From figure 5.1.2 it is observed that,

1. The viscosity depends on shear rate for all the runs. More specifically, the viscosity follows a pattern, in which it initially decreases with increasing shear rate at low shear rates up to approximately 100 s^{-1} . Then, it reaches a plateau, and subsequently it increases gradually with increasing shear rate, for higher shear rates, showing a shear thickening behaviour.
2. Comparing the subsequent runs with one another, it is observed that the viscosity decreases for each consecutive run, indicating that once the solution has been subjected to a higher shear rate its viscosity decreases for lower shear rates as well and this decrease is not reversible. It is also observed that the plateau for the first few runs is longer lasting up to a shear rate of 400 s^{-1} whereas it is decreasing for every subsequent run down to 200 s^{-1} . Therefore, the viscosity of PMA solutions depends both on shear rate and shearing history.

As an explanation for these phenomena, it has been proposed that the field of shear builds up a network through the intermolecular force but concurrently severs it as well, and the former effect predominates in these systems, for higher shear rates. It is considered ambiguous whether the increase of the viscosity reflects a transition of chain conformation in the field of flow (Sakurai et al., 1993). In general, a conformation transition of PMA has been interpreted in terms of competition between electrostatic repulsion between charges on the polymer chain and some attractive interactions such as hydrogen bond between carboxyl or carboxylate groups, van der Waals or hydrophobic interactions between methyl groups (Sakurai et al., 1993). The conformational change of the PMA chain from a compact coil to an expanded coil is governed by dissociation of the carboxyl groups and by the intermolecular and intramolecular hydrophobic and/or hydrophilic bonding abilities. Therefore, the increase of viscosity does not result from the deformation or orientation of polymer

coils, but it may be due to the increased chance of mutual collision of PMA coil under shear stress (Katsumichi Ono and Kenkichi Murakami, 1977).

The concentration and molecular weight of the polymer may also be common and essential factors that affect shear thickening behaviour. The hydrogen bonding ability of PMA molecules (Towlson and Wright, 1983) the hydrophobic interaction between PMA molecules, or a balance between hydrophilic bonding ability and the hydrophobic one of PMA molecules may be essential factors to induce shear thickening behaviour.

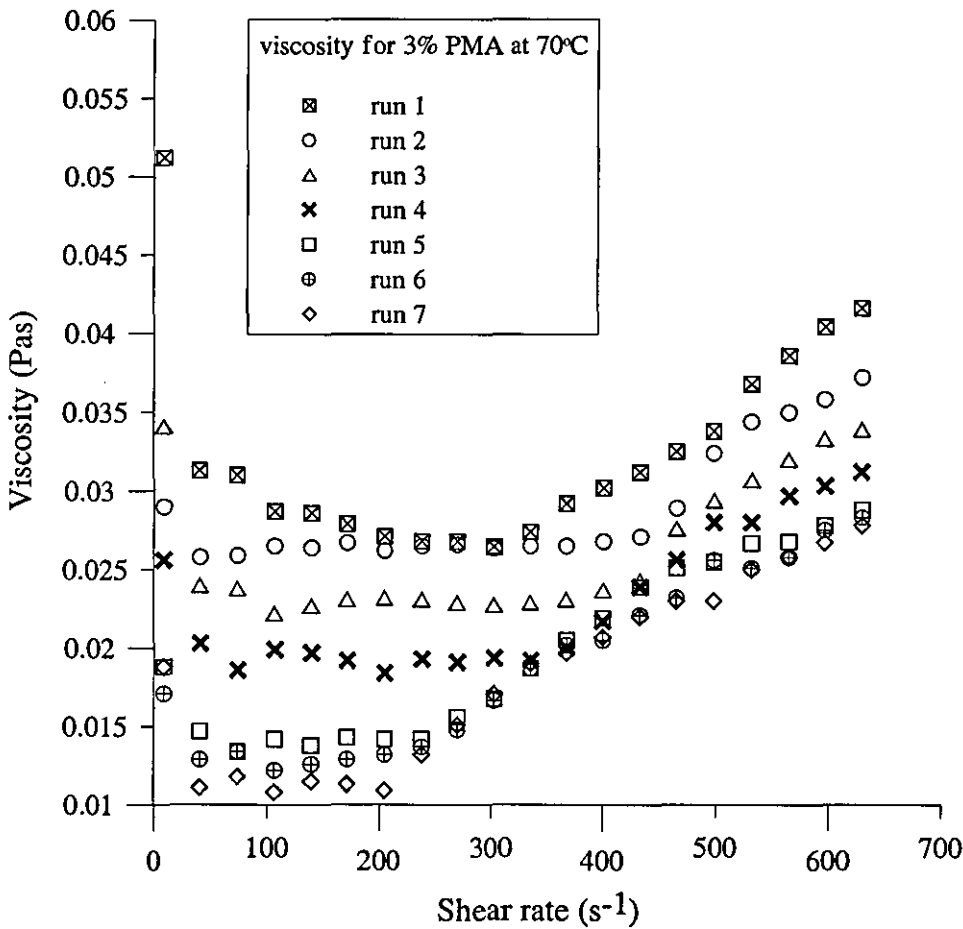


Figure 5.1.2. Viscosity for increasing shear rate, for 3% PMA at 70°C, and pH 3.

The decrease of the solution viscosity for the subsequent runs could also be attributed to the network being built up by the field of shear. As this network is being built up, the viscosity decreases for each subsequent run. At the end of the first run, the field of shear has caused the development of a network to a certain extent. Because of this network, when the same sample is attributed to a subsequent run, its viscosity is lower

(figure 5.1.2). The network is being developed for each subsequent run (runs 1 to 5), and hence the solution viscosity decreases. When the network has been fully developed for these conditions, the viscosity does not decrease any more, and remains constant for every subsequent run (runs 6-7).

5.1.2. Ammonium polymethacrylate (APMA)

The rheological behaviour of APMA solutions was also examined. The effects of shearing time, shear rate and pH on the viscosity of aqueous solutions of APMA were tested.

Shearing time: First of all, the effect of shearing time for constant shear rate was examined. As shown in figure 5.1.3, a 0.78% APMA solution was subjected to constant shear of 108 s^{-1} (which is close to the value of the shear rate in the reactor) for 1200s; the viscosity seems to be constant and there is no effect of the shearing time on it.

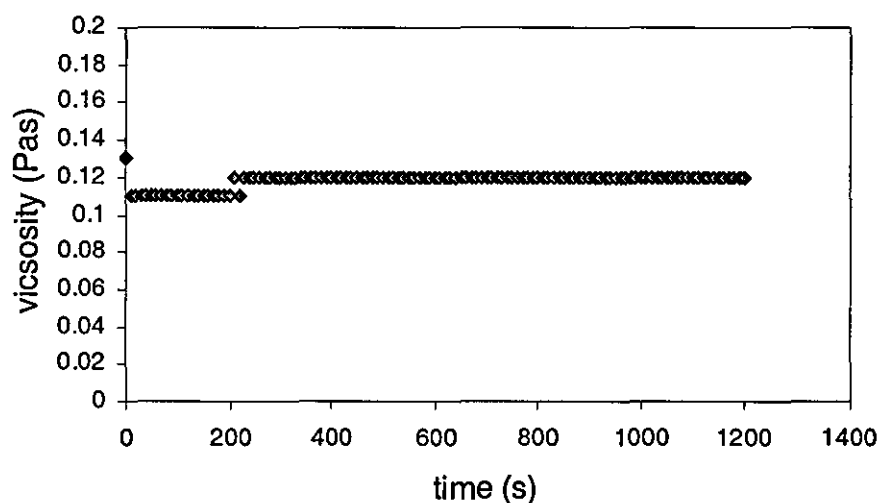


Figure 5.1.3. Viscosity under constant shear 108 s^{-1} , for a 0.78% APMA solution, at 70°C , and pH 9 versus time.

pH and shear rate: The effect of shear rate and pH was examined concurrently. The pH of APMA solutions of the same polyelectrolyte concentration was adjusted to various values by the addition of NH_3 , and their viscosity was measured over a range of shear rates from 0 to 648 s^{-1} .

Figure 5.1.4 shows the effect of both shear rate and the pH on the solution viscosity at 70°C, for a 0.93% APMA solution. APMA, unlike PMA, shows a shear thinning behaviour, as the viscosity decreases with increasing shear rate, indicating that the neutralisation of PMA eliminates the shear thickening behaviour. The repulsion between the parts of the polymer chain, with the same charge, force the polymer coil to unfold and stretch while at the same time the friction between the extended polymer coils is reduced, and therefore the viscosity is reduced. The pH seems to have a significant effect on the viscosity. As the pH increases the solution viscosity decreases monotonously for certain shear rates. These observations could be explained in terms of the strong repulsive forces that are developed between the charged polymer coils. The pH increase leads to a greater extent of ionisation, to stronger repulsive forces and a more charged coil. These repulsive forces between the carboxyl anions on the polymer chain, cause the PMA molecules to occupy a more stretched and extended conformation while also preventing the yielding of intermolecular bonds which could be regarded as the origin of the viscosity increase (Ohoya et al., 2000).

Shear history: Figure 5.1.5. also shows that, like PMA, the viscosity of the APMA solutions also depends on shear history. More precisely, figure 5.1.5.a, shows that for pH 8, the behaviour of APMA, when subjected to subsequent runs, resembles the behaviour of PMA. The viscosity initially decreases for shear rates up to 500s^{-1} , but for higher shear rates it starts to increase, resembling the shear thickening behaviour of APMA. The difference between the two materials is that, in the case of PMA, the shear thickening behaviour occurs at lower shear rates, of 200s^{-1} . For pH 9, the solution viscosity decreases for every subsequent run, and this decrease is more evident for lower shear rates. Once the solution has been subjected to higher shear rates, the viscosity decreases even for lower shear rates, as shown in figure 5.1.5.b. Accordingly, comparing the response of PMA and APMA for $\text{pH} \geq 9$, to subsequent runs, it is concluded that these materials behave in a different way for high shear rates. The viscosity of PMA solutions increases with increasing shear rates while the viscosity of APMA decreases, gradually. The only similarity is that in both cases the viscosity of PMA and APMA solutions for $\text{pH} \geq 9$, depends on the shearing history.

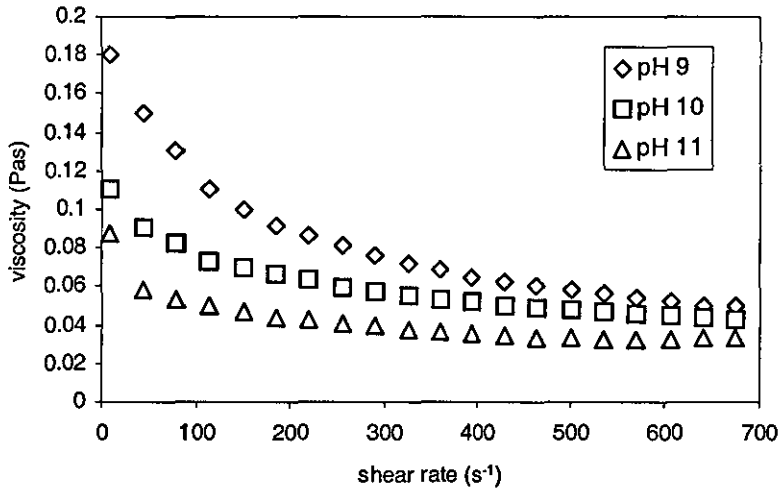


Figure 5.1.4. The effect of pH and shear rate on the viscosity of a 0.93% APMA solution at 70°C

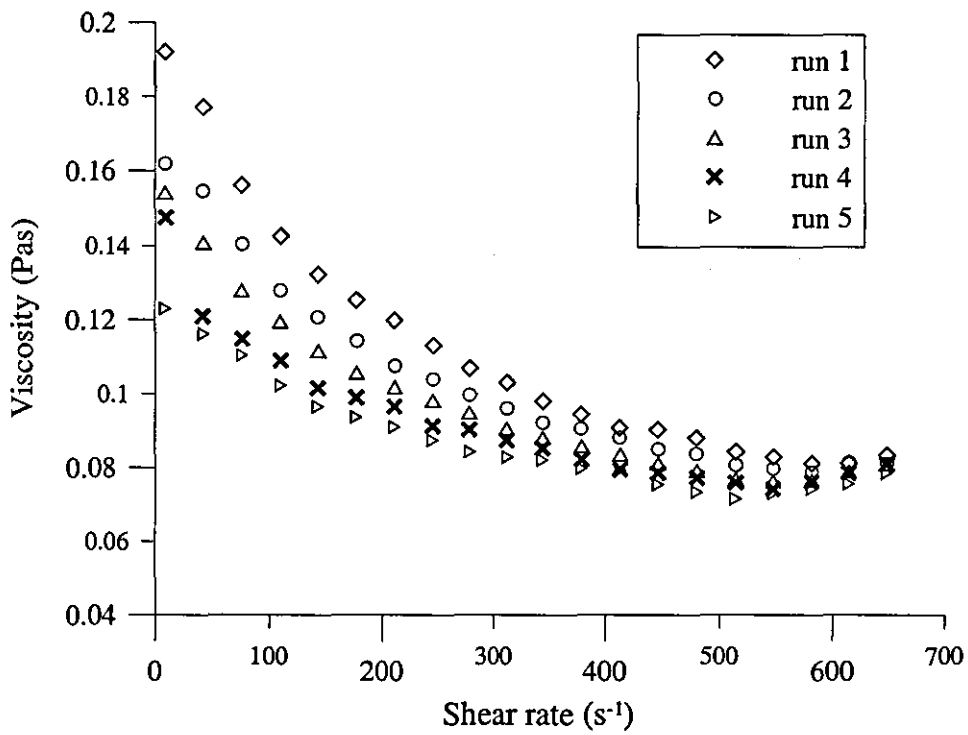


Figure 5.1.5.a) Effect of subsequent runs of shear on the viscosity of 0.93% APMA solution, at pH 8 and 70°C

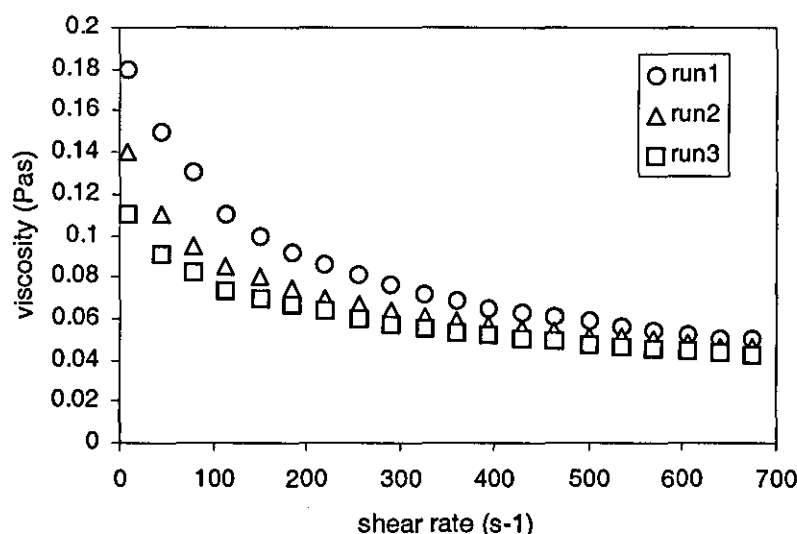


Figure 5.1.5.b) Effect of subsequent runs of shear on the viscosity of 0.93% APMA solution, at pH 9 and 70°C

5.1.3. Sodium polymethacrylate (PMA-Na)

Shearing time: Aqueous PMA-Na solutions of various concentrations were subjected to a constant rate in order to find out the effect of shearing time on the solution viscosity. Figure 5.1.6 shows that the viscosity remains stable and is not affected by the elapse of shearing time. Therefore, PMA-Na does not exhibit rheopectic behaviour.

pH and shear rate: The effect of the pH and of the shear rate on PMA-Na aqueous solutions was also examined. Comparing the viscosity response to the pH changes (figure 5.1.7) for increasing shear rate, it is observed that the viscosity remains constant for pH values varying from 8 to 12 and it changes when the pH drops to 7. Within the range of pH values from 12 to 8, the viscosity follows the same pattern; it decreases sharply at low shear rates and it becomes almost constant at shear rates higher than 400 s^{-1} . Therefore, the pH does not affect the solution viscosity when it ranges between 8 and 12. The viscosity drops significantly and becomes pH dependent for pH values below 8.

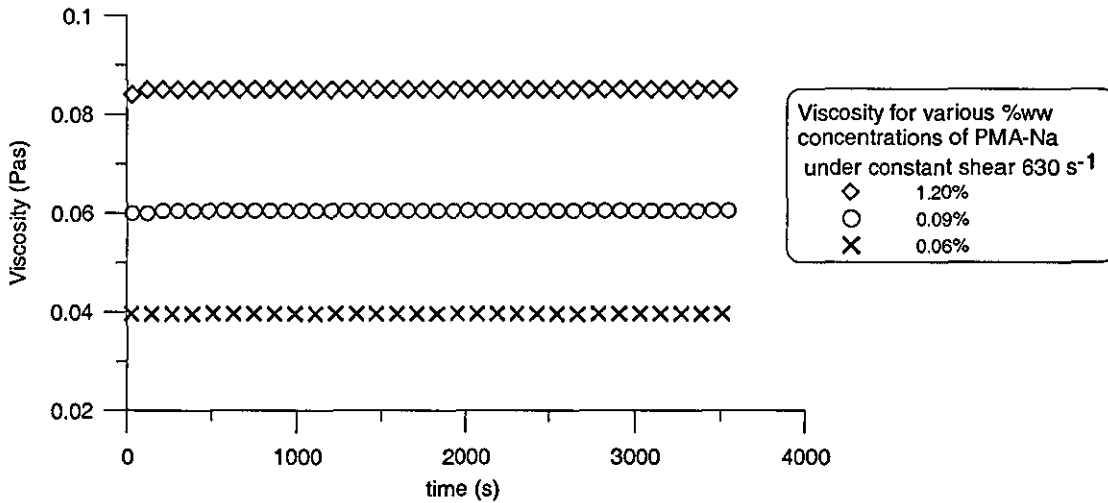


Figure 5.1.6. Effect of shearing time on viscosity

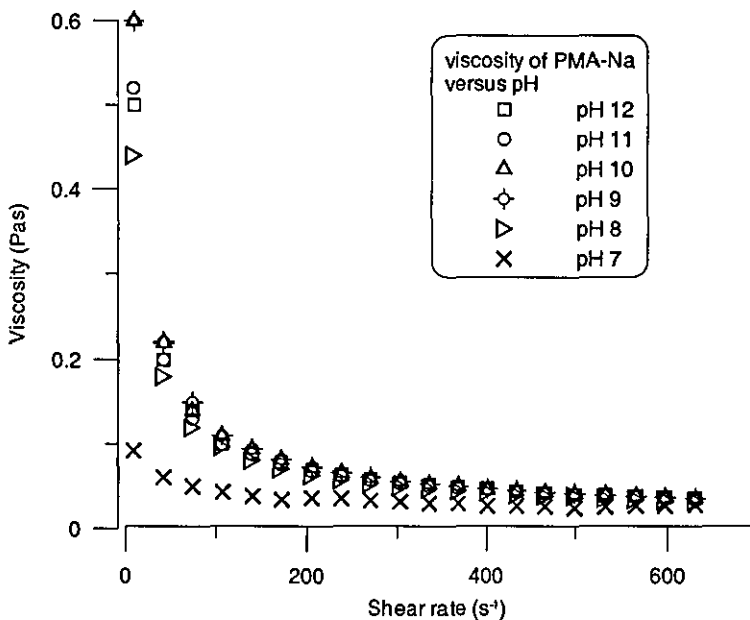


Figure 5.1.7. Effect of the pH on the viscosity of 0.6% PMA-Na aqueous solution

Shearing history: Figure 5.1.8 shows that when the pH decreases to 7 (figure 5.1.8.a), the viscosity pattern changes and it resembles the behaviour of polymethacrylic acid by becoming dependent on the shearing history. When the pH increases within the range, from 8 to 12 (figures 5.1.8.b and c), subsequent runs do not affect the viscosity. Therefore, the viscosity profile of the PMA-Na solutions is independent of the shear history within this range of pH values. Comparing the response of PMA and PMA-Na (within a pH range 12-8) to subsequent runs, it is concluded that these materials behave in a different way at high shear rates:

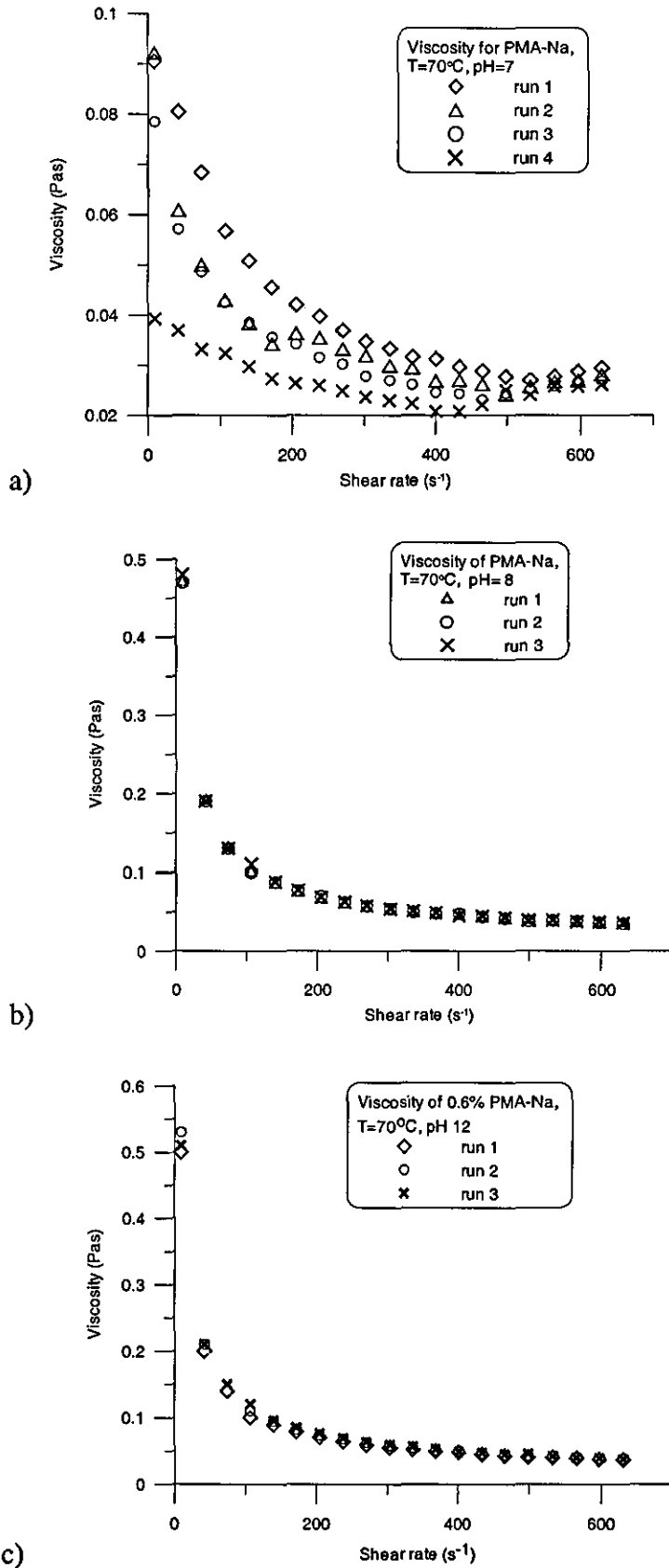


Figure 5.1.8. Viscosity dependence on shear rate and history for various pH values:

a)pH 7, b)pH=8, c)pH=12

1. the viscosity of PMA solutions increases with increasing shear rates while the viscosity of PMA-Na decreases gradually and after 400 s^{-1} it becomes almost constant.
2. the viscosity of PMA solutions depends on the shearing history, whereas the viscosity of the sodium salt is not influenced at all.

These differences between PMA and PMA-Na may be explained in terms of the strong repulsive interaction between the ionised carboxyl anions in the presence of NaOH. The presence of NaOH may prevent from yielding intramolecular and intermolecular bonds.

5.1.4. Conclusions

The conclusions that can be deduced from the investigation of the rheological behaviour of PMA, and its ammonium and sodium salts, are:

- All the solutions examined, (PMA, APMA, and PMA-Na), show a time independent rheological behaviour.
- PMA solutions exhibit a shear thickening behaviour, whilst APMA and PMA-Na solutions exhibit a shear thinning behaviour. The rheological behaviour of PMA solutions seems to change when the polymethacrylic acid is neutralised either with NH_3 or with NaOH.
- PMA and APMA show a shear history-dependent behaviour. Once the PMA or APMA solutions have been subjected to high shear rates, their viscosity decreases even for low shear rates. On the contrary, PMA-Na solutions do not show any dependence on shear history.
- The viscosity of APMA solutions depends on pH. For increasing pH, the solutions' viscosity decreases. The viscosity of PMA-Na solutions does not depend on pH.

- For $\text{pH} < 9$, APMA solutions resemble the behaviour of PMA, showing a slight shear thickening behaviour for high shear rates. PMA-Na solutions resemble the behaviour of PMA for $\text{pH} < 8$, showing, also a dependence on shear history.

5.2. Interfacial tension

The interfacial tension between PMA-Na or APMA, and MMA was measured for various stabiliser concentrations and pH values.

5.2.1. APMA

The influence of APMA concentration, and of the pH, on the interfacial tension between APMA solutions and MMA was examined within a range of APMA concentrations from 0.78 to 1.56% APMA, and within a range of pH values from 8-12, at 70°C, as shown in figure 5.2.1. It was observed that the interfacial tension does not change significantly with increasing APMA concentration, in fact it remains almost constant over all the concentration range. pH did not seem to have any significant effect on the interfacial tension either, as the interfacial tension remains almost constant, over all the pH range. The interfacial tension ranged from 12×10^{-3} N/m to 13×10^{-3} N/m for all the APMA concentrations and pH values used.

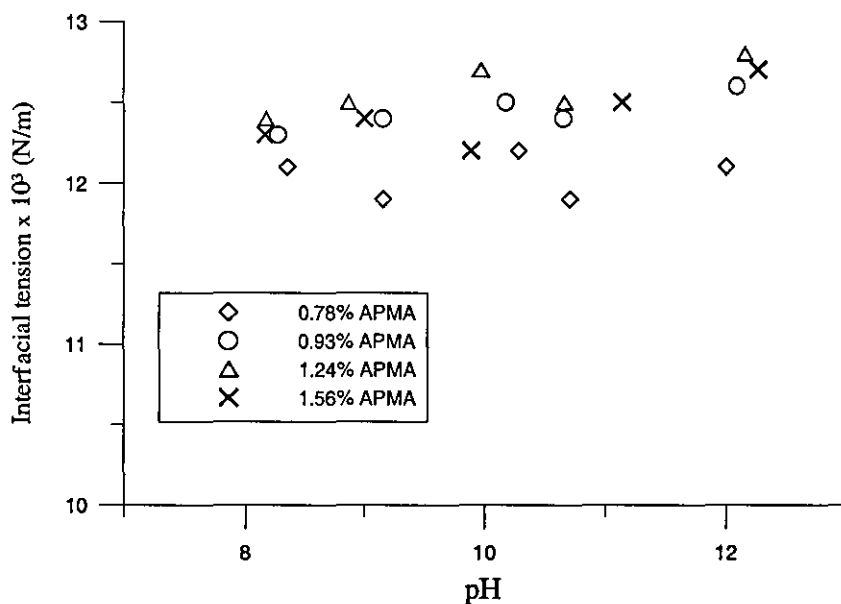


Figure 5.2.1. Interfacial tension between the monomer and the APMA continuous phase versus pH at 70°C

5.2.2. PMA-Na

The effect of pH and of PMA-Na concentration on the interfacial tension between PMA-Na solutions and MMA was examined for PMA-Na concentrations from 0.5 to 1.2 % PMA-Na and within a range of pH values, from 10 to 12, at 70°C, as shown in figure 5.2.2. The interfacial tension ranged between $12.9 \times 10^{-3} \text{ N/m}$ to $14.8 \times 10^{-3} \text{ N/m}$ over all the PMA-Na concentration range. The pH did not have any effect on the interfacial tension. The interfacial tension remained constant for every solution, over all the pH range.

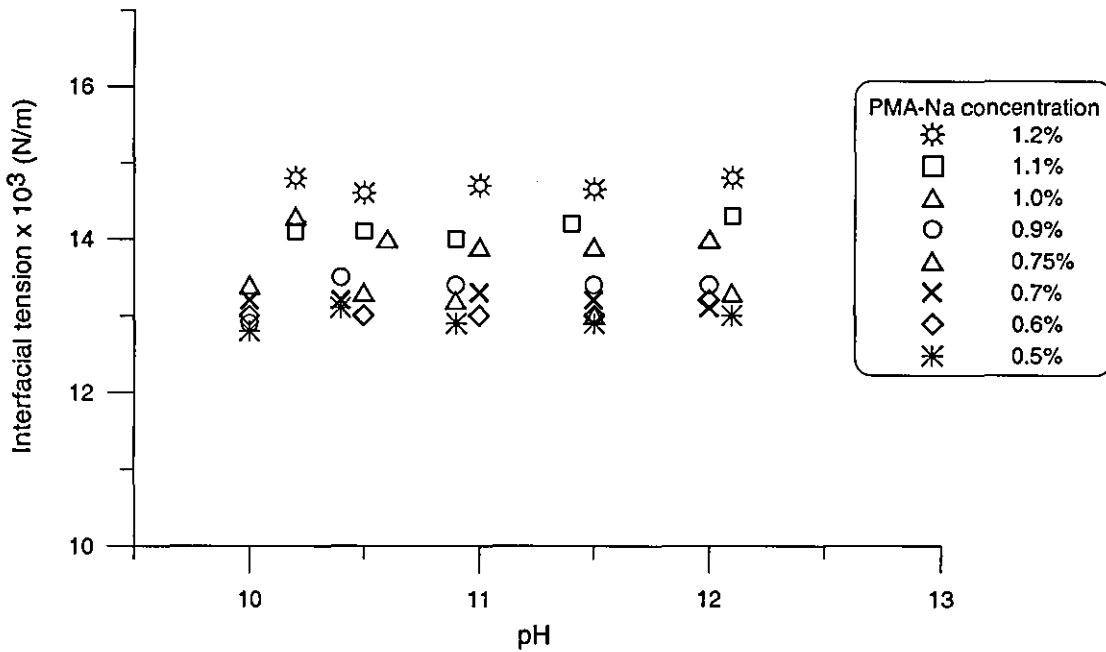


Figure 5.2.2. Interfacial tension between the monomer and the PMA-Na continuous phase versus pH at 70°C

5.2.3. Conclusions

The conclusions drawn from these measurements is that

- The increase in stabiliser concentration does not have any significant effect on the interfacial tension between the continuous phase and the monomer. The interfacial tension remains almost constant over all the range of stabiliser concentrations
- The pH does not affect the interfacial tension between the two phases

5.3. Factors that affect the drop and particle sizes and their distributions

In this chapter, the factors that affect the drop and particle sizes were also investigated. Drop and particle sizes and distributions were measured, and their variation as a function of these factors was examined. These factors are the stabiliser concentration and continuous phase viscosity, impeller speed, pH, temperature, monomer hold-up and dispersed phase viscosity

5.3.1. Effect of the stabiliser concentration - continuous phase viscosity

In order to investigate the effect of the concentration of the polyelectrolyte stabilisers PMA-Na and APMA on the drop and particle size distributions, suspension polymerisation experiments were run with different polyelectrolyte concentrations, at 70°C, and at 750rpm (12.5 s⁻¹). The initial pH of the continuous phase at 70°C, is adjusted to 10 for all runs. The particle size distributions of the polymer beads produced with PMA-Na and APMA are depicted in figures 5.3.1 and 5.3.2 , respectively. When the concentration of the stabilisers in the continuous phase increases, the particle sizes in both cases decrease and the particle size distributions become slightly broader, especially towards the smaller sizes. This means that the maximum drop diameters decrease, while not only do the minimum drop diameters decrease in size but they also increase in number, justifying the broadening of the distribution especially towards the smaller sizes.

The particular feature of these stabilisers is that they are viscous gels and they produce aqueous solutions which are also very viscous. Hence with increasing concentration of the stabiliser in the continuous phase, the viscosity of the continuous phase also increases. More specifically, for PMA-Na concentrations ranging from 0.5 to 1.2%, the continuous phase viscosity would range from 0.15 to 0.38 Pas. For APMA concentrations ranging from 0.78% to 1.56%, the viscosity ranged between 0.116 to 0.168 Pas. The broadening of the distribution as the stabiliser concentration increases might be caused by the simultaneous increase of the viscosity of the continuous phase (Jahanzad et al., 2004 (a)).

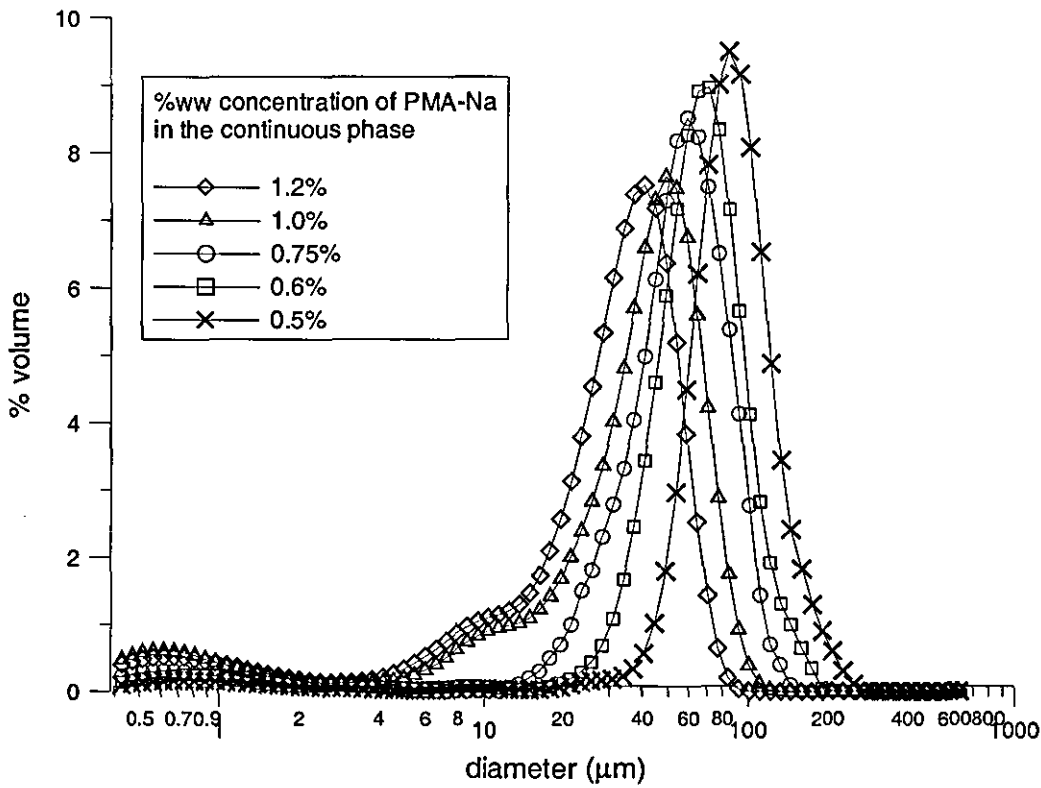


Figure 5.3.1. Particle size distributions for increasing PMA-Na concentration in the continuous phase, at 70°C , 12.5s^{-1} , and initial $\text{pH}=10$

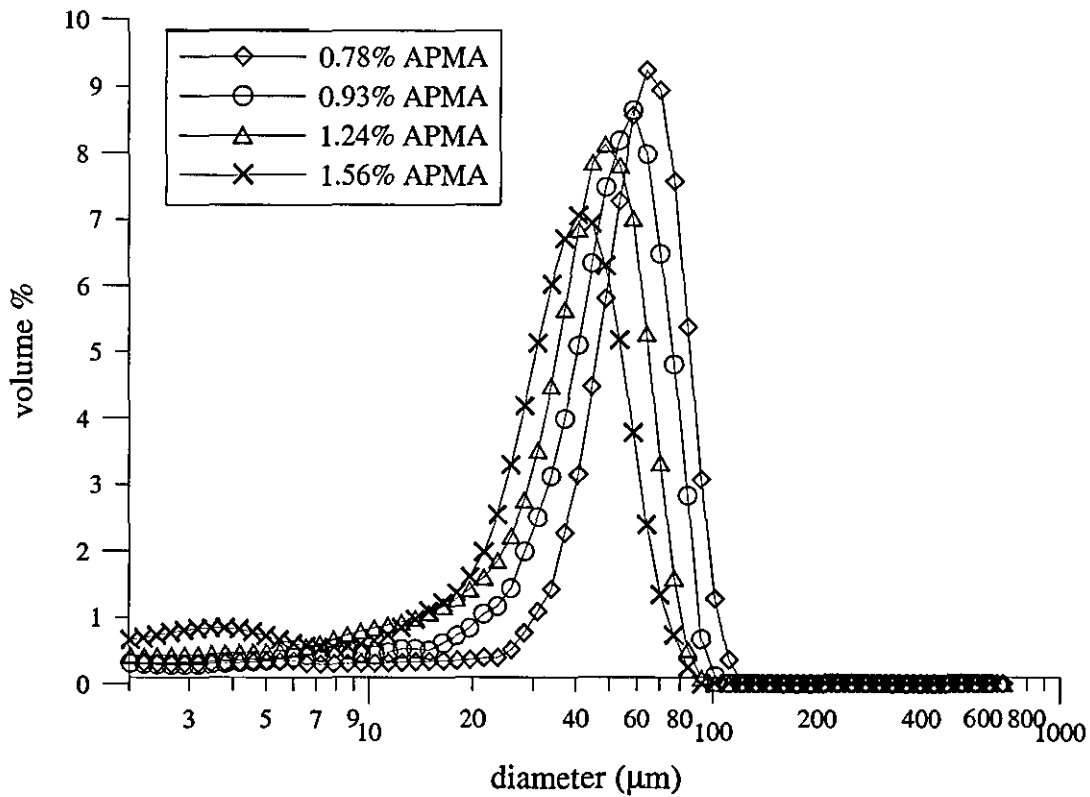


Figure 5.3.2. Effect of increasing APMA concentration in the continuous phase, at 70°C , 12.5s^{-1} , and initial $\text{pH}=10$

The drop size distribution at any time is a result of the dynamic equilibrium between breakage and coalescence. Decreasing the drop breakage rate or increasing the drop coalescence rate results in larger drop sizes. On the other hand, increasing the drop breakage rate or decreasing the drop coalescence rate results in smaller drop sizes.

In the case of PMA-Na and APMA, where the viscosity of the continuous phase plays a very important role in determining the hydrodynamic conditions in the vessel, the increase of the continuous phase viscosity results in an increase of the viscous shear forces exerted on the drops which, in turn, cause the breakage rate to increase. At the same time the increased viscosity hinders the coalescence because of the thicker film trapped between colliding drops and the coalescence rate decreases. For a breakage to occur, it is necessary that enough energy be supplied to the drop to overcome the forces that resist breakage as a function of surface tension. The energy for the breakage will come from the field outside the drop, either as kinetic energy in the turbulent eddies, or as shear energy, or as a combination of both. As the viscosity of the continuous phase increases, the viscous stress increases leading to an increase of the breakage rate. The drop coalescence is also influenced by several factors. One of them is the collision rate between the drops. Another factor, is the coalescence efficiency between the drops. This is a function of the time that two colliding drops remain in contact. And the time required for the intervening liquid film to drain out to achieve film rupture and thus coalescence. For systems of higher continuous phase viscosities, a lower film drainage rate would be expected and thus a lower coalescence rate.

Figure 5.3.3, shows the effect of the continuous phase viscosity on the Sauter mean diameter, with a)PMA-Na and b)APMA. In both cases the Sauter mean diameter decreases with the increase of the continuous phase viscosity. This may be attributed to the decrease of the coalescence rate that is also supported by the fact that the particle size distribution becomes broader towards the smaller sizes when the viscosity increases.

These two factors, concentration and viscosity of the continuous phase, can not be decoupled in order to distinguish between the effects on the particle sizes caused by each one of them. A factor that can provide a useful source of information for the

behaviour of the polyelectrolyte stabilisers is the variation of the interfacial tension with increasing stabiliser concentration.

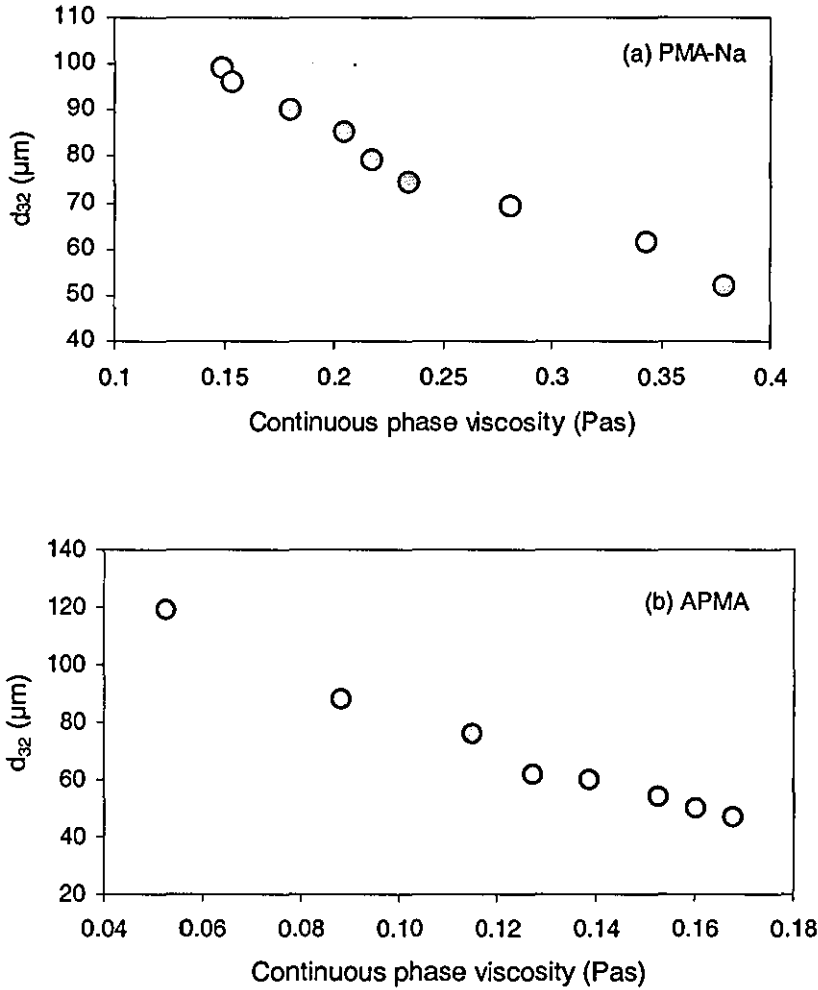


Figure 5.3.3. Effect of the continuous phase viscosity on the Sauter mean diameter, at 70°C , 12.5s^{-1} , and initial pH =10 for a)PMA-Na and initial pH =9 for b)APMA

Comparing the Sauter mean diameters of the beads produced by the two stabilisers (figure 5.3.4), it is observed that for the same continuous phase viscosity values, APMA produces smaller particles than PMA-Na. More specifically, for the same continuous phase viscosity of 0.153 Pas, the d_{32} of the particles produced with PMA-Na is 96 μm , whereas the d_{32} of the particles produced with APMA is 54 μm . One factor that could probably explain the difference is the interfacial tension between the monomer and the two stabilisers. Lower interfacial tension means lower resistance to

breakage and consequently leads to smaller particle sizes. Therefore, if the interfacial tension of the system APMA+MMA is lower than the interfacial tension of the system PMA-Na +MMA, smaller drops would be expected for the first one.

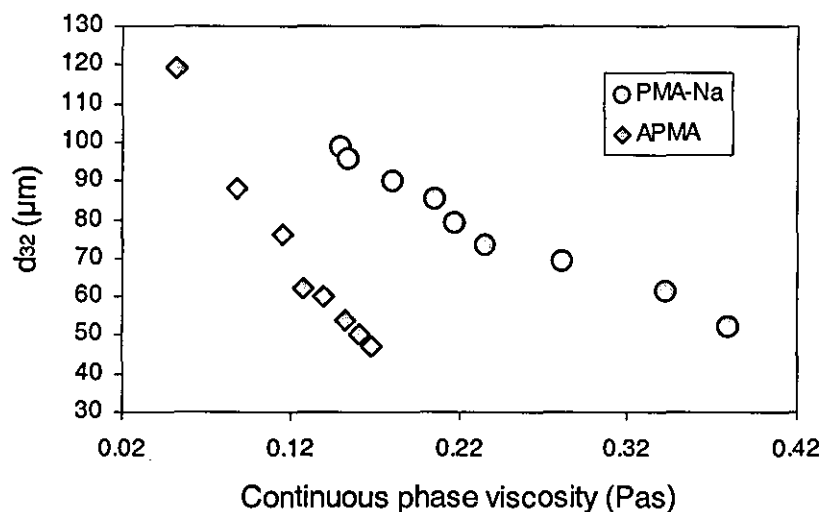


Figure 5.3.4. d_{32} for PMA-Na and APMA, at 70°C , 12.5s^{-1} , for increasing continuous phase viscosity

There are two questions to be answered by the interfacial tension measurements:

- For samples produced with the same stabiliser, which is the determining factor causing the diminution of the drop sizes, the increase of the stabiliser concentration through decreasing the interfacial tension, or the increase of the continuous phase viscosity?
- Comparing samples produced with PMA-Na and APMA, what causes the difference in the drop sizes for samples produced with the same continuous phase viscosity?

In figure 5.3.5, the interfacial tension between PMA-Na and monomer and APMA and monomer is depicted for increasing stabiliser concentration at the reaction temperature (70°C). The interfacial tension for both of the solutions is low.

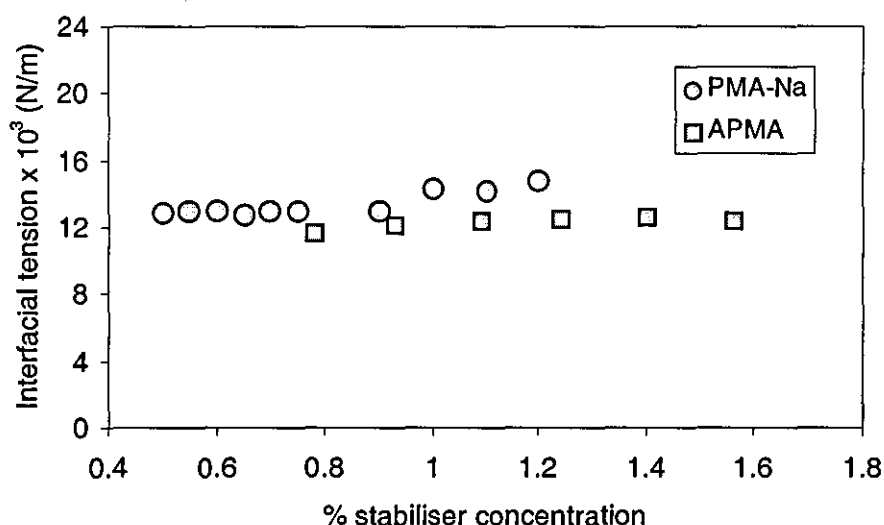


Figure 5.3.5. Interfacial tension between monomer and the continuous phase for increasing stabiliser concentration, at 70°C

Two significant observations can be made from these data. First, the interfacial tension varies only slightly over the whole range of stabiliser concentrations. In fact, it remains almost constant over all the concentration range. Therefore, there is no significant influence of the increase of the stabiliser concentration on the interfacial tension. The second observation is that the interfacial tension between PMA-Na solutions and the monomer ranges between 12.8×10^{-3} N/m and 14.9×10^{-3} N/m and is slightly higher than the interfacial tension between APMA solutions and the monomer, that ranges between 11.7×10^{-3} N/m and 12.4×10^{-3} N/m. But is this small difference sufficient to explain the difference between the produced particle sizes? The answer is no, and therefore, the diminution of the particle sizes with increasing stabiliser concentration could not be attributed to interfacial phenomena. For polymer samples produced with the same stabiliser, it could possibly be attributed to the increased viscosity of the continuous phase.

Although, the increased continuous phase viscosity can probably justify this diminution, it cannot justify the formation of different drop sizes for the same continuous phase viscosity, when APMA is used instead of PMA-Na. This could probably be caused by the different nature and properties of the two materials. One of the factors that might account for this, is the different shear thinning behaviour of the two stabilisers. More specifically, the viscosity index, n , for PMA-Na solutions is

lower than the viscosity index for APMA solutions. Lower viscosity index is associated with an increasing shear thinning behaviour. Increasing shear thinning (or lower viscosity index) in the laminar flow region leads to larger drops (Shimizu et al., 1999; Kumar et al, 1993). With increasing shear thinning, the shear stress tending to deform the drop decreases and, as a result, the maximum drop diameter increases.

5.3.2. Effect of the stirring speed

Increasing the stirring speed during the suspension polymerisation has been found to lead to a decrease of the particle sizes, when the flow in the reactor is turbulent (Zerfa and Brooks, 1996 (b), Leng and Quarderer, 1982). When, it is not turbulent, it has also been found to lead to a decrease of the drop sizes (Boye et al. 1996). A decrease initially, followed by an increase of the Sauter mean diameter for increasing stirring speed and high hold-up fraction dispersion systems has also been reported (Chatzi and Kiparissides, 1995). The initial decrease was attributed to the increase of the breakage rate with increasing impeller speed. The subsequent increase was attributed to the diminishing molecules of the stabiliser on the interface because of the large increase of the interfacial area. The increase of the coalescence frequency with increasing impeller speed (Howarth, 1964), in combination with the diminution of the stabiliser molecules lead to an increase of the drop sizes.

The effect of the stirring speed on the particle sizes when the non Newtonian PMA-Na and APMA solutions are used as suspending agents was investigated. Suspension polymerisation experiments were run for various stirring conditions, at 70°C, and initial pH 10 for PMA-Na. Figures 5.3.6 and 5.3.7 present the particle size distributions (PSDs) for 0.6% and 1.2% PMA-Na, and for 3 stirring speeds. As can be observed in these figures, the particle sizes, which reflect the initial drop sizes, for these conditions increase with increasing stirring speed. For a certain stabiliser concentration, the increase of the stirring speed causes an increase in the particle size. This is not what would be expected, if the flow was turbulent. It was not consistent with previous work suggesting that, for a low coalescing system such as this, one of the parameters favouring the droplet breakup, is higher impeller speed which generally decreases the minimum transition time required for the system to reach

steady state, and leads to smaller drop sizes (Chatzi et al., 1991). The particle size distribution becomes more narrow, though, with increasing stirring speed, as expected.

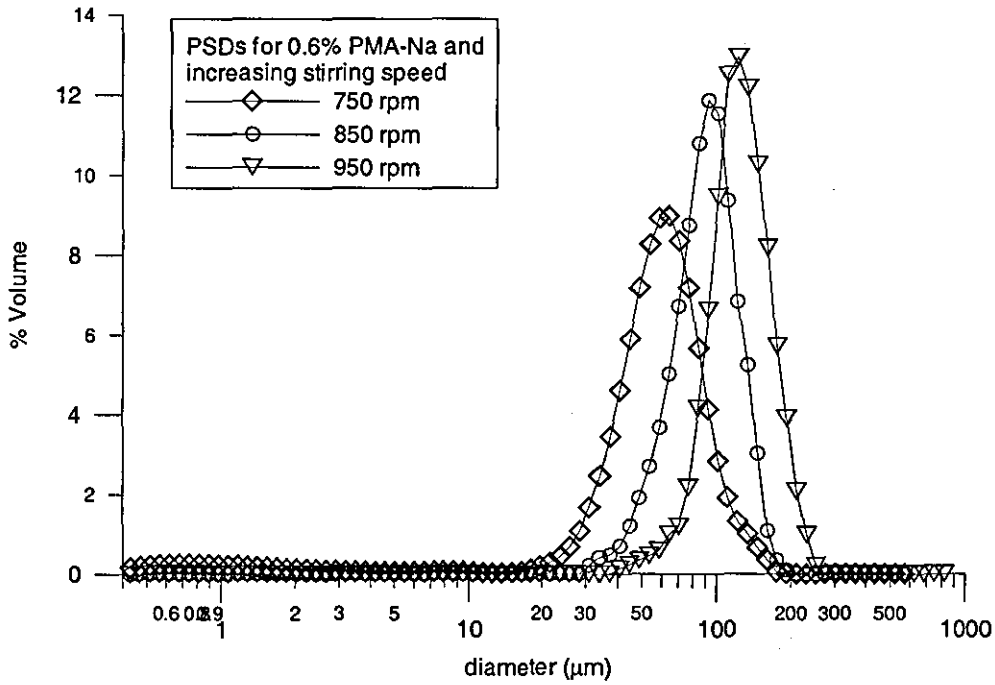


Figure 5.3.6. PSDs for 0.6% PMA-Na and increasing stirring speed at 70°C, and initial pH=10

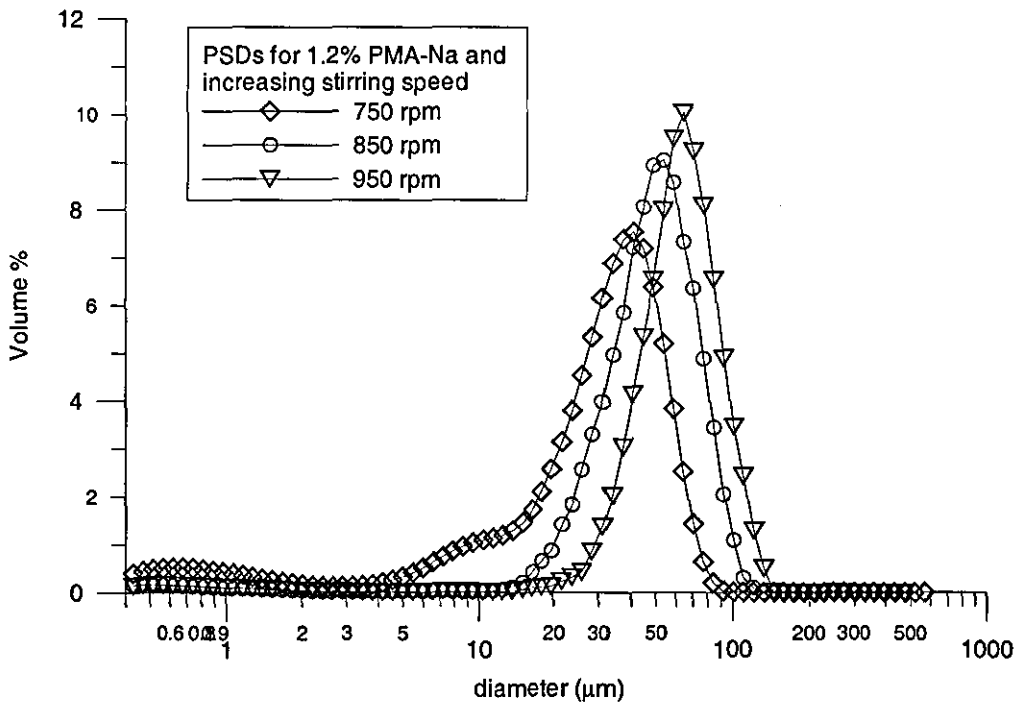


Figure 5.3.7. PSDs for 1.2% PMA-Na and increasing stirring speed at 70°C, and initial pH=10

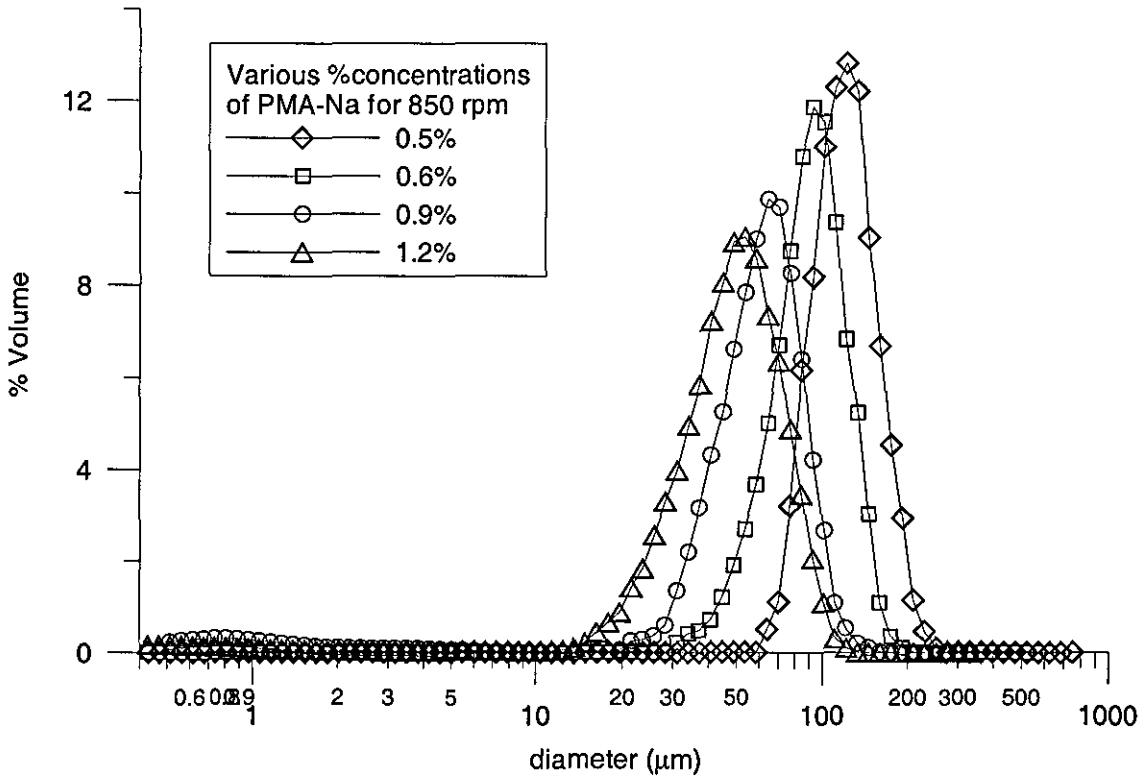


Figure 5.3.8. PSDs for various PMA-Na concentrations at 850 rpm, at 70°C, and initial pH=10

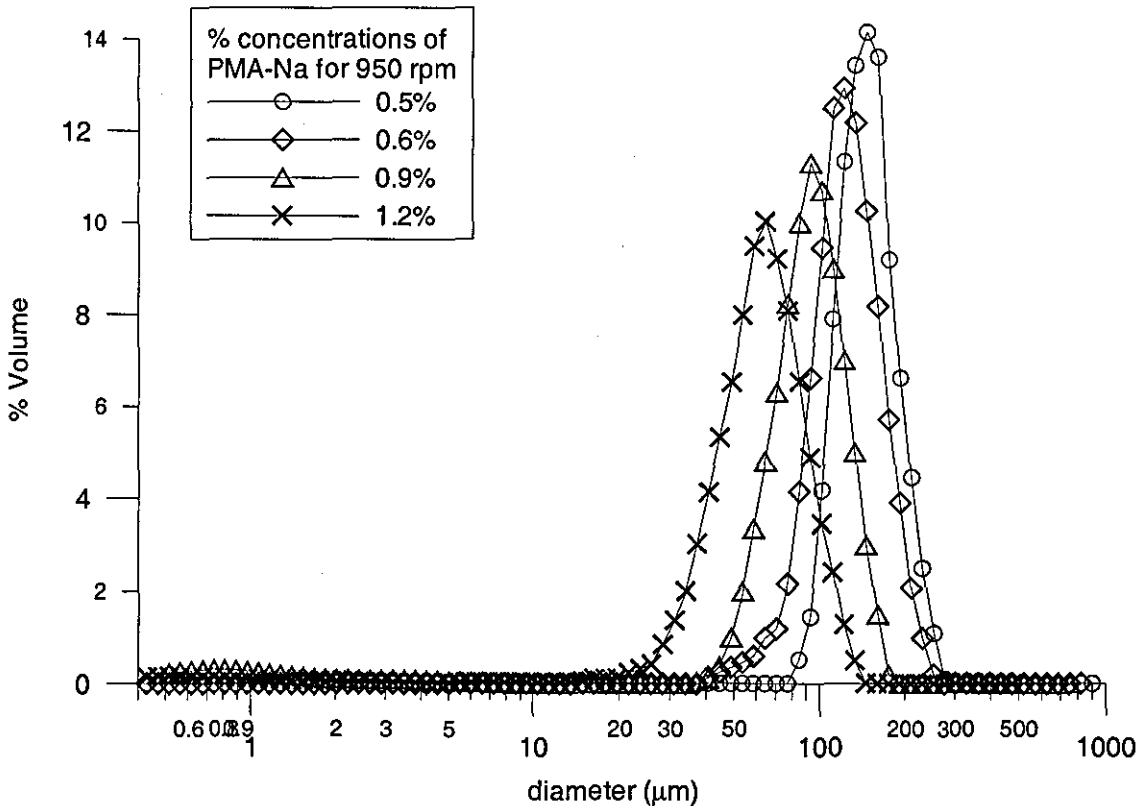


Figure 5.3.9. PSDs for various PMA-Na concentrations at 950 rpm, at 70°C, and initial pH=10

Figures 5.3.8 and 5.3.9 show the PSDs produced with various concentrations of PMA-Na at 850 rpm and 950 rpm respectively. The distributions follow the same pattern they followed at 750 rpm or 12.5 s^{-1} (figure 5.3.1). The particle sizes diminish with increasing stabiliser concentration and viscosity, and simultaneously their distribution becomes broader towards the smaller sizes.

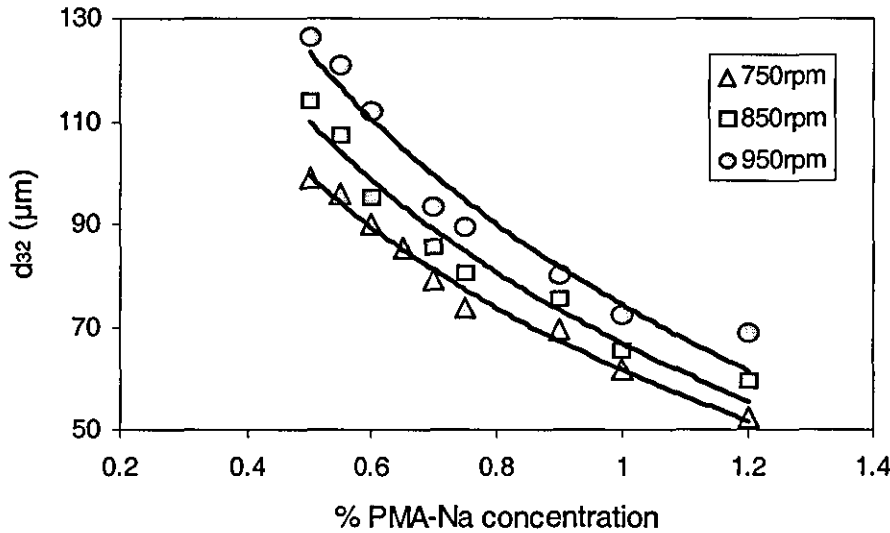


Figure 5.3.10. d_{32} for increasing stabiliser concentration at different stirring speeds

The Sauter mean diameters decrease with increasing stabiliser concentration but increase with increasing stirring speed as shown in figure 5.3.10. They follow the same trend for all the different speeds.

5.3.3. Effect of monomer hold-up

Monomer hold-up (or monomer volume fraction) has been found to have a significant effect on the particle sizes. Increasing the monomer hold-up during suspension polymerisation leads to an increase of the particle sizes when turbulent conditions prevail in the reactor, and for certain hold-ups. Boye et al. (2000) studied dispersions of high hold-up and found that, for hold-ups up to 0.5, the drop breakup occurs via the inertial breakup mechanism and that the particle size increases with increasing hold-up. For hold-ups higher than 0.6 the dispersion showed strong non-Newtonian characteristics and the apparent viscosity of the dispersion increased significantly. For

these conditions, the shear breakup mechanism prevailed and the drop size decreased for increasing hold-up. Stamatoudis and Tavlarides (1985) studied dispersions for high continuous phase viscosities and found that the drop sizes increase for increasing hold-up.

Here, the effect of the monomer hold-up (ϕ) on the particle sizes for the PMA-Na system has been studied for 3 different PMA-Na concentrations, 0.6, 0.9 and 1.2% and for hold-ups ranging from 0.05 to 0.3. The particle size distributions of the polymer produced with 0.6% PMA-Na for increasing ϕ are depicted in figure 5.3.11. The particle size distribution is more narrow for smaller hold-ups and becomes broader for higher hold-ups. For hold-ups from 0.05 to 0.2 the PSD is shifted towards smaller sizes as the hold-up increases. When the hold-up increases to 0.2, a small second peak is formed in the large size range of the distribution indicating the occurrence of coalescence. For an even higher hold-up, 0.25, the PSD becomes even broader and is shifted towards larger sizes, while the second peak becomes significantly larger indicating that coalescence occurs to a greater extent. Therefore, the effect of the increasing hold-up on the PSD is not monotonous. Initially, for low hold-ups the particle sizes decrease as the hold-up increases. For higher hold-ups, the particle sizes increase for increasing hold-up. This behaviour could be attributed to two competing factors, the viscosity of the system and the coalescence rate. As the hold-up increases, the viscosity of the system increases. This viscosity increase causes the formation of smaller particles which is consistent with the decreasing particle sizes for low hold-ups (0.05 to 1.5). The coalescence rate also increases for increasing ϕ , but for low ϕ , this effect may be counterbalanced by the viscosity increase which enhances the drop breakup by shear. For $\phi \geq 0.2$, the viscosity increase causes the formation of smaller particles but the coalescence rate also increases causes the formation of a second small peak at higher sizes. As the hold-up increases even further (0.2 to 0.25), the coalescence rate increases to such an extent that, it can not be counterbalanced by the increasing viscosity. Therefore, for higher hold-ups the particle sizes increase. For systems with hold-ups equal to 0.3, or higher, coalescence occurs to a great extent and the PSD becomes very broad and multimodal, while coagulation of the particles to bigger agglomerates is also observed.

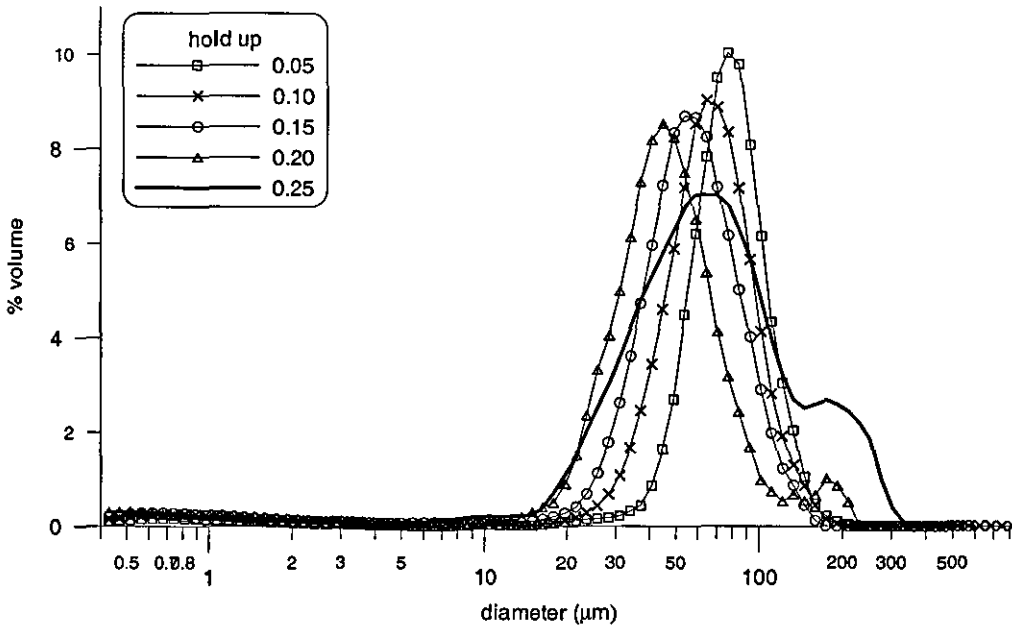


Figure 5.3.11. PSDs for increasing holdup and 0.6% PMA-Na, at pH 10 and 750rpm

The effect of the increasing hold-up on the Sauter mean diameter for 3 different PMA-Na concentrations, 0.6, 0.9 and 1.2% is shown in figure 5.3.12. Initially, for low hold-ups, from 0.05 to 0.15, a similar trend is evident for all PMA-Na concentrations. For the lower PMA-Na concentration, 0.6%, d_{32} starts to increase for hold-ups higher than 0.15, and the increase becomes sharp for hold-ups higher than 0.2. As the PMA-Na concentration increases to 0.9%, the capacity of the system against coalescence increases, and the increase of the particle sizes is mitigated. In fact only a slight increase for hold-ups higher than 0.15 occurs, and the particle sizes increase for hold-ups higher than 0.2. When the stabiliser concentration is increased, even further, to 1.2%, the capacity of the system against coalescence is even more enhanced, and the drop sizes decrease up to a hold-up of 0.2, and a slight increase occurs for hold-up equal to 0.25. The point where the coalescence starts to prevail over the viscosity, causing an increase of the particle size with increasing ϕ , is affected by the stabiliser concentration in the continuous phase. Hence, for higher stabiliser concentrations the capacity of the system against coalescence is enhanced and the increase of the particle sizes correspond to higher hold-ups. For 0.6% PMA-Na the coalescence takes over for ϕ equal to 0.15, whereas for 1.2% PMA-Na the coalescence takes over for ϕ equal to 0.2.

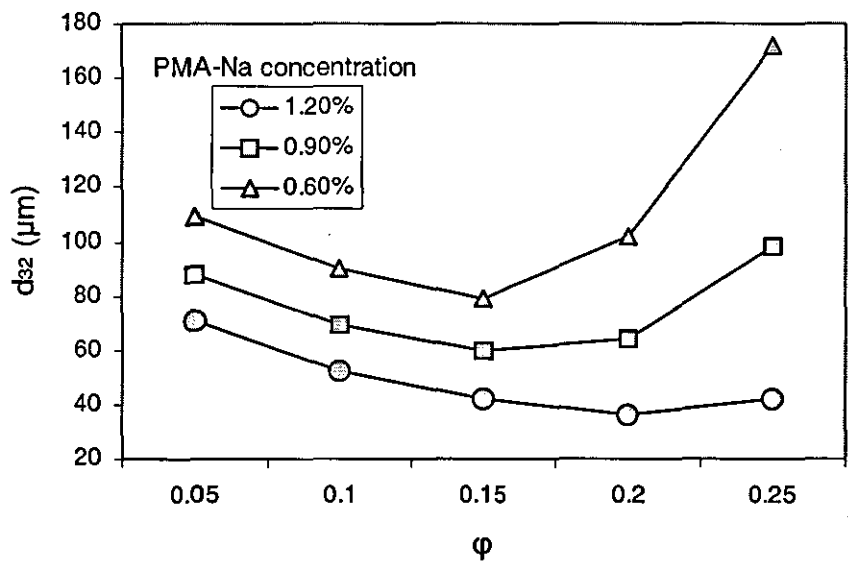


Figure 5.3.12. d_{32} for increasing hold-up and various PMA-Na concentrations, at pH 10

5.3.4. Effect of the viscosity of the dispersed phase

The particle size distributions broaden significantly as the dispersed phase viscosity increases (figure 5.3.13). Not only do the maximum diameters become larger but also the number of drops with small diameters increases. These observations are consistent with previous studies on the dispersed phase viscosity (Calabrese et al, 1986 (a); Arai et al., 1977) that referred to turbulent flow in tanks. The effect of the dispersed phase viscosity on the maximum diameter is shown in figure 5.3.14. The increase of the dispersed phase viscosity causes the drop sizes to increase.

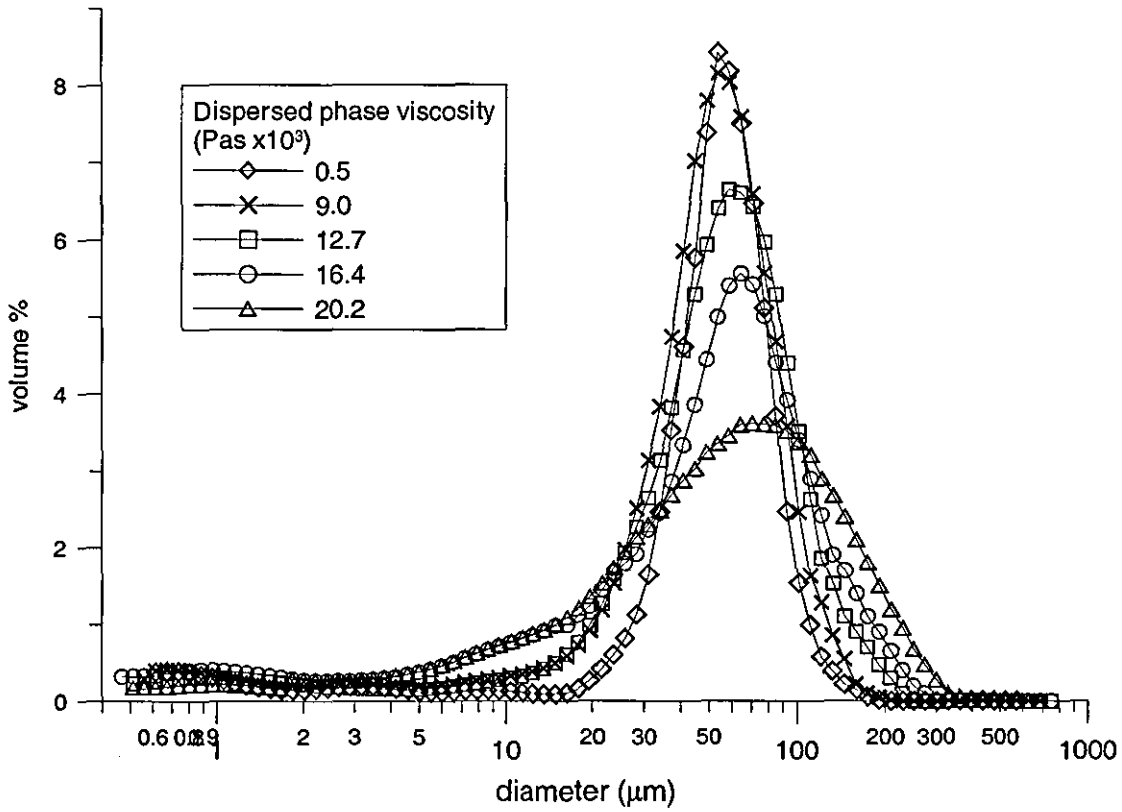


Figure 5.3.13. PSD for increasing dispersed phase viscosity, for PMA-Na, at 70°C and 12s^{-1}

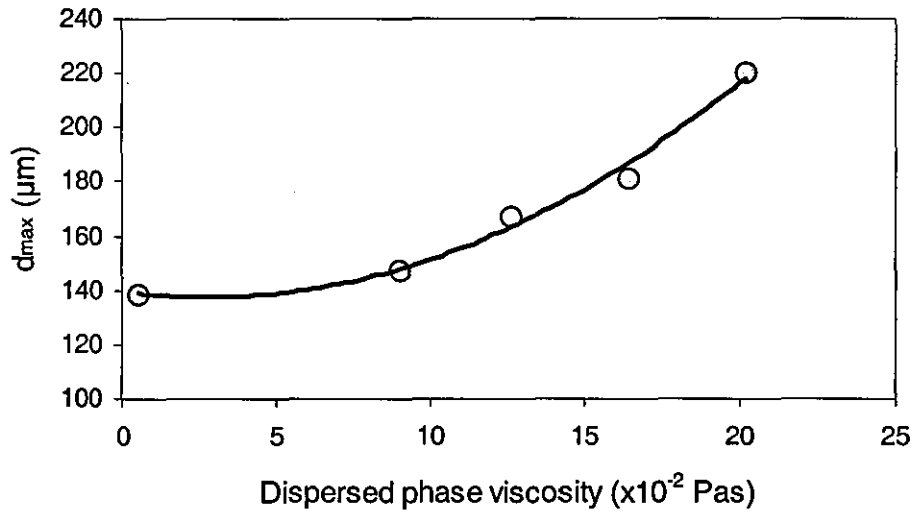


Figure 5.3.14: The effect of the dispersed phase viscosity on d_{max} for PMA-Na, at 70°C and 12s^{-1}

5.3.5. Effect of pH

One of the features that make these polyelectrolyte stabilisation systems differ from many other systems is their sensitivity to pH. The pH of the continuous phase has a profound effect on the particle sizes and on their distribution. In order to investigate this effect, suspension polymerisation experiments were run for the same conditions, while the pH was varied. The BPO concentration for these runs was 0.04 mole/l and the PMA-Na concentration was 0.45%. The pH was adjusted to the desirable value by the addition of 5M NaOH solution, in the continuous phase before the treatment of the continuous phase with N_2 and, of course, before the addition of MMA. The pH of the continuous phase before the addition of NaOH was 10 at the reaction temperature, 70°C, for all the solutions. The pH of the continuous phase decreases when the monomer is added and it decreases even further during the course of polymerisation reaction. This pH decrease is presented in figure 5.3.15 for various initial pH values. The pH decrease follows the same pattern in all cases, despite the different initial conditions. It decreases sharply when the monomer is added and then it decreases gradually during the course of polymerisation until it reaches a plateau at approximately pH 8. It is noted that despite the big difference in the initial pH values (10, 11, and 12), the final pH values (7.89, 8.17 and 8.32, respectively) do not differ significantly.

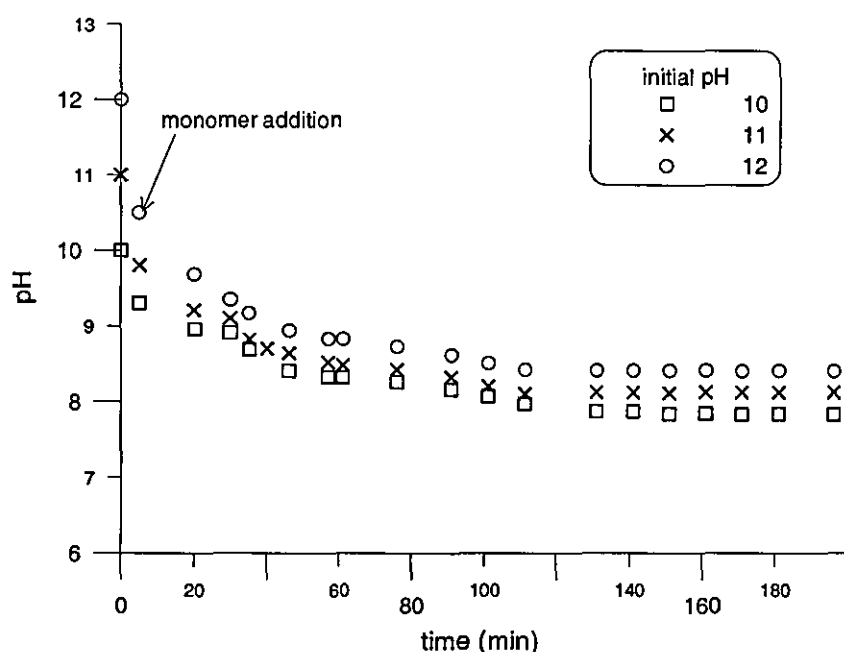


Figure 5.3.15. pH decrease during the course of polymerisation, at 70°C

The particle size distributions produced from experiments conducted as described above, for a pH range from 10.5 to 13, are depicted in figure 5.3.16. There are two different phenomena that accompany the increase of the initial pH during suspension polymerisation. First of all, the particle sizes diminish with pH increase and their distributions are shifted towards smaller sizes. Secondly, apart from the initial main peak, two more secondary peaks appear. Both of them correspond to small particles. The first of the secondary peaks, designated from now on, 'peak 1', corresponds to very small particles with diameters that range from 0.4 to 1.5 μm . The second of the secondary peaks, designated 'peak 2', corresponds to larger particles with diameters that range between 1.5 and 15 μm . These secondary peaks appear only when the pH had been adjusted to values higher than the initial pH of the solution.

Once the secondary peaks appear, each one of them is influenced by further pH increase in a different way. The main peak is also influenced by the pH increase in a different way. As can be observed, in figure 5.3.16, the area of peak 1, increases with increasing pH, while peak 2 decreases with increasing pH. The area of the main peak, also decreases with increasing pH, while at the same time the peak is shifted to smaller diameters.

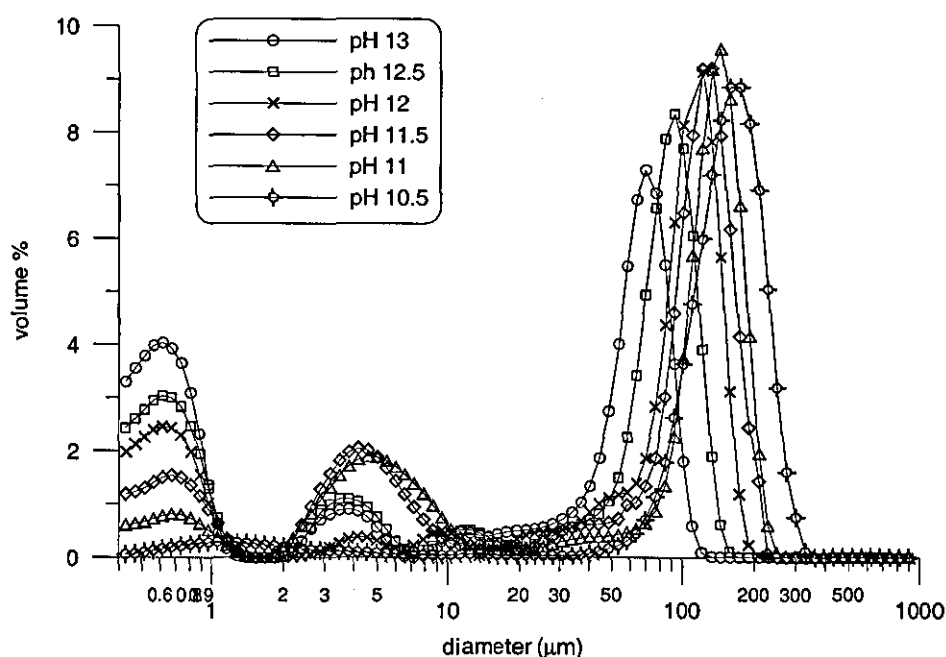


Figure 5.3.16. Effect of increasing initial pH on the PSD, for 0.45% PMA-Na

The influence of the increasing pH on each one of the three peaks is depicted separately in figures 5.3.17. Figure 5.3.17.a shows the effect of the pH on peak 1. As the pH increases, the area of peak 1 increases, meaning that the volume % or the number of fine particles that correspond to diameters from 0.4 to 1.5 μm increases. The range of the diameters is not influenced by the pH increase, but only the area of the peak. Figure 5.3.17.b., shows the effect of the increasing pH on peak 2. This peak appears as the pH rises higher than 10.5 to 11. Then, with a further increase of the pH the peak area decreases, and it also becomes bimodal for pH values equal to 12 or higher. The effect of the increasing pH on the main peak is depicted in figure 5.3.17.c. As can be observed, the increase of the pH values causes both the main peak area and the corresponding diameters to decrease. Hence, pH has a dual effect on the main peaks. Firstly, the main peaks become more narrow with increasing pH. Secondly, the particle sizes decrease and the main peaks are shifted towards smaller diameters.

The corresponding variations of d_{32} , for each one of the three peaks and for the total distribution, with increasing pH are depicted in figure 5.3.18, where figure 5.3.18.a. depicts d_{32} for peaks 1 and 2, figure 5.3.18.b. shows d_{32} for peak 3 and figure 5.28.c. depicts d_{32} of the total distribution.

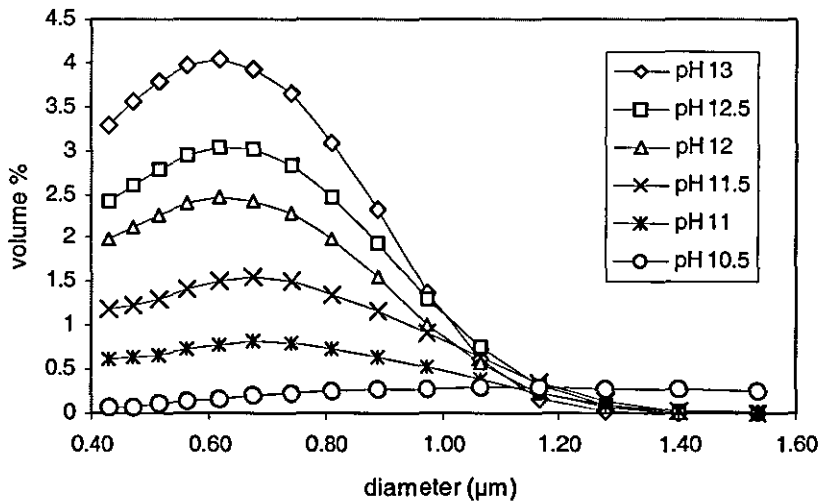


Figure 5.3.17.a. Effect of increasing pH on peak 1

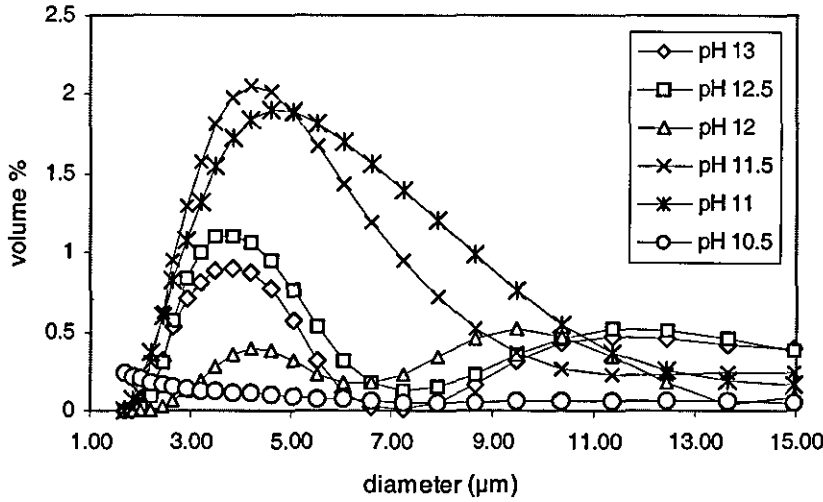


Figure 5.3.17.b. Effect of increasing pH on peak 2.

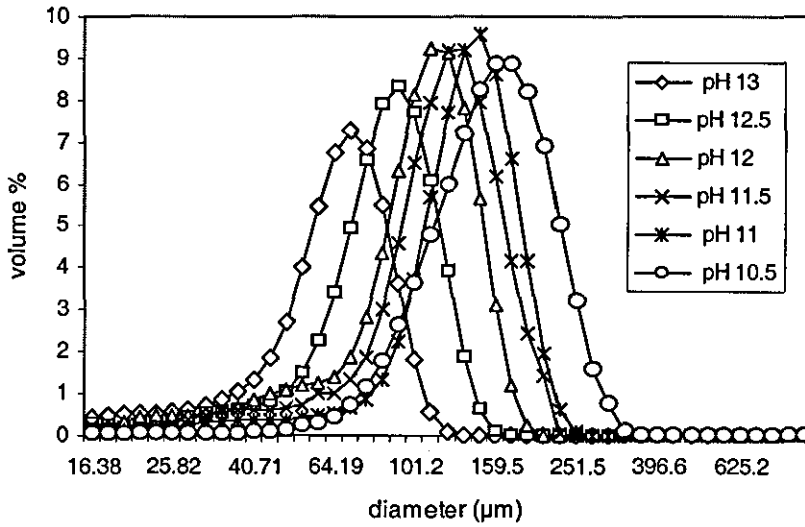


Figure 5.3.17.c. Effect of increasing pH on the main peak.

Peaks 1 and 2 are formed for pH values higher than 10.5 as was shown in figures 5.3.17.a. and 5.3.17.b. Therefore, the d_{32} values given for pH 10.5, in figure 5.3.18.a, for peaks 1 and 2, (0.87 μm and 3.1 μm , respectively), do not correspond to a peak. In fact, they correspond to a small fraction of fine particles that have diameters within the same ranges with peak 1 and 2, and they are only presented, in the figure, for comparison. Once these peaks are formed, for pH higher than 10.5, they have a constant d_{32} . For peak 1, d_{32} has a constant value, of 0.6 μm , over the pH range. Peak 2, also has an almost constant value of 4.5 μm , overall the pH range. Therefore, pH does not seem to affect the value of d_{32} for the two secondary peaks.

Figure 5.18.b shows the effect of pH on the main peak (peak 3). As the pH increases, d_{32} for peak 3 decreases significantly, from 139.9 μm for pH 10.5 to 55 μm for pH 13. Therefore, the pH has a significant effect on the d_{32} of the main peak causing it to decrease significantly. Summarising, the pH increase does not have any influence on d_{32} for the two secondary peaks 1 and 2, but it has a very strong effect on d_{32} of the main peak 3, causing it to decrease significantly.

The effect of the pH on d_{32} for the total particle size distribution is shown in figure 5.3.18.c. The total d_{32} decreases significantly as the pH increases. d_{32} for the total distributions shows very low values as the pH increases, compared to the corresponding values of the main peak (peak 3), suggesting that there is a strong influence of the two secondary peaks on the total d_{32} . The value of d_{32} for pH 10 before the secondary peaks appear was 135 μm ; a value very close to d_{32} for the main peak. But as the pH increases, the deviation of the total d_{32} from the d_{32} for peak 3 becomes larger, indicating that the influence of the small peaks becomes stronger. Therefore, the influence of the secondary peaks becomes stronger with increasing pH.

The increasing influence of the secondary peaks on the total d_{32} could be explained if the % volume or the number of the particles that belong to each diameter range is taken into consideration. Figure 5.3.19 shows the effect of pH on the % volume of particles that form each peak. For increasing pH the volume of the secondary peaks increases significantly, whereas the volume of the main peak decreases. For pH 10.5 the secondary peaks have not yet been formed and the volume of the fine particles that belong to the same diameter range with peak 1 and 2 are taken into consideration. Once the secondary peaks are formed, at pH from 10.5 to 11, their total volume increases with pH. The volume of peak 1 increases significantly with increasing pH. Peak 2 is initially larger for pH 11, then it diminishes gradually as the pH increases further. Therefore, both the main peak (peak 3) and peak 2 diminish as the pH increases. The overall tendency, for increasing pH, is to form fine particles within the diameter range 0.4 to 1.5 μm .

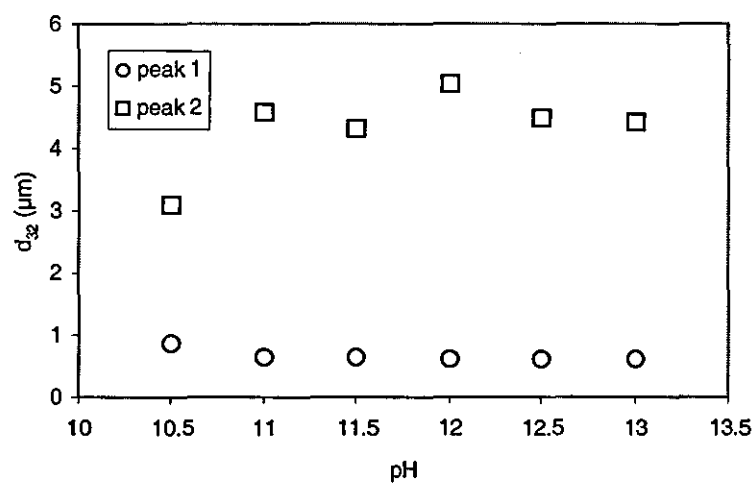


Figure 5.3.18.a. Effect of pH on peaks 1 and 2

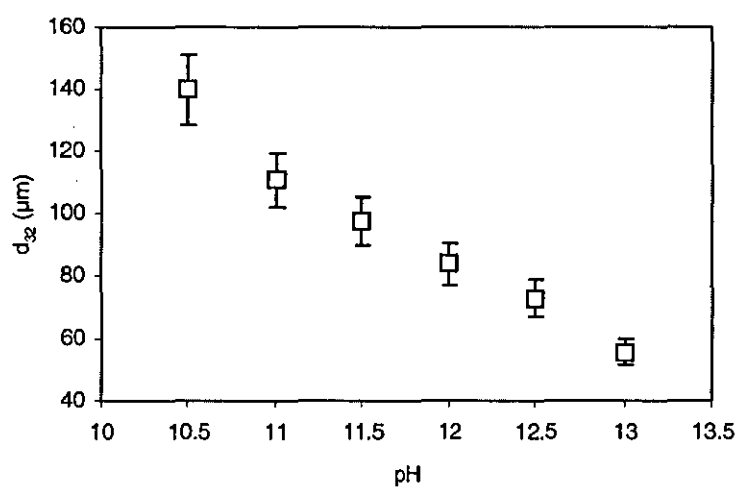


Figure 5.3.18.b. Effect of pH on the main peak (peak 3)

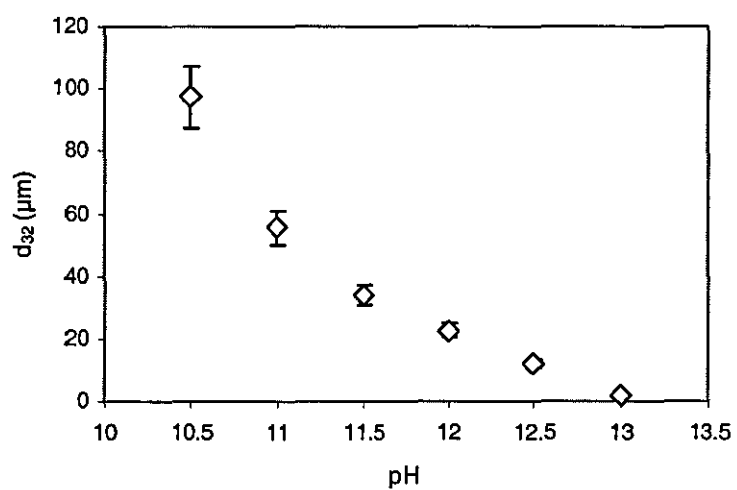


Figure 5.3.18.c. d_{32} for total distribution and increasing pH

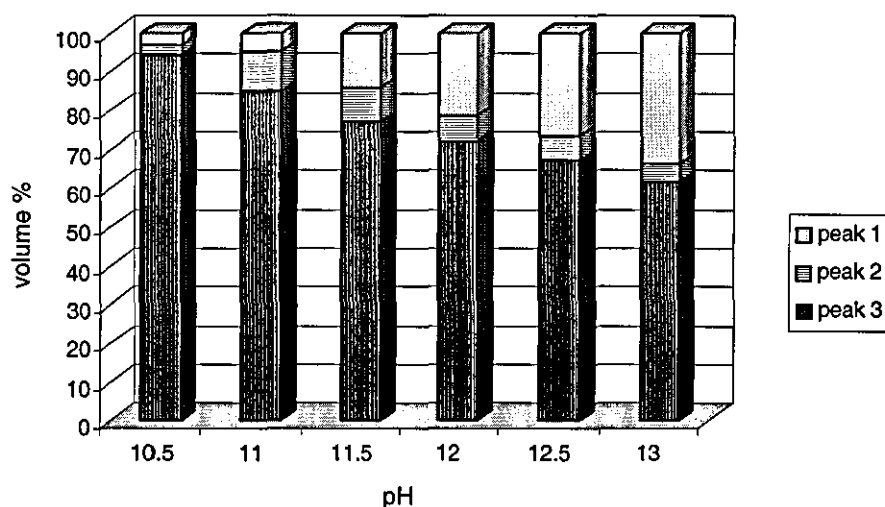


Figure 5.3.19. Volume % of each peak for increasing pH

5.3.6. Effect of temperature

The effects of the variation in reaction temperature (T) in suspension polymerisation are multiple. The temperature variation affects the attributes of both phases, continuous and dispersed. More specifically, it affects

- the rate of polymerisation
- the way the stabiliser distributes between the two phases
- the viscosity of both phases,
- the pH of the continuous phase, which has been proved to play an important role in the determination of the particle sizes

The influence of the temperature on so many different factors complicates the determination of the effect on the drop and particle sizes to a great extent. It is a multivariate problem, and the factors have to be decoupled, in order to ease the deduction of conclusions.

Two series of experiments are run in order to study the effect of T . For the first series of experiments, designated 'A', polymerisation experiments are run for the same conditions, with the same BPO concentration, but at different temperatures. In this case all the above mentioned variables change simultaneously leading to a combined

effect. The conditions used for these series are BPO concentration 0.06 mole/l, PMA-Na concentrations 0.6%, 0.9% and 1.2%, temperatures 60, 70, 75 and 80°C, stirring speed 12.5s^{-1} , and \square 0.1. The same stock stabiliser solution was used for the preparation of the continuous phase in all cases, and therefore, the initial pH varied only because of the temperature variations. No additional pH adjustment took place. The pH was 10.5 at 70°C, 10.8 at 60°C, 10.3 at 75°C, and 10.2 at 80°C.

For the second series of experiments, designated 'B', suspension polymerisation experiments were run for various temperatures and different BPO concentrations. For this series the BPO concentrations are such, that the rate of polymerisation is maintained constant in all cases. The BPO concentrations used were 0.06 mole/l at 70°C, The variables, in this case, will be the viscosity and the pH.

The effect of temperature on the viscosity of the continuous phase for both series is depicted in figure 5.3.20. The viscosity of the continuous phase decreases for increasing reaction temperature. Lower viscosity causes the formation of larger particles, as was shown in chapter 5.3.2. Therefore, in the absence of other influences, the temperature increase would be expected to lead to larger particles.

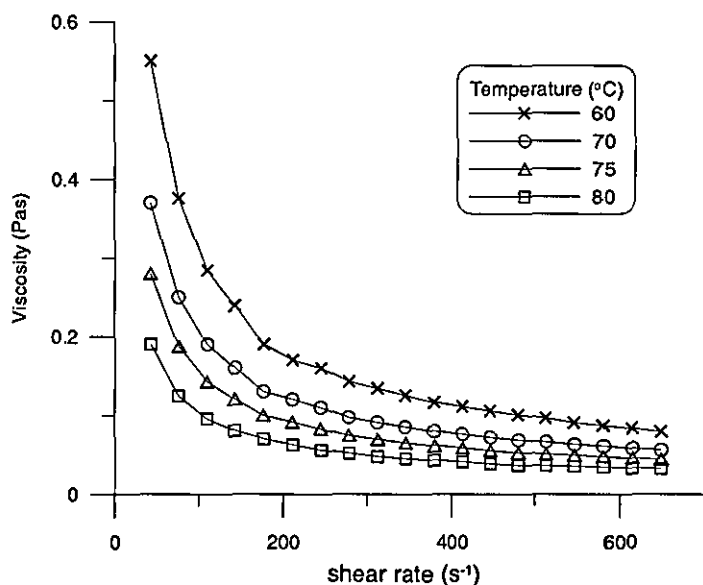


Figure 5.3.20. Continuous phase viscosity (0.6% PMA-Na) for various temperatures, for series A and B

The effect of the temperature on the pH of the continuous phase for both series is depicted in figure 5.3.21. Figure 5.3.21 shows the pH decrease with time during the

polymerisation, for various temperatures. The initial pH decreases with increasing temperature. In the absence of other influences, a pH decrease would also be expected to lead to larger particles as was shown in section 5.3.5.

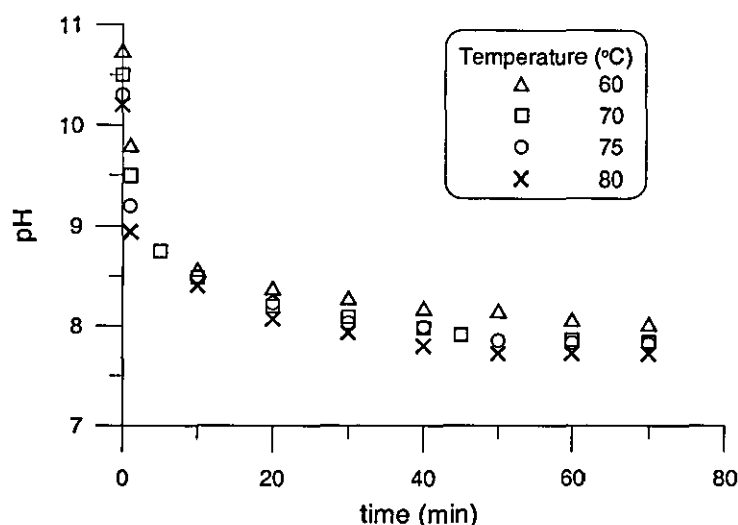


Figure 5.3.21. pH decrease with time for various temperatures

Series A: The conversion versus time for various temperatures, for the same BPO concentration is shown in figure 5.3.22. The increase of temperature has a strong effect on the reaction kinetics, increasing the polymerisation rate two to threefold for every 10°C of increase (Odián, 1991). The increase of the polymerisation rate causes the viscosity of the dispersed phase to increase more rapidly. This viscosity increase results in a decrease of the breakage rate that could lead to larger particles. The PSDs of beads produced for increasing temperature are shown in figure 5.3.23. The particle sizes increase for increasing temperature, and this increase could be attributed to the combined effect of the increasing polymerisation rate, the pH decrease and the viscosity decrease of the continuous phase. The distributions also become more narrow for increasing temperature, which could be attributed to the decrease of the continuous phase viscosity.

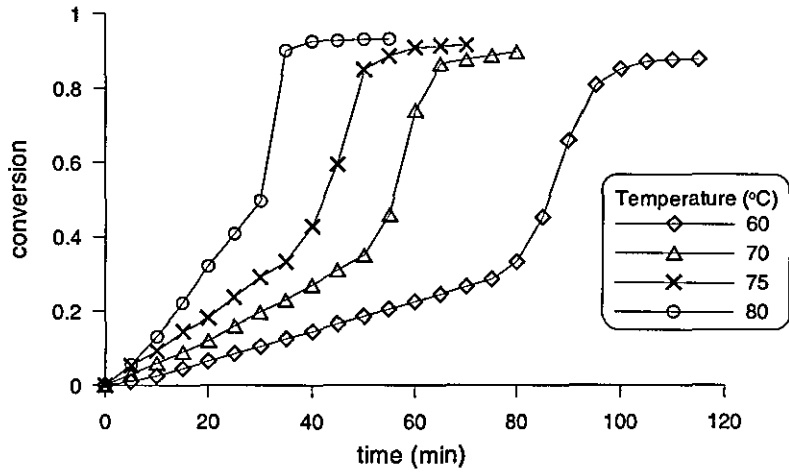


Figure 5.3.22. Conversion-time for various temperatures, and BPO 0.06mole/l

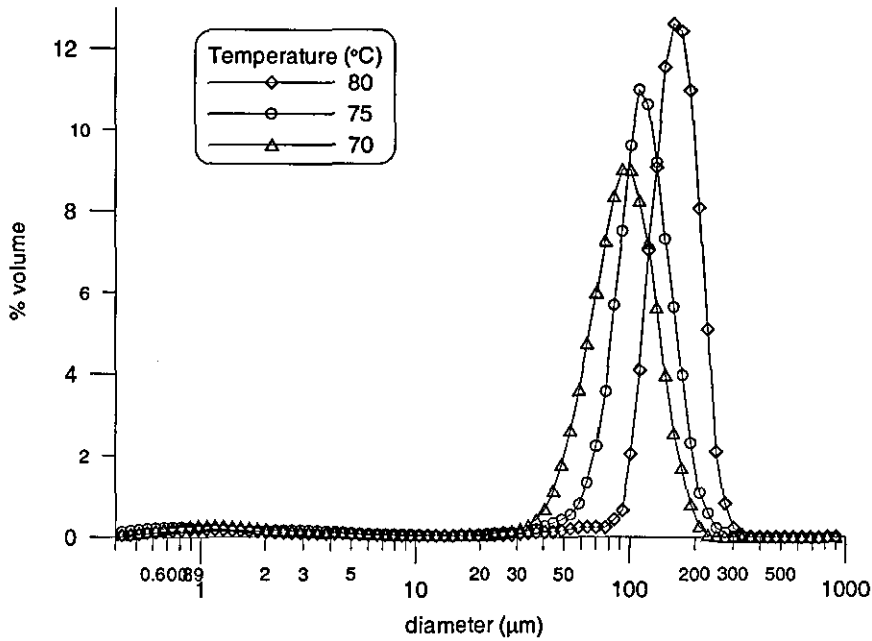


Figure 5.3.23. PSDs for various temperatures and 0.6% PMA-Na

Figure 5.3.24 shows the effect of the increasing temperature on d_{32} for various PMA-Na concentration. d_{32} increases for increasing temperature. Though, as the stabiliser concentration increases, the breakage rate is enhanced and d_{32} decreases.

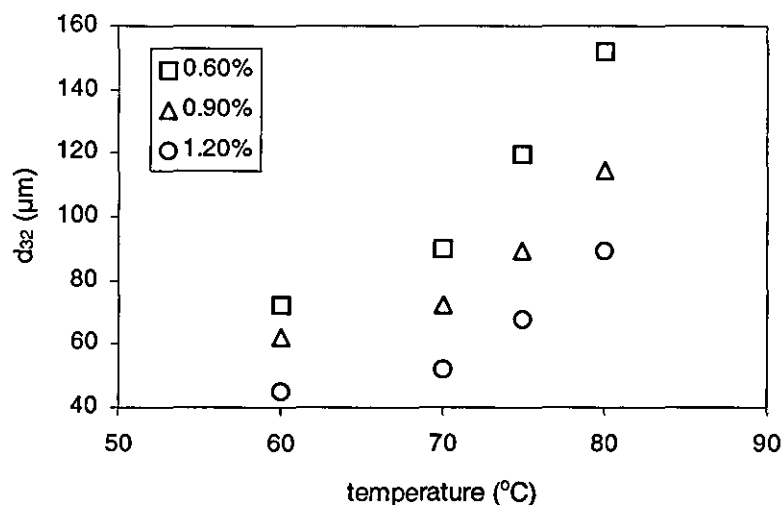


Figure 5.3.24. d_{32} series A and for PMA-Na concentrations 0.6, 0.9 and 1.2%

Series B: The conversion –time data for suspension polymerisation experiments run for various temperatures, by adjusting the BPO concentration in order to achieve equal polymerisation rates for all the runs, are depicted in figure 5.3.25. The BPO concentration is adjusted to 0.01 mole/l for 80 $^{\circ}\text{C}$, and to 0.025 mole/l for 75 $^{\circ}\text{C}$. The BPO concentration at 70 $^{\circ}\text{C}$, is 0.06 mole/l.

The Sauter mean diameters for these runs are shown in figure 5.3.26. They increase for increasing temperature but decrease for the same temperature and increasing PMA-Na concentration.

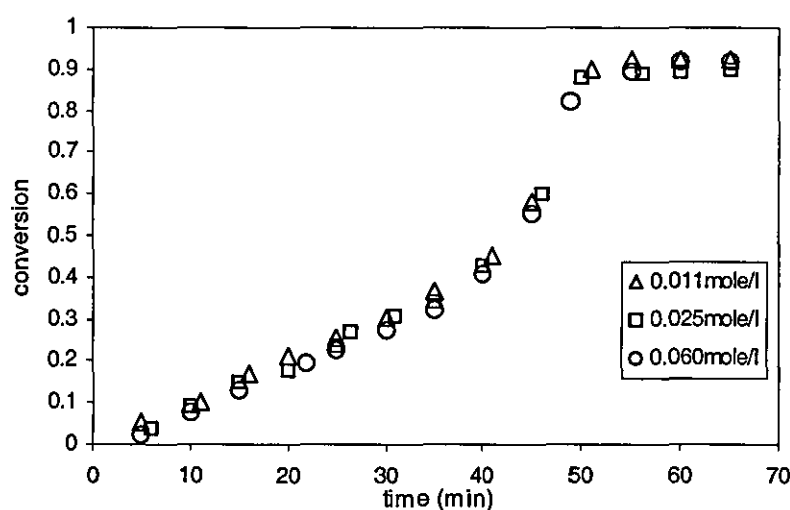


Figure 5.3.25. Conversion-time at various T, and BPO concentration adjusted to achieve the same reaction rate

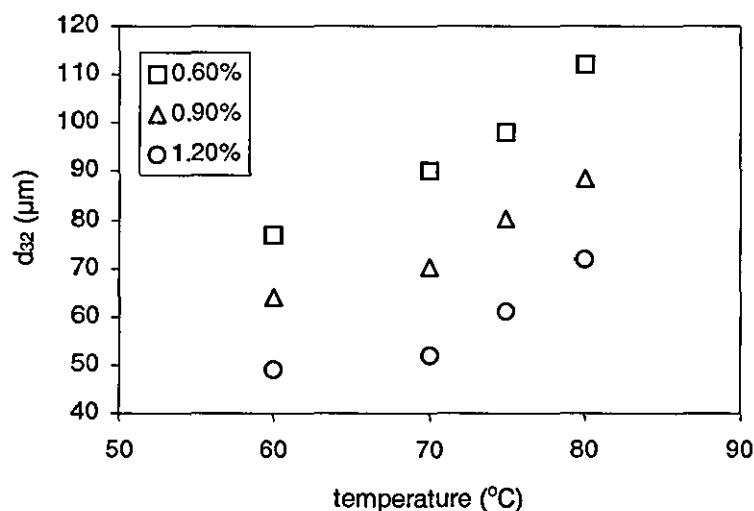


Figure 5.3.26. d_{32} of the final particles for series B and for PMA-Na concentrations: 0.6, 0.9 and 1.2%

Comparing the Sauter mean diameters for the two series A and B (figure 5.3.27), for increasing and constant polymerisation rate, respectively, the net effect of the polymerisation rate can be deduced. The polymerisation at 70°C , was used as a reference point and in both cases the same BPO concentration was used. Therefore, there is no difference in d_{32} between the two series A and B.

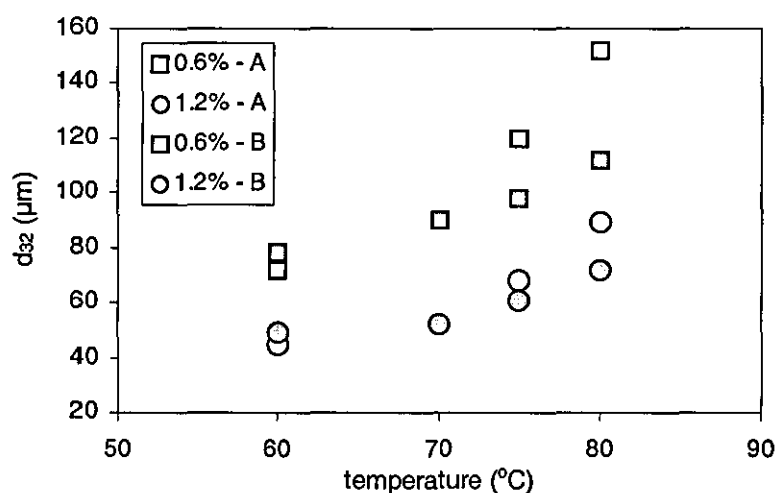


Figure 5.3.27. d_{32} for series A and B and for PMA-Na concentrations 0.6 and 1.2%

For the runs at 60°C , the BPO concentration was increased from 0.06 mole/l to 0.35 mole/l in order to achieve a higher polymerisation rate, equal to the polymerisation

rate for 70 °C. In the other cases, for 75 and 80°C, the BPO concentration was decreased in order to achieve a lower polymerisation rate, equal to the polymerisation rate at 70 °C.

This increase of the polymerisation rate for 60 °C for series B, results in a higher Sauter mean diameter. In the other cases, where the polymerisation rate is higher for series A, the higher Sauter mean diameters are also observed for series A. The Sauter mean diameters for 75 °C increase from 71.8 µm for series B, to 89 µm for series A, for 0.6% PMA-Na. The increase in d_{32} is higher for 80 °C, from 112 µm to 152 µm. This increase in the Sauter mean diameter between series A and B reflects the net effect of the increase in the polymerisation rate induced by the increase in temperature. The increase in d_{32} for increasing temperature in series B reflects the effect of the effect of temperature on the pH and the viscosity of the continuous phase.

5.3.7. Effect of the chain transfer agent

The effect of the chain transfer agent, which is n-dodecyl mercaptan (DMA) is examined here. The initiator concentration is 0.08 mole/l monomer, in all cases. The concentration of the chain transfer agent is 0.025 mole/l monomer. The conversion time data for the runs with and without n-dodecyl mercaptan are given in figure 5.3.28. Two stabiliser concentrations were used, 0.6% and 0.4% PMA-Na. The higher of the two concentrations is sufficient to maintain a constant d_{32} over all the conversion range, as described in section 5.4.1. For the second stabiliser concentration the particle size increases with increasing conversion. The initial pH of the continuous phase in all cases was 10.

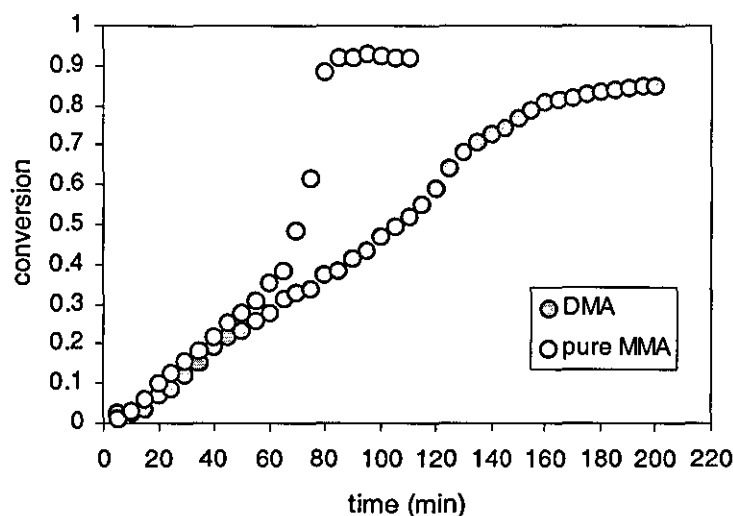


Figure 5.3.28. Conversion-time data for polymerisation with and without DMA

For the higher stabiliser concentration, 0.6% PMA-Na, the PSDs, over the total range of particle sizes, for two runs are presented in figure 5.3.29. The first run was carried out with the addition of chain transfer agent in the monomer phase, whereas the second run was carried out without DMA. For this concentration the particles in both cases are within the same range, and the PSDs are almost identical. The PSD for the run without DMA is a little higher than the PSD for the run with DMA. The addition of DMA results in a slightly shorter main peak.

A more significant difference exists in the fine particles' distributions, as shown in figure 5.3.30, for particles with diameters smaller than $10\mu\text{m}$. The volume of the fine particles for the run with DMA is significantly larger than the volume of the fine particles for the run without DMA. The dissolution of the monomer phase in the water phase may account for this difference. Because of the longer time that the polymerisation requires in the presence of DMA, the dissolution of the monomer in the aqueous phase may occur to a greater extent. The dissolution of the monomer in the water phase is one of the possible sources for the appearance of fine particles during the polymerisation.

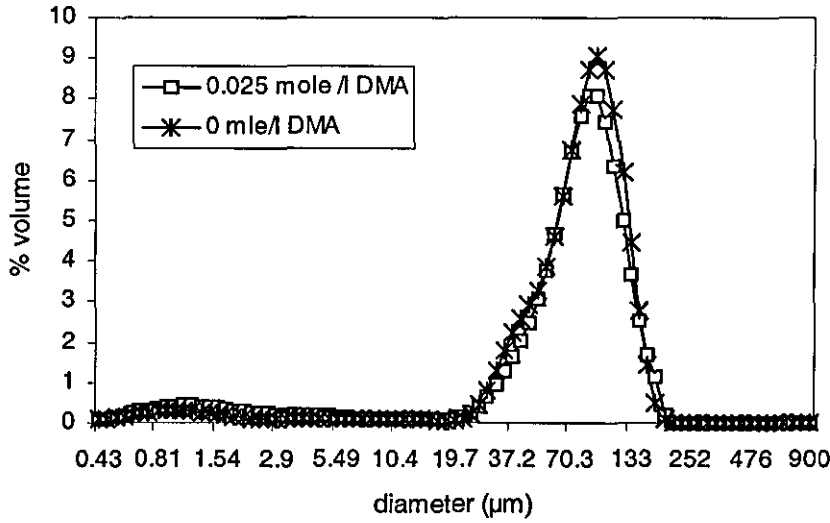


Figure 5.3.29. PSDs for runs with DMA and pure monomer, for 0.6% PMA-Na

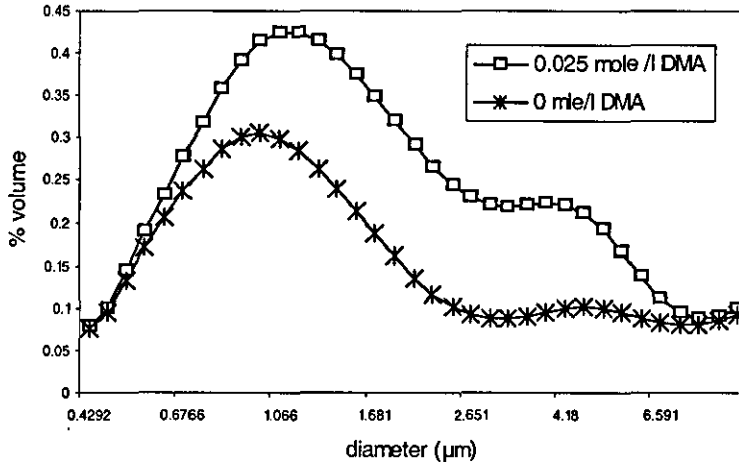


Figure 5.3.30. PSDs of fine particles, for runs with DMA and pure monomer, and for 0.6% PMA-Na

For the lower stabiliser concentration examined, 0.4% PMA-Na, the evolution of the particle size distribution for all particle sizes is depicted in figure 5.3.31. The particle sizes increase with increasing conversion. The shape of the PSD does not change significantly with conversion. It becomes slightly shorter and broader as conversion increases. The d_{\max} of the final polymer beads produced with DMA is 300 μm , whereas the d_{\max} of the polymer beads produced without DMA is 396 μm . Therefore, the maximum diameter is significantly smaller when DMA is used. This might be attributed to the lower rate of viscosity build up in the presence of DMA. Because the polymer produced in the presence of DMA has significantly lower molecular weight,

the rate of viscosity build up is lower, and therefore the resistance to breakage is lower, resulting in smaller particle sizes.

Figure 5.3.32, shows the evolution of the PSD for the fine particles, for 0.4% PMA-Na. Also here, there is a slight decrease of the volume of the fine particles with increasing conversion.

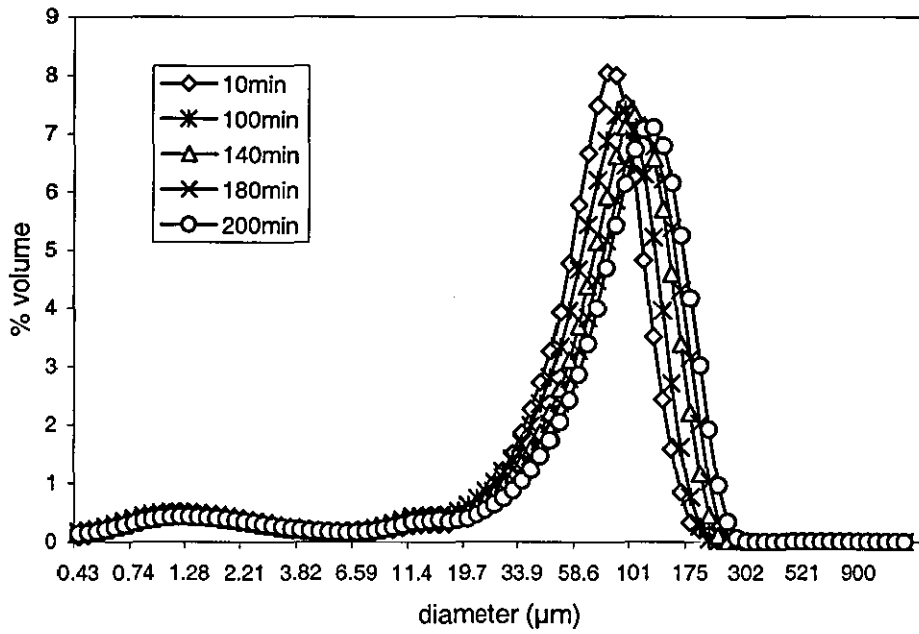


Figure 5.3.31. Evolution of the PSD, with DMA, and for 0.4% PMA-Na

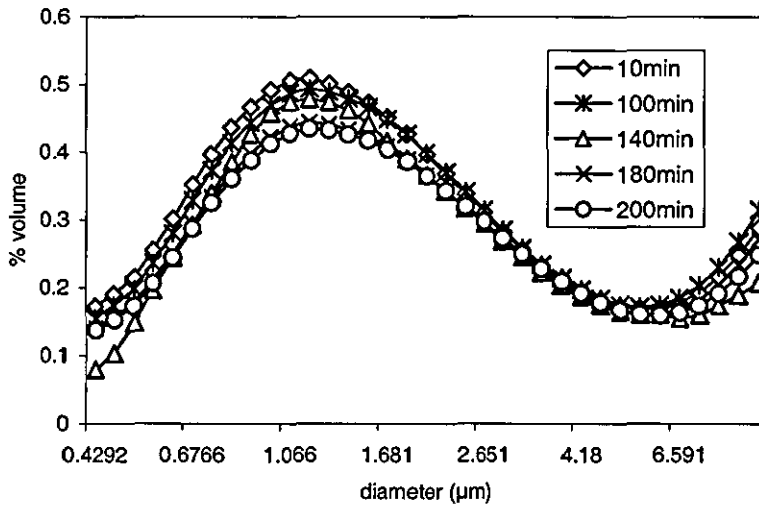
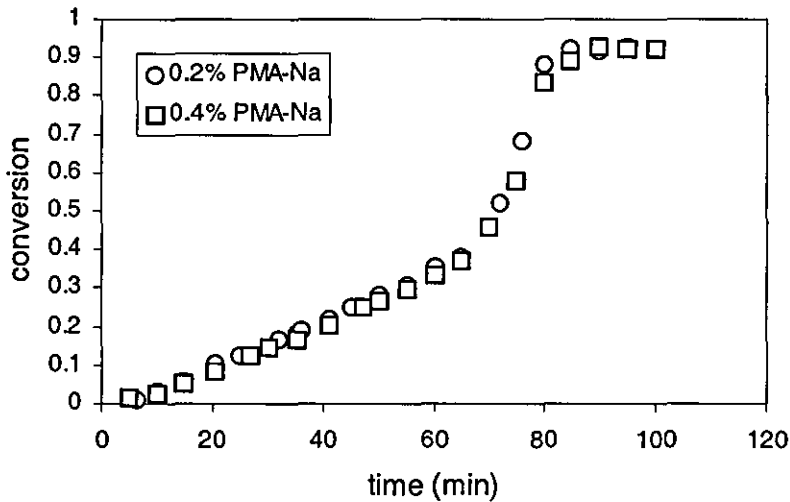


Figure 5.3.32. Evolution of the PSD for the fine particles, with DMA, and for 0.4% PMA-Na

5.3.8. Evolution of the particle size distribution during suspension polymerisation

In this section the evolution of the particle size distribution is examined. The stabiliser used was PMA-Na and the initiator concentration was 0.04 mole/l, and the initial pH 10. The conversion time data for these runs are presented in figure 5.3.33. Two cases are presented, for stabiliser concentrations 0.2% and 0.4% PMA-Na. In the first case the stabiliser concentration is low and significant coalescence occurs during the course of the polymerisation and mainly during the gel effect. In the second case the extent of coalescence is limited.



Figures 5.3.33. Conversion time data for 0.04 mole/l BPO, at 70°C, with 0.2% and 0.4% PMA-Na

Figures 5.3.34 and 5.3.35 show the evolution of the particle size distribution for 0.2% PMA-Na. The first of the two figures shows the evolution for particles with diameters larger than 10 μm , whereas the latter one shows the evolution of the fine particles (with diameters smaller than 10 μm) throughout the polymerisation reaction. For particles with diameters larger than 10 μm (figure 5.3.35) the particle sizes increase with conversion and their size distribution shifts to larger sizes. Coalescence occurs to a significant extent during the polymerisation reaction and especially during the gel effect, leading to the formation of a second broad peak at sizes larger than the main peak. The main peak becomes broader and shorter while the second broad peak increases in volume with increasing conversion. During the first 30 minutes, the main

peak of the distribution only shifts slightly to larger sizes. At 40 minutes, which corresponds to a conversion of about 23%, the second peak appears and starts to increase in volume thereafter.

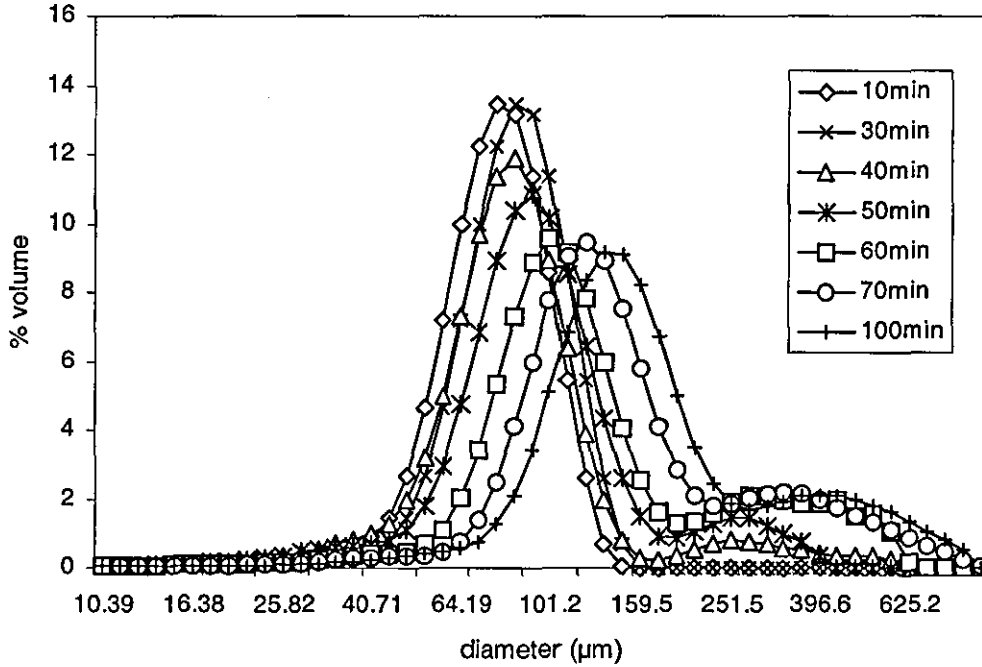


Figure 5.3.34. Evolution of the PSD for particles with diameter larger than $10\mu\text{m}$, and 0.2% PMA-Na

For particles with diameters smaller than $10\mu\text{m}$ (figure 5.3.35), there is a secondary peak of fine particles. This peak maintains a constant range of particle diameters throughout the polymerisation, but its volume decreases with increasing conversion. For the first 30 minutes the distribution of the fine particles remains almost constant. After 40 minutes the fine particles start to coalesce and their total volume, in the small size range, decreases with increasing conversion. Thus the higher concentration of fine particles occurs at the beginning of the polymerisation, and, as the polymerisation proceeds, the fine particles' concentration decreases.

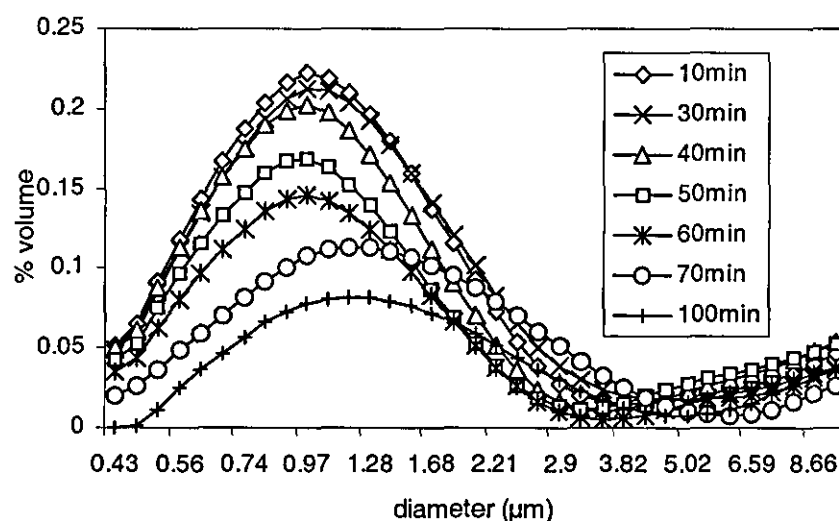


Figure 5.3.35. Evolution of the PSD for particles with diameter smaller than $10\mu\text{m}$, and 0.2% PMA-Na

In the second case, for a higher PMA-Na concentration 0.4% PMA-Na, the evolution of the particle size distribution differs significantly. Figure 5.3.36. shows the evolution of the particle sizes with diameters larger than $10\mu\text{m}$. The particle sizes increase with increasing conversion and their distribution shifts to larger sizes, but maintains the same shape throughout the polymerisation reaction. The coalescence seems to occur to a smaller extent because of the higher stabiliser concentration and the higher continuous phase viscosity. As a result, the second peak at sizes larger than the main peak does not appear in this case. For the first 40 minutes the main peak is only slightly shifted towards larger sizes. The most significant shift is observed after 40 minutes, for conversion higher than 23%, which was the conversion where the most significant changes were observed for 0.2% PMA-Na.

The fine particles' peak, shown in figure 5.3.37, decreases in volume with increasing conversion. The peak maintains almost the same volume for the first 40 minutes and then starts to decrease in volume because of coalescence of the fine particles. The decrease of the fine particles' peak occurs to a smaller extent, compared to the decrease of the same peak for a smaller stabiliser concentration, 0.2% (figure 5.3.35). This is attributed to the limited extent of coalescence in this system because of the higher stabiliser concentration.

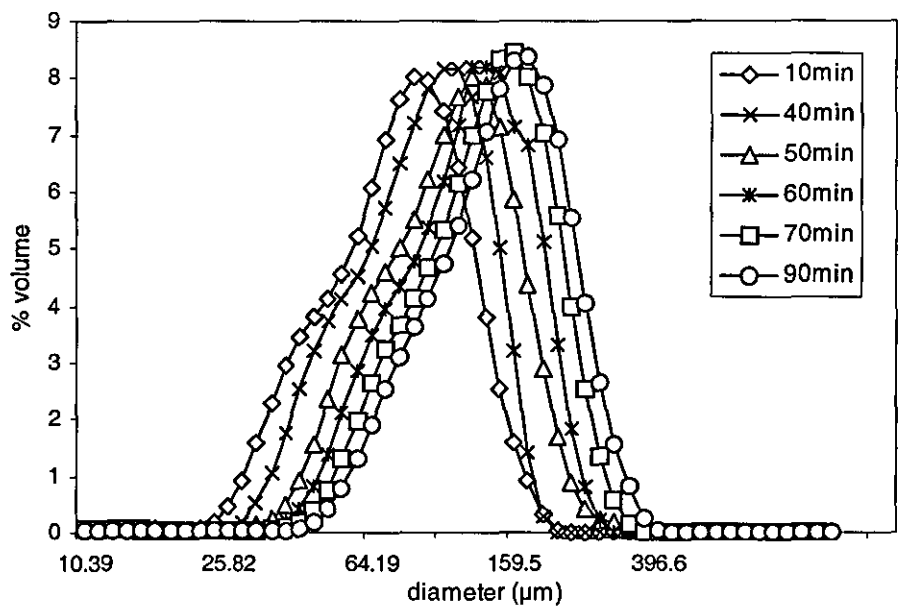


Figure 5.3.36. Evolution of the PSD for particles with diameter larger than 10µm, and 0.4% PMA-Na

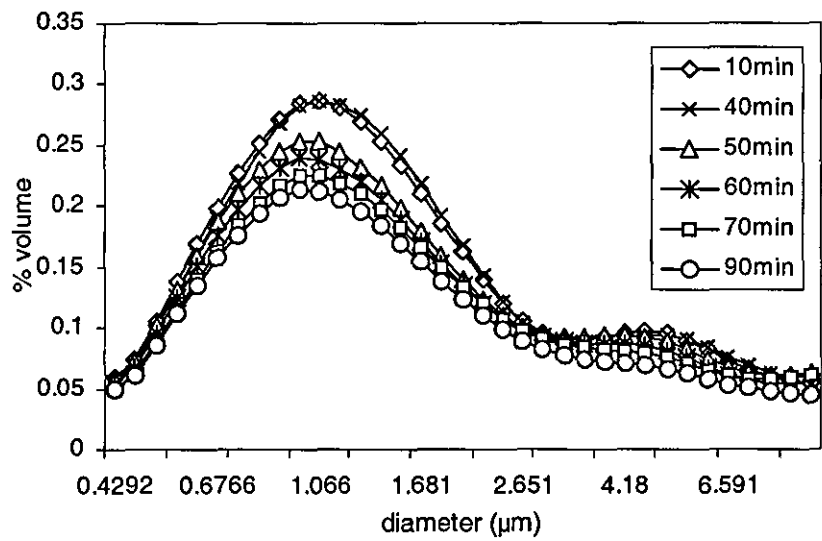


Figure 5.3.37. Evolution of the PSD for particles with diameter smaller than 10µm, and 0.4% PMA-Na

5.3.9. Conclusions

The main conclusions drawn from the series of experiments investigating factors that may influence the drop and particle sizes are:

- *Continuous phase viscosity:* The continuous phase viscosity has a strong effect and plays an important role on the determination of the drop and particle sizes. For both PMA-Na and APMA, an increase in the continuous phase viscosity causes a diminution of the particle sizes, and vice versa. The PSDs shift to smaller sizes and become slightly broader as the continuous phase viscosity increases. For the same continuous phase viscosity, APMA solutions produce smaller particles than PMA-Na solutions.
- *Stirring speed:* Increasing the impeller speed leads to an increase of the particle sizes. This is attributed to the non-Newtonian nature of the continuous phase. Increasing the stirring speed, causes the viscosity of the non-Newtonian continuous phase to decrease. According to the previous conclusion, since the viscosity decreases, the particle sizes increase.
- *Hold-up:* For increasing hold-up, d_{32} initially decreases, reaches a minimum and then starts to increase. The hold-up, for which d_{32} becomes minimum, increases for increasing stabiliser concentration and continuous phase viscosity.
- *Dispersed phase viscosity:* Increasing the dispersed phase viscosity causes the d_{32} to increase and the PSD to broaden significantly.
- *pH:* Increasing the initial pH of the continuous phase, causes the particle sizes to diminish, and leads to the formation of two secondary peaks, at size ranges up to 1.5 μm for the first one, and within the range from 1.5 to 10 μm for the second. The total volume of the secondary peaks increases with increasing pH, while the volume of the main peak decreases. The first peak increases monotonously, while the second peak, increases initially and then decreases. The overall trend is to form fine particles within the diameter range 0.4 to 1.5 μm .
- *Temperature:* Increasing the reaction temperature causes the particle sizes to increase. This decrease of the particle size is a combined effect caused, mainly, by

the viscosity decrease of the continuous phase as the temperature increases, and by the increase of the polymerisation rate. The effect of the temperature on the particle size is more evident for lower stabiliser concentrations.

- *Chain transfer agent (CTA):* In the presence of a chain transfer agent the volume of the particles with diameters smaller than 10 μm increases, and the size of the maximum diameter decreases significantly. The increase of the volume of fine particles may be caused by the dissolution of the monomer in the continuous phase to a greater extent, in the presence of a CTA. The diminution of the maximum particle size could be attributed to the lower rate of viscosity build up in the drops.

5.4. Factors required for the investigation of the dispersion mechanism

Among the factors that influence the drop and particle sizes examined, the continuous phase viscosity was proved to play a very important role, not only for increasing stabiliser concentration, but also for increasing stirring speed, and for increasing temperature. The viscosity of the reaction mixture for increasing hold-up also was a determining factor for the formation of the drops. This strong effect of the viscosity could be an important factor that determines the drop breakup mechanism in the initial dispersion. In order to determine the dispersion mechanism, we have to measure, calculate or estimate the required factors. These factors are the apparent viscosity of the continuous phase, the Kolmogorov macroscale of turbulence, the dissipated power, the interfacial tension, the density of the two phases, the interfacial tension and the maximum drop diameters. The factors required for the determination of the dispersion mechanism are presented and calculated in this chapter.

Three series of suspension polymerisation experiments were run in order to investigate the dispersion mechanism when polyelectrolyte stabilisers (PMA-Na and APMA) are used for the suspension polymerisation of MMA (table 5.4.1). For the first series of experiments, designated A, sodium polymethacrylate (PMA-Na) is used as a suspending agent. Series A consists of 3 groups of experiments for 3 different impeller speeds, A₁ for 750 rpm or 12.5 s⁻¹, A₂ for 850 rpm or 14.17 s⁻¹ and A₃ for 15.83 s⁻¹. For the second series, designated B, ammonium polymethacrylate (APMA) was used as suspending agent in the continuous aqueous phase, and the impeller speed was 750 rpm or 12 s⁻¹. For series A and B, the dispersed, organic, phase was pure MMA, while for the third series, designated C, PMMA was predissolved in MMA prior to polymerisation in order to examine the combined effect of the viscosities of the two phases. PMA-Na was used as a suspending agent for series C.

The dispersed phase volume fraction was 0.1 for all series. The initiator concentration in the monomer was always the same 0.04 mole/l. For series A the PMA-Na concentration in the continuous phase varied from 0.5 to 1.2 % resulting in an increase of the continuous phase viscosity. In series A, the viscosity and the density of the dispersed phase were constant in all experiments, and equal to the viscosity and density of the pure monomer, which are 0.5x10⁻³ Pas and 910 kgm⁻³ respectively, at the reaction temperature. For series B, the APMA concentration in the continuous

phase varied from 0.78% to 1.56% resulting in increasing continuous phase viscosity also. For series C, the PMA-Na concentration remained constant at 0.6%, resulting in constant continuous phase viscosity, but the viscosity of the organic phase was increased by dissolving solid PMMA prior to polymerisation. The polymerisation temperature was 70°C. The stabiliser concentrations used for these series of experiments were chosen by using the criteria for the required stabiliser concentration that are presented in the following chapter (5.4.1). The initial pH for all the experiments run with PMA-Na was 10, while the initial pH for all the runs with APMA was 9.

Table 5.4.1. Experimental conditions

<i>Series</i>	<i>Groups</i>	<i>Stabiliser</i>	<i>Initial pH</i>	<i>Organic phase</i>	<i>Impeller speed</i>	<i>Stabiliser concentration</i>
A	A ₁	PMA-Na	10	MMA	12.5 s ⁻¹	0.5-1.2%
	A ₂	PMA-Na	10	MMA	14.17 s ⁻¹	0.5-1.2%
	A ₃	PMA-Na	10	MMA	15.83 s ⁻¹	0.5-1.2%
B		APMA	9	MMA	12.5 s ⁻¹	0.78-1.56%
C		PMA-Na	10	MMA+ PMMA	12.5 s ⁻¹	0.6%

5.4.1. Required stabiliser concentration

The determination of the dispersion mechanism requires knowledge of the maximum drop sizes, d_{\max} , rather than an average drop diameter, because d_{\max} appears in established hydrodynamic relationships, whereas the average d does not. The maximum drop sizes could be considered equal to the maximum particle sizes when sufficient quantity of stabiliser is used, to prevent coalescence from occurring (Konno et al. 1982, Larzak et al. 1998, Jahanzad et al., 2004). In order to determine the stabiliser concentration that satisfies the previous requirement, suspension polymerisation experiments were run with a wide range of stabiliser concentrations and the evolution of the Sauter mean drop diameter was monitored throughout the reaction. In figures 5.4.1, a and b, the Sauter mean drop diameters for various conversion intervals and for various stabiliser concentrations are depicted for series

A₁ and B, respectively. As can be observed, for series A₁ (figure 5.4.1.a) and PMA-Na concentrations lower than 0.5%, the Sauter mean drop diameter increases with the conversion, which means that the drops coalesce as their viscosity increases. For PMA-Na concentrations higher than 0.5%, the mean drop sizes remain constant over all the conversion range. Therefore, PMA-Na concentrations higher than 0.5% could be considered sufficient to prevent coalescence during the course of polymerisation and, for these conditions, the drop diameters could be considered equal to the final particle diameters. For series B (figure 5.4.1.b), and APMA concentrations equal to 0.62%, or higher, could be considered sufficient to prevent coalescence over all the range of conversion, whereas for lower concentrations there was significant coalescence occurring and the Sauter mean diameter increased with conversion.

Figure 5.4.2 shows the sauter mean diameters with increasing conversion for the C series of experiments. The Sauter mean diameter is shown to increase as the dispersed phase viscosity increases, but coalescence is prevented with a 0.6% w/w stabiliser concentration and the drop sizes remain constant until the end of the reaction.

Therefore, over this range of concentrations the particle size distributions can be considered to reflect the drop size distributions.

Figure 5.4.3 shows the drop/particle size distribution from an early stage of the reaction, when the conversion from monomer to polymer is only 0.19, through the gel effect for conversion 0.38 and at the end of the reaction for conversion 0.91. The drop / particle size distribution seems to remain the same throughout the course of the reaction and it is not shifted to larger sizes after the gel effect, which means that with the stabiliser concentrations used, coalescence is prevented from occurring and the final particles reflect the initial drop sizes.

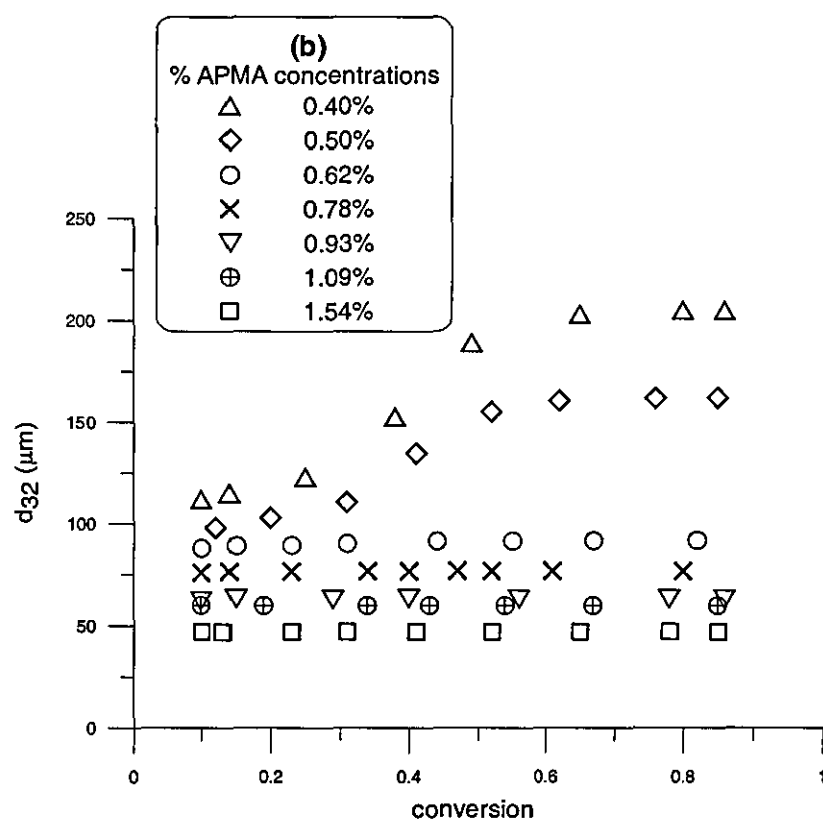
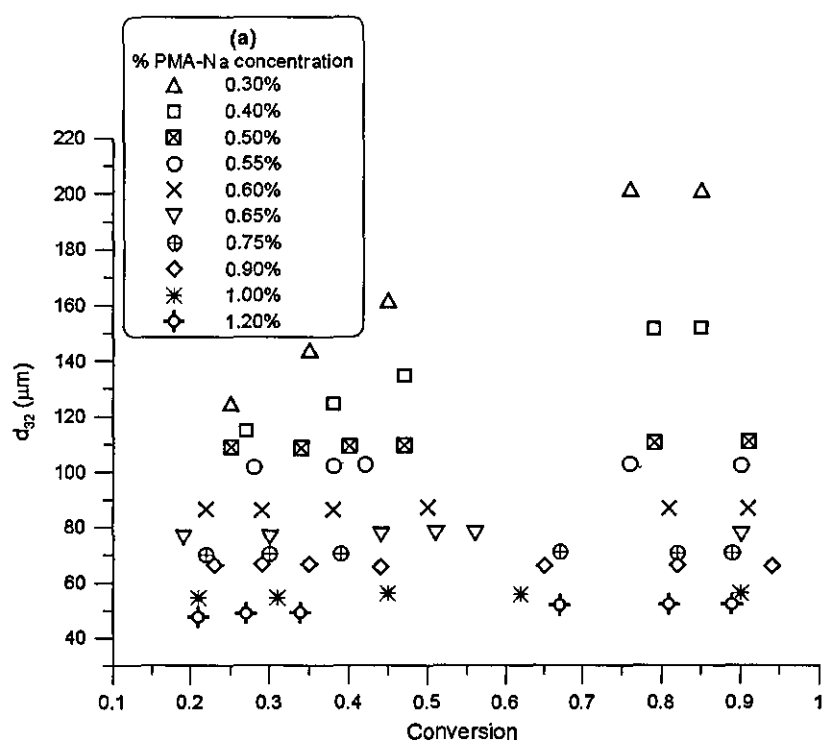


Figure 5.4.1: Evolution of d_{32} with conversion for various stabiliser concentrations at 70°C, (a) PMA-Na (b) APMA

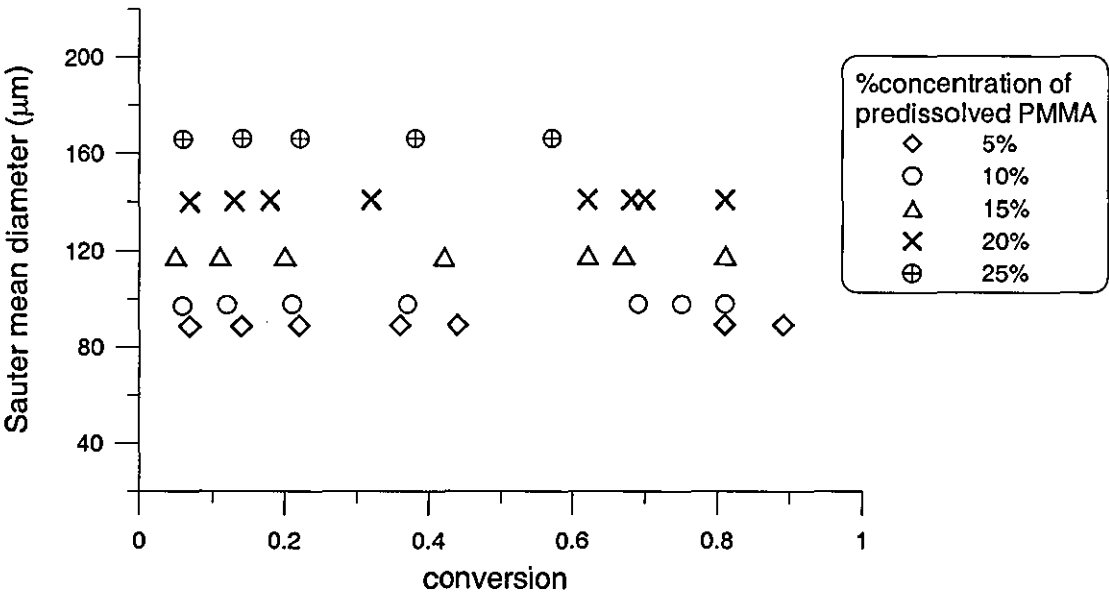


Figure 5.4.2: Sauter mean diameter with the conversion for various concentrations of predissolved PMMA, for 0.6% PMA-Na

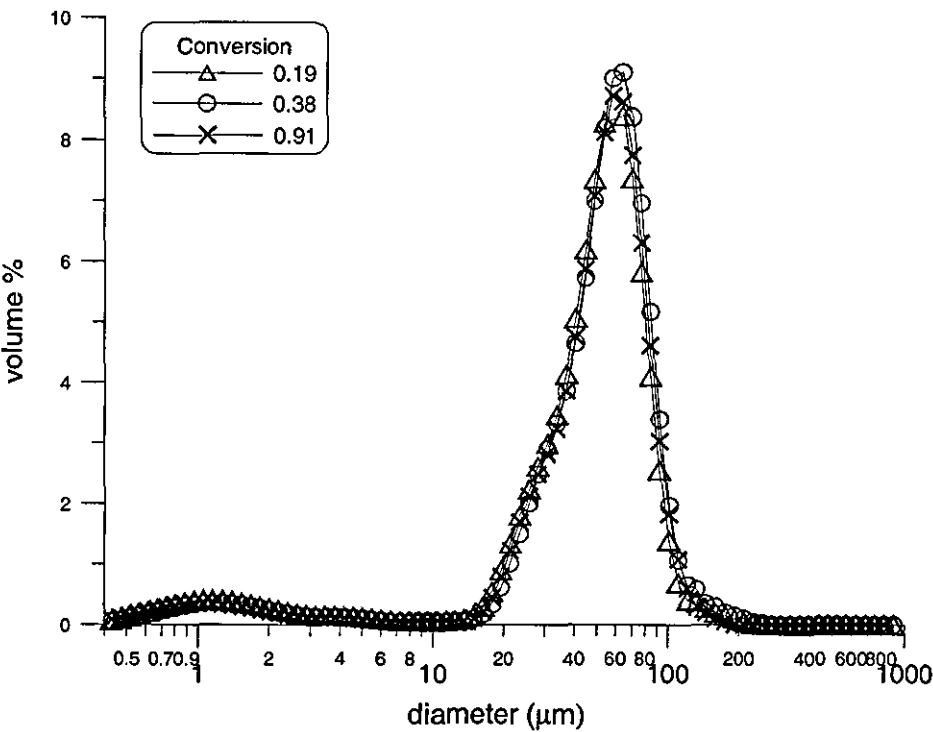


Figure 5.4.3. PSD for increasing conversion for 0.6% PMA-Na

5.4.2. Apparent viscosity of the non-Newtonian continuous phase.

The viscosity of the continuous phase is a shear dependent variable and therefore its value can only be considered for a specific shear rate. Although, the viscosity can be measured over a wide range of shear stress values, as shown in figures 5.4.4 and 5.4.5, for PMA-Na and APMA respectively, the shear stress that prevails in the reactor tank is not known and hence the corresponding viscosity could not be determined, unless an appropriate theory was used, to estimate the pair of values shear stress and corresponding viscosity. For this reason, the pair of variables: apparent viscosity and shear rate in the reactor tank are estimated by using the theory proposed by Metzner and Otto (1957). According to this theory, an average shear rate, $(du/dr)_A$, must exist in an agitated vessel. This average shear rate is such that the apparent viscosity corresponding to $(du/dr)_A$ is equal to the viscosity of the Newtonian fluid which would show exactly the same power consumption under identical conditions, at least in the laminar region. This average shear rate is linearly related to the rotational speed of the impeller. According to this theory proposed by Metzner and Otto, the average shear rate and hence apparent viscosity depend only on the rotational speed of the impeller

$$\left(\frac{du}{dr}\right)_A = k_s N \quad (5.4.1)$$

where k_s = constant and N = rotational speed of the impeller. The assumption that average fluid shear rates are related only to impeller speed has led to a useful correlation of the power requirements for agitation of non-Newtonian fluids.

Ducla et al. (1983) determined the effective viscosity of the continuous phase by using the power consumption in stirred tanks based on the concept of the effective rate of deformation proposed by Metzner and Otto. That rate is proportional to the rotational speed of the impeller: $\gamma_e = kN$ where k is a function of the vessel geometry and not of the rheological properties of the fluid and it is essentially the same constant as the k_s used by Metzner and Otto.

In this work the rheological properties were assumed to be represented by a power-law model

$$\tau = K\gamma^n \quad (5.4.2)$$

To obtain the average shear rate, the equations (5.4.1) and (5.4.2) are combined as follows: $\tau = K\gamma^n = K\left(\frac{du}{dr}\right)_A^n = K(k_s N)^n$. Hence, the apparent viscosity can be calculated from the equation:

$$\mu_{app} = K(k_s N)^{n-1} \quad (5.4.3)$$

This flow model has been widely used for shear dependent viscosity i.e. shear thinning ($n < 1$).

Metzner and Otto calculated the constant k_s for various impellers including 6-bladed disc turbines, marine propellers, anchors. but their study does not include 4-bladed impellers. Thus, the constant k_s is calculated by the equation established by Calderbank and Moo-Young (1959), where B_k = constant, n = the viscosity index:

$$k_s = B_k \left(\frac{4n}{3n+1} \right)^{\frac{n}{1-n}} \quad (5.4.4)$$

When 4 baffles are used with $n < 1$ and the ratio of the Tank and impeller diameters is $T/D > 1.5$ the value of B_k can be estimated from the literature (Skelland, 1967, Skelland and Kanel 1990). Here, the value of B_k was found to be $11 \pm 10\%$.

Determination of K and n indices

For the determination of the indices K and n used in equation (5.4.3), shear stress versus shear rate data for various concentrations of PMA-Na and APMA that are depicted in figures 5.4.1 and 5.4.2 were fitted by regression to the power law equation. The K and n values that derive from these data, as well as the k_s values calculated from equation 5.4.4, are reported in table 5.4.2. The constant k_s is calculated by using the aforementioned values of the viscosity index n , and $B_k = 11$.

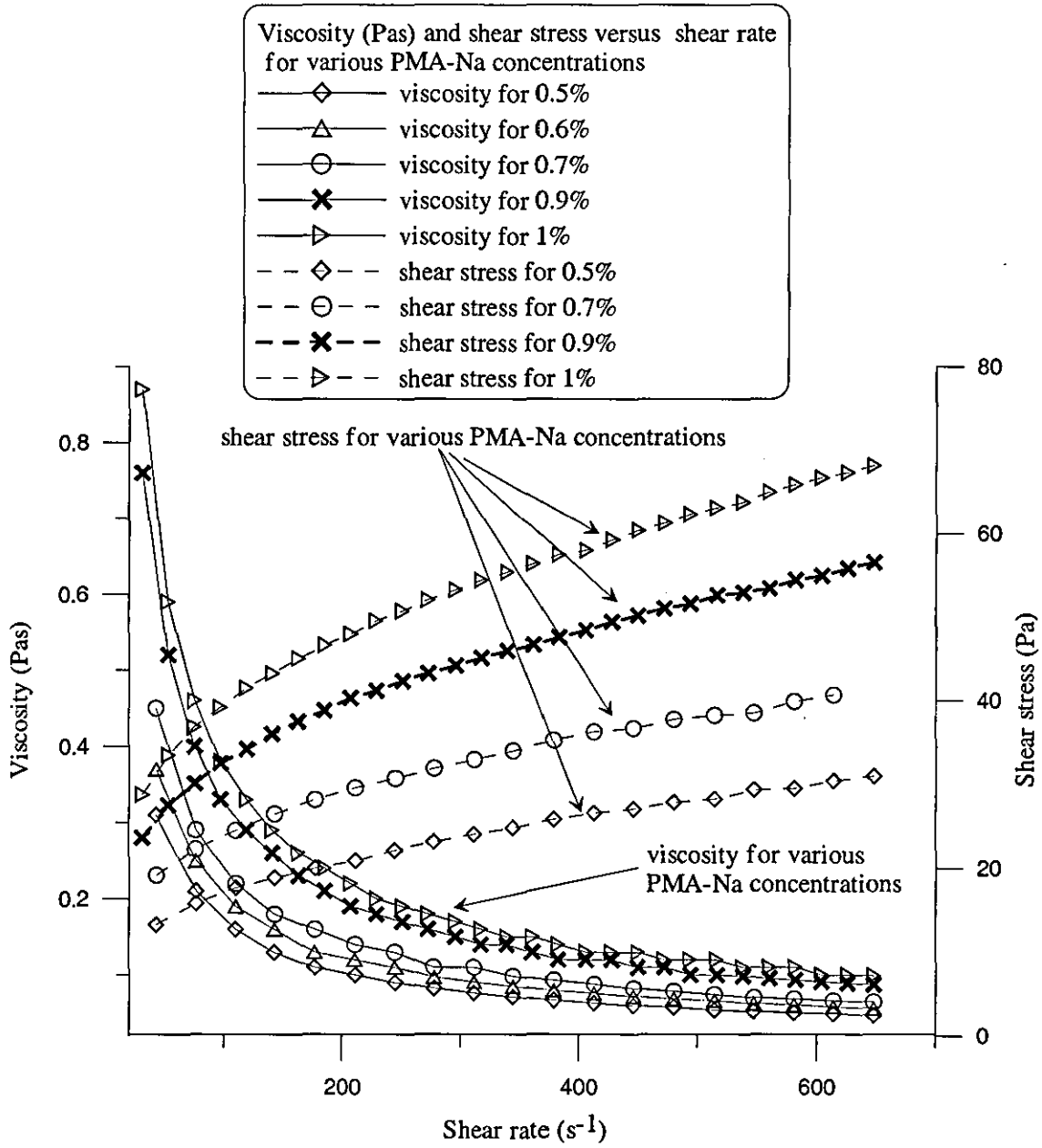


Figure 5.4.4: Viscosity and shear stress versus shear rate for various PMA-Na concentrations at the reaction temperature ($70^{\circ}C$)

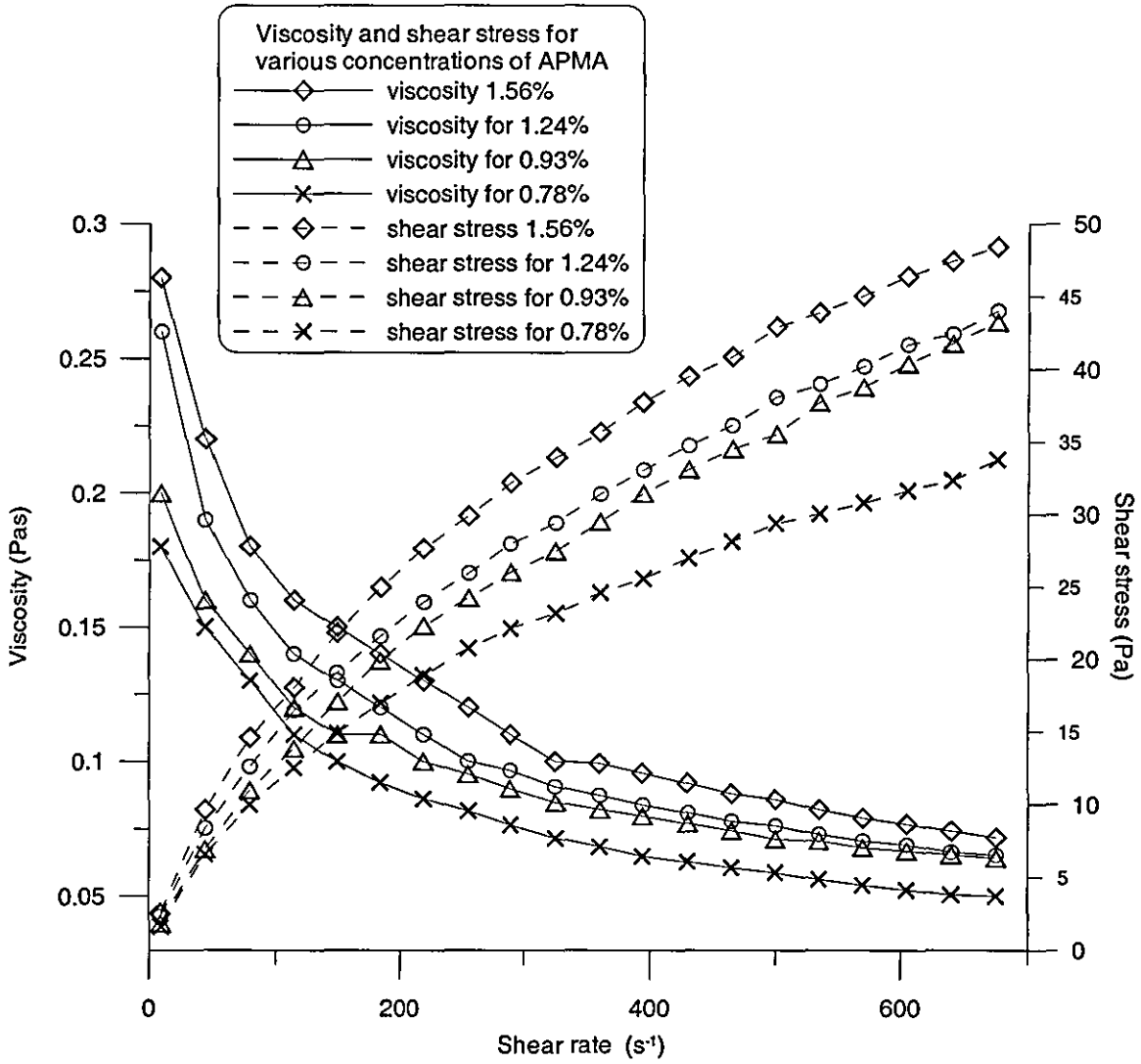


Figure 5.4.5: Viscosity and shear stress versus shear rate for series B₁, for various APMA concentrations at the reaction temperature (70°C), at pH 9

As can be observed in table 5.4.2., the viscosity index n for APMA solutions is higher for the viscosity index of PMA-Na solutions, meaning that the two stabilisers exhibit a different shear thinning behavior.

The viscosity of the reaction mixture is calculated by using the following expressions (Vermeulen, 1955)

$$\mu_m = \frac{\mu_{appc}}{1 - \phi} \left(1 + \frac{1.5\mu_d\phi}{\mu_d + \mu_{appc}} \right) \quad (5.4.5)$$

where

μ_m = viscosity of reaction mixture

μ_d = viscosity of dispersed phase and

μ_{appc} = apparent viscosity of continuous phase

Table 5.4.2: Values of K , viscosity index n , and k_s , for series A

Type of stabiliser	% concentration	K (Pas^n)	n	k_s
PMA-Na	1.2	9.884	0.321	8.99
	1.0	9.627	0.306	9.79
	0.9	8.502	0.291	9.82
	0.75	6.975	0.294	9.81
	0.7	6.324	0.289	9.82
	0.65	6.223	0.290	9.05
	0.6	4.583	0.326	9.76
	0.55	3.363	0.356	8.95
	0.5	3.793	0.326	9.76
APMA	0.78	0.948	0.550	8.76
	0.93	0.780	0.613	8.72
	1.09	1.086	0.561	8.73
	1.24	1.221	0.557	8.76
	1.40	1.307	0.553	8.76
	1.56	1.396	0.549	8.76

5.4.3. Density and interfacial tension

The measured values for the density of the continuous phase and the interfacial tension between the polyelectrolyte solutions and the monomer are given in table 5.4.3

The density of the reaction mixture is then calculated by using the following expression (Vermeulen, 1955)

$$\rho_m = \varphi\rho_d + (1-\varphi)\rho_c \quad (5.4.6)$$

where ρ_m = density of reaction mixture

ρ_d and ρ_c = density of dispersed and continuous phase respectively

Table 5.4.3. Density and interfacial tension for various PMA-Na and APMA concentrations.

% PMA-Na concentration	1.2	1.0	0.9	0.75	0.7	0.65	0.6	0.55	0.5
Density (kgm ⁻³)	1010	1008	1007	1006	1005	1005	1004	1004	1003
Interfacial tension x10 ³ (N/m)	14.9	14.3	12.9	13.0	13.0	12.7	13.0	13.0	12.8
% APMA concentration	1.56	1.40	1.24	1.09	0.93	0.78			
Density (kgm ⁻³)	994	994	993	993	993	992			
Interfacial tension x10 ³ (N/m)	12.4	12.6	12.5	12.4	12.1	11.7			

5.4.4. Dissipated power

The dissipated power, P , is calculated by using the power number N_p estimated by empirical equations (Nagata, 1975), which have been widely used (Sumi and Kamiwano, 2001; Roychoudhury et al., 1999; Chen et al., 1998; Moreira et al., 1995), in a general form covering both laminar and turbulent regions. More specifically the first term of the right hand side in the following equation corresponds to the laminar region, whereas the latter term corresponds to the turbulent region.

$$N_p = \frac{A}{Re} + B \left(\frac{10^3 + 0.6 Re}{10^3 + 1.6 Re} \right)^y \quad (5.4.7)$$

where

$$A = 14 + b/T(670(D/T - 0.6)^2 + 185) = 100$$

$$B = 10^{\{1.3 - 4(b/T - 0.5)2 - 1.14(D/T)\}} = 6.3$$

$$y = 1.1 + 4(b/T) - 2.5(D/T)^5 - 7(b/T)^4 = 2.52$$

$$\text{and } Re = \frac{ND^2 \rho_m}{\mu_m} \quad (5.4.8)$$

T is the tank diameter, and D and b are the impeller diameter and width respectively. It should be noted that the power required by two paddles at an arbitrary distance apart is equal to the power consumed by a single paddle with double width. Additionally, the power required by an impeller having four blades is equal to that required for a paddle with double width. Thus, for this case that two impellers with four blades are used the dimension b (impeller width) should be multiplied by a factor 4.

The dissipated power is then calculated from the equation given below

$$P = N_p \rho_c N^3 D^5 \quad (5.4.9)$$

and the dissipated power per unit mass is given by

$$\varepsilon = \frac{P}{\rho V} \quad (5.4.10)$$

where V is the reactor volume

The values calculated for N_p and P, and the energy dissipation rate ε are presented in table 5.4.4 for series A, and 5.4.5 for series B.

5.4.5. Kolmogorov turbulence macroscale

The Kolmogorov scale is defined by the equation

$$\eta = \varepsilon^{-1/4} \nu_c^{3/4} \quad (5.4.11)$$

where ε is the dissipated power per unit mass of the stirred suspension and ν_c is the kinematic viscosity of the continuous phase. It is a very important parameter because it provides information about the viscosity influence on the droplet breakup.

All the quantities required for the determination of the dispersion mechanism are presented in table 5.4.4, for series A, in table 5.4.5, for series B, and table 5.4.6, for series C. Among these, there is also the viscosity ratio, $p = \mu_d / \mu_{appc}$, where μ_d is the viscosity of the dispersed phase and μ_{appc} is the apparent viscosity of the continuous phase.

Table 5.4.4. Results for PMA-Na (series A): Viscosity, Re , N_P , power, dissipated power, Kolmogorov scale, viscosity ratio, maximum diameter, and Taylor number

<i>Stirring speed</i>	<i>% PMA-Na concentration</i>	μ_{app} (<i>Pas</i>)	Re	N_P	P (<i>W</i>)	ε (<i>W/kg</i>)	$\eta \times 10^6$ (<i>m</i>)	$p \times 10^3$	d_{max} $\times 10^6$ (<i>m</i>)	Ta
750rpm	1.2	0.379	53.2	7.43	1.500	3.000	2049	1.330	101	116.9
	1.0	0.343	58.8	7.18	1.448	2.896	1920	1.470	112	139.9
	0.9	0.281	71.8	6.72	1.353	2.706	1682	1.797	142	170.7
	0.75	0.234	86.0	6.33	1.274	2.548	1490	2.155	158	204.6
	0.7	0.217	92.6	6.08	1.221	2.483	1419	2.440	167	231.4
	0.65	0.205	98.1	6.06	1.218	2.436	1366	2.460	176	246.4
	0.6	0.180	111.6	5.80	1.165	2.330	1254	2.801	187	265.5
	0.55	0.153	131.2	5.48	1.100	2.200	1126	3.296	212	312.1
	0.5	0.149	134.5	5.43	1.090	2.180	1108	3.379	230	320.0
850rpm	1.2	0.348	58.6	7.19	2.115	4.230	1764	1.448	110	129.6
	1.0	0.314	64.8	6.95	2.042	4.084	1651	1.603	125	143.2
	0.9	0.257	79.2	6.50	1.908	3.815	1444	1.964	149	175.1
	0.75	0.214	94.9	6.13	1.796	3.592	1280	2.354	169	209.6
	0.7	0.199	102.1	5.98	1.751	3.501	1219	2.535	178	225.5
	0.6	0.165	122.6	5.61	1.644	3.288	1079	3.048	229	271.0
	0.55	0.141	143.5	5.31	1.552	3.104	972	3.573	228	317.0
	0.5	0.137	147.5	5.25	1.535	3.070	955	3.677	258	325.9
950rpm	1.2	0.323	69.2	6.80	2.791	5.581	1556	1.561	121	152.9
	1.0	0.291	76.4	6.58	2.696	5.391	1454	1.731	137.5	168.9
	0.9	0.237	93.2	6.16	2.521	5.042	1269	2.124	157	205.8
	0.75	0.198	110.9	5.81	2.375	4.750	1126	2.546	179	245.1
	0.7	0.184	119.0	5.67	2.316	4.632	1073	2.740	184	262.8
	0.6	0.154	141.7	5.33	2.179	4.358	950	3.284	251	313.1
	0.55	0.131	164.0	5.05	2.058	4.116	859	3.837	246	362.3
	0.5	0.127	168.9	4.99	2.033	4.067	842	3.962	276	373.2

Table 5.4.5. Results for APMA (series B): Viscosity, Re , N_p , power, dissipated power, Kolmogorov scale, viscosity ratio, maximum diameter, and Ta for 750 rpm

% APMA concentration	μ_{app} (Pas)	Re	N_p	P (W)	ε (W/kg)	$\eta \times 10^6$ (m)	$px10^3$	d_{max} $\times 10^6$ (m)	Ta
0.78	0.115	155	2.75	0.545	1.08	515	4.708	161	272
0.93	0.127	140	2.84	0.563	1.11	552	4.247	146	245
1.09	0.139	128	2.91	0.579	1.14	585	3.895	129	225
1.24	0.153	117	3.00	0.596	1.18	623	3.541	114	205
1.40	0.160	111	3.04	0.605	1.20	644	3.373	102	195
1.56	0.168	106	3.09	0.614	1.23	685	3.221	95	186

Table 5.4.6. Results from series C: % concentration of PMMA predissolved in MMA, maximum diameter, Kolmogorov length, interfacial tension, viscosity, viscosity ratio, power number, power and dissipated power

%PMMA in MMA	$d_{max} \times 10^6$ (m)	$\lambda \times 10^6$ (m)	Interfacial tension $\times 10^3$ (N/m)	Initial dispersed phase viscosity (cP)	$px10^3$	$f(p)$	N_p	P (W)	ε (W/kg)
5	186.5	1286	14.5	0.505	3.0	1.0006	5.868	1.168	2.336
10	202.4	1299	15.9	9.0	54.2	1.0096	5.899	1.175	2.350
15	247.8	1303	17.3	12.66	76.3	1.0133	5.910	1.179	2.357
20	278.1	1308	18.8	16.4	98.8	1.0169	5.921	1.182	2.365
25	332.6	1313	20.7	20.21	121.8	1.0204	5.933	1.186	2.372

5.4.6. Conclusions

From this section, it can be concluded that

- The viscosity index, provided by the fit of the data to the power law model, is higher for APMA solutions than the viscosity index for PMA-Na solutions
- The d_{max} is, when either PMA-Na or APMA solutions are used as continuous phase, lower than the Kolmogorov macroscale of turbulence

5.5. Determination of the dispersion mechanism

The low values of the Re in tables 5.4.3 and 5.4.4 indicate that the turbulence was not fully developed. This is also indicated by the values of the Taylor number, as it has been found that for $Ta < 400$ the prevailing dispersion mechanism was the viscous shear mechanism (Jegat, 2001). These indications have to be verified by the experimental data which must be consistent with the prevailing mechanism. Having measured and estimated all the variables required to determine the dispersion mechanism, the two theories for droplet breakage, Kolmogorov's theory of isotropic turbulence and Taylor's theory of viscous shear breakup, are now examined.

According to Kolmogorov's theory for inertial breakup in isotropic homogeneous turbulence (Shinnar and Church, 1960), when $D \gg d \gg \eta$, the maximum drop diameters in a dispersion are given by

$$d_{\max} \propto \varepsilon^{-2/5} \left(\frac{\sigma}{\rho_c} \right)^{3/5} \quad (5.5.1)$$

If the viscosity of the continuous phase plays an important role in the drop breakup process and $D \gg \eta \gg d$, then the drop diameters are given by

$$d_{\max} \propto \left(\frac{\sigma \nu_c}{\varepsilon \rho_c} \right)^{1/3} \quad (5.5.2)$$

Therefore, if Kolmogorov's theory is applicable for the suspension polymerisation experiments conducted with sodium polymethacrylate as a suspending agent, then the maximum drop diameters should be given by one of the two aforementioned expressions.

According to Taylor's theory of viscous shear breakup, and in the case of laminar or semi laminar flow, or when the turbulence is not fully developed, the maximum diameter is given by

$$d_{\max} \propto \frac{\sigma}{G \mu_{appc} f(p)} \quad (5.5.3)$$

where G is the velocity gradient, $p = \left(\frac{\mu_d}{\mu_{appc}} \right)$ is the initial viscosity ratio of the dispersed and continuous phases and

$$f(p) = \left(\frac{19p + 16}{16p + 16} \right) \quad (5.5.4)$$

is a function of the viscosity ratio.

5.5.1. Experimental results and inertial breakup mechanism

In the case that the flow in the reactor is turbulent and the inertial breakup mechanism is responsible for the drop breakup, equation (5.5.2) should be valid, where $D \gg \square \gg d$,

and d_{max} should be proportional to $\left(\frac{\sigma v_c}{\epsilon \rho_c} \right)^{1/3}$. A plot of $\ln d_{max}$ versus $\ln \left(\frac{\sigma v_c}{\epsilon \rho_c} \right)$ is

presented in figure 5.5.1 for series A₁ (PMA-Na) and figure 5.5.2 for series B (APMA). The figures show that there is a linear relationship between $\ln d_{max}$ and

$\ln \left(\frac{\sigma v_c}{\epsilon \rho_c} \right)$, but with a slope of -1.19 for PMA-Na and approximately -0.6 for APMA,

instead of $1/3$. When $(\sigma v_c / \epsilon \rho_c)$ increases d_{max} decreases, which is contrary to the theoretical predictions that d_{max} increases as $(\sigma v_c / \epsilon \rho_c)$ increases. Therefore, a different break-up mechanism should be considered in the case where $\eta \gg d$

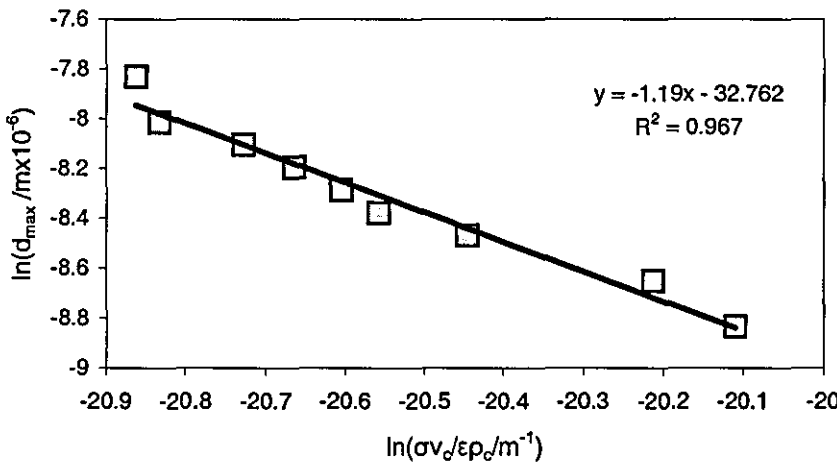


Figure 5.5.1. $\ln d_{max}$ versus $\ln (\sigma v_c / \epsilon \rho_c)$ for PMA-Na (series A₁)

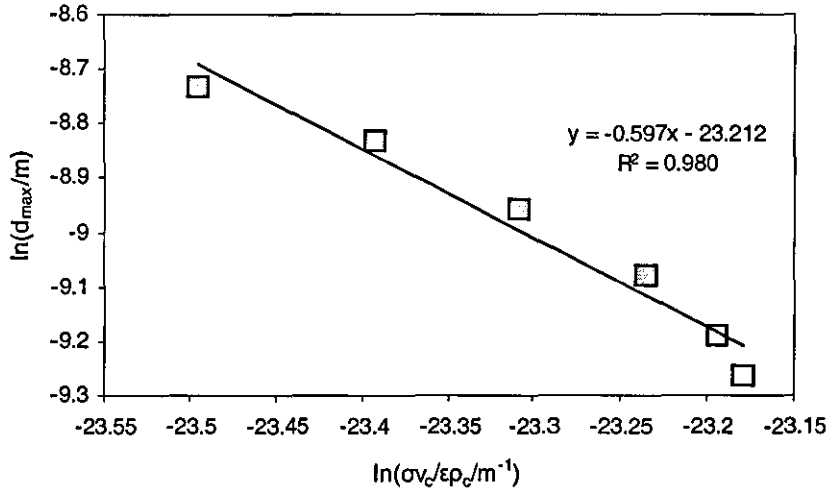


Figure 5.5.2. $\ln d_{\max}$ versus $\ln (\sigma v_c / \epsilon p_c)$ for APMA (series B)

5.5.2. Experimental results and viscous shear break up mechanism

If we assume laminar or semi-laminar flow in the reactor and $\eta \gg d$, the maximum diameter is given by equation (5.5.3). Then the maximum drop diameters should depend on the interfacial tension σ , the continuous and dispersed phase viscosities and the velocity gradient or abrasion velocity G . It should be noted that the velocity gradient, G , could not be measured in the reactor and hence equation (5.5.3) should be used with care. Keeping the stirring speed constant for all the experiments cannot ensure that G remains constant, because G itself depends on the viscosity and the viscosity changes.

However, the existence of a linear relationship between d_{\max} and $\frac{\sigma}{\mu_{appc} f(p)}$ would give strong evidence to support the validity of the viscous shear mechanism for the drop breakup. Therefore, d_{\max} versus $\frac{\sigma}{\mu_{appc} f(p)}$ is plotted, in figures 5.5.3 and 5.5.4 for series A and B, respectively. In figure 5.5.3, all the maximum diameters obtained for various stirring speeds and PMA-Na concentrations, versus $\frac{\sigma}{\mu_{appc} f(p)}$, are depicted. It is shown that in all cases, the relationship between the two variables is

linear. Figure 5.5.4, shows that the relationship for APMA is also linear. Thus, the data seem to be consistent with Taylor's theory. The low values of Re and Ta , seem to be consistent with this theory, also. Therefore, the viscous shear mechanism could be considered suitable to describe the breakage of the droplets.

As can be observed in table 5.4.3, increasing the stirring speed causes the maximum drop diameter to increase. The non-Newtonian nature of the continuous phase and the breakage mechanism can also explain this increase. Changing the stirring speed, causes the viscosity of the continuous phase, which is the determining factor controlling the drop sizes, to change. As the stirring speed increases, the shear stress exerted on the continuous phase increases and the viscosity decreases. Since the shear breakup mechanism is responsible for the drop breakage, lower viscosity means larger drops.

In figure 5.5.5, all the maximum diameters obtained for various stirring speeds and PMA-Na concentrations are depicted versus the ratio $\frac{\sigma}{\mu_{app,c} f(p)}$. All of them follow the same trend regardless of the speed variations.

If d_{max} is plotted versus the Taylor number for the different stirring speeds, as shown in figure 5.5.6, a linear relationship seems to be valid for each case. By plotting the different cases together and comparing them, as in figure 5.5.7, it seems that the overall proportionality constant for d_{max} and Taylor number is 0.8. A linear relationship between Ta and d_{max} seems to exist for APMA as well as shown in figure 5.5.7 (b).

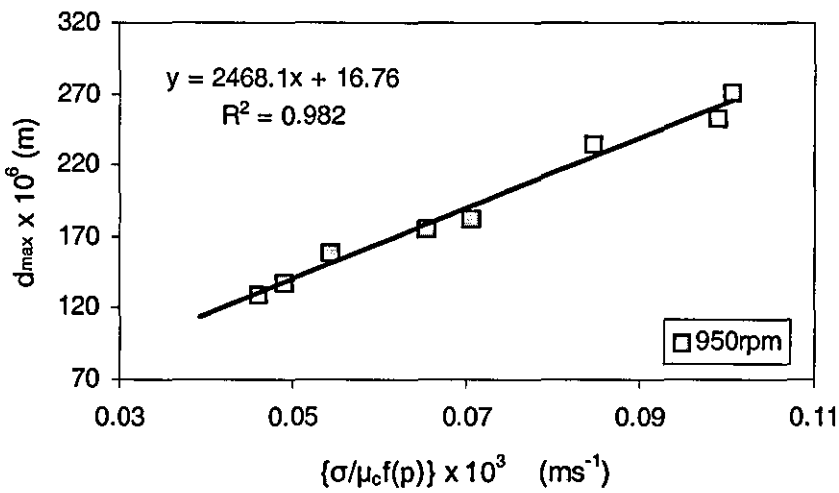
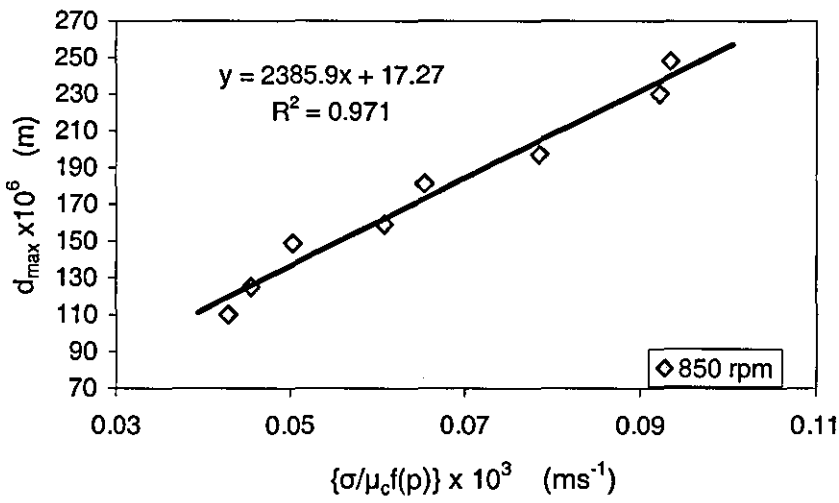
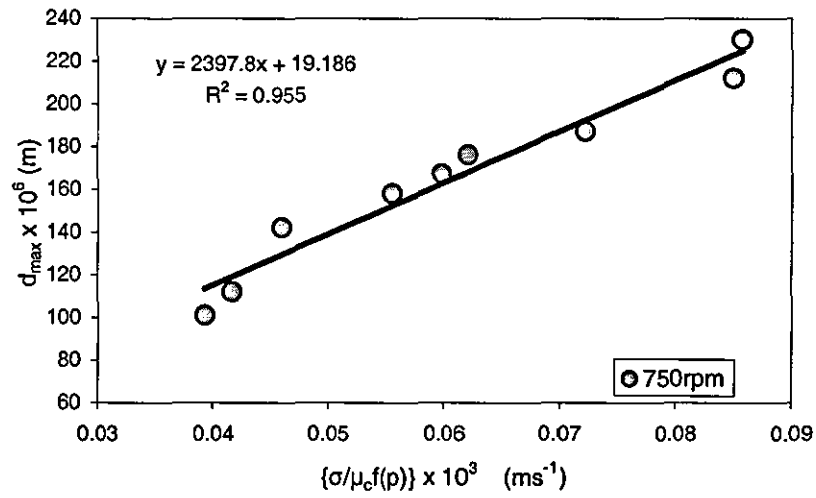


Figure 5.5.3. d_{\max} versus $\sigma/\mu_c f(p)$ for PMA-Na and various stirring speeds

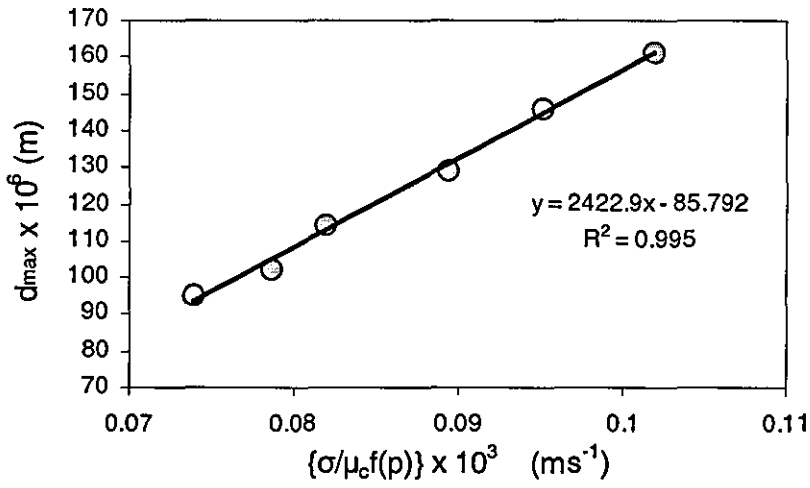


Figure 5.5.4. d_{\max} versus $\sigma/\mu_c f(p)$ for APMA

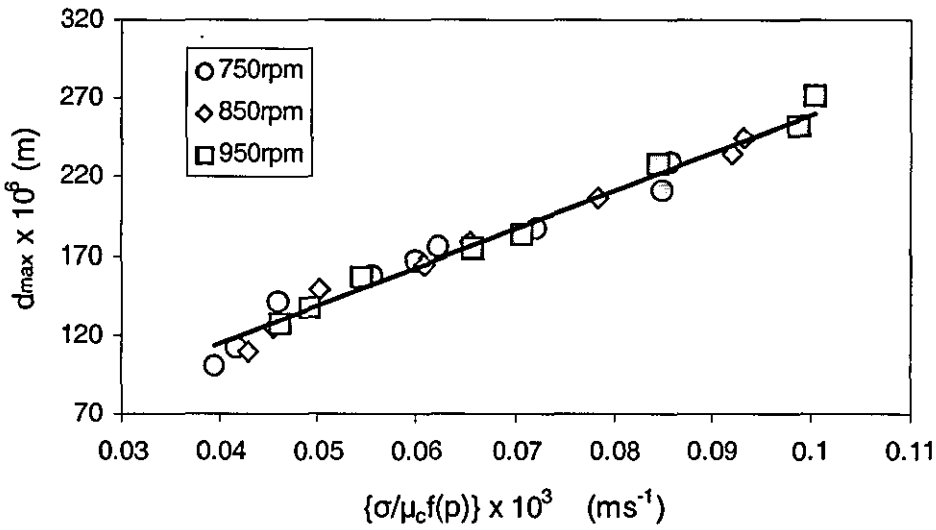
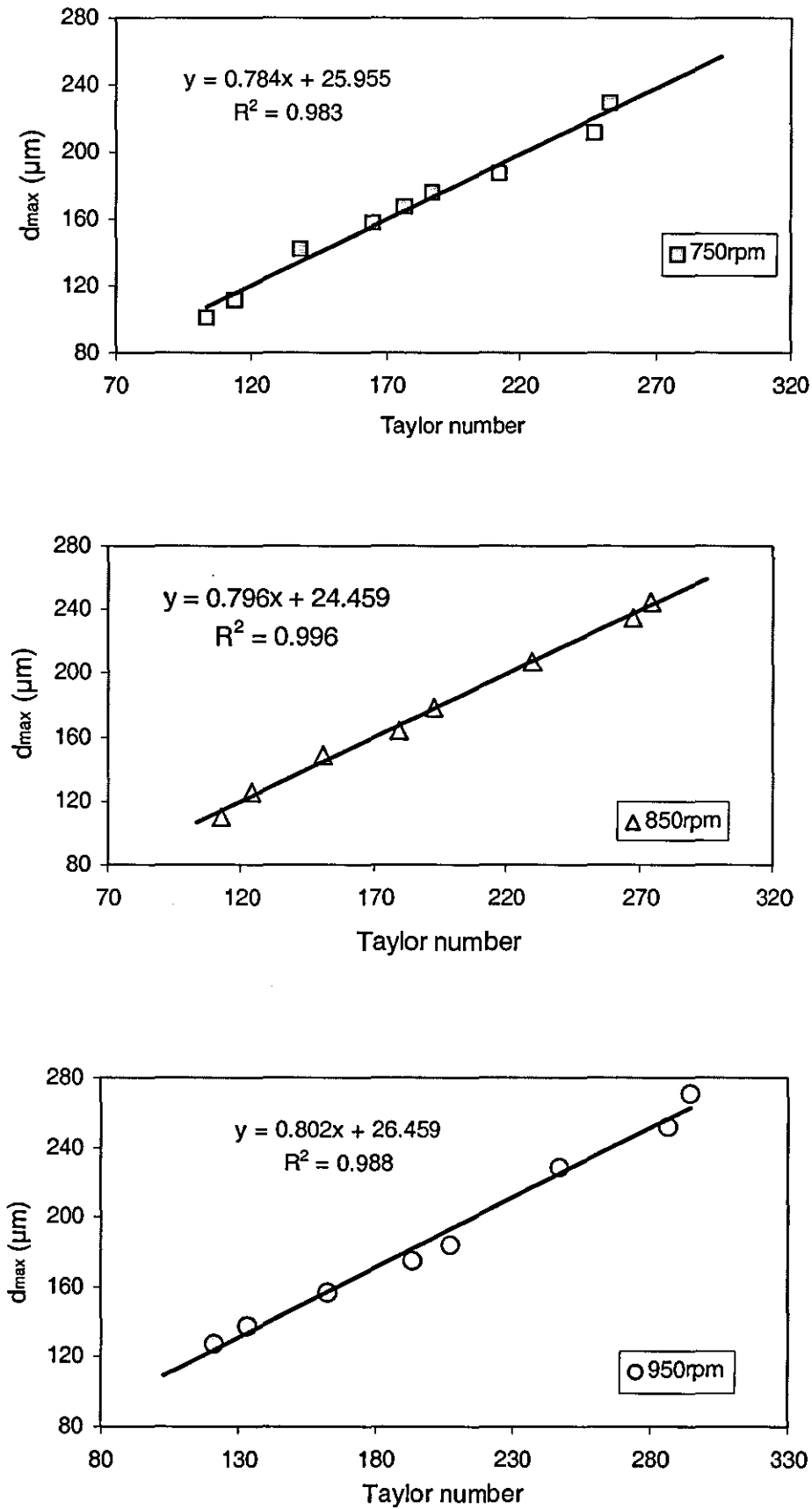


Figure 5.5.5. d_{\max} versus $\sigma/\mu_c f(p)$ for PMA-Na. Comparison of the stirring speeds.

Figure 5.5.6. d_{\max} versus Taylor number for various stirring speeds

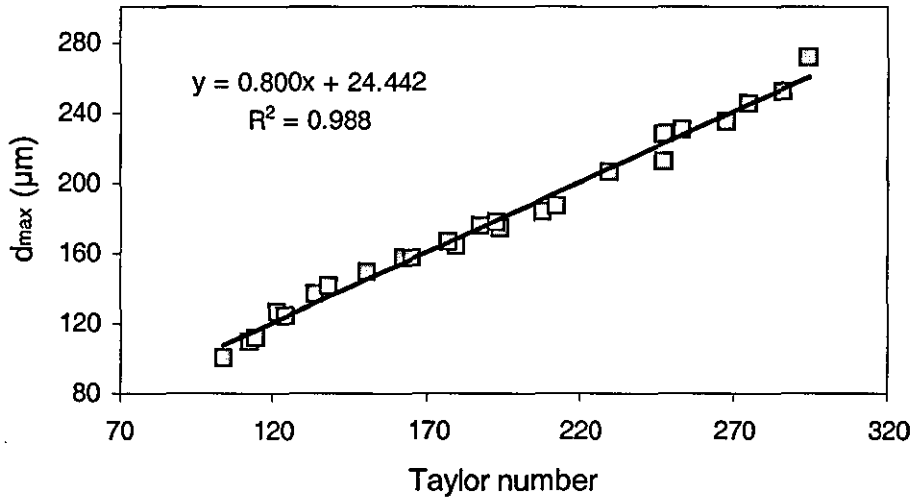


Figure 5.5.7 (a). d_{\max} versus Taylor number for all stirring speeds (series A)

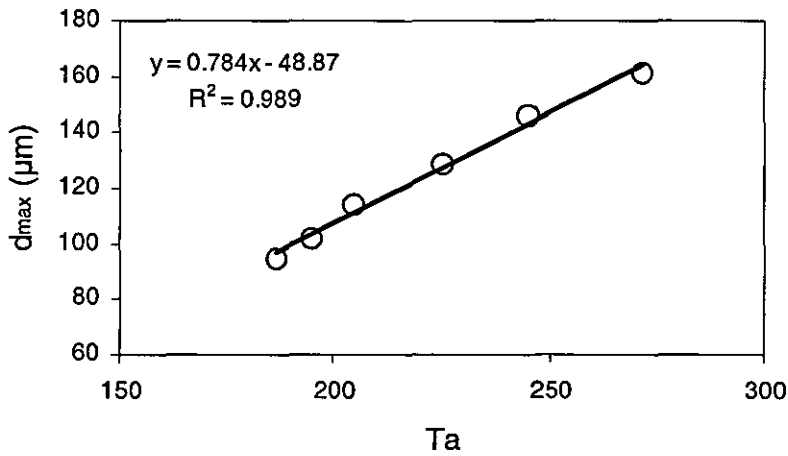


Figure 5.5.7 (b). d_{\max} versus Taylor number for APMA (series B)

5.5.3. Effect of the dispersed phase viscosity

In order to examine the effect of increases in dispersed phase viscosity on the dispersion mechanism, the dispersed phase viscosity was increased by dissolving PMMA in the monomer prior to polymerisation (series C). In this series of

experiments, the concentration of the PMA-Na in the continuous phase, and therefore the viscosity of the continuous phase, remained constant at 0.6% of PMA-Na and 0.166 Pas respectively. The dispersed phase viscosity increases from 0.5×10^{-3} Pas to 20×10^{-3} Pas. The results for series C are presented in table 5.4.6. The influence of the dispersed phase viscosity could only be examined for an initial viscosity ratio $p < 1$. For $p = 1$ or $p > 1$ the organic phase could not be properly dispersed in the viscous aqueous phase. Figure 5.5.8 shows d_{max} plotted versus $\frac{\sigma}{\mu_{appc} f(p)}$ and it is shown

that these two variables are related linearly.

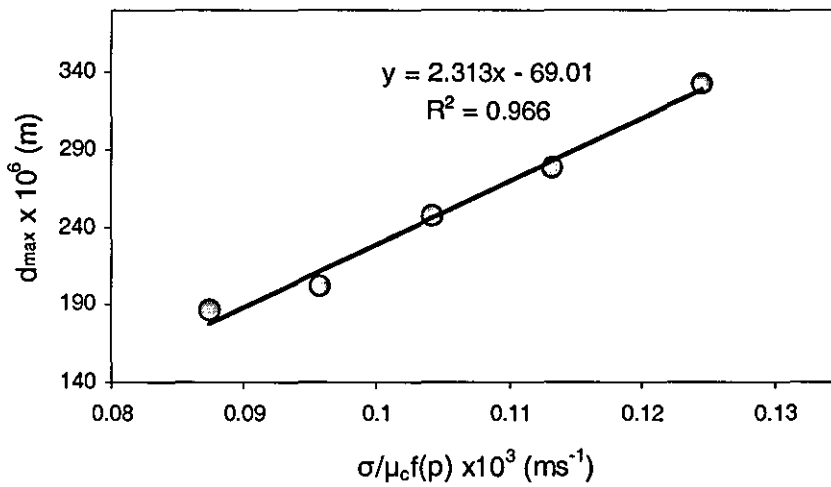


Figure 5.5.8. d_{max} versus $\sigma / \mu_c f(p)$ for increased dispersed phase viscosity

When the polymerisation of MMA alone is compared with polymerisation of MMA+PMMA (figure 5.5.9), the straight lines that derive from the data points by regression have almost the same slope, 2.398 for the MMA runs and 2.313 for the MMA+PMMA runs, indicating that the dispersion mechanism remains the same.

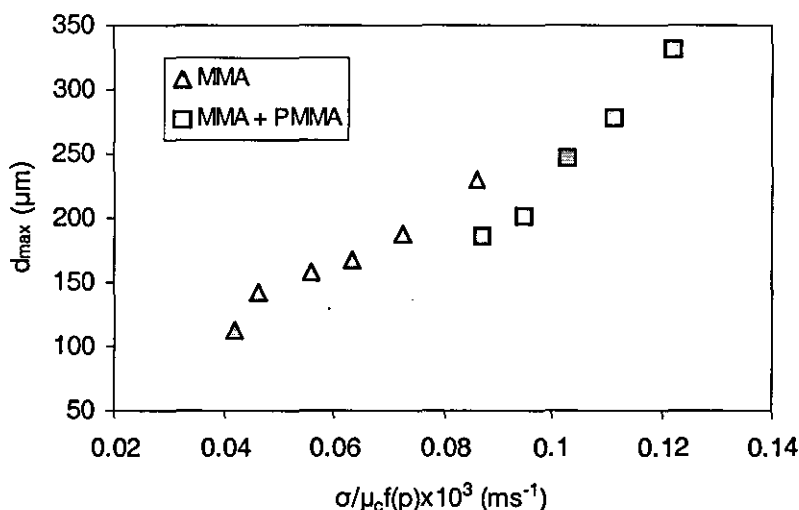


Figure 5.5.9. d_{\max} versus $\frac{\sigma}{\mu_c f(p)}$ at 750rpm. Comparison for simple runs (MMA only) and runs with predissolved PMMA

5.5.4. Conclusions

The aim of this series of experiments was to investigate the mechanism of drop formation in the suspension when PMA-Na and APMA are used as suspending agents. From the experimental results it can be concluded that:

- For PMA-Na concentrations higher than 0.5% and APMA concentrations higher than 0.62% in the continuous phase, coalescence is prevented and d_{32} remains constant over all the conversion range. Therefore, for these concentrations the final particle sizes can be considered to reflect the initial drop sizes.
- The continuous phase viscosity seems to be the main factor that determines the particle sizes.
- The results show that for high continuous phase viscosities, the inertial breakup theory cannot explain the drop breakup. The d_{\max} values obtained from the suspension polymerisation experiments show a good agreement with Taylor's theory. It can be reasonably deduced that the viscous shear breakup mechanism controls the dispersion process when PMA-Na is used as a suspending agent in laboratory scale reactors and when the Reynolds number has a low value. This

would not be expected in large scale industrial reactors where the Reynolds numbers are higher by some orders of magnitude

- Increasing the dispersed phase viscosity by the addition of PMMA to the monomer prior to polymerisation does not affect the dispersion mechanism for viscosity ratios lower than 1.
- The low values of Re and Ta are consistent with the viscous shear breakup mechanism.

5.6. Stabilisation mechanism

Most of the information and the studies in the literature refer to polyelectrolyte solutions, such as APMA and PMA-Na as dispersant agents for ceramic powders and there is no information (to our knowledge) on the use of PMA-Na and APMA as suspending agents for suspension polymerisation processes. Polyelectrolyte species, though, may also be considered as an optional approach for the suspension polymerisation processes.

5.6.1. pH

When polyelectrolyte stabilisers are used for the suspension polymerisation of MMA, the pH of the continuous phase affects the particle sizes, as was shown in chapter 5.3.5. The pH has a very strong effect on d_{32} , and more specifically, a significant diminution of the Sauter mean diameter is caused with the pH increase for various stabiliser concentrations. When the initial pH at the beginning of the reaction was increased by the addition of NaOH or NH_3 in the continuous phase for PMA-Na or APMA respectively, the particle sizes decreased, while two secondary peaks were formed at the small diameter range of the main peak. The effect of the pH on d_{32} of the main peak, for various stabiliser concentrations and pH values are depicted in figure 5.6.1, for PMA-Na and in figure 5.6.2, for APMA. For these figures the d_{32} of the main peak is used, instead of the d_{32} of the total distribution, because for higher pH values, the secondary peaks exert a stronger influence on d_{32} , and deter the deduction of conclusions for the main peak, which represents the bulk volume of polymer product. The d_{32} for the total distribution is also depicted in figure 5.6.3. From these figures, it is evident that in order to produce particles of certain size range, one could either increase the stabiliser concentration or the pH. For example, if the desirable particle size is $d_{32} \sim 70 \mu\text{m}$, this could be produced either with 0.9% of PMA-Na at pH 10, or with 0.7% PMA-Na at pH 11, or with 0.5% PMA-Na at pH 12.

The pH increase also affected the quantity of stabiliser required to prevent coalescence during suspension polymerisation, and maintain a constant d_{32} throughout the polymerisation. The required quantity of stabiliser decreased for increasing pH.

More specifically, for an initial pH ~ 9 , the required concentration of APMA that prevents coalescence during suspension polymerisation of MMA, maintaining d_{32} constant over all the conversion range was found to be 0.78% (see chapter 5.5.1). As the pH increases to higher values the required concentration decreases to 0.62% and 0.47% for pH 10 and 11 respectively. The same observations were made for PMA-Na. For pH 10, the required amount of PMA-Na to stabilise the MMA dispersion was found to be 0.5% (see chapter 5.5.1). As the pH increased the required PMA-Na quantity decreased to 0.45% and 0.4 % for pH 11 and 12, respectively. Figure 5.6.3, shows the effect of the pH on the amount of stabiliser required to prevent coalescence over all the conversion range. The relationship between the pH and the required stabiliser concentration seems to be linear for APMA and almost linear for PMA-Na.

Another significant effect of the pH is that the stabiliser concentration required to stabilise a dispersion decreases as the pH increases. It should be noted that small concentrations of stabiliser were not sufficient to stabilise the dispersion at pH ~ 9 for APMA, but the same concentrations could stabilise the dispersion when the pH was increased above 10, while at the same time a further pH increase to about 11 causes the particle sizes to diminish. The required stabiliser concentration to stabilise a MMA dispersion versus pH is depicted in figure 5.6.4.

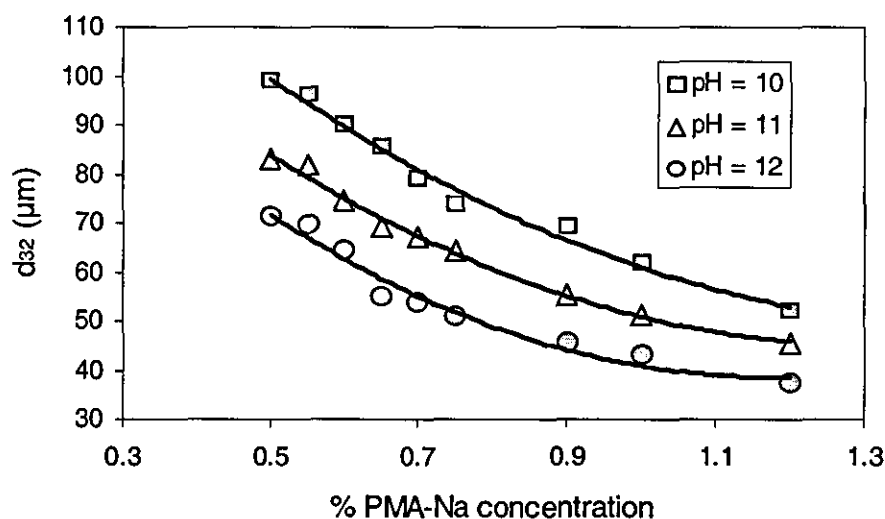


Figure 5.6.1. d_{32} for various PMA-Na concentration at various pH values

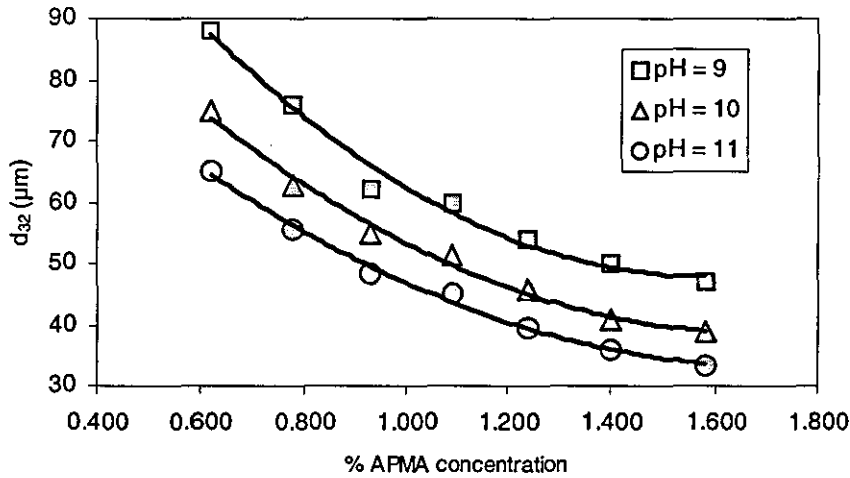


Figure 5.6.2. d_{32} for various APMA concentration at various pH values

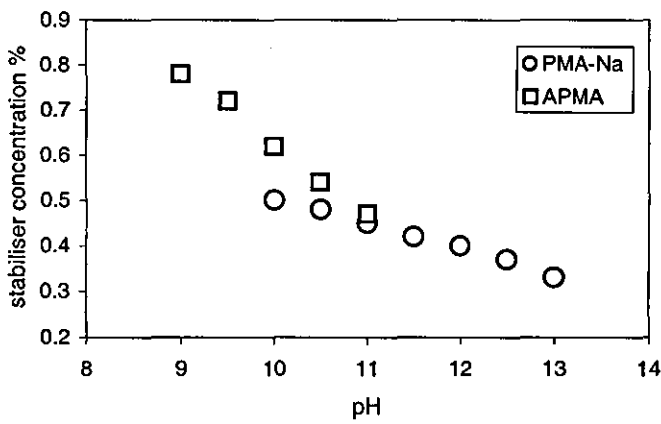


Figure 5.6.3. Amount of stabiliser required to prevent coalescence for increasing pH

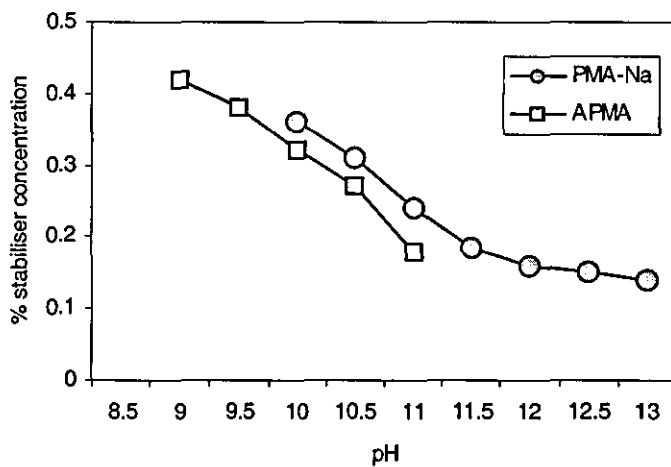


Figure 5.6.4. Stabiliser concentration required to stabilise a dispersion for increasing pH

The factors that may change with the pH are the viscosity and the degree of ionisation for APMA solutions, but only the degree of ionisation for PMA-Na solutions, since their viscosity has been shown to be independent of the pH for $\text{pH} > 8$. Each of these factors will be examined in order to find out their contribution to the dispersion stabilisation process. The viscosity decrease will be examined only for APMA solutions, since the viscosity of PMA-Na solutions does not depend on pH.

5.6.2. Viscosity decrease (APMA)

Since drop breakage has been shown to occur via a viscous shear mechanism, a decrease in the viscosity would be expected to lead to bigger particles. This is the case when the pH is not manipulated and lower viscosity leads to bigger particles. But, when the pH is increased, the viscosity decreases and smaller particles are produced. This might happen because the viscosity decrease changes the flow field. If turbulence is enhanced, the viscous shear mechanism may no longer prevail. A decrease in particle size could result from a shift towards a turbulence mechanism. But the viscosity measurements showed that this was not happening. Despite this decrease, the viscosity of the continuous phase remains within the range that is compatible with the viscous shear breakup mechanism, and hence bigger particles would be expected with the viscosity decrease, instead of smaller ones. Therefore, in this case, it is not a change in the flow field that caused the particle size diminution and, despite the viscosity drop, the prevailing mechanism remains the same.

5.6.3. Ionisation / Dissociation degree.

Two mechanisms for drop stabilization, steric and electrosteric, may coexist and their contribution varies depending on the pH. As the pH increases, the ionization/dissociation degree increases, the number of charged sites on the polymer coil also increases and the repulsive forces start playing an important role in the conformation and the behaviour of the polymer chains. Thus, the contribution of the electrosteric mechanism for drop stabilization increases with increasing pH. Therefore, it is

considered more probable that it is the enhancement of the electrosteric stabilization mechanism, which now prevails over the steric stabilization, that caused the particle size diminution.

It was found that a particular concentration of APMA might be insufficient to stabilise a dispersion, and to prevent coalescence, at pH~9 but it was effective at pH~11. A possible explanation could be that, at pH ~9, the steric stabilization is more likely to prevail and the stabiliser quantity is insufficient to provide physical hindrance to coalescence. As the pH increases, the electrosteric stabilization is more likely to prevail and stabilization of the dispersion becomes feasible. This is because the charged polymer coils stretch and take up a more extended conformation. They expand on the drop surfaces as well, and in this way the charges enhance the stability of the dispersion.

5.6.4. Conclusions

The experimental work showed that the pH played a very important role in the stabilisation of the dispersion.

- The pH had a profound effect on the particle sizes and, at a constant stabiliser concentration, increasing the pH caused the particle size to decrease. Not only did the pH increase cause a decrease of particle sizes for various stable dispersions but, at a given stabiliser concentration, it induced stability in dispersions that were unstable at a lower pH. This was attributed to increases in the charges on the polymer coil and in the strength of repulsive forces.
- The enhancement of the stabilisation of the dispersion was considered to have been achieved through the contribution of the electrosteric stabilisation mechanism.

CHAPTER 6. FACTORS THAT AFFECT THE ONSET OF THE GEL EFFECT

According to the free volume theory (Neil et al., 1998) which is the prevailing theory used to interpret the gel effect, the x_{crit} depends on the reaction temperature but does not depend on the molecular weight of the polymer produced prior to the onset of the gel effect. This theory, like all the theories used to interpret this phenomenon, has received criticism and it has been suggested that the molecular weight of the polymer produced prior of the gel effect influences the x_{crit} but indirectly. More specifically, it has been suggested that as the molecular weight (M) of the polymer produced prior to the onset of the gel effect increases, the concentration dependence of the termination rate constant k_t , which is controlled by translational diffusion, increases. The diminution of k_t is more pronounced at high conversion. Therefore, increasing M has a more evident effect on k_t and hence on the onset of the gel effect. If this is the case, the initiator concentration which determines the M of all the polymer produced throughout the polymerisation should have an effect on the onset of critical conversion as well.

Therefore, there are two cases that need to be examined. According to the first, the x_{crit} does not depend on M of the polymer produced prior to gel effect. According to the second, the M of the polymer produced prior to gel effect influences the critical conversion but indirectly. In order to test these theories, the effect, if there is any, of the initiator concentration on x_{crit} is examined, as well as the relationship, between the M of the final polymer and the x_{crit} .

In this chapter factors that may affect the onset of the gel effect, in terms of the critical concentration, are examined. The effect of the reaction temperature and the effect of the initiator concentration on the critical conversion are examined experimentally and a statistical approach is used to assess and evaluate the results. The effect of the type of stabiliser on the x_{crit} is also examined and the molecular weight of the polymer produced is also considered.

6.1. Experiments

The main experimental work for this chapter includes three series of experiments:

Series A: Experiments were run with constant BPO concentration, 0.04 mole/l, and the same stabiliser type and concentration, 0.6% PMA-Na, for varying temperature, in order to examine the effect of temperature on x_{crit} . Series A, consists of 3 groups, group A₁ for 70°C, group A₂ for 75 °C, and group A₃ for 80°C. Pure monomer was used as organic phase. The x_{crit} and the final conversion for each group is shown in table 6.1.1. The initial pH of the continuous phase was adjusted to 10.

Series B: Series B, consists of two groups, group B₁ and group B₂. Experiments were run, for both series, at 70°C, with the same stabiliser concentration, 0.6% PMA-Na, for various BPO concentrations, 0.04, 0.06, 0.08, 0.10, and 0.12 mole/l BPO, in order to examine the effect of initiator concentration on x_{crit} . Polymerisation experiments with each BPO concentration are repeated many times. Pure monomer was used as organic phase for both groups. The initial pH of the continuous phase for all runs was 10. For both groups, x_{crit} was calculated, as described in section 3.3.5. The only difference between the two groups is that for the group B₂, apart from x_{crit} , molecular weight measurements were also carried out, as shown in table 6.1.3., whereas for B₁ only the x_{crit} data are presented, in table 6.1.2.

Series C: Experiments run with 0.78% APMA, for various BPO concentrations, 0.04, 0.06, 0.08 and 0.10 mole/l BPO, at 70°C, in order to examine the effect of the stabiliser type on x_{crit} . Pure monomer was used as organic phase. The initial pH of the continuous phase was adjusted to 9.

Table 6.1.1. Results for series A

A ₁		A ₂		A ₃	
70°C		75°C		80°C	
x _{crit}	conversion	x _{crit}	conversion	x _{crit}	conversion
0.299	0.9125	0.3253	0.876	0.3295	0.933
0.3028	0.9144	0.3139	0.9153	0.3321	0.908
0.2963	0.908	0.3201	0.923	0.3411	0.918
0.3139	0.918	0.3244	0.944	0.3433	0.931
0.297	0.923	0.3254	0.871	0.3102	0.9412
0.3065	0.917	0.3132	0.87	0.3127	0.9531
0.2808	0.9067	0.32	0.9203	0.321	0.925
0.3077	0.9142	0.3279	0.8982	0.315	0.9308
0.297	0.909	0.312	0.926	0.3146	0.9518
0.2948	0.8959	0.3102	0.931	0.3356	0.9451
0.3107	0.9054	0.3265	0.9058	0.3317	0.944
0.2957	0.8866	0.3204	0.859	0.3327	0.954
0.307	0.873	0.3127	0.897	0.3316	0.9373
0.287	0.893	0.3259	0.871	0.3439	0.942
0.2931	0.9172	0.3236	0.967	0.3235	0.8997
0.287	0.8893	0.3247	0.925	0.3193	0.931
0.3129	0.925	0.3082	0.899	0.3429	0.942
0.299	0.867	0.3213	0.947	0.3323	0.9385
0.2976	0.896	0.3284	0.9267	0.3329	0.9618
0.2898	0.931	0.3044	0.9206	0.3476	0.923

Table 6.1.2. Results for series B₁.

BPO concentration (mole/l)				
0.04	0.06	0.08	0.10	0.12
0.2785	0.2931	0.3028	0.3091	0.3326
0.283	0.2948	0.3102	0.3132	0.3347
0.2834	0.2957	0.311	0.3213	0.3357
0.285	0.2963	0.3127	0.3247	0.3395
0.2901	0.2977	0.3133	0.3253	0.3458
0.2977	0.299	0.3167	0.3254	0.3479
0.298	0.3054	0.3201	0.3284	0.3499
0.2983	0.307	0.3204	0.3329	0.3569
0.2986	0.3076	0.3236	0.3411	0.3585
0.3082	0.3086	0.3259	0.3439	0.3587
0.3139	0.3107	0.3316	0.3476	
0.3148	0.3127			
	0.3146			
	0.3156			
	0.3157			
	0.3181			
	0.3193			
	0.32			
	0.3201			

Table 6.1.3. Results for series B₂

<i>BPO</i> concentration mole/l	<i>x_{crit}</i>	<i>conversion</i>	<i>M_n</i>	<i>M_w</i>	<i>M_z</i>	<i>M_v</i>	<i>polydispersity</i>
0.04	0.299	0.9125	358258	1059576	1923498	904490	2.96
	0.3028	0.9144	269573	966361	1780432	858000	3.55
	0.2963	0.908	343608	949407	1694845	849255	2.76
	0.3139	0.918	329051	932259	1639694	834527	2.83
	0.297	0.923	310204	924790	1655782	824595	2.98
	0.3065	0.917	290779	925401	1671233	822956	3.18
	0.2808	0.9067	290259	909254	1628956	809316	3.13
	0.3077	0.9142	327805	890609	1570455	799392	2.72
	0.297	0.909	258797	838703	1541843	741949	3.24
	0.2948	0.8959	286301	832335	1522810	739876	2.91
0.06	0.3076	0.8995	290703	812371	1451099	725296	2.8
	0.3098	0.9257	247381	810941	1507064	716966	3.28
	0.3117	0.8922	266420	760613	1363722	678663	2.86
	0.321	0.9213	234523	779913	1805663	668732	3.48
	0.3156	0.9275	224063	769743	1805663	668732	3.48
	0.3044	0.9187	271925	722482	1285269	646804	2.66
	0.2976	0.8949	226310	750259	1771224	643479	3.32
	0.2898	0.8983	219431	727984	1666084	627640	3.32
	0.303	0.923	255909	694173	1247822	620761	2.71
	0.3065	0.942	217596	663568	1217655	589982	3.05
0.08	0.315	0.9263	220648	662976	1216425	586206	3.15
	0.315	0.944	224616	658554	1216296	583664	2.93
	0.3129	0.937	221990	637714	1163227	568265	2.87
	0.3279	0.9287	234176	625954	1146579	558925	2.67
	0.312	0.9318	194645	623392	1191337	547805	3.2
	0.2963	.0.928	193730	668593	1476263	544820	3.18
	0.3102	.0.916	232395	604708	1106623	539803	2.6
	0.3356	0.896	184133	599475	1165852	524574	3.24
	0.3317	0.9167	209799	587560	1078780	524088	2.8
	0.3052	0.908	182578	610199	1685861	502301	3.39
0.1	0.3265	.0.921	171036	582185	1202592	494447	3.2
	0.3327	0.931	172909	574928	1076988	479325	3.17
	0.3157	0.925	180592	582081	1047890	502459	3.12
	0.3082	0.9286	177284	504491	975632	449013	2.87
	0.33044	0.947	147386	526482	1246233	447111	3.57
	0.3235	.0.9356	134471	518589	1109654	445313	3.86
	0.3193	0.948	142336	526482	1246233	445111	3.57
	0.3433	0.9568	146293	514382	1231379	439424	3.52
	0.3244	0.9385	168549	507837	1169026	438532	3.01
	0.3321	0.9185	163954	507837	1169026	437932	3.01
	0.3429	0.9265	137085	491439	1125378	399308	3.25
	0.3195	0.9181	132152	467207	1269670	393956	3.54
	0.3184	.0.935	135873	459042	1135279	430000	3.26
	0.3323	.0.928	140655	449860	1045809	405000	3.4

0.12	0.3454	0.925	133843	441524	994703	381068	3.3
	0.3296	0.929	146285	427453	854495	374732	2.92
	0.3468	0.9697	139868	417811	914908	362926	2.99
	0.3195	0.932	122175	464048	1228386	354881	2.93
	0.3457	0.916	118548	376784	825382	326045	3.18
	0.319	0.926	120869	289094	496924	262210	2.24
	0.3386	0.942	128809	289094	496924	260725	2.24
	0.3219	0.95	124506	279883	685877	224991	2.42
	0.3305	0.927	123870	273579	643279	262210	2.43
	0.3461	0.925	123974	268965	642380	228495	2.51
	0.351	0.906	122609	263570	635342	223549	2.32

Table 6.1.4. Results for series C

<i>BPO</i> concentration mole/l		<i>BPO</i> concentration mole/l	
	x_{crit}		x_{crit}
0.04	0.18199	0.08	0.167
	0.2147		0.16544
	0.1875		0.1754
	0.19765		0.1765
	0.1754		0.1643
	0.1977		0.18675
	0.18654		0.18654
	0.1979		0.1589
	0.217		0.1567
	0.1782		0.18975
	0.2247		0.1655
0.06	0.2065	0.1	0.1567
	0.1875		0.1608
	0.1754		0.14987
	0.1643		0.15677
	0.1865		0.1678
	0.1986		0.1567
	0.194		0.15447
	0.1699		0.15667
	0.1795		0.16778
			0.1643

6.2. Preliminary tests of the variables

The statistical tests used to assess the relationship between the variables, like the Analysis of Variance (ANOVA), require that the variables satisfy some assumptions before the tests are performed. If these assumptions are not valid, the test results cannot be considered reliable. The assumptions made when ANOVA is applied, are the following:

- The population from which the samples were obtained must be normally or approximately normally distributed
- The samples must be independent of each other
- The variances of the populations must be equal.

Before the application of ANOVA, these assumptions have to be tested and verified. For the first assumption of normality, the values of x_{crit} , for series A, B and C, and the values of the viscosity average molecular weight (M_v), for series B, are tested for normality, by a Normal probability plot (P-P plot) as shown in figure 6.2.1, where cumulative proportions of x_{crit} and M_v are plotted against the expected cumulative proportions of the variable if the normal distribution was followed. If the selected variable matches the normal distribution, the points cluster around the diagonal straight line. The more the experimental points deviate from the diagonal straight line the more their distribution deviates from normality.

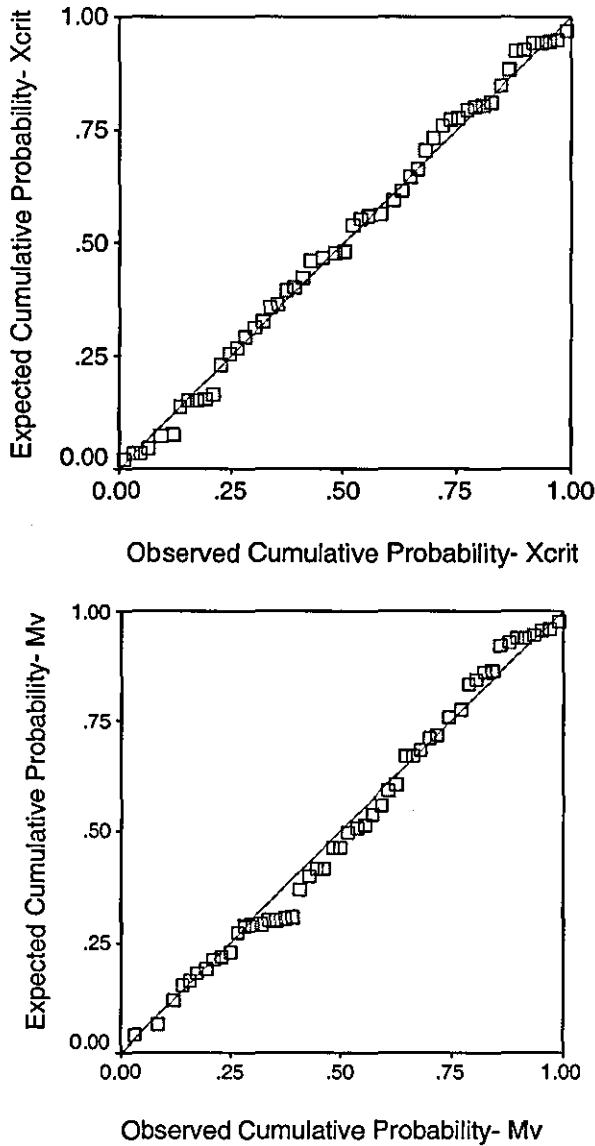


Figure 6.2.1. P-P plots for x_{crit} and Mv

The experimental points, in both cases, for x_{crit} and Mv , do not deviate significantly from the straight line and therefore they can be considered to follow the normal distribution. The samples are independent runs and therefore, they satisfy two of the three requirements for the application of ANOVA. The third requirement of equal variances is examined in each case together with the application of ANOVA.

6.2.1. Conclusions

The probability – probability plots for x_{crit} and Mv showed that the values of the variables do not deviate significantly from normality and they may be considered to follow a normal distribution.

6.3. Effect of temperature on x_{crit}

According to the free volume theory, x_{crit} depends on the reaction temperature. The alleged relationship between these two variables is examined in order to verify it or reject it, by using ANOVA. A number of experiments (series A) run for three different temperatures but for the same BPO concentration (0.06 mole/l) were used, with PMA-Na as stabiliser. The variance of the x_{crit} values for each temperature are depicted in figure 6.3.1. A trend for an increase of x_{crit} with increasing temperature becomes evident.

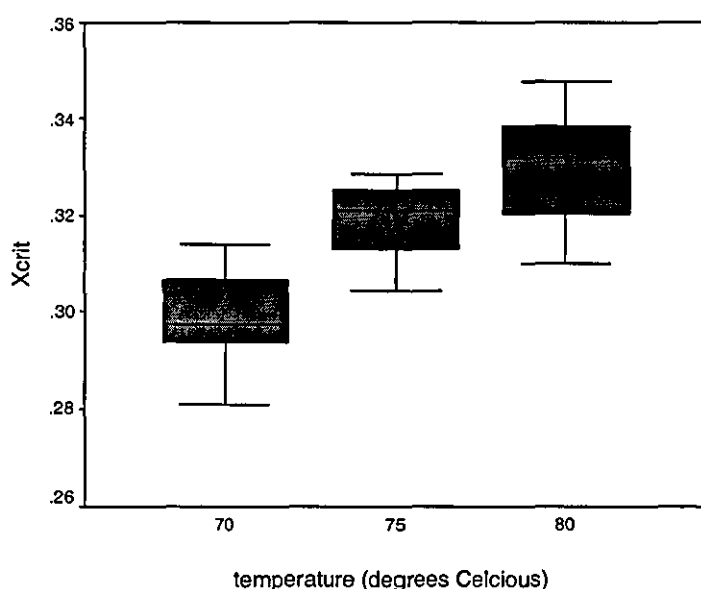


Figure 6.3.1. x_{crit} for various temperatures

The descriptive statistics, including the mean, standard deviation, standard error, the lower and upper bounds for 95% confidence interval and the minimum and maximum, for x_{crit} for various temperatures are shown in table 6.3.1, where λ is the number of experiments. The mean values of x_{crit} for each temperature seem to differ.

Table 6.3.1. Descriptive statistics for x_{crit} and various temperatures (series A)

Temperature C)	λ	Mean x_{crit}	Std. Deviation	Std. Error	95% Confidence Interval for Mean		Minimum	Maximum
					Lower Bound	Upper Bound		
70	20	0.298771	0.0090225	0.0020175	0.294549	0.302994	0.2808	0.3139
75	20	0.319415	0.0072433	0.0016196	0.316025	0.322805	0.3044	0.3284
80	20	0.329667	0.0112894	0.0025244	0.324384	0.334951	0.3102	0.3476
Total	60	0.315951	0.0158759	0.0020496	0.311850	0.320052	0.2808	0.3476

The test of homogeneity of variance is shown in table 6.3.2, where the number of treatments is $u=3$ (represents the 3 different temperatures for subgroups A_1 , A_2 and A_3) and the number of experiments for each treatment is $\lambda=20$. Therefore, the degrees of freedom for this test are $df1 = u-1=2$ and $df2=u(\lambda -1)=57$. This test shows that the p-value (sig.) is 0.177 which is higher than the 0.05 level. When the Levene's test (described in chapter 4.4) is significant (the value under "Sig." is less than 0.05), the two variances are significantly different. When it is not significant (Sig. is greater than 0.05), the two variances are not significantly different; that is, the two variances can be considered equal.

Table 6.3.2. Test of Homogeneity of Variances

Levene Statistic	df1	df2	Sig.
1.784	2	57	0.177

Table 6.3.3, shows the ANOVA for the x_{crit} for the various groups determined by the temperature. The p-value is lower than 0.01 which means that the group means are different.

Table 6.3.3. ANOVA

	Sum of Squares	df	Mean Square	F	Sig.
Between Groups	.010	2	.005	56.858	.000
Within Groups	.005	57	0		
Total	.015	59			

The Tukey test (described in section 4.6), shown in table 6.3.4, shows that all the means differ from one another.

Table 6.3.4. Tukey test

(I) Temperature	(J) Temperature	Mean Difference	Std. Error	Sig.	95% Confidence Interval	
					Lower Bound	Upper Bound
70	75	-0.0206*	0.00295	.000	-0.0277	-0.0135
	80	-0.0309*	0.00295	.000	-0.0380	-0.0238
75	70	0.0206*	0.00295	.000	0.0135	0.0278
	80	-0.0102*	0.00295	.003	-0.0174	-0.0032
80	70	0.0309*	0.00295	.000	0.0238	0.0380
	75	0.0102*	0.00295	.003	0.0032	0.0174

* The mean difference is significant at the .05 level.

The values noted with a * in the previous table represent statistically significant differences between the group means which were tested. This means that x_{crit} depends on temperature. More specifically, x_{crit} was found to increase for higher reaction temperatures, which is in agreement with published results and has been justified in terms of the free volume theory.

6.3.1. Conclusions

From the analysis of the experimental results with ANOVA, it is shown that critical conversion, x_{crit} , increases for increasing polymerisation temperature, as has been explained in terms of the free volume theory.

6.4. Effect of the initiator concentration on x_{crit}

The effect of the initiator concentration on the monomer conversion to polymer is shown in figure 6.4.1. With increasing initiator concentration the overall reaction rate increases, but does this increase of the initiator concentration have any effect on the x_{crit} ?

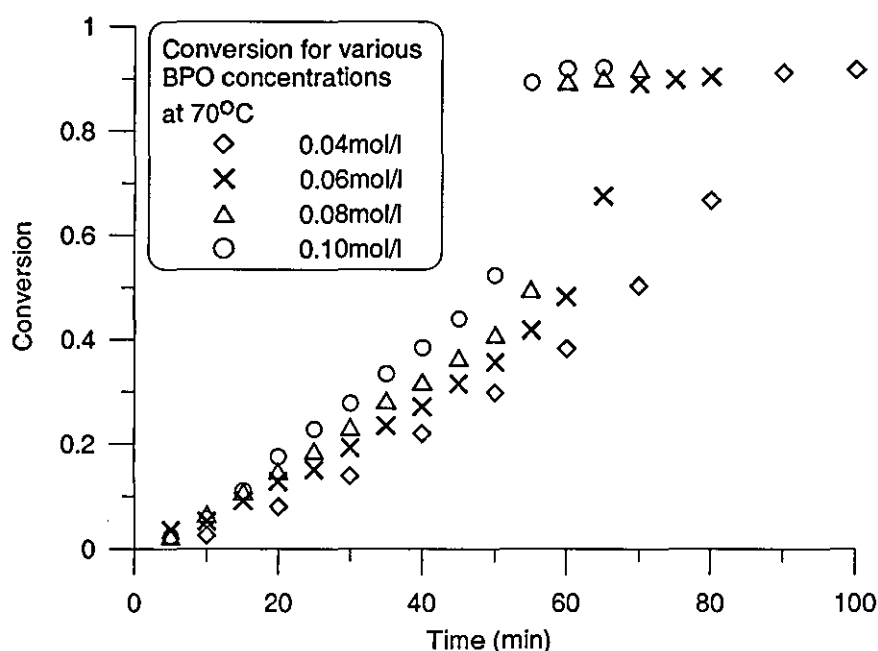


Figure 6.4.1. Effect of initiator concentration on monomer conversion, for PMA-Na and pH 10

The statistical process used to investigate the relationship between x_{crit} and initiator concentration consists of the following steps:

1. Investigate whether x_{crit} varies with BPO concentration. Analysis of variance (ANOVA) was carried out, using x_{crit} and BPO concentration.
2. Investigate whether x_{crit} varies with M of polymer produced.
 - Classify the samples into groups according to their viscosity average M_v , using the K-means clustering method.
 - Examine, whether x_{crit} values for these groups are equal, using ANOVA. If the mean x_{crit} values of these groups of samples with different M_v are equal then there is no relation between M_v and x_{crit} .

6.4.1. One way Analysis of Variance (A-NOVA)

The x_{crit} was calculated for 122 suspension polymerisation runs, series B (groups B₁ and B₂), with 5 different initiator concentrations 0.04, 0.06, 0.08, 0.10 and 0.12 mole/l and constant temperature (70°C) under isothermal conditions. Analysis of variance was used in order to find if there is any statistically significant difference between x_{crit} values for various initiator concentrations. The experimental hypothesis for this test is simply that there may be a difference in x_{crit} between the five groups of BPO concentrations: that is the experimental hypothesis is non-directional. In this case, the corresponding null hypothesis is that there is no difference, and a large difference in either direction would be evidence against it. ANOVA was performed for the x_{crit} and the BPO concentration was used as the grouping variable. The statistical descriptive statistics for these runs are reported in table 6.4.1, and they include the mean values of x_{crit} , the standard deviation, the lower and upper bound and the minimum and maximum values.

Table 6.4.1. Descriptive statistics for x_{crit}

BPO Concentration (mole/l)	λ	Mean	Std.	Std. Error	95% Confidence	Interval	Minimum	Maximum
		Deviation		for Mean				
				Lower Bound	Upper Bound			
.04	22	.2974	.0110	.0024	.2925	.3022	.2785	.3170
.06	34	.3061	.0102	.0018	.3025	.3097	.2870	.3210
.08	23	.3170	.0112	.0024	.3121	.3219	.2963	.3356
.10	22	.3276	.0112	.0024	.3226	.3325	.3082	.3476
.12	21	.3407	.0121	.0026	.3352	.3462	.3190	.3587
Total	122	.3164	.0184	.0017	.3131	.3197	.2785	.3587

The mean values of each one of the five groups differ, but it cannot be determined whether this difference is due to random variance or systematic variance caused by the independent variable, which in this case is the BPO concentration.

In figure 6.4.2 the boxplot shows the variance of the values of x_{crit} for the 5 cases of BPO loading, where the box represents the interquartile range which contains 50% of the values. The whiskers are lines that extend from the box to the highest and lowest values, excluding outliers. A line across the box indicates the median. As shown in

the boxplot, the higher x_{crit} values for 0.04 mole/l are within the same range with the lower values for 0.06 mole/l BPO. The same thing can be observed for all the successive values of BPO concentrations; there is significant overlap of values for various BPO concentration. The higher x_{crit} values for a certain concentration are within the same range with the lower values of the next concentration examined. It is, therefore, considered expedient to compare the means of the two groups of values via a more rigid statistical method, like ANOVA, that would take into consideration the variance of the x_{crit} values.

The application of this method requires, apart from the normality and the independent sample requirements, that the variances of the variable at every level (level = BPO concentration) are equal.

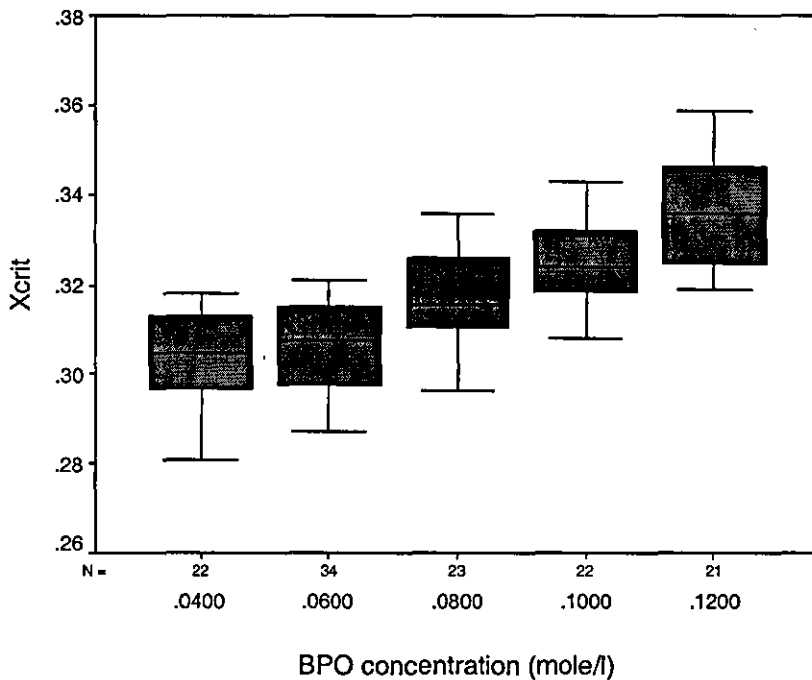


Figure 6.4.2. x_{crit} for various BPO concentrations

The equality of variances is examined by Levene's test (table 6.4.2), which is less dependent on the assumption of normality than most other tests. The Levene's test examines the homogeneity or equality of group variances, which means whether the groups have approximately equal variance on the dependent variable. When the Levene's test is significant (the value under "Sig." is less than 0.05), the two variances are significantly different. When it is not significant (Sig. is greater than 0.05), the two variances are not significantly different; that is, the two variances can be

considered equal. In this case, the significance is 0.879, which is greater than 0.05. We can assume that the variances are approximately equal. The third assumption has been met.

Table 6.4.2. Test of Homogeneity of Variances for x_{crit}

<i>Levene Statistic</i>	<i>df1</i>	<i>df2</i>	<i>Sig.</i>
.298	4	117	0.879

Since all of the assumptions are met, the analysis of variance can be performed, as shown in table 6.4.3. When the value of the F distributions, which is the ratio of the variance between the groups over the variance within the groups, is much larger than 1, as in this case ($F = 54.527$), the means of the groups are different. If the means were equal then the F distribution should be equal to 1. The probability value (sig.) is lower than the significance level of 0.05, which means that the null hypothesis of the equality of means is rejected. Therefore, the mean values of x_{crit} for the various groups are statistically different at a significance level 0.05. Therefore, there seems to be a statistically significant difference between the values of x_{crit} for the different BPO concentrations, and the null hypothesis is rejected.

Table 6.4.3. ANOVA for the mean values of x_{crit} for various BPO concentrations

	<i>Sum of Squares</i>	<i>df</i>	<i>Mean Square</i>	<i>F</i>	<i>Sig.</i>
Between Groups	.027	4	0.007	54.527	0.000
Within Groups	.014	117	0.000		
Total	.041	121			

The mean values of the variable groups are statistically different and hence the x_{crit} is affected by the BPO concentration, and more specifically as can be observed in figure 6.4.3, where the mean values of x_{crit} are plotted against BPO concentration, the x_{crit} values increase with increasing BPO concentration.

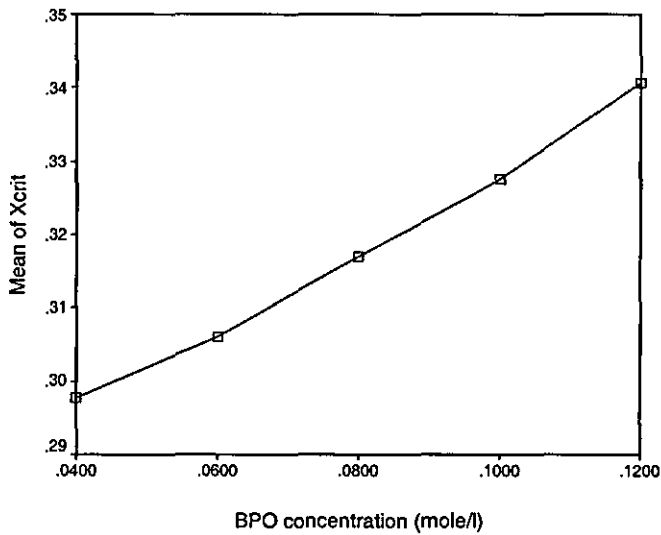


Figure 6.4.3. Mean values of x_{crit} for increasing BPO concentration

The linear association of the two variables of interest, x_{crit} and BPO concentration (mole/l), was also tested by the Pearson correlation coefficient, as shown in table 6.4.4. A correlation coefficient is a statistic devised for the purpose of measuring the strength, or degree, of a supposed linear association between two variables. The Pearson coefficient ranges between 0 and 1, corresponding to no linear and linear relationships respectively. The Pearson coefficient (table 6.4.4) for the two variables is 0.805, which is significant at the 0.01 level and indicates that there is a linear association between them.

Table 6.4.4. Pearson correlation

		BPO concentration (mole/l)	x_{crit} at 70°C
BPO concentration (mole/l)	Pearson Correlation	1	.805**
	Sig. (2-tailed)	.	.000
	N	122	122
x_{crit}	Pearson Correlation	.805**	1
	Sig. (2-tailed)	.000	.
	N	122	122

** Correlation is significant at the 0.01 level (2-tailed).

6.4.2. K-means cluster analysis

The viscosity average molecular weight, M_v , of the final polymer is used as the variable for the cluster analysis by K-means of 55 suspension polymerisation samples (series B₂). Therefore, the criterion for the classification of these samples is only their similarity in terms of molecular weight values. The clusters to be produced by K-means will consist of samples with similar molecular weights. The initial cluster centres are shown in table 6.4.5. The final cluster centres chosen to maximise the distance among cases in different clusters (after 20 iterations) are shown in table 6.4.6, whereas the distances between the final cluster centres are shown in table 6.4.7.

Table 6.4.5. Initial Cluster Centres

Cluster	1	2	3	4	5
Cluster center	904490	224991	799392	326045	716966

Table 6.4.6. Final Cluster Centres

Cluster	1	2	3	4	5
Cluster center	837816	255378	674964	413620	535419

Table 6.4.7. Distances between Final Cluster Centres

Cluster	1	2	3	4	5
1		582438	162852	424195	302396
2	582438		419585	158242	280041
3	162852	419585		261343	139544
4	424195	158242	261343		121799
5	302396	280041	139544	121799	

The smallest distance is found between clusters 4 and 5, and it is 121×10^3 , whereas the biggest distance is found between clusters 1 and 2, and it is 582×10^3 .

The number of cases in each cluster is given in table 6.4.8.

Table 6.4.8 Number of Cases (experiments) in each Cluster

Cluster	Cases
1	8
2	7
3	12
4	15
5	13
Valid	55

The samples comprising each cluster are shown in figure 6.4.4, and they are labelled by the BPO concentration used for their production. Each cluster consisted of samples with similar *M_v*. The samples comprising each cluster were mainly produced by the same BPO concentration, one BPO concentration is predominant in each cluster. Figure 6.4.4 shows the number of the samples produced by a certain BPO concentration that belong to each cluster. Clusters 1 and 2 consist solely of samples produced by 0.04 and 0.12 mole/l BPO, respectively. 90% of the samples produced by 0.06 mole/l and 20% of the samples produced by 0.04 mole/l BPO belong to cluster 3. All of the samples (100%) produced by 0.10 mole/l BPO and 40% of the samples produced by 0.12% belong to cluster 4. Cluster 5 consists of 100% of the samples produced by 0.08 mole/l BPO and 10% of the samples produced by 0.06 mole/l BPO.

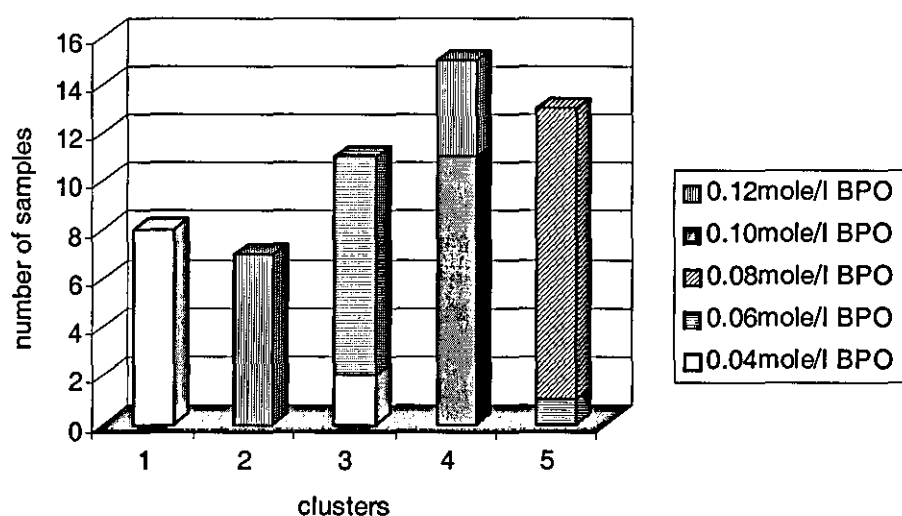


Figure 6.4.4. Samples (labelled with BPO concentration) comprising the clusters

Figure 6.4.5, shows the percentage of the sample type in each cluster, reflecting the degree of homogeneity of the clusters. Clusters 1 and 2 consist 100% of samples produced by 0.04 and 0.12 mole/l BPO respectively. Cluster 3 consists 80% of samples with 0.06 mole/l BPO and 20% of samples with 0.04 mole/l BPO. Cluster 4 consists of 70% of 0.10 mole/l BPO samples and 30% of 0.12mole/l BPO samples. Finally, cluster 5 consists 90% of 0.08 and 10% of 0.06 mole/l BPO samples.

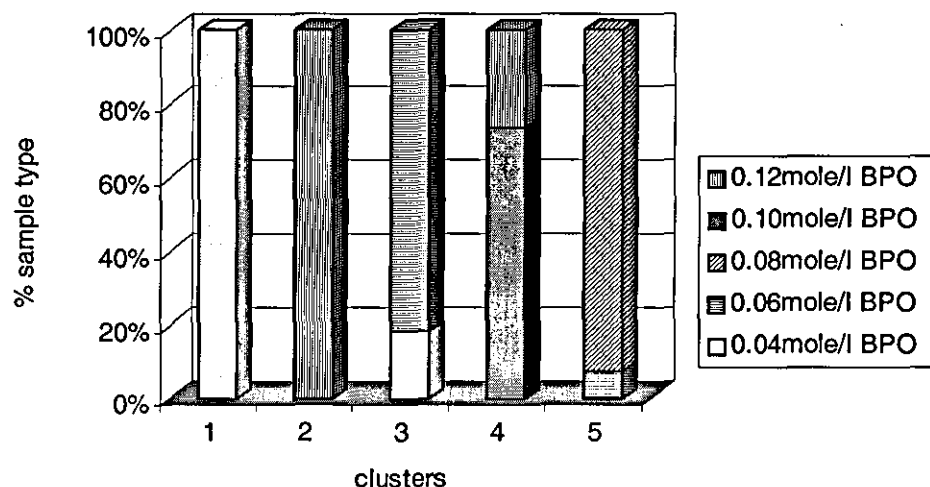


Figure 6.4.5. Percentage of samples type in each cluster

The mean values of x_{crit} for each cluster shown in table 6.4.9, together with the rest of the descriptive statistics, differ. Whether this difference is due to the variation of the viscosity average molecular weight or random error will be verified by the application of ANOVA.

Table 6.4.9. Descriptive statistics for x_{crit} in the clusters

Cluster	n	Mean x_{crit}	Std. Deviation	Std. Error	95% Confidence Interval for Mean		Minimum	Maximum
					Lower Bound	Upper Bound		
1	8	0.2881	0.0069	0.0025	0.2823	0.2939	0.2785	0.2977
2	7	0.3361	0.0126	0.0047	0.3245	0.3477	0.3190	0.3510
3	12	0.3074	0.0091	0.0026	0.3017	0.3132	0.2898	0.3210
4	15	0.3290	0.0116	0.0030	0.3226	0.3355	0.3082	0.3468
5	13	0.3176	0.0122	0.0034	0.3102	0.3249	0.2963	0.3356
Total	55	0.3165	0.0184	0.0025	0.3116	0.3215	0.2785	0.3510

The test of homogeneity of variance, in table 6.4.10, shows that the variance is homogeneous. The p-value (sig.) is (0.261) higher than 0.05 and therefore the group variances can be considered almost equal, permitting the application of ANOVA.

6.4.10. Test of Homogeneity of Variances for x_{crit} in the clusters

<i>Levene Statistic</i>	<i>df1</i>	<i>df2</i>	<i>Sig.</i>
1.359	4	50	.261

The application of ANOVA, as shown in table 6.4.11, verifies that there is a statistically significant difference in the cluster means. The p-value is lower than 0.01 and therefore the difference between the cluster means is significant at a 0.01 level.

Table 6.4.11. ANOVA for x_{crit} in the clusters

	<i>Sum of Squares</i>	<i>df</i>	<i>Mean Square</i>	<i>F</i>	<i>Sig.</i>
Between Groups	0.013	4	0.003	26.726	0.000
Within Groups	0.006	50	0.000		
Total	0.018	54			

Each cluster is homogeneous in relation to the Mv. Since, the mean x_{crit} between the clusters vary, the conclusion that can be drawn is that the x_{crit} and the Mv are related.

When the Pearson correlation is used to determine whether there is a linear correlation between the two variables, as in table 6.4.12, it is shown that there is a strong relationship between x_{crit} and Mv. Consequently, the Mv does influence the onset of the gel effect.

Table 6.4.12. Pearson Correlations

	x_{crit}	Mv
x_{crit} Pearson Correlation	1	-0.814**
Sig. (2-tailed)		0.000
N	55	55
Mv Pearson Correlation	-0.814**	1
Sig. (2-tailed)	0.000	
N	55	55

** Correlation is significant at the 0.01 level (2-tailed).

When the M_v and the x_{crit} for each cluster are plotted, it becomes clear that the two variables are inversely proportional, and hence for decreasing M_v the x_{crit} increases.

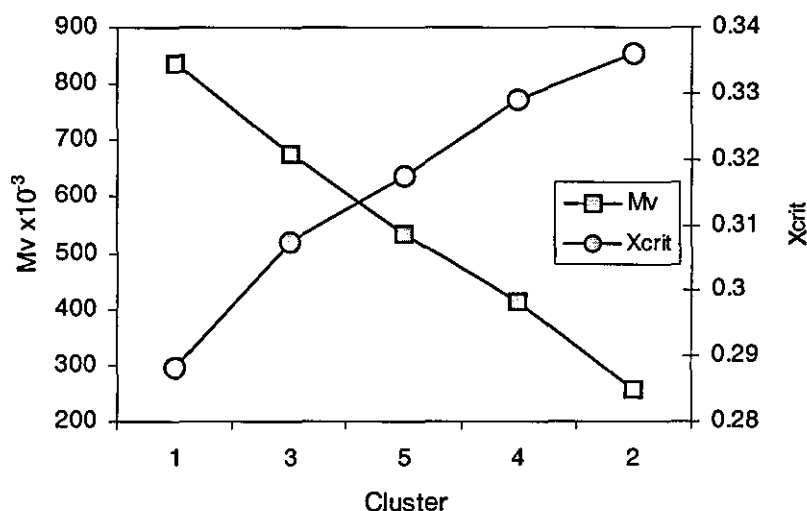


Figure 6.4.6. M_v and x_{crit} for each cluster

Eventually, the critical conversion does depend on the molecular weight of the polymer produced in the polymerisation reaction.

6.4.3. Effect of predissolved polymer on x_{crit}

In order to examine the effect of the molecular weight of the polymer produced prior to the onset of gel effect on x_{crit} , some simulation experiments were carried out. In those experiments, polymer PMMA of various molecular weights was dissolved in monomer, prior to polymerisation, and the x_{crit} was calculated as described in subchapter 3.3.5. The concentration of the predissolved polymer was 20% in all cases, corresponding to a conversion of 20%. The viscosity average molecular weights of the predissolved polymer and the corresponding x_{crit} are given in table 6.4.13. For each experiment, three replicates were run and the average x_{crit} was then calculated. The stabiliser used was PMA-Na, and its concentration was 0.6% for all the runs. The polymerisation temperature was 70°C. The BPO concentration was constant for all the runs, 0.08 mole/l. For this initiator concentration at 70°C, and for runs with pure monomer, the corresponding x_{crit} (see subchapter 6.4.1) is 0.3170.

In order to provide a reference case, a run with pure monomer was carried out and the polymerisation was stopped after 50 min with the addition of inhibitor and cooling of the reaction mixture at the same time. The conversion reached after 50 min was 0.336, slightly higher than the x_{crit} . The molecular weight and the molecular weight distribution of the polymer produced up to that point was measured with GPC (figure 6.4.7). The M_v of the sample was 178,000. This M_v does not correspond to x_{crit} , but it can provide a good estimate for the order of magnitude of M_v , at the onset of gel effect. Therefore, the M_v of the polymer produced prior to gel effect, for the run with pure monomer, is considered to be approximately 178,000.

Table 6.4.13. Viscosity average molecular weight M_v , concentration of predissolved PMMA, x_{crit} and BPO concentration

Cases	M_v at gel effect	M_v of predissolved PMMA	Concentration of predissolved PMMA	x_{crit}	BPO concentration (mole/l)
Reference case	178000	-	0	0.317	0.08
1	-	21000	20%	0.365	0.08
2	-	354000	20%	0.307	0.08
3	-	631000	20%	0.285	0.08
4	-	858000	20%	0.267	0.08

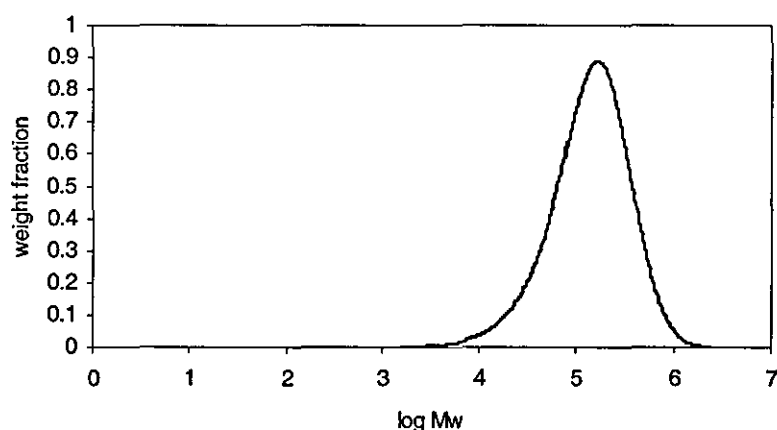


Figure 6.4.7. MWD of PMMA at 0.336 conversion

As shown in figure 6.4.8, the critical conversion increases with decreasing M_v of predissolved polymer. The trend is similar with the trend observed in figure 6.4.6,

(chapter 6.4.2) for the x_{crit} and the M_v of the final polymer produced, for runs with pure monomer as dispersed phase.

As observed in table 6.4.13, for case 1, where the M_v is very low, 21000, lower than the M_v of the reference case, the x_{crit} is significantly higher than the x_{crit} of the reference case. For the other 3 of the cases with predissolved PMMA, the M_v of the predissolved monomer is higher than the M_v of the reference case, and therefore, the x_{crit} is significantly lower, than the x_{crit} of the reference case.

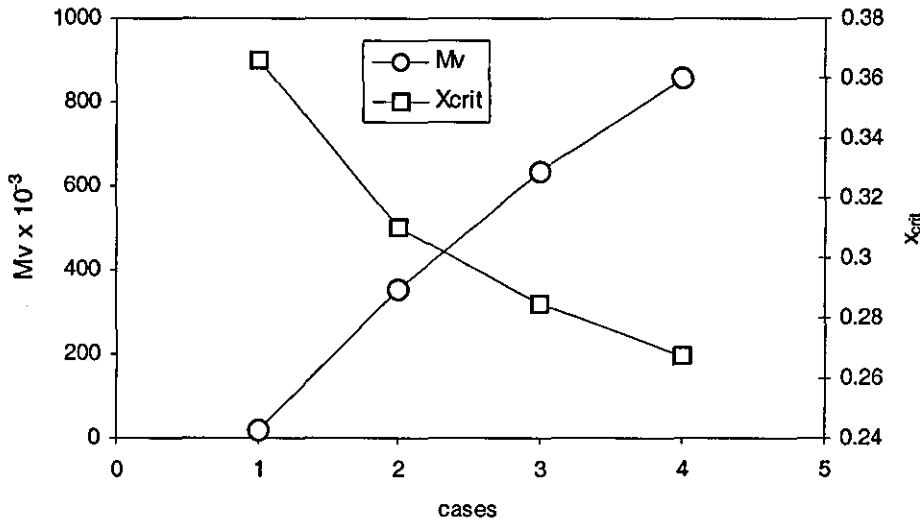


Figure 6.4.8. M_v of predissolved PMMA and corresponding x_{crit}

6.4.4. Conclusions

The conclusion deduced from the statistical assessment of the experimental results are:

- The analysis of variance applied on groups of samples produced with various BPO concentrations showed that mean values of x_{crit} of the groups increase for increasing BPO concentration
- When the samples are clustered using the viscosity average molecular weight as a grouping variable, the clusters produced, which are similar in terms of M_v , have means (x_{crit}) which also increase for decreasing M_v . Therefore, the relationship between M_v and x_{crit} has been verified.

6.5. Effect of the type of stabiliser on x_{crit}

Two different stabilisers were used for the experimental investigation of the factors that affect the x_{crit} , PMA-Na and APMA, for series A and C, respectively. The type of stabiliser used, seems to influence the conversion–time data indicating that there may exist an influence on the reaction kinetics. Figure 6.5.1, shows the conversion time curves for the two stabilisers, for the same initiator loading. As observed in this figure, the use of APMA seems to cause an acceleration of the reaction rate and the reaction reaches higher conversion at earlier times.

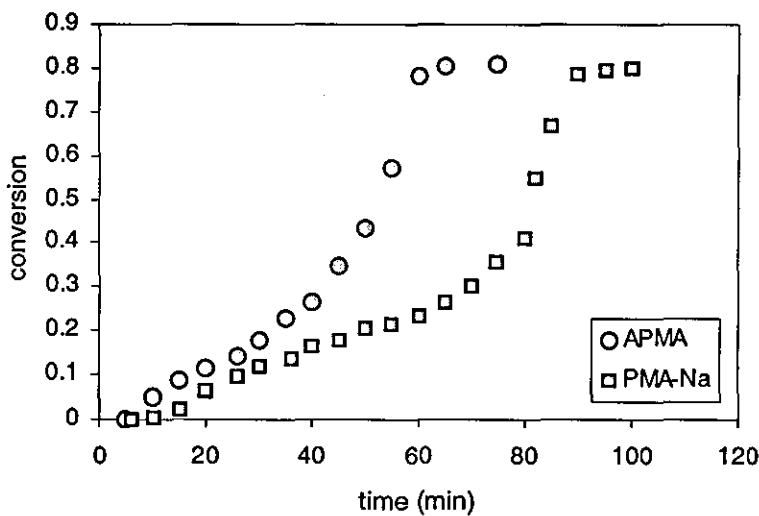


Figure 6.5.1. The effect of the type of stabiliser on conversion

The descriptive statistics for the two stabilisers PMA-Na and APMA are given in table 6.5.1. The mean critical conversion values calculated for the runs performed with APMA are significantly lower than the corresponding values for the runs with PMA-Na. The influence of APMA, first observed on the time-conversion curves, is also evident on the x_{crit} data.

Table 6.5.1. Descriptives

Stabiliser	λ	Mean	Std. Deviation	Std. Error Mean
APMA	11	0.1963	.0165	.0050
PMA-Na	10	0.2968	.0107	.0034

6.5.1. T-test

In order to compare the mean values of x_{crit} for the two groups of experiments run with the two stabilisers and the same initiator loading, a T- test is performed. As shown in table 6.5.2, there is a statistically significant difference between the mean values of x_{crit} for the two stabilisers.

When the probability (sig.) value is lower than 0.05, the hypothesis of equality of means is rejected. Therefore, there is a statistically significant difference between the x_{crit} values of the two groups, produced with APMA and PMA-Na.

Table 6.5.2. Independent Samples T-test

	<i>Levene's Test for Equality of Variances</i>								
	<i>Test for Equality of Means</i>								
	F	Sig.	t	df	Sig. (2-tailed)	Mean Difference	Std. Error Difference	95% Confidence Interval of the Difference	
								Lower	Upper
Equal variances assumed	1.950	.179	-15.581	19	.000	-.0955	.0061	-.1084	-.0827
Equal variances not assumed			-15.905	17.242	.000	-.0955	.0060	-.1082	-.0829

Both, the conversion time curves and the x_{crit} data indicate that there is a significant influence of the stabiliser on the reaction kinetics. x_{crit} values published on previous work for PVA - BPO systems (Neil et al., 1996), are consistent with the x_{crit} values for the system PMA-Na - BPO. The deviation from previously published values is observed for the APMA - BPO system. Therefore, it must be APMA and not PMA-Na that plays a role or has some kind of influence on the reaction kinetics. This of course, also indicates that there must be some sort of interaction between the two phases.

The mechanism via which APMA interacts or interferes with the MMA+BPO system is not known, and a number of questions are raised about the mechanism and the factors that determine this interaction. One of these is whether the concentration of

APMA affects the reaction kinetics and x_{crit} . A second one is how the concentration of BPO affects x_{crit} when APMA is used.

6.5.2. Combined effect of increasing BPO and APMA concentrations

But what happens to the reaction kinetics when the BPO concentration is increased, for runs where APMA is used in the continuous phase? What interaction between the two phases occurs?

The conversion-time data for increasing BPO concentration and APMA, used as stabiliser, are depicted on figure 6.5.2, for 70°C. The reaction rate increases as it would be expected according to previous results for PMA-Na. The critical conversion would also be expected to increase because x_{crit} was shown to increase with increasing initiator concentration. As shown on figure 6.5.3, though, the critical conversion seems to decrease for increasing BPO concentration.

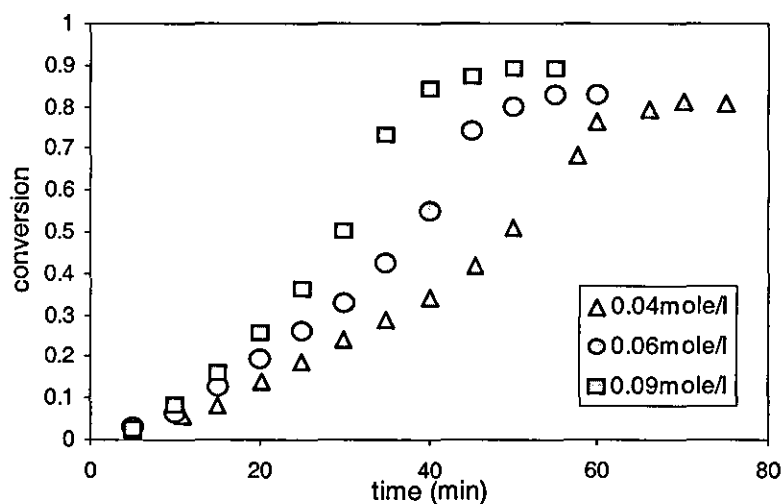


Figure 6.5.2. Conversion for increasing BPO concentration, with APMA at 70°C

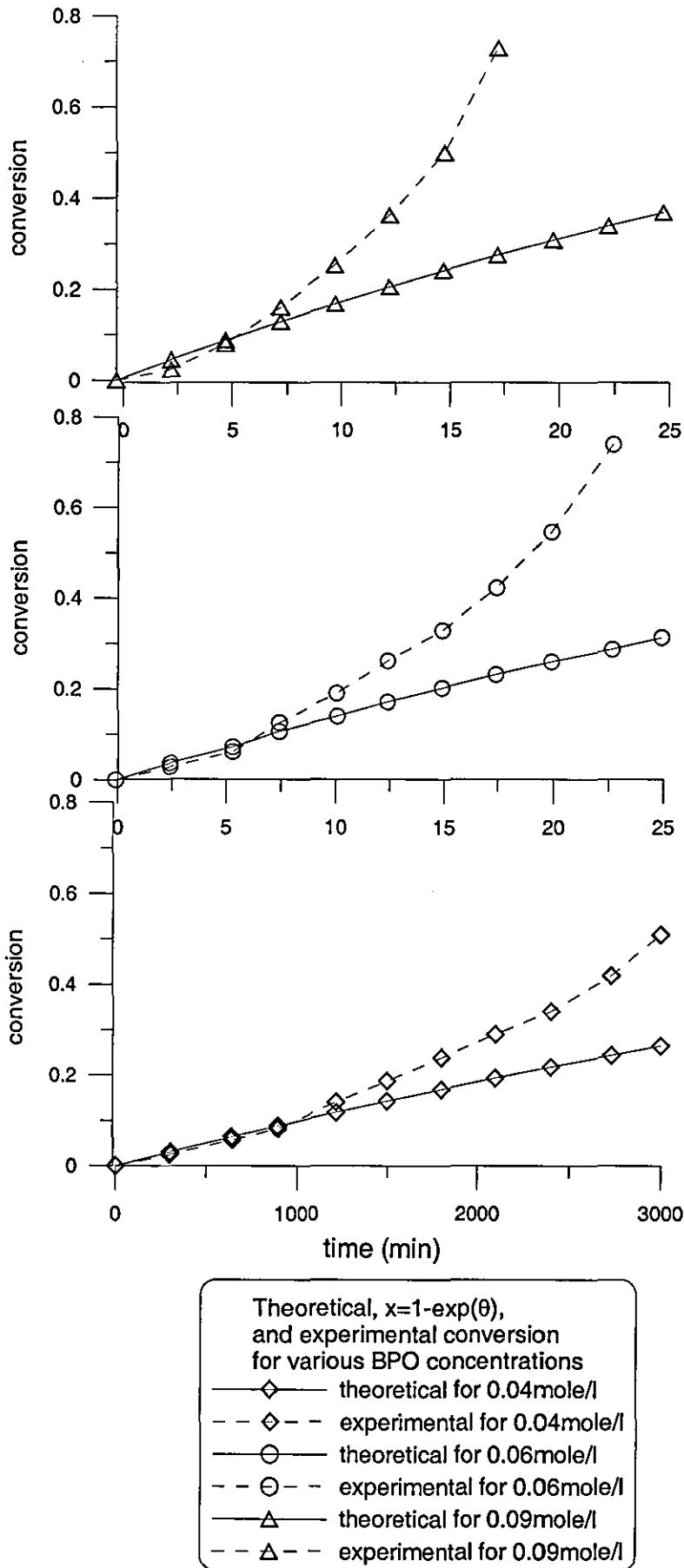


Figure 6.5.3 x_{crit} for increasing BPO concentration, for APMA

By comparing the variation of x_{crit} for increasing BPO concentrations for the two stabilisers (figure 6.5.4), two contradicting trends are observed. While for increasing BPO concentration x_{crit} increases when PMA-Na is used, it decreases when APMA is used. This decrease cannot be explained and is not consistent with the recent findings presented on chapter 6.4.1 showing that increasing initiator concentration leads to an increase of x_{crit} . It could probably be attributed to the interactions of BPO with the stabiliser.

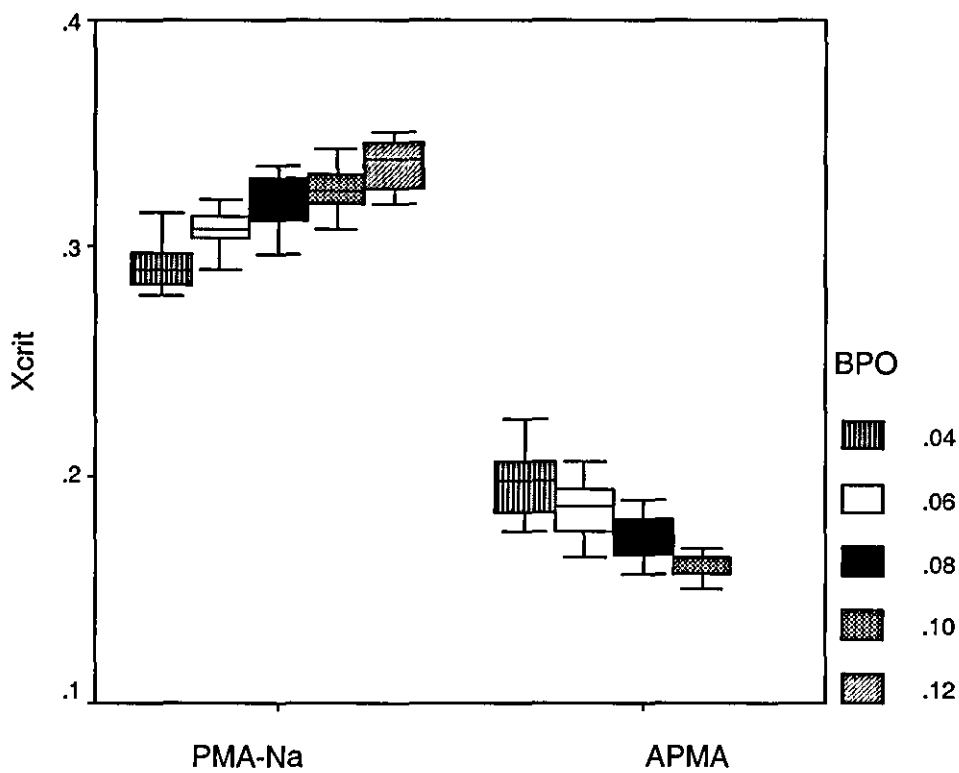


Figure 6.5.4 Comparison between PMA-Na and APMA for increasing BPO concentration

The question raised by these phenomena is whether this observed x_{crit} decrease reflects an earlier gel effect onset, or is in fact just manifestation of interactions that have not been so far determined.

6.5.3. Effect of APMA concentration on x_{crit}

Since APMA affects the reaction mechanism, the concentration of APMA might have an influence on the reaction kinetics as well. Runs for various APMA concentrations are depicted in figure 6.5.5.

As can be observed, an increase of the reaction rate takes place for increasing APMA concentration. The corresponding (to these runs) values of x_{crit} also decrease for increasing APMA concentration.

This might be attributed to two possible causes:

- the increase of the concentration of APMA as a chemical reagent for the reaction/interaction between APMA and BPO
- the increase of the interfacial area between the continuous and the dispersed phase. As APMA concentration in the continuous phase increases, the drops become smaller and the interfacial area between the two phase increases. If the interaction of APMA and BPO is associated with the interfaces and the interfacial area between the two phases, increasing the interfacial area might lead to an increasing interaction rate.

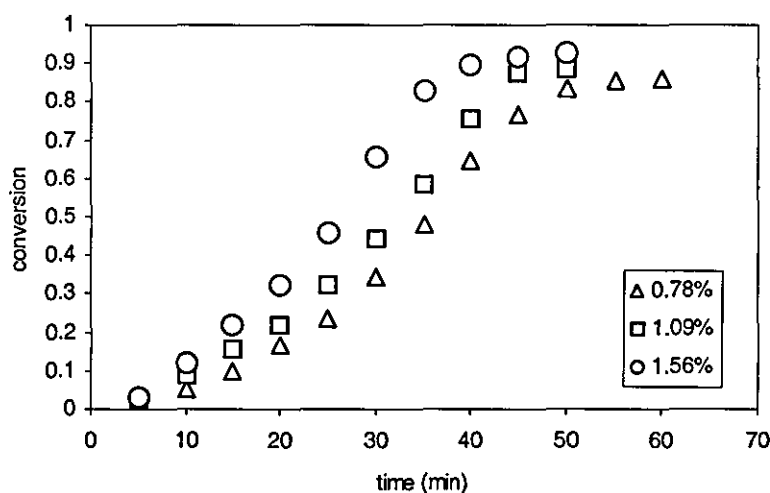


Figure 6.5.5. Conversion for increasing APMA concentration in the continuous phase

These two factors have to be decoupled, and the effect of each one of them has to be investigated separately, in order to find out what are the factors that determine this type of interaction.

6.5.4. Effect of interfacial area

If the interfacial area between the continuous and dispersed phases, has any influence on the phenomena of autoacceleration observed so far, then by varying the interfacial area, x_{crit} will change as well. In order to vary the interfacial area without changing the stabiliser concentration, the stirring speed is varied. As shown in section 5.3.2, increasing the stirring speed leads to increasing drop sizes and therefore to a decrease of the interfacial area. Hence, experiments with the same APMA and BPO concentration were run for increasing stirring speeds. The particle size distributions of the samples produced are depicted in figure 6.5.6.

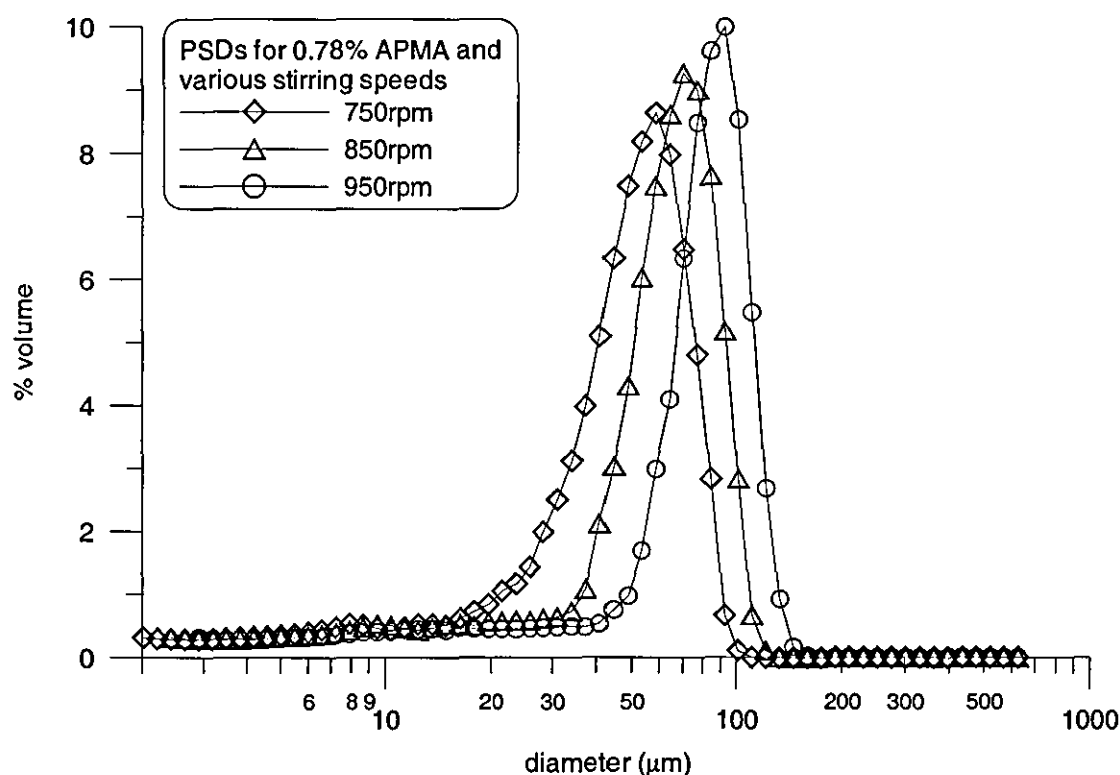


Figure 6.5.6. Particle size distributions for APMA and increasing stirrer speed, at pH 9

The interfacial area for these runs is calculated from the drop size distribution with the procedure described in the experimental part, chapter 3.3.4

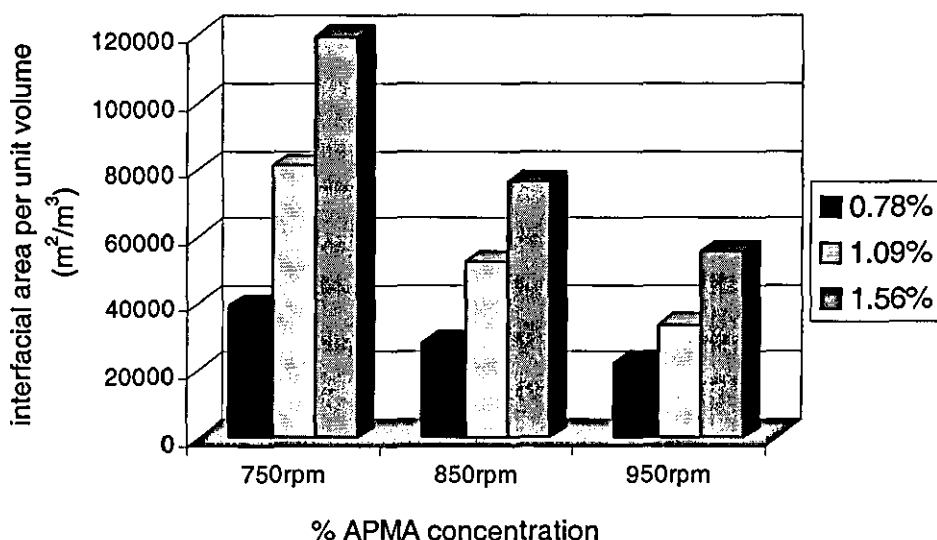


Figure 6.5.7. Interfacial area for increasing APMA concentration

The interfacial area is a function of two variables, of the APMA concentration and the stirring speed. As shown in figure 6.5.7, the interfacial area increases with increasing APMA concentration for a certain stirring speed, but decreases for increasing stirring speed for all stabiliser concentrations. Higher stabiliser concentrations produce smaller drops and hence larger interfacial areas for the same monomer concentration. When the stirring speed increases, larger drops are produced, as shown in chapter 3.3.4, and hence the interfacial area decreases.

The conversion-time data depicted in figure 6.5.8, for constant stabiliser concentration in the continuous phase, show that the reaction rate accelerates for decreasing stirring speed, and therefore increasing interfacial area.

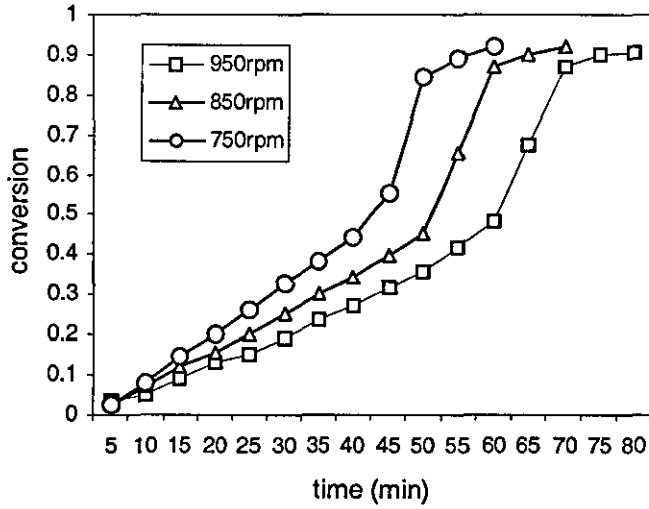


Figure 6.5.8. Conversion for 0.78% APMA and increasing stirring speed and BPO 0.06mole/l.

Figure 6.5.9, shows that for increasing stirring speed the values of x_{crit} diminish. For these runs the increase of the interfacial area is achieved by lowering the stirring speed. Hence, there must exist an influence of the interfacial area on the reaction kinetics, and this influence is manifested by an acceleration for decreasing stirring speed.

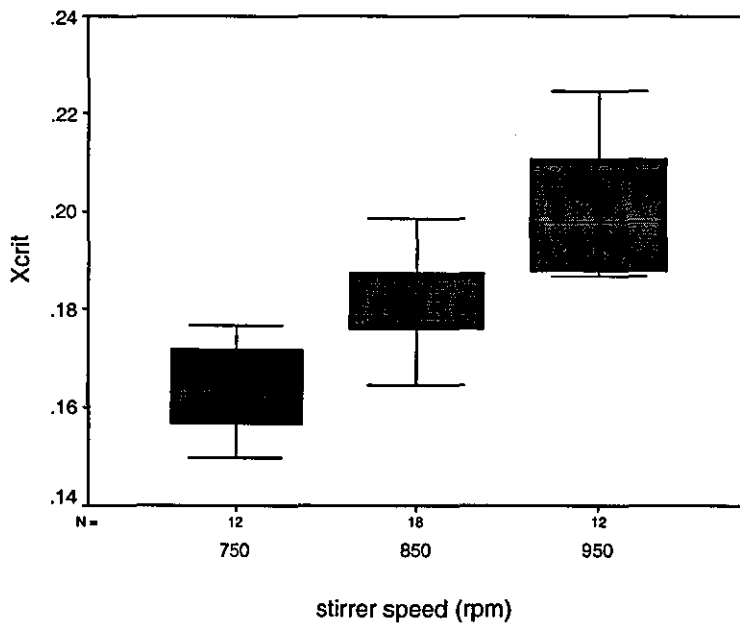


Figure 6.5.9. x_{crit} for APMA and increasing stirrer speed

The x_{crit} values for increasing interfacial area are depicted in figure 6.5.10, where it is shown that x_{crit} decreases for increasing interfacial area. Hence there must exist a relation between the interfacial area and x_{crit}

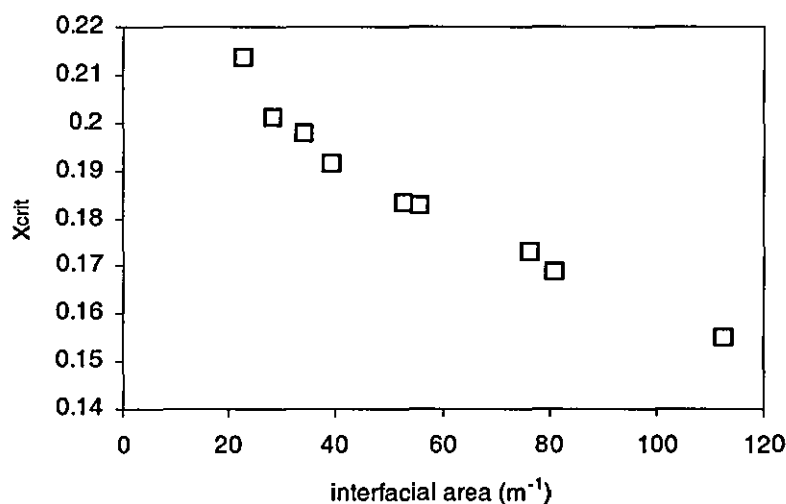


Figure 6.5.10. x_{crit} for increasing interfacial area

Summarising, the observations made so far are regarding the use of APMA as a stabiliser and its effect on the polymerisation kinetics:

- When APMA is used, the x_{crit} decreases with increasing BPO concentration, in contradiction with the trend that x_{crit} follows when other stabilisers are used (PMA-Na and PVA)
- For increasing APMA concentrations, the reaction rate accelerates
- For increasing interfacial area, achieved by lowering the stirring speed and for the same APMA concentration the reaction rate also accelerates
- For increasing interfacial area the x_{crit} diminishes

These observations indicate that there must exist an influence of APMA on polymerisation kinetics and more specifically, there must exist an interaction of APMA and BPO, that takes place or is related to the interface between the two liquid phases. What kind of interaction this is may become a little bit more obvious if the molecular weight distributions and averages of the samples produced with APMA under various conditions are examined.

6.5.5. Conclusions

The effect of the stabiliser type on x_{crit} was examined in this chapter, for two stabilisers PMA-Na and APMA. The results so far lead to the following conclusions:

- When APMA is used, for the same conditions as PMA-Na, an acceleration of the reaction rate occurs. When APMA solutions are used, the x_{crit} decreases with increasing BPO concentration, in contradiction with the trend that x_{crit} follows when other stabilisers are used (PMA-Na and PVA). APMA interacts with the reacting system and interferes with the reaction kinetics causing an acceleration of the polymerisation rate.
- For increasing APMA concentrations, the polymerisation rate accelerates and x_{crit} diminishes
- For increasing interfacial area, achieved by lowering the stirring speed and for the same APMA concentration, the reaction rate accelerates, and x_{crit} diminishes. This suggests that the interaction of APMA with the reacting system takes place in a way that is related to the interfacial area.

6.6. Effect of AMPA on Mw

The two factors that affect the polymerisation rate, APMA concentration and interfacial area, may also affect the molecular weight of the polymer produced. By examining the effect of these factors on the molecular weight the interference of APMA with the reaction kinetics may be clarified.

6.6.1. Effect of APMA concentration on MWD

In order to clarify the kind of interaction between APMA and BPO, experiments run with PMA-Na are compared with APMA runs. These suspension polymerisation experiments were run, at 70°C, with the same BPO concentration 0.04 mole/l and monomer volume fraction (0.1), but with different stabiliser concentrations PMA-Na and APMA. The concentration of the stabilisers was such that the drop sizes produced, or the drop size distributions produced, were almost identical in both cases, and that the specific interfacial area was almost equal as well (52,000 and 55,000 m⁻¹, for APMA and PMA-Na, respectively). Therefore, the only different factor in these cases was the stabiliser type.

The MWDs produced under these conditions are shown in figure 6.6.1. It is observed that, although the BPO concentration and the reaction temperature that are the factors affecting the MWD are the same in both cases, the M of the sample produced with APMA is lower than that of the sample produced with PMA-Na. If the stabiliser type, did not play any role influencing the reactions kinetics the MWD and the molecular weight averages would be identical. But in this case the molecular weight averages differ significantly. In fact the Mv for these samples are approximately 830,000 for PMA-Na and 560,000 for APMA.

This kind of difference between the Mv averages should not take place for the same BPO concentration. Lower Mv means that a larger number of free radicals were produced that could initiate the polymerisation of a larger number of polymer chains. This can only mean that APMA interacts with BPO, facilitating the decomposition of BPO and the formation of free radicals. In fact, APMA seems to act as a catalyst for the decomposition of BPO. This type of interaction, has not been reported before. Although, the catalytic effect of tertiary amines on the decomposition of BPO has been reported (Maltha, 1956; Yefremova et al., 1985; Vasquez et al., 1998), the

catalytic effect of the ammonium salt of polymethacrylic acid has not been reported previously.

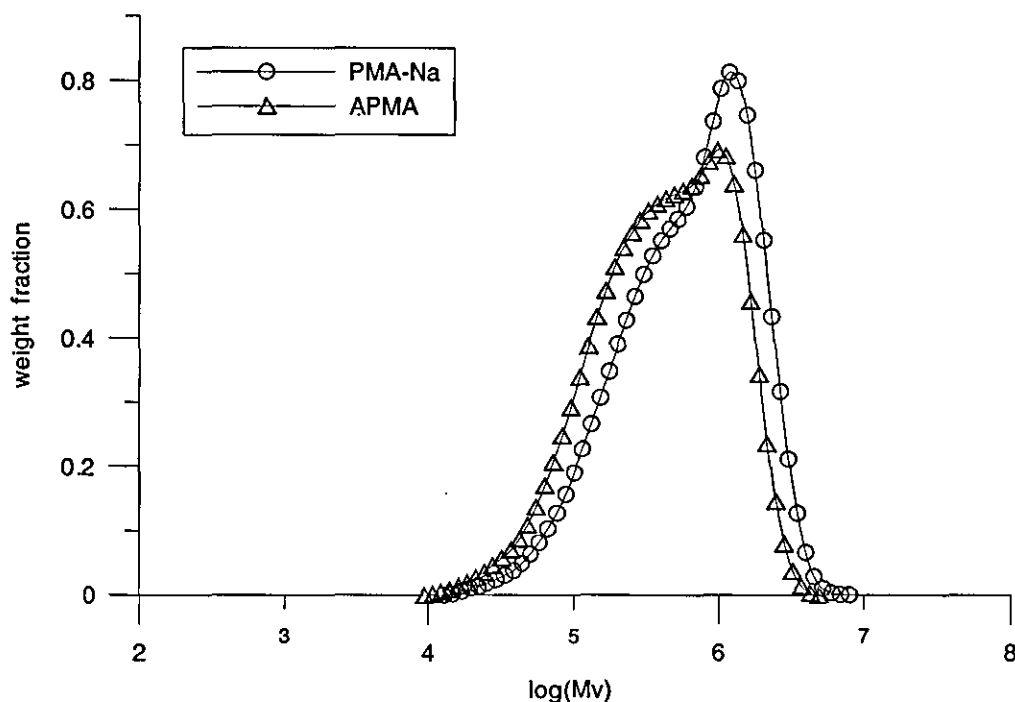


Figure 6.6.1. MWDs for PMA-Na and APMA, produced under similar conditions

The fact that APMA causes the formation of free radicals by facilitating the decomposition of BPO can also explain, apart from the lower Mv of the samples produced by APMA, some of the previous observations summarised in chapter 6.5.3. Hence, the acceleration of the reaction rate is caused by the larger number or concentration of free radicals formed. The corresponding decrease of the x_{crit} observed with increasing BPO could be explained by the increase of the decomposition rate of BPO.

The decomposition rate of BPO increases, and hence the actual decomposition rate constant of BPO, also increases. But because this interaction between APMA and BPO was not known, this increase was not taken into consideration, when classical kinetics calculations were used for the determination of x_{crit} , as was described in chapter 3.3.5. Therefore, the values of the decomposition rate constant of BPO used in classical kinetics calculations are lower than the actual ones. The use of lower values than the real ones for the decomposition rate constant gives lower values for

the theoretically predicted conversion-time data when classical kinetics is used. This means that the theoretically predicted curve is shifted to lower values, than the actual ones, and therefore, the experimental conversion-time data start to deviate from the theoretical curve, earlier on time scale, than the actual onset of the gel effect. This earlier deviation, results in underestimating the x_{crit} . Finally, the lower x_{crit} values observed were only an underestimate of the x_{crit} because of the initiator decomposition rate increase, which in turn was caused by the catalysing effect of APMA on BPO decomposition. Since, the kinetics of this APMA-BPO interaction are not known, the real values of x_{crit} cannot be estimated.

6.6.2. Effect of interfacial area on MWD

The effect of the interfacial area on the molecular weight was also examined by running suspension polymerisation experiments with the same BPO concentration (0.04 mole/l), at the same temperature, 70°C, the same monomer volume fraction (0.1), and the same APMA concentration in the continuous phase (0.78%). The increase of the interfacial area was achieved by lowering the stirring speed. The MWDs of the samples produced for 3 different stirring speeds are shown in figure 6.6.2. The interfacial area corresponding to the three stirring speeds are: 81,000, 69,000 and 52,000 m^{-1} , for 750, 850 and 950 rpm respectively. As shown in this figure, M increases for increasing stirring speed, or increases for decreasing interfacial area.

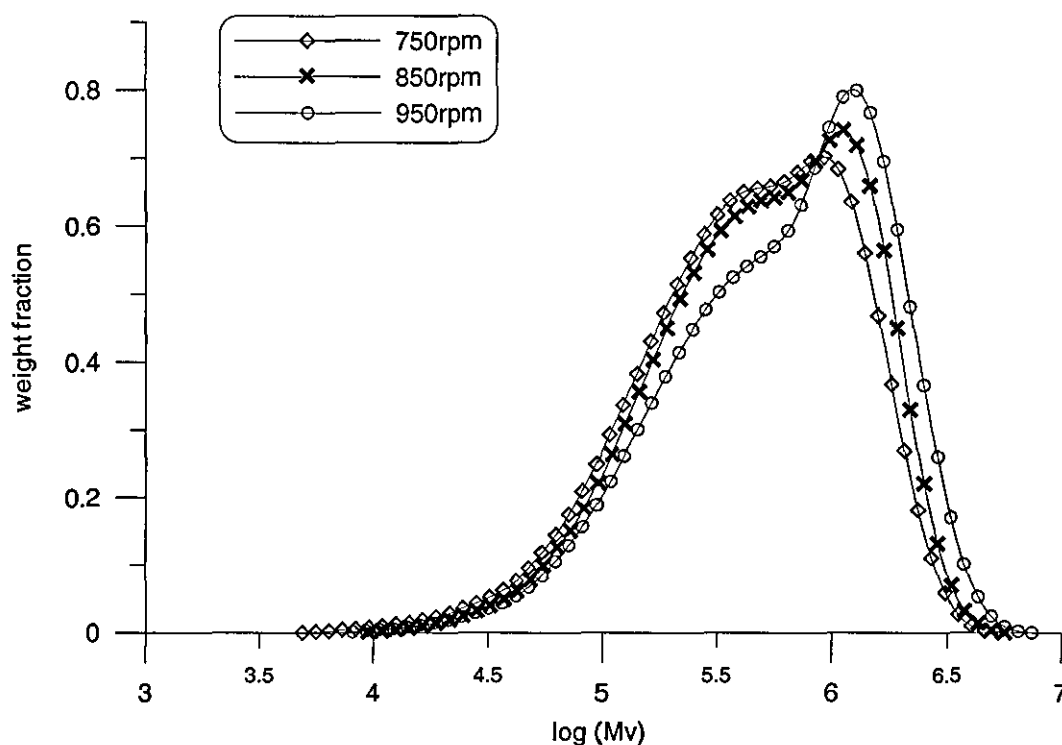


Figure 6.6.2. MWDs for increasing stirrer speed, produced with 0.93% APMA, at initial pH 9

The effect of the interfacial area on the M means that the interaction between APMA and BPO is related to the interfacial area between the two liquid phases, or takes place on the interface. Hence, as the interfacial area increases for decreasing stirring speed, the interaction of APMA and BPO takes place to a greater extent. APMA causes the formation of more free radicals and therefore a lower molecular weight polymer is produced.

6.6.3. Conclusions

The main conclusions drawn from the effect of APMA on the molecular weight of the polymer produced, are:

- APMA influences the reaction kinetics by catalysing the decomposition of BPO. The decomposition rate of BPO increases, producing a larger number of free radicals, which lead to the acceleration of the polymerisation rate and to polymer product with lower molecular weight.

- The increase of the interfacial area, has as a result, the decrease of the molecular weight of the polymer produced. This occurs because the increase of the interfacial area facilitates the catalysing effect of APMA on BPO leading to the production of lower MW polymer.

SECTION 4. CONCLUSIONS AND FUTURE WORK

7. GENERAL CONCLUSIONS

The use of the sodium and ammonium salts of polymethacrylic acid, PMA-Na and APMA, as suspending agents for the suspension polymerisation of MMA was investigated. The particular characteristics of these stabilisers is that they are polyelectrolytes, which determines their chemical behaviour, and they are viscous gels producing viscous continuous phases, which determines the flow conditions in the reactor. The experimental investigation carried out includes experimental work focused on

- the rheological behaviour of PMA and its salts, PMA-Na and APMA and the interfacial properties between PMA-Na or APMA and MMA
- the behaviour of PMA-Na and APMA as suspending agents for the suspension polymerisation, the dispersion mechanism and the stabilisation mechanism
- the factors that affect the onset of the gel effect.

7.1. Rheological behaviour and interfacial properties

The viscosity of PMA, PMA-Na and APMA was examined for any dependence on shear rate or shearing time, and pH, that they may exhibit, and the conclusions deduced were that:

- All the solutions examined, (PMA, APMA, and PMA-Na), show a time independent rheological behaviour.
- PMA solutions exhibit a shear thickening behaviour, while APMA and PMA-Na solutions exhibit a shear thinning behaviour. The rheological behaviour of PMA solutions seems to change when the polymethacrylic acid is neutralised either with NH_3 or with NaOH . The neutralisation seems to eliminate the shear thickening behaviour. This may be attributed to the repulsion between the parts of the polymer chain with the same charge, which force the polymer coil to unfold and

stretch causing the friction between the extended polymer coils and therefore the viscosity to reduce.

- PMA and APMA show a shear history-dependent behaviour. Once the PMA or APMA solutions have been subjected to high shear rates, their viscosity decreases even for low shear rates. On the other hand, PMA-Na solutions do not show any dependence on shear history.
- The viscosity of APMA solutions depends on pH (within the range of pH values from 9 to 11). For increasing pH, the solutions' viscosity decreases. For $\text{pH} < 9$, APMA solutions resemble the behaviour of PMA, showing a slight shear thickening behaviour for high shear rates. The viscosity of PMA-Na solutions does not depend on pH (within the range of pH values from 8 to 12). PMA-Na solutions resemble the behaviour of PMA for $\text{pH} < 8$, showing, also a dependence on shear history.
- The increase of the stabiliser concentration does not have any significant effect on the interfacial tension between the continuous phase and the monomer. The interfacial tension remains almost constant over all the range of stabiliser concentrations. The pH does not affect the interfacial tension between the two phases either.

7.2. Behaviour of PMA-Na and APMA as suspending agents

The behaviour of the polyelectrolyte stabilisers was examined in terms of the factors that influence the drop or particle sizes and the dispersion and stabilisation mechanisms.

7.2.1 Factors that affect the drop / particle sizes

The factors that affect or determine the drop formation and the final particle sizes, when PMA-Na or APMA are used as suspending agents, are the following:

- *Continuous phase viscosity*: The continuous phase viscosity has a strong effect and plays an important role on the determination of the drop and particle sizes. In

both cases of PMA-Na and APMA, an increase in the continuous phase viscosity causes a diminution of the particle sizes, and vice versa. The PSDs shift to smaller sizes and become slightly broader as the continuous phase viscosity increases. For the same continuous phase viscosity, APMA solutions produce smaller particles than PMA-Na solutions.

- *Stirrer speed:* Increasing the impeller speed above a particular value leads to an increase of the particle sizes. This is attributed to the non-Newtonian nature of the continuous phase. Increasing the stirring speed causes the viscosity of the non-Newtonian continuous phase to decrease, and therefore, the particle sizes increase.
- *Hold-up:* For increasing hold-up, d_{32} initially decreases, reaches a minimum and then starts to increase. The hold-up, for which d_{32} becomes minimum, increases for increasing stabiliser concentration and continuous phase viscosity.
- *Dispersed phase viscosity:* Increasing the dispersed phase viscosity causes the d_{32} to increase and the PSD to broaden significantly.
- *pH:* Increasing the initial pH of the continuous phase causes the particle sizes to diminish, as well as the formation of two secondary peaks, at size ranges up to 1.5 μm for the first one, and within the range from 1.5 to 10 μm for the second. The total volume of drops within the secondary peaks increases with increasing pH, while the volume within the main peak decreases. The size of the first peak increases monotonously, while the size of the second peak, increases initially and then decreases. The overall trend is to form fine particles within the diameter range 0.4 to 1.5 μm .
- *Temperature:* Increasing the reaction temperature causes the particle sizes to increase too. This decrease of the particle size is a combined effect caused, mainly, by the viscosity decrease of the continuous phase as the temperature increases, and the increase of the polymerisation rate. The effect of the temperature on the particle size is more evident for lower stabiliser concentrations.
- *Chain transfer agent (CTA):* In the presence of a chain transfer agent the volume of the particles with diameters smaller than 10 μm increases, and the size of the maximum diameter decreases significantly. In the presence of a CTA the polymerisation requires longer time, which causes the dissolution of monomer in the continuous phase to a greater extent. The increased dissolution of monomer

causes the formation of a larger number of fine particles. The diminution of the maximum particle size could be attributed to the lower rate of viscosity build up in the drops.

7.2.2. Dispersion mechanism

- The viscosity index provided by the fit of the data to the power law model, is higher for APMA solutions than the viscosity index for PMA-Na solutions, suggesting that they exhibit a different shear thinning behaviour
- For PMA-Na concentrations higher than 0.5% and APMA concentrations higher than 0.78% in the continuous phase, coalescence is prevented and d_{32} remains constant over all the conversion range. Therefore, for these concentrations the final particle sizes can be considered to reflect the initial drop sizes.
- The results show that for high continuous phase viscosities, the inertial breakup theory cannot explain the drop breakup. The d_{max} values obtained from the suspension polymerisation experiments show a good agreement with Taylor's theory. It can be reasonably deduced that the viscous shear breakup mechanism controls the dispersion process when PMA-Na is used as a suspending agent in laboratory scale reactors and when the Reynolds number has a low value. This would not be expected in large scale industrial reactors where the Reynolds numbers are higher by some orders of magnitude
- Increasing the dispersed phase viscosity by the addition of PMMA to the monomer prior to polymerisation does not affect the dispersion mechanism for viscosity ratios lower than 1.

7.2.3. Stabilisation mechanism

The experimental work showed that the pH played a very important role in the stabilisation of the dispersion.

- The pH had a profound effect on the particle sizes and, at a constant stabiliser concentration, increasing the pH caused the particle size to decrease. Not only did

the pH increase cause a decrease of particle sizes for various stable dispersions but, at a given stabiliser concentration, it induced stability in dispersions that were unstable at a lower pH. This was attributed to increases in the charges on the polymer coil and in the strength of repulsive forces.

- The enhancement of the stabilisation of the dispersion was considered to have been achieved through the contribution of the electrosteric stabilisation mechanism.

7.3. Factors that affect the onset of the gel effect

The onset of the gel effect, in terms of x_{crit} was examined for increasing temperature, initiator concentration and molecular weight of the polymer produced,

- x_{crit} increases for increasing polymerisation temperature, as has been explained in terms of the free volume theory.
- x_{crit} increases for increasing BPO concentration, and decreasing molecular weight. The effect of the M_v on x_{crit} has been verified.
- When APMA is used, for the same conditions as PMA-Na, an acceleration of the reaction rate occurs. When APMA solutions are used, the x_{crit} decreases with increasing BPO concentration, in contradiction with the trend that x_{crit} follows when other stabilisers are used (PMA-Na and PVA). APMA interacts with the reacting system and interferes with the reaction kinetics causing an acceleration of the polymerisation rate. Also, for increasing APMA concentration, the polymerisation rate accelerates and x_{crit} diminishes
- For increasing interfacial area, achieved by lowering the stirring speed, and for constant APMA concentration the reaction rate also accelerates, and x_{crit} diminishes, suggesting that the interaction of APMA with the reacting system takes place or that the interaction is related to the interfacial area.
- APMA influences the reaction kinetics by catalysing the decomposition of BPO. The decomposition rate of BPO increases, producing a larger number of free

radicals, which lead to the acceleration of the polymerisation rate and to polymer product with lower molecular weight.

- With APMA, the increase of the interfacial area leads to decrease of the molecular weight of the polymer produced. This occurs because the increase of the interfacial area facilitates the catalysing effect of APMA on BPO leading to the production of lower MW polymer.

8. SUGGESTIONS FOR FURTHER WORK

This experimental results produced within the frame of this project, and the conclusions drawn, have elucidated the use of polyelectrolyte stabilisers for the suspension polymerisation processes. Interesting subjects that have been raised within this project and are recommended for future investigation are:

1. The effect of ammonium polymethacrylate on the kinetics of the decomposition rate of BPO. The catalysing effect of APMA on BPO has not been reported before (to our knowledge) and investigation would produce useful information about the effect of APMA on the decomposition rate of BPO.
2. The role of the drop sizes and of the interfacial area on the interaction between APMA and BPO. APMA, when used with BPO, can act both as a stabiliser and as an accelerator. This dual action can have significant potential for the suspension polymerisation processes.
3. Further investigation on the evolution of drops and particles in non-turbulent flows in suspension polymerisation, and in other systems
4. Further investigation on the formation of fine particles during suspension polymerisation
5. Further investigation on the effect of the non-Newtonian, shear thinning behavior on the drop and particle evolution, in suspension polymerisation.
6. The Molecular weight dependence and concentration dependence of the termination rate constant, k_t

REFERENCES

- Abuin, E., and Lisi, A (1977), 'Methyl methacrylate polymerisation at high conversion II. Factors determining the onset of the gel effect', J. Macromol. Sci.-Chem. A 11 (2), 287-293
- Abuin, E., and Lissi, E.A. (1979), 'Methyl methacrylate polymerisation at high conversion III. Effect of a chain-transfer agent', J. Macromol. Sci.-Chem. A 13 (8), 1147-1156
- Abuin, E., Conteras, E., Gruttner, E., and Lissi E.A. (1977), 'Methyl methacrylate polymerisation at high conversion. I. Influence of the molecular weight of the polymer produced', J. Macromol. Sci.-Chem. A 11 (1), 65 -72
- Achilias, DS, Sideridou, I., (2002). 'Study of the effect of two BPO/amine initiation systems on the free-radical polymerisation of MMA used in dental resins and bone cements. J of Macromolecular science-Pure and applied chemistry A39 (12), 1435-1446
- Ades, D., and Fontanille, M., (1978). 'Polymerization of Phenyl Glycerol Ether Methacrylate by Benzoyl Peroxide: Acceleration of Polymerization by Sulfinates of Tertiary Amines', Journal of Applied Polymer Science 23 (1), 11-23
- Ahn, SM., Chang, SC., and Rhee, H-K. (1996), Application of Optimal Temperature Trajectory to batch PMMA polymerisation reactor', J. Appl. Polym. Sci. 69, 59-68
- Alvarez, Jesús, Alvarez, José, and Hernández Martín (1994), A population balance approach for the description of particle size distribution in suspension polymerization reactors, Chemical Engineering Science, Volume 49 (1,) 99-113
- Arai, K., and Saito S. (1976), 'Simulation model for the rate of bulk polymerisation over the complete course of reaction', J.Chem.Eng. Japan 9 (4), 302-311
- Arai, K., Konno M., and Matunaga Y. (1977). Effect of dispersed-phase viscosity on the maximum stable drop size for breakup in turbulent flow. J. Chem. Eng. Japan 10 (4), 325-330

- Azad, A.R.M., and Fitch R.M., (1978). 'Particle size distribution in suspension polymerisations: Effect of low molecular weight compounds', *Polymer Colloids II*, Fitch R.M. (Ed.), Plenum Press, New York, 95-119
- Beattie, J.K., and Djerdjev A., (2000). 'Rapid electroacoustic method for monitoring dispersion: zeta potential titration of alumina with ammonium poly(methacrylate)', *J. Am. Chem. Soc.* 83 (10), 2360 -2369
- Berndtsson B, Turnen L., 1954. *Kunststoffe* 44, 430
- Bogunjoko, J.S.T., and Brooks. B.W. (1983 (a)), 'Kinetics of free-radical polymerisation at high viscosities', *Makrom. Chem.* 184, 1603-1612
- Bogunjoko, J.S.T., and Brooks, B.W. (1983 (b)), 'Molecular weight distributions of poly(methyl methacrylate) produced at high viscosities', *Makrom. Chem.* 184, 1623-1630
- Borwankar, R.P., Chung, S.I., and Wasan, D.T., (1986), 'Drop Sizes in Turbulent Liquid-Liquid Dispersions Containing Polymeric Suspension Stabilizers', *Journal of Applied Polymer Science*, 32, 5749-5762
- Boye, A.M., Lo, M-Y. A., Shamlou, A.P. (1996), 'The effect of two-liquid phase rheology on drop breakage in mechanically stirred vessels', *Chemical Engineering Communications* 143, 149-167
- Brauer, G.M., Stansbury j.W., Antonucci J.M., (1981), 'Dental Research' 60, 1343-1348
- Brooks, B.W., (1977), 'Viscosity effects in the free-radical polymerisation of methyl methacrylate', *Proc.R.Soc.Lond.A* 357, 183-192
- Brooks B.W., 1990, Basic Aspects and Recent Developments in Suspension Polymerisation, *Makromol. Chem. Macromol. Symp.*, 35/36, 121-140
- Calabrese, R.V., Chang, T.P.K., Dang, P.T. (1986 (a)), 'Drop breakup in turbulent stirred-tank contactors. Part I: Effect of dispersed-phase viscosity', *AIChE Journal* 32 (4), 657-666

- Calabrese, R.V., Wang, C.Y., Bryner, N. (1986 (b)), 'Drop breakup in turbulent stirred-tank contractors. Part III: Correlations for mean size and drop size distribution', *AIChE J.* 32 (4), 677-687
- Calderbank P.H., Moo-Young M.B., (1959), 'The prediction of power consumption in the agitation of non-Newtonian fluids', *Transactions-Institution of Chemical Engineers* 37, 26-33
- Cebollada, A.F., Schmidt, M.J., Farber, J.N., Capiati, N.J., Valles, E.M., (1989), 'Suspension polymerisation of vinyl chloride. I. Influence of viscosity medium on resin properties', *J. Appl. Polym. Sci.* 37, 145-154
- Cesarano, J. III, Aksay, I.A., Bleier, A., (1988). 'Stability of aqueous α -Al₂O₃ suspensions with poly(methacrylic acid) polyelectrolyte', *Journal of American Chemical Soc.* 71 (4), 250-258
- Chatzi, E.G. and Kiparissides, C., (1995), 'Steady-state drop-size distributions in high holdup fraction dispersion systems', *AIChE J.* 41 (7), 1640-1652
- Chatzi, E.G., Boutris, C.J., and Kiparissides, C., (1991), 'On-line monitoring of drop size distribution in agitated vessels. 2. Effect of stabilizer concentration', *Ind. Eng. Chem. Res.* 30, 1307-1313
- Chen, B, Keshive, M, Deen, WM, (1998), 'Diffusion and reaction of nitric oxide in suspension cell cultures', *Biophys J* 75 (2): 745-754
- Cho, J.M., and Dogan, F., (2001), 'Colloidal processing of lead lanthanum zirconate titanate ceramics', *J. Material Sci.* 36, 2397-2405
- Cioffi, M., Hoffmann, A.C., and Janssen, L.P.B.M., (2001), 'Rheokinetics and the influence of shear rate on the Trommsdorff (gel) effect during free radical polymerisation', *Polymer Eng. Science* 41 (3), 595 - 602
- Clarke-Pringle T.L., Mac Gregor, J.F., (1998), 'Optimization of molecular-weight distribution using batch to batch adjustments', *Ind. Eng. Chem. Res.* 37, 3660-3669
- Cobb, G.W., (1998), 'Introduction to design and analysis of experiments. Springer-Verlag', New York.

- Cooper, A.R., (1989), 'Determination of molecular weight', John Willey & Sons
- Coulaloglou, C.A., and Tavlarides, L.L., (1976), 'Drop size distributions and coalescence frequencies of liquid-liquid dispersions in flow vessels', *AIChE Journal*, 22 No.2, 289-297
- Coulaloglou, C.A., Tavlarides, L.L., (1977), 'Description of interaction processes in agitated liquid-liquid dispersions', *Chemical Engineering Science* 32 (11), 1289-1297
- Crowley, T., and Choi, K.Y., (1997), 'Discrete optimal control of molecular weight distribution in a batch free radical polymerisation process', *Ind. Eng. Chem. Res.* 36, 3676 -3695
- Cunningham, M.F., and Mahabadi, H.K., (1996), 'Kinetics of high conversion free-radical polymerisation. 1. Understanding kinetics through study of pseudoinstantaneous molecular weight distributions', *Macromol.* 29, 835-841
- Das, P.K., (1996), 'Prediction of maximum diameter of viscous drops in a turbulent dispersion', *Chem. Eng. Techn.* 19 (1), 39-42
- Dean, A., Voss D., (1999), 'Design and analysis of experiments', New York, Springer
- Deshiikan, S.R., Papadopoulos, K.D., 1995. London-VDW and EDL effects in the coalescence of oil drops. *J. Colloid and Interface Sci.*, 174 (2), 302-312
- Desnoyer, C., Masbernat, O., Gourdon, C., (2003). Experimental study of drop size distributions at high phase ratio in liquid-liquid dispersions. *Chemical Eng. Sci.* 58, 1353-1363.
- Dowding, P.J., Vincent B., (2000), 'Suspension polymerisation to form polymer beads', *Colloids and Surfaces A*, 161, 259-269
- Doxastakis, G., Sherman, P., (1984), 'Interaction of sodium caseinate with monoglyceride and diglyceride at the oil water interface in corn oil in water emulsions and its effect on emulsion stability', *Colloid and Polymer Science* 262 (11), 902-905

- Driscoll, K.F., and Ponnuswamy, S.R., (1990), 'Optimization of a batch polymerisation reactor at the final stage of conversion. II. Molecular weight constraint', *J. Appl. Polym. Sci.* 39, 1299
- Ducla, J.M., Desplanches, J., Chenalier, J.L., (1983), 'Effective viscosity of non-Newtonian fluids in a mechanically stirred tank', *Chemical Engineering Communications* 21, 29-36
- Dvornic, P.R., and Jacovic, M., (1981), 'The viscosity effect on autoacceleration of the rate of free radical polymerisation', *Polym. Eng. Sci.* 21 (12), 792-796
- Gaillard, C., Camps, M., Proust, J.P., Hashieh, I.A., Rolland, P., Bois, A., (2000), 'Copolymerisation of 1,2 bis(2-methylpropenoxy)ethane and divinylbenzene in aqueous suspension. Part I: control of the diameters of the beads of 1,2(2-methylpropenoxy)ethane – divinylbenzene copolymer', *Polymer* 41, 595-606
- Gillc, V., Golob, J., Modic, R., (1986), 'Drop coalescence in liquid/liquid dispersions by flow through glass fibre beds', Part II. *Chemical Engineering Research & Design* 64 (1), 67-70
- He, Y., Howes, T., Lester, J.D., Ko, G.L., (2002), 'Experimental study of drop-interface coalescence in the presence of polymer stabilisers', *Colloid surface A* 207 89-104
- Hinze, J.O., (1955), 'Fundamentals of the hydrodynamic mechanism of splitting in dispersion processes', *AIChE Journal* 1 (3), 289-295
- Howarth, W.J., (1963), 'Coalescence of drops in a turbulent flow field', *Chemical Engineering Science* 19, 33-38
- Howarth W.J., (1967), 'Measurement of coalescence frequency in an agitated tank' *AIChE J.* 13 (5), 1007-1067
- Jahanzad, F., Sajjadi, S., Brooks B.W., (2005), Characteristic intervals in suspension polymerisation reactors: An experimental and modelling study, *Chemical Engineering Science*, 60 (20), 5574-5589

- Jahanzad F., Brooks B.W., Sajjadi S., (2004 (a)), "New Insight in the Suspension Polymerization of Methyl Methacrylate" , *8th International Workshop on Polymer Reaction Engineering*
- Jahanzad, F., Sajjadi, S., Brooks, B.W., (2004 (b)), 'On the evolution of particle size average and size distribution in suspension polymerisation processes', *Macromolecular Symposia* 206, 255-262
- Jean, J.H., and Wang, H.R., (1998), 'Dispersion of aqueous barium titanate suspension with ammonium salt of poly(methacrylic acid)', *J. Am. Ceram. Soc.* 81 (6), 1589-1599
- Jegat, C., Bois, A., Camps, M., (2001), 'Continuous phase viscosity influence on maximum diameters of poly(styrene-divinylbenzene) beads prepared by suspension polymerisation', *Journal of Polymer Science* 39, 201-210
- Jegat, C., Jacob, L., Camps, M., Bois, A., (1998), 'The viscosity influence study on poly(styrene-Co-divinylbenzene) beads in suspension polymerisation', *Polymer Bulletin* 40, 75-81
- Karam, H.J., Bellinger, J.C., (1968), 'Deformation and breakup of liquid droplets in a simple shear flow', *Industrial and Engineering Chemistry Fundamentals* 7(4), 576-581
- Katsumichi, Ono, Kenkichi, Murakami, (1977), 'Kinetics of gelation of aqueous poly(methacrylic acid) solutions under shear stress', *Polym. Let. Edition* 15, 507
- Kawashima, W., Iwamoto, T., Niwa, T., Takeuchi, T., Hino, T., (1993). 'Size control of Ibuprofen microspheres with an acrylic polymer by changing the pH in an aqueous dispersion', *Chemical and Pharmaceutical Bulletin* 41 (1), 191-195
- Kelso, J.F., and Ferrazzoli, T.A., (1989), 'Effect of powder surface chemistry on the stability of concentrated aqueous dispersions of alumina', *J.Am.Ceram.Soc.*, 72 (4), 625
- Kiparissides, C., Moustakis, I., Hamielec, A., (1993), 'Electrostatic and steric stabilization of PVC primary particles', *J.Appl. Polym. Sci.* 49, 445-459

- Konno, M., Arai, K., Saito, S., (1982), 'The effect of on coalescence of dispersed drops in suspension polymerisation of styrene', *Journal of Chemical Engineering of Japan* 15 (2), 131-135
- Koshy, A., Das, T.R., Kumar, R., Gandhi, K.S., (1988), 'Breakage of viscoelastic drops in turbulent stirred dispersions', *Chemical Engineering Science* 43, 2625-2631
- Kraume, M., Gabler, A., Schulze, K., (2004), 'Influence of physical properties on drop size distributions of stirred liquid-liquid dispersions', *Chemical Engineering and Technology* 27 (3), 330-334
- Kumar, S., Ganvir, V., Satyanand, C., Kumar, R., Gandhi, K.S., (1998), 'Alternative mechanisms of drop breakup in stirred vessels', *Chemical Engineering Science* 53 (18), 3269-3280
- Kumar, S., Kumar, R., Gandhi, K.S., (1991), 'Alternative mechanisms of drop breakage in stirred vessels,. *Chemical Engineering Science* 46, 2483-2489.
- Kumar S., Kumar R., Gandhi K.S., (1993). A new model for coalescence efficiency of drops in stirred dispersions, *Chemical Engineering Science* 48 (11), 2025-2038
- Lachinov M.B., Simonian R.A., Georgieva T.G., Zubov V.P. and Kabanov V.A., 'Nature of gel effect in radical polymerisation', *J. Polym. Sci.: Polym. Chem.* 17, 613 (1979)
- Lagisetty, J.S., Das, P.K., Kumar, R., Gandhi, K.S., 1986. Breakage of viscous and non-Newtonian drops in stirred dispersions. *Chemical Engineering Science* 41 (1), 65-72
- Lazrak N., Le Bolay N., Ricard A., 1998. Droplet stabilisation in high holdup fraction suspension polymerisation reactors, *European Polymer Journal* 34 (11), 1637-1647
- Leng, D.E., Quadrerer, G.J., 1982. Drop dispersion in suspension polymerisation. *Chemical Engineering Communications* 14, 177-201
- Lerner, F., Nemet, S., 1999. Effects of poly(vinyl acetate) suspending agents on suspension polymerisation of vinyl chloride monomer. *Plastics, Rubber and Composites* 28 (3), 100-104

Louie B.M. and Soong D.S., (1985 (a)), 'Optimization of batch polymerisation process – Narrowing the MWD. I. Model simulation', J. Appl. Polym. Sci. 3707-3749

Louie B.M. and Soong D.S., 'Optimization of batch polymerisation process – Narrowing the MWD. II. Experimental study', J. Appl. Polym. Sci. 30, 3825 (1985 (b))

Madriga E.L. and San Roman J., (1984). 'Effect of 1-n-dodecanethiol on the molecular weight distribution of poly(methyl methacrylate) synthesized by suspension polymerisation', J. Macromol. Sci.-Chem. A 21 (2), 167-177

Madriga E.L., San Roman J. and Benedi P., (1990). 'High conversion polymerisation of methyl methacrylate in the presence of n-dodecylmercaptan', J. Appl. Polym. Sci. 41, 1133-1140

Maggioris D., Goulas A., Alexopoulos A.H., Chatzi E.G., Kiparissides C., (2000). Prediction of particle size distribution in suspension polymerisation reactors: effect of turbulence nonhomogeneity. Chemical Engineering Science 55, 4611-4627

Maltha P., Damen L., (1956). Kunststoffe 46, 324

Margaritova M.F., Rusakona K.A., (1969). Study of reactions of benzoyl peroxide with amines, Polym Sci USSR, v 11, n 12, 1969, 3116-3122

Maschio G. and Scali C., (1999). 'Analysis of the molecular weight distribution in free radical polymerisation: modeling of the MWD from the analysis of experimental GPC curves', Macromol. Chem. Phys. 200 (7), 1708-1721

Maschio G. and Scali C., (1992). 'Optimal operating conditions of the batch reactors for the polymerisation of methyl methacrylate', Chimica e l'industria, 74(4), 16-23

Maschio G., Bello T. and Scali C., (1994). 'Optimal operation strategies to control the molecular weight distribution of polymer products', Chem. Eng. Sci. 49 (24B), 5086

Mason, R.L., Gunst R.F., Hess R.F., (2003). Statistical design and analysis of experiments :with applications to engineering and science. New York, Chichester, Wiley

- Metzner, A.B., Otto, R.E., (1957). Agitation of Non-Newtonian Fluids. A.I.Ch.E. Journal 3 (1), 3-10
- Moad G., Solomon D.H., (1995). The chemistry of free radical polymerisation, Pergamon Press Oxford, U.K., 72-73
- Montgomery D.C., (1991). Design and analysis of experiments. John Wiley & sons, New York
- Moreira J. L. Santana P.C., Feliciano A.S., et al. , (1995). Effect of viscosity upon hydrodynamically controlled natural aggregates of animal-cells grown in stirred vessels. Biotechnol Progr 11 (5): 575-583
- Morgan G.A., Mahwah, N.J., L. Erlbaum, (2004). SPSS for introductory statistics :use and interpretation. London, Eurospan
- Nagata S., 1975. Mixing: principles and applications, Kodansha Ltd, John Wiley and Sons, Tokyo, London, New York
- Narsimhan G., Gupat J.P., Ramkrishna D., (1979). A model for transitional breakage probability of droplets in agitated lean liquid-liquid dispersions. Chemical Engineering Science 34, 257-265
- Neil G.A. and Torkelson J.M., (1999). 'Modeling insight into the diffusion-limited cause of the gel effect in free radical polymerisation', Macromol. 32, 411-422
- Neil G.A., Wisnudel M.B. and Torkelson J.M., (1996). 'A critical experimental examination of the gel effect in free radical polymerisation: do entanglements cause autoacceleration?', Macromol. 29, 7477-7490
- Neil G.A., Wisnudel M.B. and Torkelson J.M., (1998). 'An evaluation of free volume approaches to describe gel effect in free radical polymerisation', Macromol. 31, 4537-4545
- Ni, X., Johnstone, J. C., Symes, K. C., Grey, B. D., Bennett, D. C., (2001), Suspension Polymerization of Acrylamide in an Oscillatory Baffled Reactor: from Drops to Particles, AIChE Journal, 47 (8), 1746-1757

- O'Shaughnessy B. and Yu J., (1994). 'Autoacceleration in free radical polymerisation 1. Conversion', *Macromol.* 27, 5067-5078
- Ohoya S., Hashiya S., Tsubakiyama K. and Matsuo T., (2000). 'Shear induced viscosity change of aqueous polymethacrylic acid solution', *Polym. J.* 32 (2), 133-139
- Ohoya T., Suzuki A., Kikuchi K., (1999). Importance of grafting in the emulsion polymerisation of MMA using PVA as a protective colloid. Effect of initiators. *Colloids and Surfaces A: Physicochemical and Engineering Aspects* 153, 123-125
- Oldfield, F.F., Yasuda, H.K., (1999). ESR study of MMA polymerization by a peroxide/amine system: Bone cement formation. *Journal of Biomedical Materials Research* 44, n 4, 436-445
- Ormondroyd S., (1988). The Influence of Poly(vinyl alcohol) suspending agents on Suspension Poly(vinyl chloride) Morphology, *British Polymer Journal*, 20, 353-359
- Park J.Y. and Blair L.M., (1975). The Effect of Coalescence on Drop Size Distribution in an Agitated Liquid-Liquid Dispersion, *Chemical Engineering Science*, 30, pp. 1057-1064
- Pittman C.U., Jada S.S., (1982). Effect of polymer-bound amine accelerators on the radical-initiated curing of unsaturated polyesters with styrene. *Ind. Eng. Chem. Prod. Res. Dev.* 21, 281-284
- Reddy S.R., Fogler H.S., (1980). Emulsion stability of acoustically formed emulsions. *J. Physical chemistry* 84 (12), 1570-1575
- Roychoudhury PK, Gomes J, Bhattacharyay SK, et al. (1999). Production of urokinase by HT 1080 human kidney cell line. *Artif Cell Blood Sub* 27 (5-6): 399-402
- Ruiz M.C., Lermenda P., Padilla R., (2002). Drop size distribution in a batch mixer under breakage conditions. *Hydrometallurgy* 63, 65-74.
- Ryabov A.V., Panova G.D., Emel'yanova D.N., Myasnikov B.V. and Smirnova L.A., (1972). Influence of stabilizers on the particle size distribution of suspension poly(methyl methacrylate), *Sov. Plast.* 29

- Sakurai M., Imai T., Yamashita F., Nakamura K., Komatsu T., Nakagawa T., (1993). 'Temperature dependence of viscosities and potentiometric behavior of aqueous poly(acrylic acid) and poly(methacrylic acid) solutions', *Polym. J.* 25 (12), 1247
- Santhiya, D., Subramanian S., Natarajan K.A. and Malghan S.G., (2000). Surface chemical studies on alumina suspension using ammonium poly(methacrylate), *Colloids & Surf. A* 164, 143-154
- Scali C., Ciari R., Bello T. and Maschio G., (1995). 'Optimal temperature for the control of the product quality in batch polymerisation: simulation and experimental results', *J. Appl. Polym. Sci.* 55, 945
- Shih C.J. and Hon M.H., (1999). 'Electrokinetic and rheological properties of aqueous TiN suspensions with ammonium salt of poly(methacrylic acid)', *J. Europ. Ceram. Soc.* 19, 2773
- Shimizu, K., Minekawa, K., Hirose, T., Kawase, Y., (1999). 'Drop breakage in stirred tanks with Newtonian and non-Newtonian fluid systems'. *Chemical Eng. Journal* 72, 117-124
- Shinnar R., Church, J.M., (1960). 'Statistical theories of turbulence in predicting particle size in agitated dispersions'. *Industrial & Engineering Chemistry* 52 (3), 253-256
- Shreekumar, Kumar R., Gandhi K.S., (1996). 'Breakage of a drop of inviscid fluid due to a pressure fluctuation at its surface'. *Journal of Fluid Mechanics* 328, 1-17
- Skelland A.H.P., (1967). *Non-Newtonian flow and heat transfer*, Wiley, New York
- Skelland, A.H.P., Kanel, J.S., (1990). Minimum impeller speeds for complete dispersion of non-Newtonian liquid – liquid systems in baffled vessels. *Industrial and Engineering Chemistry Research* 29, 1300-1306
- Soh S.K., Sundberg D.C., (1982). J. 'Diffusion controlled vinyl polymerisation' *Polym. Sci.* 20, 1299-1313
- Sovova H., (1981). Breakage and coalescence of drops in a batch stirred vessel – II. Comparison of model and experiments. *Chem. Eng. Sci.* 36 (9), 1567-1573

- Sprow F.B., (1967). 'Distribution of drop sizes produced in turbulent liquid-liquid dispersion'. *Chemical Engineering Science* 22, 435-442
- Stamatoudis, M., Tavlarides, L.L., (1985). 'Effect of continuous phase viscosity on the drop sizes of liquid – liquid dispersions in agitated vessels'. *Industrial & Engineering Chemistry Process Design and Development* 24, 1175-1181
- Stone H.A., (1994). 'Dynamics of drop deformation and breakup in viscous flows'. *Annu. Rev. Fluid Mech.*, 26, 65-102
- Sumi Y, Kamiwano M., (2001). 'Development and mixing characteristics of a multistage impeller for agitating highly viscous fluids'. *J Chem Eng JPN* 34 (4): 485-492
- Sundlof, B.R., Carty, W.M., 2000. Dispersion of alumina. *Science of whitewares II, Proc.Conf. New York*, 237-248
- Tarnogrodzki A., (1993). 'Theoretical prediction of the critical Weber number'. *Int. J. Multiphase Flow* 19 (2), 329-336
- Taylor G.I., (1934). 'The formation of emulsions in definable fields of flow'. *Proceedings of the Royal Society A CXLVI*, 501-523
- Taylor, G.I., (1932). 'The viscosity of a fluid containing small drops of another fluid'. *Proceedings of the Royal Society A CXXXVIII*, 41-48
- Tefera N., Weickert G., Westerterp K.R., (1997). 'Modelling of free radical polymerisation up to high conversion. 1. A method for the selection of models by simultaneous parameter estimation'. *J. Appl. Polym. Sci.* 12, 1649-1661
- Tobin T., Muralidhar R., Wright H., and Ramkrishna D., (1990). 'Determination of coalescence frequencies in liquid-liquid dispersions: Effect of drop size dependence'. *Chem. Eng. Sci.* 45 (12), 3491-3504
- Tobin T., Rakrishna D., (1992). 'Coalescence of charged droplets in agitated liquid-liquid dispersions'. *AIChE J.* 38 (8), 199-1205

- Tobin T., Ramkrishna D., Muralidhar R., (1991). 'An investigation of drop charge effects on coalescence in agitated liquid-liquid dispersions'. AIChE Symp. S., 88 (286), 60-64
- Towlson S.M., Wright P.V., (1983). 'Potentiometric hysteresis and ultra-violet spectroscopy of isotactic poly(methacrylic acid)', Polym. Commun. 24, 79-82
- Tulig T.J. and Tirrell M., (1981). 'Toward a molecular theory of the Trommsdorff effect', Macromol. 14, 1501-1511
- Valentas K.J., Bilous O., Amundson N., (1966). 'Analysis of breakage in dispersed phase systems'. Industrial and Engineering Chemistry Fundamentals 5 (20), 271-279
- Vazquez B., Levenfeld B., Roman J.S., 1998. Role of amine activators on the curing parameters, properties and toxicity of acrylic bone cements. Polymer international 46 (3), 241-250
- Velev O.D., Gurkov T.D., Chakarova Sv.K., Dimitrova B.I., Ivanov I.B., Borwankar R.P., (1994). 'Experimental investigations on model emulsion systems stabilized with non-ionic surfactant blends'. Colloids and Surfaces A: Physicochemical and Engineering Aspects 83 (1), 43-55
- Vermeulen, T., Williams, G.M., Langlois, G.E., (1955). 'Interfacial area in liquid-liquid and gas -liquid agitation'. Chemical Eng. Progress 51, 85F-94F
- Vivaldo-Lima E., Wood P.E., Hamielec A.E and Penlidis A., (1997). 'An updated review on suspension polymerisation'. Ind. Eng. Chem. Res., 36, 939-965
- Von Hopff H., Lussi H., Gerspacher P., (1964). 'Zur kenntnis der perlpolymerisation 2. Mitt praktische anwendung der dimensionsanalyse auf das system MMA – mowiol 70/88', Makromol. Chem. 78, 37-46
- Walstra, P., (1993). 'Principles of emulsion formation', Chemical Engineering Science 48 (2), 333-349
- Wang C.Y. and Calabrese R.V., (1986). 'Drop break up in turbulent stirred-tank contactors, Part II: Relative influence of viscosity and interfacial tension', AIChE Journal, 32 No.4, 667-676

- Wang X. and Ruckenstein E., (1993). 'On the gel effect in the presence of a chain transfer agent in methyl methacrylate polymerisation and its copolymerisation with various acrylates', *J. Appl. Polym. Sci.* 49, 2179-2188
- Werts A.P., (1971). 'What you should know about promoters for RT- cure polyesters'. *Plastics Technol.* 17 (13), 36-37
- Yan H.G., Kalfas G. and Ray W.H., (1991). 'Suspension Polymerisation', *JMS – Rev. Macromol. Chem. Phys.*, C31(2&3), 215-299
- Yang B., Takahashi K., Takeishi M., (2000). 'Styrene drop size and size distribution in an aqueous solution of poly(vinyl alcohol)'. *Ind. Eng. Chem. Res.* 39, 2085-2090.
- Yefremova Ye. P., Chikhacheva I. P., Stavrova S. D., Bogachev Yu. S., Zhuravleva, I. L., Pravednikov A. N., (1985). 'Mechanism of formation of initiating radicals in the peroxide-tertiary amine system'. *Polymer Science USSR* 27 (3), 595-601
- Zerfa M., Brooks B.W., (1996 (a)). 'Drop coalescence processes in suspension polymerisation of vinyl chloride'. *Journal of Applied Polymer Sci.* 60 (12), 2077-2086
- Zerfa M., Brooks B.W., (1997). 'Experimental Investigation of Vinyl Chloride Drop Behavior During Suspension Polymerisation', *Journal of applied polymer science*, 65, 127-134
- Zerfa M., Brooks B.W., (1998), 'Experimental Investigation of PVA adsorption at the vinyl chloride/water interface in monomer suspensions', *Colloids and Surfaces A*, 132, 267-273
- Zerfa, M., Brooks, B.W., (1996 (b)). 'Prediction of vinyl chloride drop sizes in stabilised liquid-liquid agitated dispersion'. *Chemical Engineering Science* 51 (12), 3223-3233
- Zhang S.X., Harmon Ray W., (1997). 'Modelling and experimental studies of aqueous polymerisation processes. 3. Mass transfer and monomer solubility effects', *Ind. Eng. Chem. Res.* 36, 1310-1321

Zhu S., Hamielec A.E., (1989). 'Chain length dependent termination for free radical polymerisation', *Macromolecules* 22, 3093-3098

Zhu S., Tian Y., Hamielec A.E. and Eaton D.R., (1990). 'Radical trapping and termination in free-radical polymerisation of MMA', *Macromol.* 23, 1144-1150

